R85-3

TC171
.M41
.H99
no.298

MIT LIBRARIES
3 9080 00314 9330

SPILLWAY ANALYSIS IN DAM SAFETY EVALUATION

by
DAVID E. LANGSETH
and
FRANK E. PERKINS

RALPH M. PARSONS LABORATORY
HYDROLOGY AND WATER RESOURCE SYSTEMS

Report No. 298

Prepared under the support of the
National Science Foundation

December 1984

MIT

BARKER ENGINEERING LIBRARY
MASS. INST. TECH.
NOV 18 1985
LIBRARIES

DEPARTMENT
OF
CIVIL
ENGINEERING

SCHOOL OF ENGINEERING
MASSACHUSETTS INSTITUTE OF TECHNOLOGY
Cambridge, Massachusetts 02139

R85-3

SPILLWAY ANALYSIS IN DAM SAFETY EVALUATION

by

David E. Langseth

and

Frank E. Perkins

RALPH M. PARSONS LABORATORY

HYDROLOGY AND WATER RESOURCE SYSTEMS

Report Number 298

Prepared under the support of the

National Science Foundation

DECEMBER 1984

MIT Libraries

77 Massachusetts Avenue
Cambridge, MA 02139
http://libraries.mit.edu/ask

DISCLAIMER NOTICE

Due to the condition of the original material, there are unavoidable flaws in this reproduction. We have made every effort possible to provide you with the best copy available.

Thank you.

Some pages in the original document contain text that is illegible.

ABSTRACT

This work develops, tests, and applies a non-dimensional flood damage model which includes both overtopping and non-overtopping dam failures. The model represents a catchment, reservoir, dam, channel, and damage site. Peak reservoir flood inflow, initial reservoir stage, and overtopping failure stage are represented as stochastic variables. The model computes the expected value of total flood damage and of the damages attributable to natural floods, overtopping failures, and non-overtopping failures. The model also computes overtopping failure probability.

Four dams are used as case studies. Parameters of the catchment, reservoir, and dam are estimated from real data. Channel and damages site parameters are hypothetical. Sensitivity of model results to variations of uncertain model parameters is examined. Channel and damage site parameters are also varied. Estimates of expected damage and failure probability are shown to vary substantially as parameters which are difficult to estimate are varied within reasonable ranges. It is also shown that expected damage can decrease, increase, pass through a minimum, or remain fairly constant as spillway size is increased. The influence of spillway size varies with the initial reservoir stage.

ACKNOWLEDGEMENTS

The authors wish to thank Messrs. Perkins Gould, Phillip Manley, and Joseph Finnegan of the New England Division, U.S. Army Corps of Engineers, Mr. Denton Nichols of the New England Power Service Corporation, and Mr. William Wandle of the U.S. Geological Survey for providing agency reports and data which were used in this work.

This research was done as part of a research project on "Risk-Based Assessment of the Safety of Dams", sponsored by the National Science Foundation under Grant No. PFR-7815989. Any opinions, findings, conclusions, or recommendations expressed herein are those of the authors and do not necessarily reflect the views of the NSF.

TABLE OF CONTENTS

LIST OF TABLES

LIST OF FIGURES

CHAPTER 5

APPENDIX F

Chapter 1

INTRODUCTION

Wise dam designers have long recognized the need to provide spillways for the safe passage of flood water through a dam. Banks (1964), in the report of the American Society of Civil Engineers (ASCE) Task Force on Spillway Design Floods, states

> The hydraulic engineer looks upon the spillway as a device whose primary function is to protect the dam from structural failure and incidentally, [sic] protect downstream property against an extraordinary release of stored water in excess of natural flood inflow to the reservoir. The cost of a spillway and accompanying surcharge storage space constitutes insurance, not only for the dam itself, but for downstream life and property. Consequently, the hydraulic engineer designs the spillway to protect the dam and reservoir against failure and to control the rate of release, although he may not intend the dam and reservoir to provide other than incidental flood control for the protection of downstream properties.

Jansen (1980) reports that inadequate or non-existent spillways have caused dam failures from the beginning of recorded history through to modern times. Among the more well known dam breaches caused by an inadequate spillway is the failure in 1889 of the South Fork dam on the Conemaugh River above Johnstown, Pennsylvania. An ASCE investigating committee determined that the spillway as designed should have prevented the dam from being overtopped. Unfortunately, the spillway as built was only half as large as the design specified. The flooding in Johnstown was so severe before the breach occurred that it is hard to determine how much additional damage was due to the breach, but had the spillway been built as designed, at least the dam might not have been destroyed.

Designing spillways requires the exercise of judgment and compromise. A larger spillway will provide greater protection for the dam, but

spillways are not free. Simply building a larger spillway is not always feasible. Again quoting from Banks (1964)

> Engineers responsible for the development of water resource projects recognize that the provision of spillways and surcharge storage capacity for dams of all types constitutes a major problem in planning and design that frequently has profound effect on the economics and physical feasibility of a project. The policies that guide the engineer in making such provision are derived from basic economic, ethical, and political considerations as well as the fundamental technical criteria of hydrology, hydraulics and structural design. As a result, the complex spillway design flood problem is resolved largely by experience and judgment rather than by rigid technical procedure.

The economic tradeoff most fundamentally related to spillway design, between the cost of the spillway and the cost and probability of a failure, has been implicitly recognized through establishment of design standards, such as those shown in Table 1.1 (from Snyder, 1964). (A spillway design flood is the largest flood for which a spillway is designed.) This tradeoff, however, is rarely made explicit or quantified, making accurate comparison between the resources spent on dam safety and the resources spent elsewhere difficult.

This work develops and applies a model through which some of the economic tradeoffs in spillway design, and in reservoir operation as it relates to dam safety, may be examined. The model represents a catchment, dam, river channel below the dam, and damage site. Similar models have been used extensively for flood damage estimation. This model differs from commonly used models in that the possibility of a dam failure is explicitly recognized. The probability of overtopping failure and the damage due explicitly to the failure are computed.

The primary purpose of this work is to examine the effects of spillway size and reservoir operation on the potential for flood damage downstream

Table 1.1

Classification of Dams

(from Snyder, 1964)

Category	Impoundment Danger Potential		Failure Damage[a] Potential		Spillway Design Flood
	Storage, in acre-feet	Height, in feet	Loss of life	Damage	
(1)	(2)	(3)	(4)	(5)	(6)
Major;failure cannot be tolerated	>50,000	>60	Considerable	Excessive or as matter of policy	Probable maximum; most severe flood considered reasonably possible on the basin
Intermediate	1,000 to 50,000	40 to 100	Possible but small	Within financial capability of owner	Standard project; based on most severe storm or meteorological conditions considered reasonably characteristic of the specific region
Minor	<1,000	<50	None	Of same magnitude as cost of dam	Frequency basis; 50-100 yr recurrence interval

[a]Based on consideration of height of dam above tailwater, storage volume, and length of damage reach, present and future potential population and economic development of the flood plain.

from a dam, with special emphasis on the damage that may be caused by dam failures.

Section 1.1 describes the motivation for this work, Section 1.2 reviews some background literature, and Section 1.3 discusses the general features of this work.

1.1 Motivation

Attention has recently been focused on spillways at existing dams because of the National Dam Inspection Program. The National Dam Inspection Act, PL 92-367 (see Appendix E), passed in August 1972, authorized the U.S. Army Corps of Engineers (Corps) to conduct an inventory of all non-Federal dams which either impounded at least fifty acre-feet of water or were more than twenty-five feet high, inspect those dams which were judged to pose a threat to human life or property, and establish a program to regulate dam safety in the future. The inventory was completed in 1975. Approximately 55,000 dams were identified, approximately 9,000 of which were selected for the inspection program. The inspection program was funded in 1977, in the wake of some spectacular dam failures, notably those of the Teton Dam in Idaho and the Kelly Barnes Lake Dam in Georgia. The Corps of Engineers recommended that the states be responsible for continuing dam safety inspections.

The inspection program was divided into two parts, called Phase I and Phase II. Phase I was designed to "identify expeditiously those dams which may pose hazards to human life or property" (Corps, 1975). The Corps was responsible for Phase I inspections. Phase II studies are required "when the results of the Phase I investigation indicate the need for additional in-depth studies, investigation, or analyses" (Corps,

1975). The owners of the dams were responsible for Phase II inspections. Corps (1975) describes guidelines for the inspection program.

Phase I investigations consist of an examination of the easily available engineering data, a visual inspection, and a simple evaluation of spillway adequacy. Phase II investigations consist of all additional work needed to design repairs or modifications to the dam, including more detailed hydrologic and hydraulic analyses.

Figure 1.1 and Table 1.2 show the size and hazard classifications used in the national inspection program. Table 1.3 shows the recommended spillway design flood as a function of the size and hazard classifications of a dam.

Approximately 8,800 dams were inspected as part of the Phase I inspection program. 2,917 of these dams were found to be unsafe. A summary published after the first year of the program, during which 1,793 dams were inspected, showed that approximately 90 percent of the deficiencies were due to inadequate spillways (Corps, 1978a). (Similar statistics about the types of deficiencies found were not available for the complete program.) Assuming the 90 percent rate held for the rest of the program, 2,625 of the 2,917 unsafe dams had deficient spillways. If the average cost were $200,000 each, the bill for repairing these spillways would be $525 million dollars. Engineering News Record (1980) cited a preliminary draft of a report by the Federal Emergency Management Agency which suggested that the total repair bill for the dams identified in the Phase I inspections could range from a low of $1.5 billion to a high of $7.5 billion.

Wise use of resources applied to this problem requires determination of how much it is really worth spending to enlarge spillways and where

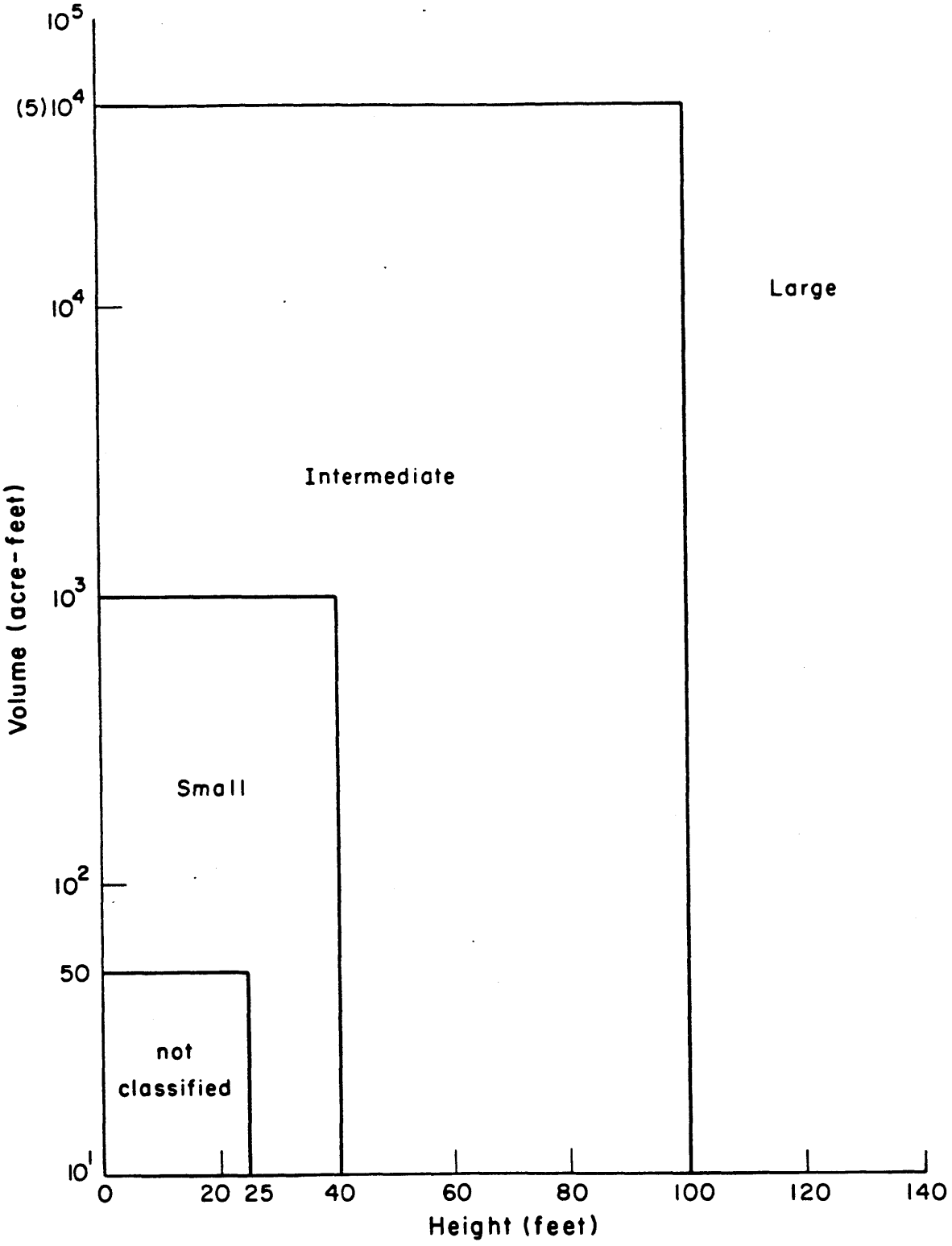

Figure 1.1: Size Classification of Dams used in The National Dam Inspection Program

Table 1.2

Hazard Potential Classification Used in the National Dam Safety Inspection Program

(from Corps, 1975)

Category	Loss of Life (Extent of Development)	Economic Loss (Extent of Development)
Low	None expected (No permanent structures for human habitation)	Minimal (Undeveloped to occasional structures or agriculture)
Significant	Few (No urban developments and no more than a small number of inhabitable structures)	Appreciable (Notable agriculture, industry or structures)
High	More than few	Excessive (Extensive community, industry or agriculture)

Table 1.3

Recommended Spillway Design Floods Used in the
National Dam Safety Inspection Program

(from Corps, 1975)

Hazard	Size	*Spillway Design Flood (SDF)
Low	Small	50 to 100-yr freq
	Intermediate	100-yr to 1/2 PMF
	Large	1/2 PMF to PMF
Significant	Small	100-yr to 1/2 PMF
	Intermediate	1/2 PMF to PMF
	Large	PMF
High	Small	1/2 PMF to PMF
	Intermediate	PMF
	Large	PMF

*The recommended design floods in this column represent the magnitude of the spillway design flood (SDF), which is intended to represent the largest flood that need be considered in the evaluation of a given project, regardless of whether a spillway is provided; i.e., a given project should be capable of safely passing the appropriate SDF. Where a range of SDF is indicated, the magnitude that most closely relates to the involved risk should be selected.

100-yr = 100-Year Exceedence Interval. The flood magnitude expected to be exceeded, on the average, of once in 100 years. It may also be expressed as an exceedence frequency with a one-percent chance of being exceeded in any given year.

PMF = Probable Maximum Flood. The flood that may be expected from the most severe combination of critical meteorologic and hydrologic conditions that are reasonably possible in the region. The PMF is derived from probable maximum precipitation (PMP), which information is generally available from the National Weather Service, NOAA. Most Federal agencies apply reduction factors to the PMP when appropriate. Reductions may be applied because rainfall isohyetals are unlikely to conform to the exact shape of the drainage basin and/or the storm is not likely to center exactly over the drainage basin. In some cases local topography will cause changes from the generalized PMP values, therefore, it may be advisable to contact Federal construction agencies to obtain the prevailing practice in specific areas.

the spending should begin. The spillways identified as deficient may not all be worth fixing, and they can not all be fixed at once. The methods of current practice, and the methods used in the National Dam Safety Inspection Program, cannot answer these questions because the economics, ethics, and politics which must guide spillway design are buried in the collective judgment of dam designers, as represented by guidelines such as those given in Tables 1.1 or 1.3.

Analysis of spillway design must deal with uncertain events because no one can accurately predict the floods which will occur in the future. The probability distribution of future floods can be predicted, but even that prediction is subject to large errors, errors which increase as the flood size gets larger and frequency gets smaller.

Methods for dealing with uncertain events, when the risk of damage is to be explicitly weighed against the cost of preventing damage, are frequently called risk analysis. The term risk analysis will be used in this work as a generic term applicable to any such method.

Both the Ad Hoc Interagency Committee on Dam Safety of the Federal Coordinating Council for Science, Engineering, and Technology (FCCSET, 1979) and the Office of Science and Technology Policy Independent Review Panel (OSTP, 1978) call for research in risk analysis applied to dams. OSTP (1978), in reference to Federally owned or regulated dams, said

> The evaluation of existing structures can also benefit from the use of a formal risk-based methodology. The 2,078 Federally-owned dams and about 5,000 other dams in the US on Federal land or subject to Federal licensing vary greatly in the degree of hazard that they pose to those downstream. Moreover, any Federal dam safety program has to face the facts of limited budgets and limited manpower. There may be neither sufficient funds nor sufficient trained manpower to analyze and correct every high hazard situation simultaneously. If priorities are not set by systematic evaluation, they are set in some other manner, and the public may be exposed unnecessarily to undesirable risk.

While it is unlikely that the need for sound judgment in spillway design can ever be replaced by a technical procedure, explicit evaluation of at least the economics of spillway design may help determine where scarce resources may best be applied.

This work investigates explicit evaluation of the effect of spillway design on the potential for flood damage below a dam, including the damage caused by failures.

1.2 Background and Literature Review

Section 1.2.1 briefly reviews current practice in spillway design. Section 1.2.2 reviews literature dealing with risk analysis applied to spillway design, and Section 1.2.3 reviews some literature dealing with risk analysis for dam safety in areas other than spillway design.

The literature on economic analysis of public projects, both with and without uncertainty, is extensive and will not be reviewed here. Some sources of general information and further references are Arrow and Lind (1970), Maass et. al. (1962), and James and Lee (1971).

1.2.1 Current Practice for Spillway Design

A series of four papers presented by the ASCE Task Force on Spillway Design Floods in 1964 outlined current practice in spillway design. The first of the four papers, Banks (1964), is an introduction to the other three. The other three, Snyder (1964), Koelzer and Bitoun (1964), and Ogrosky (1964) describe spillway design for large dams when there is adequate hydrologic data, large dams when there is limited hydrologic data, and small dams when there is limited hydrologic data.

The two passages from Banks (1964) quoted in the introduction to this chapter set forth the general philosophy of the task force recommendations. The task force suggested that dams could be divided into the following three categories:

Class 1: dams where failure can not be tolerated

Class 2: dams where failure would result in serious economic loss

Class 3: dams where failure would result in minor damage

The economic, ethical, and political considerations of spillway design are reflected in guidelines for spillway design floods such as those suggested by Snyder (1964) for large dams (Table 1.1), by Ogrosky (1964) for small dams (Table 1.4), or by Corps (1975) for the National Dam Safety Inspection program (Table 1.3). These three sets of guidelines are similar to each other. They differ in detail because they are based on judgment and intuition.

Snyder (1964) states that there are really only two categories of dams; those where failure can not be tolerated and those where failure can be tolerated. The guidelines given in Table 1.1 for those dams where failure can be tolerated are meant by Snyder only to illustrate the factors that should be considered.

Spillway design revolves around determination of a spillway design flood, and spillway design floods revolve around the probable maximum flood (PMF) and portions thereof.

A spillway design flood is the largest flood for which a spillway is designed, but a spillway design flood alone does not define the spillway requirement. Assumptions about other conditions, especially the initial reservoir stage, are required. For example, when Knightville Dam, on the Westfield River in Massachusetts, was designed, the spillway design

Table 1.4

Recommended Spillway Design Floods for Small Dams
(from Ogrosky, 1964)

Hazard Classification

"Class (a) - Structures located in rural or agricultural areas where failure may damage farm buildings, agricultural land, or township or county roads."

"Class (b) - Structures located in predominantly rural or agricultural areas where failure may damage isolated homes, main highways or minor railroads or cause interruption of use or service of relatively important public utilities."

"Class (c) - Structures located where failure may cause loss of life, serious damage to homes, industrial and commercial buildings, important public utilities, main highways or railroads."

Recommended Design Storms,
from which Design Floods are Developed

Two hydrographs are used in the design of each spillway. One is called the Emergency Spillway Hydrograph and is used to determine the required spillway capacity. The other, called the Freeboard Hydrograph, is used to determine spillway freeboard. Therefore, minimum rainfall criteria are established for the development of each hydrograph as follows:

Emergency Spillway Hydrograph.

P for Class (a) structure = P100
P for Class (b) structure = P100 + .12 (PMP - P100)
P for Class (c) structure = P100 + .26 (PMP - P100)

Freeboard Hydrograph

P for Class (a) structure = P100 + .12 (PMP - P100)
P for Class (b) structure = P100 + .40 (PMP - P100)
P for Class (c) structure = PMP

in which P denotes 6-hr design rainfall, P100 refers to 6-hr, 100-yr precipitation, and PMP represents 6-hr probable maximum precipitation.

flood had a peak of 113,200 cfs and a volume of 134,000 af. The reservoir was assumed to be full at the beginning of the flood, and the outlet works were assumed to be closed (Corps, 1978). When Knightville dam was reevaluated 35 years later, the spillway design flood was enlarged to have a peak of 145,000 cfs and a volume of 152,000 af, but the reservoir was assumed to be only half full at the beginning of the flood and the outlet works were assumed to be open. The spillway was adequate for both situations.

Estimation of the PMP and PMF is far from an exact procedure. The definitions of the terms are not clear, several methods of computation can be used, and a variety of assumptions are needed for each of the several methods.

Weather Bureau (1956) defined the PMP as

> The probable maximum precipitation represents the critical depth-duration-area rainfall relations for a particular area during various seasons of the year that would result if conditions during an actual storm in the region were increased to represent the most critical meteorological conditions that are considered probable of occurrence.

Weather Bureau (1978) stated

> PMP is defined as "the theoretically greatest depth of precipitation for a given duration that is physically possible over a particular drainage area at a certain time of year," (American Meteorological Society 1959). In consideration of our limited knowledge of the complicated processes and interrelationships in storms, PMP values are identified as estimates.
>
> Another definition of PMP more operational in concept is "the steps followed by hydrometeorologists in arriving at the answers supplied to engineers for hydrological design purposes" (WMO 1973). This definition leads to answers deemed adequate by competent meteorologists and engineers and judged as meeting the requirements of a design criterion.

Viessman et al. (1977) define the PMP as the "reasonable maximization of the meteorological factors that operate to produce a maximum storm."

What is now called the probable maximum precipitation used to be called the maximum possible precipitation. According to Weather Bureau (1960),

> At one time the concept of probable maximum precipitation (P.M.P.) was expressed in terms of the words 'maximum possible.' However, in considering the limitations of data and understanding implicit in an estimate of 'maximum possible' precipitation, it seemed that there was sufficient uncertainty to substitute for the expression 'maximum possible' the more realistic one 'probable maximum.' This was done with no intention or implication of making the values any different. 'Probable maximum' simply seems to be more descriptive and more realistic.

The Weather Bureau (1956, 1960, 1978), among others, estimates the PMP through a combination of examining data for severe storms, transposing severe storms to meteorologically similar areas, and estimating the maximum amount of moisture which could be transported into the area during a storm. The maximum observed rainfall at a given location defines a lower bound for the PMP at that location (Weather Bureau, 1960).

Hershfield (1961) investigated a statistical method for transposing maximum rainfall records between stations, providing a statistical estimate of the PMP. He defined the PMP as "the largest rainfall (precipitation) that a station is ever likely to experience for a particular duration." Hershfield computed the standardized deviate (number of standard deviations away from the mean) for the largest storm at each of 2,645 24-hour weather stations. All the stations had at least ten years of record. The mean and variance at each station were corrected for sample size and outliers.

The largest standard deviate was fifteen, and four deviates fell between thirteen and fifteen. Some unofficial observations were as high as twenty standard deviations from the mean. Hershfield used the mean plus fifteen standard deviations as his estimate of the PMP and compared

his results to those of Weather Bureau (1956). The two methods gave similar results near the Gulf of Mexico, but the results diverged rapidly elsewhere, Hershfield's estimate being half of that from Weather Bureau (1956) in the northern and western parts of the United States.

Hershfield did not try to estimate the probability of occurence associated with the PMF. Table 1.5 shows the return periods (reciprocal of exceedance probability) which could be inferred from the log Pearson type III probability distribution for different skewnesses. The values in Table 1.5 were derived by extrapolating curves on log-normal probability paper. Values out to a return period of 10^4 years are available in Water Resources Council (1977).

Hershfield (1965) extended Hershfield (1961) by estimating the standard deviates which enveloped the maximum rainfall data as a function of the rainfall duration.

Once the PMP is estimated, the PMF can be estimated. The PMF is usually computed as a flood caused by the PMP. The flood caused by the PMP is affected by the distribution in time and space of the rainfall and by the condition of the watershed when the storm begins. Thus, even after the PMP is estimated, several assumptions are needed to compute the PMF. These assumptions are crucial. The same storm can produce vastly different floods depending on whether it occurs when the foliage is full and the ground fairly dry or when there is no foliage and the ground is frozen and covered by a dense snowpack near its melting point. Snyder (1964), Koelzer and Bitoun (1964), Ogrosky (1964), Bureau of Reclamation (1973), Viessman et. al. (1977), Linsley et. al. (1975), and Chow (1964), among others, describe estimation procedures for the PMF.

Table 1.5

Return Periods Associated with Standard Deviates

using a Log-Pearson type III Distributon

Skewness

		1.0	2.0	5.0
standard deviations from mean	12	$10^{8.5}$	$10^{5.5}$	$10^{3.5}$
	15	10^{11}	10^{6}	$10^{4.1}$

Snyder (1964) defines the PMF as "the most severe flood or sequence of floods considered reasonably possible in the project basin." Koelzer and Bitoun (1964) define the PMF as

> the estimated flood that would result if all factors that contribute to the generation of flood were to reach their most critical values that could occur concurrently. The probable maximum flood is the estimate of the boundary between possible floods and impossible floods. The objective, therefore, is to obtain a flood that has a chance of occurence of zero or a return period of infinity.

Snyder's definition requires an assessment of what is reasonably possible, and Koelzer and Bitoun's definition requires an assessment of what is possible. Estimation of the PMP also required an assessment of either what is reasonable or what is possible. However, as suggested in the passage from Weather Bureau (1960) quoted earlier, the definition does not always alter the estimation technique. These definitions are somewhat resolved by appealing to the standard practice of major dam building agencies and consultants (as was done in the WMO (1973) definition of the PMP referenced by Weather Bureau, 1978), but they still illustrate the lack of a consensus about the meaning of the PMF.

When building large dams, especially those above heavily populated areas, it is easy to agree, without the need for formal analysis or precise agreement about definition of the PMF, that extreme conservatism in spillway design is justified. Even if the spillway is built so large that extreme floods pass through the reservoir nearly unattenuated, causing enormous downstream damage, at least that damage can not be blamed on the dam, and the dam will continue to provide its services, such as water supply or power production, if the dam does not fail.

It also seems reasonable to allow smaller spillways on dams for

which the consequences of failure are not so great. The guidelines of standard practice recognize that economic and policy considerations should be used to design a spillway when failure can be tolerated.

However, the standard practice guidelines raise two questions.

First, is there such a thing as a dam where failure can not be tolerated? If there is, perhaps the dam should be made safer by doubling, or even tripling, the spillway sizes and embankment sections determined by standard design practice. But even then there would not be an absolute assurance that the dam would not fail, and the cost would quickly become so high that tradeoffs between cost and safety would have to be made. Also, as the structure gets larger, the possibility of construction related deaths increase. Experience shows that failure does occur, even when it can not be tolerated. Thus, safety is always weighed against cost, whether implicitly or explicitly. The current practice spillway design standards define this tradeoff implicitly.

This leads to the second question; should the tradeoff between cost and safety in spillway design be evaluated implicitly, as in the current practice guidelines, or should that tradeoff be evaluated explicitly, as in a risk analysis? Risk analysis of flood control measures is well established (see for example, James and Lee, 1971 or Weiss and Midgley, 1978). If risk analysis is to be used for spillway design, the probability of failure and the damages caused by failures must be estimated. This has not normally been done in practice.

This review has thus far concentrated on United States practice. The Working Party on Floods and Reservoir Safety of the Institution of Civil Engineers (ICE) (1978) suggested the guidelines shown in Table 1.6. (The ICE is the British counterpart of the ASCE.)

Table 1.6

Reservoir Flood and Wave Standards by Dam Category
(from Institution of Civil Engineers, 1978)

Category	Initial Reservoir Condition	Dam Design Flood Inflow			Concurrent Wind Speed and Minimum Wave Surcharge Allowance
		General Standard	Minimum Standard if Rare Overtopping is Tolerable	Alternative Standard if Economic Study is Warranted	
A. Reservoirs where a breach will endanger lives in a community	Spilling long term average daily inflow	Probable Maximum flood (PMF)	0.5 PMF or 10,000 year flood (take larger)	Not Applicable	Winter: maximum hourly wind once in 10 years (Fig. 4) Summer: average annual maximum hourly wind (Fig. 3) Wave surcharge allowance not less than 0.6 m.
B. Reservoirs where a break (i) may endanger lives not in a community, (ii) will result in extensive damage	Just full (i.e., no spill)	0.5 PMF or 10,000 year flood (take larger)	0.3 PMF or 1000 year flood (take larger)	Flood with probability that minimizes spillway plus damage costs (Fig. 1); inflow not to be less than minimum standard but may exceed general standard.	
C. Reservoirs where a breach will pose negligible risk to life and cause limited damage.	Just full (i.e., no spill)	0.3 PMF or 1000 year flood (take larger)	0.2 PMF or 150 year flood (take larger)		Average annual maximum hourly wind (Fig.3) Wave surcharge allowance not less than 0.4 m.
D. Special cases where no loss of life can be foreseen as a result of a breach and very limited additional flood damage will be caused.	Spilling long term average daily inflow.	0.2 PMF or 150 year flood.	Not applicable.	Not applicable.	Average annual maximum hourly wind (Fig.3) Wave surcharge allowance not less than 0.3 m.

Notes: Where reservoir control procedure requires, and discharge capacities permit, operation at or below specified levels defined throughout the year, these may be adopted providing they are specified in the certificates or reports for the dam.
Where a proportion of PMF is specified it is intended that the PMF hydrograph should be computed and then all ordinates be multiplied by 0.5, 0.3 or 0.2 as indicated.

These guidelines differ from those discussed so far in several respects. First, ICE (1978) distinguishes between loss in a community and other life loss. The idea of a community can not be defined easily, but ICE (1978) thought that communities of various types, including ongoing organized camps, could be distinguished from isolated houses or occasional campers. Second, they include specific recommendations for initial reservoir stage and wave surcharge allowance when routing the spillway design flood. Third, they distinguish between dams which can and dams which can not withstand some overtopping. Note that these guidelines suggest that a 10,000 year return period can be estimated.

When economic study is warranted, ICE (1978) suggests that the procedure set forth in ASCE (1973) should be used. ASCE (1973) is reviewed in Section 1.2.2.

1.2.2 Risk Analysis in Spillway Design

The report of the ASCE Task Committee on the Reevaluation of the Adequacy of Spillways of Existing in 1973 was the first major publication to suggest that risk analysis should be used to evaluate spillway design. ASCE (1973) suggested that spillway adequacy should be measured by explicit evaluation of spillway performance under the complete range of possible floods, rather than through guidelines for spillway design floods such as those shown in Tables 1.1, 1.3, and 1.4. The Task Committee presented a case study in which several spillway designs for a hypothetical dam were analyzed. A curve of total cost as a function of spillway size was developed and used to find the minimum cost spillway. The total cost was measured as the sum of the expected present value of flood damage

plus the construction cost. The Task Committee did recognize that there may be non-economic reasons for selecting other than the minimum cost spillway, but suggested that these reasons should be explicitly revealed.

ASCE (1973) was controversial because it assigned a return period to the PMF and advocated assignment of a finite monetary value to loss of a human life. The discussion following publication of ASCE (1973) indicated substantial resistance, but also some sympathy, in the civil engineering profession to both of these concepts.

A return period was assigned to the PMF as a method of establishing a continuous probability distribution of flood sizes out to the largest flood for which spillways are ever designed. The Task Committee chose 10^4 years as a conservatively low return period. That is, 10^4 years was thought to be a lower bound on the true return period. Using 10^4 years would thus overestimate the flood damage costs. However, the breach discharges used by the Task Committee were unrealistically low, counteracting the effect of the low return period. The net effect from these two items is hard to judge.

The Task Committee claimed that current practice in spillway evaluation (see Section 1.2.1) implicitly placed an infinite value on human life. This is not so. Current practice in spillway design claims to explicitly place an infinite value on human life, but, in fact, places an unknown finite value on human life. There is a finite probability of failure or misuse leading to a human death for every design. Even the construction of spillways is not without fatal accidents. This potential for death means that every constructed facility, including spillways, places an implicit finite value on human life. ASCE (1973) suggested

that explicit recognition of the value placed on human lives could promote wiser use of our national resources.

The Task Committee did not claim to have presented a fully developed procedure. They identified the need for further research in the following four areas:

1) monetary values for human life and suffering

2) probabilities of extreme precipitation and floods

3) the manner and speed with which dams fail from flood surcharge and overtopping

and 4) the hydraulic characteristics and consequences of failure flood waves.

Hawkins (1974), in his discussion of ASCE (1973), suggested that the sensitivity to the wide array of assumptions required in the procedure proposed by ASCE (1973) should be examined closely before the procedure could be evaluated properly.

Pape (1980) expanded considerably on the foundation laid by the work of ASCE (1973). Pape discussed in detail the objectives and methods of risk analysis for dam safety engineering and proposed a method of analysis in which both monetary damage and life loss were considered, but not combined into a single measure of damage. This method was demonstrated in a series of case studies based on the dam and damage site used in ASCE (1973). It allows prevention of life loss to be considered as a separate objective and is particularly useful when comparing alternatives such as larger spillways and downstream warning systems. In the end, however, any decision will implicitly assign a value to human life. A single measure of damage can easily be computed explicitly by assigning a monetary value to a human life.

Pape (1980) also presented a good discussion of the available data on dam failures and proposed a model of overtopping failure probability as a function of depth and time of overtopping. The discussion of failure data includes an analysis of the variation of overtopping and non-overtopping failure rates with age. These results show that both overtopping and non-overtopping failure rates are highest during the first few years after construction. This result was not expected for overtopping failures. The parameters of the probabilistic overtopping model can not be estimated accurately with current knowledge of embankment erosion, but they can be estimated approximately from a combination of expert judgment and the limited data on dams which have survived some overtopping.

Buehler (1973, 1974, 1975, and 1976) has been one of the most persistent advocates of risk analysis for spillway design and of assigning an explicit value of human life in that risk analysis.

Buehler (1973) presents a brief discussion of the ASCE (1973) Task Committee report, focusing on the need for further research to develop the methods proposed therein. Buehler was a member of that committee.

Buehler (1974) reviewed ASCE (1973), presented a simplified version of the case study in ASCE (1973), and discussed a situation where enlarging the spillway on a low dam could increase the expected total flood damage.

Buehler (1975) discussed the imbalance in public expenditure among various programs which affect human safety, once again reviewed the ASCE (1973) report, and discussed the research needed to implement the recommendations of that report.

Buehler (1976) presented a simplified version of the procedure recommended by ASCE (1973), through which economical spillway sizes

could be chosen with a few hours work. This method required estimates of only the damage caused by a dam failure with a full reservoir and the cost of building a spillway large enough to safely pass the PMF. The results presented by Buehler (1976) are probably not accurate enough to use for designing a spillway. However, with some refinement, the method could be useful for assessment of spillway adequacy at existing dams and preliminary design of spillways for new dams.

1.2.3 Risk Analysis for Dam Safety Assessment

ASCE (1973) was the first paper (to the author's knowledge) to advocate the use of risk analysis for dam safety assessment, though ASCE (1973) was restricted to the reevaluation of spillways at existing dams. Since then several authors have suggested the use of risk analysis for other areas (besides spillway evaluation) of dam safety assessment, though this literature is not yet very extensive.

Vanmarcke (1974) proposed a method through which the total and relative effectiveness of the various components of inspection programs could be measured. The method was designed to facilitate the selection of effective inspection procedures.

Baecher, et al. (1979, 1980) examined data on dam failures and presented some methods for economic analysis of damage from dam failures. They suggested that failure costs should be included in the overall economic analysis of a dam and that, in the absence of further information, an average annual failure rate of 10^{-4} be assumed.

Vanmarcke (1979) presented two approaches to modeling the risks from dam failure. Either approach could be used to help design a balanced

safety program for a given dam or determine how much it is worth spending for dam safety. One approach used historical data about failure damages and traced the separate components of those damages. The other approach used a Markov model to forecast the damages caused by extreme events.

Yen and Tang (1979) and Shah and Franzini (1979) both proposed the use of risk analysis for dam safety assessment. Yen and Tang briefly reviewed some failure data and outlined some aspects of the hydraulic and hydrologic aspects of dam safety. Shah and Franzini suggested a general formulation for probabilistic evaluation of dam safety using the total probability theorem.

Paté (1981) studied the sensitivity of the benefit-cost ratio, with the risk of failure included, to variation in failure probability and value placed on a human life. The results, as could be expected, depended heavily on the characteristics of the downstream development. The failure costs weighed heavily in the economic analysis for dams above highly populated areas, and not so heavily for dams in sparsely populated areas.

Bohnenblust and Vanmarcke (1982) developed a linear programming procedure through which dams may be ranked in order of the net benefits which can be gained by modifying or repairing the dams.

1.3 Method

The literature reviewed in Section 1.2.3 presents a variety of methods for using information about the risk of damage caused by dam failure, but does not suggest methods whereby that risk information can be developed. The literature reviewed in Section 1.2.2 presents some methods for developing that risk information for spillway design, but, as is expected of early efforts, left much work to be done. ASCE (1973)

identified four specific technical issues which needed further work and the discussion following publication of ASCE (1973) identified further areas of concern. Pape (1980) presented a probabilistic overtopping failure model and an economic analysis procedure, both of which provide useful insights into spillway evaluation but are too far beyond the state of current practice to be immediately useful.

This work is intended to examine closely 1) the sensitivity of the type of risk analysis proposed by ASCE (1973) to several of the more uncertain elements in that analysis and 2) the change in downstream flood risk and failure probabilities caused by changes in the spillway design and reservoir operation. Two possible approaches to this task are 1) examination of historical data and 2) computation from a model of the system. The available data are adequate to gain a tentative grasp of average flood risks and failure probabilities for broad classes of dams, but totally inadequate to say anything about a given dam, much less to predict quantitatively what will happen when anything is changed. Thus we turn, as did ASCE (1973), to a derivation of the flood risk and failure probability from a mathematical model of the system.

The system we will consider consists of a catchment above a dam, the dam and reservoir, the channel downstream of the dam, and a damage site downstream of the dam. The effects of tributaries or other additions to flow between the dam and damage sites will be neglected.

The damages will be represented by the expected value (mean) of the monetary damage. The variance of damage is also computed, and could be used to compute an uncertainty cost, as suggested by Thomas (in Maass, 1962). Computation of this uncertainty cost is an option in the computer

model developed for this work. Or a utility function which represents the appropriate aversion to risk could be used (see Keeney and Raiffa, 1976). Baecher et al. (1980) discuss this issue and argue that the simple expected value is an appropriate measure of the economic risk from dam failures. They suggest that utility theory does not offer sufficient advantage to justify the burden of developing the necessary utility functions. They further suggest that from a national viewpoint, the risks are sufficiently distributed through federal disaster relief and other insurance programs that the uncertainty costs may be neglected. Regional and local viewpoints may, of course, differ, but dealing with such topics is outside the scope of this work.

When a dam fails there is potential for human death. There is also potential for human death during the construction of the dam (an average of 5.5 deaths per dam in Tennessee Valley Authority experience. See Buehler, 1975), while persons are swimming in or boating on the reservoir, and while the river is flooding through natural causes.

The explicit recognition of the possibility of human death due to malfunction of public or quasi-public facilities is a controversial topic, and designers of dams have been reluctant to recognize the possibility of human deaths caused by dams. Recall the classification of dams proposed by Banks (1964) which was cited in Section 1.2.1. Class 1 was dams where failure "can not be tolerated."

Incorporating an explicit value for human life when evaluating public facilities is itself a large issue, beyond the scope of this work. This issue is as much social, political, and emotional as technical. As such, there is little to be gained and possibly much to lose by including the issue here. The intent of this work is to explore the influence of

explicit recognition of the possibility of failure on the flood damage potential below a dam, and, in particular, to explore how spillway design and reservoir operation influence that damage potential. The value of life issue, while it must be confronted as part of a total program for risk analysis, could easily steal attention from the results of this work.

Though it is recognized that the normal outlet works and emergency spillway are normally designed for different purposes, the outlet works to serve the day to day functions of the dam and the spillway to protect the dam structure during floods, they are treated equally, as conduits for passage of water through the dam, in this work. The downstream damage sites do not care if the water is coming through outlet works, through the spillway, over the top of the dam, or even, perhaps, through a breach in the dam. (The damage from a dam breach wave may be more severe than from a natural flood wave of equal size, because of greater dynamic stresses or lesser advance warning, but there is little data from which conclusions about this effect may be drawn.)

This work develops a model of the catchment, dam and reservoir, stream channel, and damage site which accounts for the possibility of dam failure. Both overtopping and non-overtopping failures are included. In addition to estimating the total flood damage, the portions of the total which can be attributed directly to failures are estimated.

There is no fundamental difference in philosophy between the model developed here and the procedures recommended by ASCE (1973). Also, the individual elements of the model are not new developments. This is, however, the first time (to the author's knowledge) that they have been

combined in a comprehensive flood damage model, which includes dam failures, in such a way that the effects of parameter variation can be studied easily. This is also the first time that the portions of the total damage which can be attributed to failures has been estimated.

The model is solved analytically, rather than numerically, whenever it is possible to do so without sacrificing features of the model considered crucial to this work. This is done primarily to ease the computational burden of the extensive parameter variation studies presented in Chapters 4 and 5. Chapter 2 and Appendix B describe the development of the model.

Chapter 3 describes the physical characteristics of and parameter estimation for the four dams used in the parameter variation studies presented in chapter 4 and 5.

Several of the model parameters are difficult to estimate. Some are difficult to estimate because the process being modeled is not well known, and some are difficult because the process was not well modeled (where increasing the sophistication of the individual element would have made the overall model unwieldy). Chapter 4 examines the sensitivity of the results to variations in these parameters.

Chapter 5 examines the changes in damage potential caused by changes in the spillway size and reservoir operation. These results show that total damage can increase, decrease, or pass through a minimum as the spillway size is increased. Reservoir operation is represented by the initial reservoir stage. Decreased reservoir stages always decrease damage, but the relative reduction varies with spillway size.

Chapter 6 discusses the conclusions which may be drawn from this work.

Several areas of interest are not pursued in this work. The economic analyses are incomplete. Neither the value of the dam structure nor the lost benefits from operation of the dam are estimated. The construction costs of different spillways and changes in benefits due to reservoir level changes are neglected. The minimum total cost spillway is not computed. What is computed are the damage potential downstream of the dam and the probability of failure.

The potential differences between damage functions appropriate for natural flood waves and damage functions for dam breach waves were not examined. Two damage functions, one for breach flood waves and one for natural flood waves, were incorporated in the model, primarily for future use, but the effect on the results of using two different damage functions was not investigated here.

The influence of warning systems and other non-structural flood control measures was not investigated, except as they may be implicitly incorporated into the variations of the damage function parameters. In real situations these may be good alternatives to modifying a dam and should be investigated. The literature on both structural and non-structural flood damage mitigation is extensive and will not be discussed here.

Current practice guidelines for spillway design have been developed through years of efforts by a variety of persons involved with and concerned about dam design. They embody a substantial amount of both earnest deliberation and successful practice, and thus should not be discarded lightly. In fact, there should be no presumption that they will ever be discarded. But risk analysis holds some promise if, as is the case for any tool, it is developed carefully and used wisely. Thus, it too should not be discarded lightly, before the procedures for its use

have been thoroughly investigated and its potential usefulness thoroughly examined. Even if risk analysis never replaces the methods of current practice, it may help illuminate the implications of current practice guidelines and thus aid in their further development; or risk analysis may develop as a tool to be used in conjunction with the methods of current practice. This work investigates the development of one important piece of risk analysis applied to spillway design.

CHAPTER 2

MODEL DEVELOPMENT

2.1 INTRODUCTION

Chapter 2 describes a non-dimensional mathematical model of a catchment, reservoir, river channel, and damage site, which can be used to predict the probability distribution of flood damages downstream from a dam. A deterministic model which computes damages caused by a flood is developed first. Then the deterministic model and the stochastic properties of its parameters are used to derive the probability distribution of damages.

The deterministic model routes reservoir inflow from the catchment through the reservoir, routes the reservoir discharge, part of which may be from a dam breach, through the river channel, and finally computes the damages caused by the flood in the river channel. Sections 2.2 and 2.3 describe the flood routing models, and Section 2.4 describes the damage model.

The mean and variance of flood damage are then derived using the deterministic model and the probability distributions of the reservoir inflow flood, the initial reservoir stage, and the stage at which the dam is assumed to fail by overtopping. Section 2.5 describes the stochastic variables, and Section 2.6 describes the derivation of the probability distribution. Table 2.3, shown at the end of this chapter, lists all of the model parameters.

Appendix B presents all of the mathematical development of this model.

Three types of events which may produce damaging floods downstream of the dam are modeled. The first is a reservoir inflow flood, such as that caused by rainfall or snowmelt, which passes through the dam without causing a breach (Successful Passage flood). The second is a dam breach during a reservoir inflow flood (Overtopping Failure), usually caused by external erosion as the reservoir stage nears or exceeds the crest of the dam. The stage at which the dam fails is a model parameter for Overtopping Failure. The third is a dam breach during times of normal river flow (Non-Overtopping Failure), usually caused by problems such as earthquakes or excessive seepage. Examples of events which cause floods, but are not described in this model, are landslides into the reservoir and floods generated by an upstream dam breach.

The names of these three types of floods are capitalized here and throughout this work to remind the reader that these are specific classes of events which have been defined for use in this work.

For Successful Passage floods, reservoir inflow flood size and initial reservoir stage are modeled as stochastic variables. For Overtopping Failures, a third stochastic variable, the stage at which the dam fails, is added. For Non-overtopping Failure, reservoir stage is modeled as a stochastic variable and the probability of failure is allowed to vary with reservoir stage. Reservoir inflow flood size and initial reservoir stage are commonly modeled as stochastic variables, and methods for modeling their behavior are well established. Much less is known about either the stage at which a dam will fail when overtopped or the probability of Non-Overtopping Failure for a given reservoir stage, and procedures for modeling their behavior are somewhat arbitrary.

Water movement through the the reservoir, dam, river channel, and damage site system may be represented by a variety of models. The appropriate choices depend on the purpose of the model. This model has two purposes. The first purpose is to study the damage variations caused by system property variations. Because the computational burden of these studies can be high, models in which the system properties are represented by a small number of parameters serve this purpose best. Also, for this purpose, models which can be solved explicitly are preferred to models which must be solved numerically, because the computational burden is usually lower for explicit solutions. The second purpose is to compute a probability distribution of damages for a given dam. Models which are as accurate as possible, given budget constraints, serve this purpose best.

Unfortunately, the two purposes conflict. Accuracy often declines as the number of parameters declines, and models which must be solved numerically are usually more accurate than those which may be solved explicitly. The first purpose dominates the second in this work. Thus, approximate models with few parameters and explicit solutions are preferred to more accurate models which must be solved numerically. This preference is constrained by the desire to estimate the model parameters from physical properties of the system, and thus not be dependent on historical data of system behavior. As models become more approximate, the likelihood that historical data will be needed to estimate the parameters increases. It can be difficult to give physical meaning, meaning which is essential in parameter variation studies, to parameters which can be estimated only from historical data. This consideration is most important for the reservoir model.

2.2 FLOOD ROUTING

2.2.1 Review Of Methods

Movement of flood waves through reservoirs and channels has been predicted with methods ranging from gage relations to numerical solution of the dynamic wave equations (see Linsley et al., 1975). Yevdejvich (1964) discusses the general characteristics of several routing methods and provides an extensive bibliography of flood routing literature through 1961. Fread (1981b) also reviews flood routing methods and provides a more recent, though less exhaustive, bibliography. Flood routing is also discussed in most hydraulics and hydrology texts (see, for example, Henderson, 1966, or Linsley et al., 1975). Thus, only a

brief discussion of routing methods will be given here.

Dynamic wave, diffusion analogy, storage, kinematic wave, and gage relation flood routing were considered for use in this model. Storage routing was chosen for both the reservoir and the channel routing as the best compromise between accuracy and ease of use. The rest of Section 2.2.1 briefly describes the routing models which were considered and discusses the reasons for choosing storage routing. Details of the storage routing method used here are given in Sections 2.2.2 and 2.2.3. Section 2.2.4 discusses parameter estimation methods for both reservoir and channel routing.

Numerical solution of the dynamic wave equations, which is the most accurate routing method in common use, may be used for either reservoir or channel routing. The parameters for dynamic wave routing are relatively easy to estimate. Geometry can be estimated from topographic maps, and roughness can be estimated from either extensive field data that has been summarized in hydraulics texts or comparison with other situations with which the modeler is familiar. The parameters of the dynamic wave model represent local information, which is specified for several locations and integrated over the length of the channel as the model is solved. Thus several parameters are needed to represent the overall influence of the channel on the flood wave, making dynamic wave models clumsy to use in parameter variation studies. Also, dynamic wave routing requires more computation than other flood models. The extra expense and time may be small for a single model execution, but would be large for a series of parameter variation studies.

Diffusion analogy flood routing was not developed for use in reservoirs, and no one has examined its suitability for that purpose. For channel routing, diffusion analogy flood routing has two advantages over dynamic wave flood routing for use in parameter variation studies. First, a single parameter, often called the diffusion coefficient, characterizes the influence of the channel on the flood wave. A single value of the coefficient applies to intervals of any length within a channel reach. Thus, the same coefficient is used to route a flood wave from point A to point B and from point A to point C, as long as the river does not change drastically between points B and C. Diffusion coefficients are best estimated from flood records, though a method was presented by Price (1973) for estimating coefficients from channel geometry. Second, the basic equation is well known in several branches of engineering and has been solved explicitly for some boundary conditions. Unfortunately, when the boundary conditions are the reservoir discharge equations that have been developed from storage routing through the reservoir, the diffusion analogy equations can not be solved explicitly.

Storage routing (also called hydrologic routing) can be used for either reservoirs or channels. Storage routing is commonly used for reservoirs, even when more elaborate methods, such as dynamic wave routing, are used for the channel (see Fread, 1982), because storage effects are dominant in most reservoirs, and because the model parameter is well defined by the reservoir geometry and discharge works of the dam. For channels, storage routing has two advantages over dynamic wave flood routing. Like diffusion analogy routing, a single parameter, the storage coefficient, characterizes the influence of the channel on the

flood wave. Like the diffusion coefficient, the storage coefficient is best estimated from flood records, but may be estimated from channel geometry. Unlike the diffusion coefficient, the storage coefficient applies to only one interval length within a channel reach. Thus, different values of the coefficient are needed to route a flood from point A to point B and from point A to point C. Again like diffusion analogy routing, the storage routing equations can be solved explicitly for some boundary conditions. Unlike diffusion analogy routing, the boundary conditions for which the storage routing equations can be solved explicitly include those defined by storage routing through the reservoir.

Kinematic wave routing is not suitable for this work because it does not predict attenuation of the peak discharge, which, except in narrow gorges, is the dominant effect of the river channel on the flood wave.

Gage relations (ratios between stage or discharge at different locations along a channel) are simple and sometimes accurate. The ratios need not be constants and can be developed as functions of several parameters (see Linsley et al.,1975). Gage relations will not be used because they must be estimated from flood records.

Little has been published about the relative accuracy of the various flood routing methods. Jennings and Sauer (1972) compared three storage routing models and Keefer (1976) compared dynamic wave with diffusion analogy routing. Keefer suggested that diffusion analogy routing was a good choice when only the magnitude of the peak flow was needed, the case in this work. Storage routing probably compares

favorably with diffusion analogy routing, when parameters are chosen well. Dooge (1973) shows that storage and diffusion analogy routing can compare favorably in a rectangular channel, when similar parameter estimation methods are used. The reliability of parameter estimation methods which do not use flood records is not well established for either diffusion analogy or storage routing. This problem is discussed further in Section 2.2.4.2.

Thus, of the several flood routing methods available, diffusion analogy and storage routing methods are the most suited for use in this work. Storage routing is a clear choice for the reservoir. Diffusion analogy routing has some advantages over storage routing for the channel, but the ability to solve the storage routing equations explicitly swings the choice.

The channel is treated as a single reach, rather than as several reaches, the usual practice. The works of Dooge (1973) and Sauer (1973) show the feasibility of single reach storage routing, even for long reaches. Treating the channel as a single reach facilitates parameter variation studies by reducing the number of parameters.

2.2.2 Reservoir Routing

The reservoir routing model consists of a mass conservation equation for the reservoir, an upstream boundary condition, a downstream boundary condition, and an initial condition. The upstream boundary condition is the reservoir inflow, which is determined by the hydrology of the catchment. The downstream boundary condition is determined by the discharge works of the dam. The initial condition is the state of

the reservoir at the beginning of the reservoir inflow flood. It may be given in terms of discharge, volume, or stage. Initial conditions in this work will be given in terms of stage because stage is the most commonly recorded measure of reservoir condition.

The reservoir inflow is modeled as a triangular flood hydrograph superimposed on the initial reservoir inflow,as shown in Figure 2.1. Initially, all water entering the reservoir is either discharged to the river channel, R_o, or removed from the reservoir, R_b. R_o is the initial discharge to the river channel. R_b is the reservoir draft not discharged directly to the river channel, such as water supply or irrigation drafts. R_b is assumed to be constant during a reservoir inflow flood.

No real flood looks like that shown in Figure 2.1. However, reservoir outflow can be modeled adequately using a triangular inflow hydrograph because reservoirs damp the effects of inflow hydrograph timing variations. Mathematically, the triangular shape has one advantage and one disadvantage relative to some of the non-linear functions which could have been used. The advantage is that the linear functions which describe the two limbs of the triangle are easy to work with. The disadvantage is that new equations are needed when the slope changes at t_p and t_b.

Discharge from the dam is modeled by the piecewise linear function of volume shown in Figure 2.2. This relation is fairly accurate for reservoirs located in gently rolling to hilly terrain, whose outlet works have fixed geometry. Under those conditions both discharge and volume vary with approximately the three halves power of reservoir

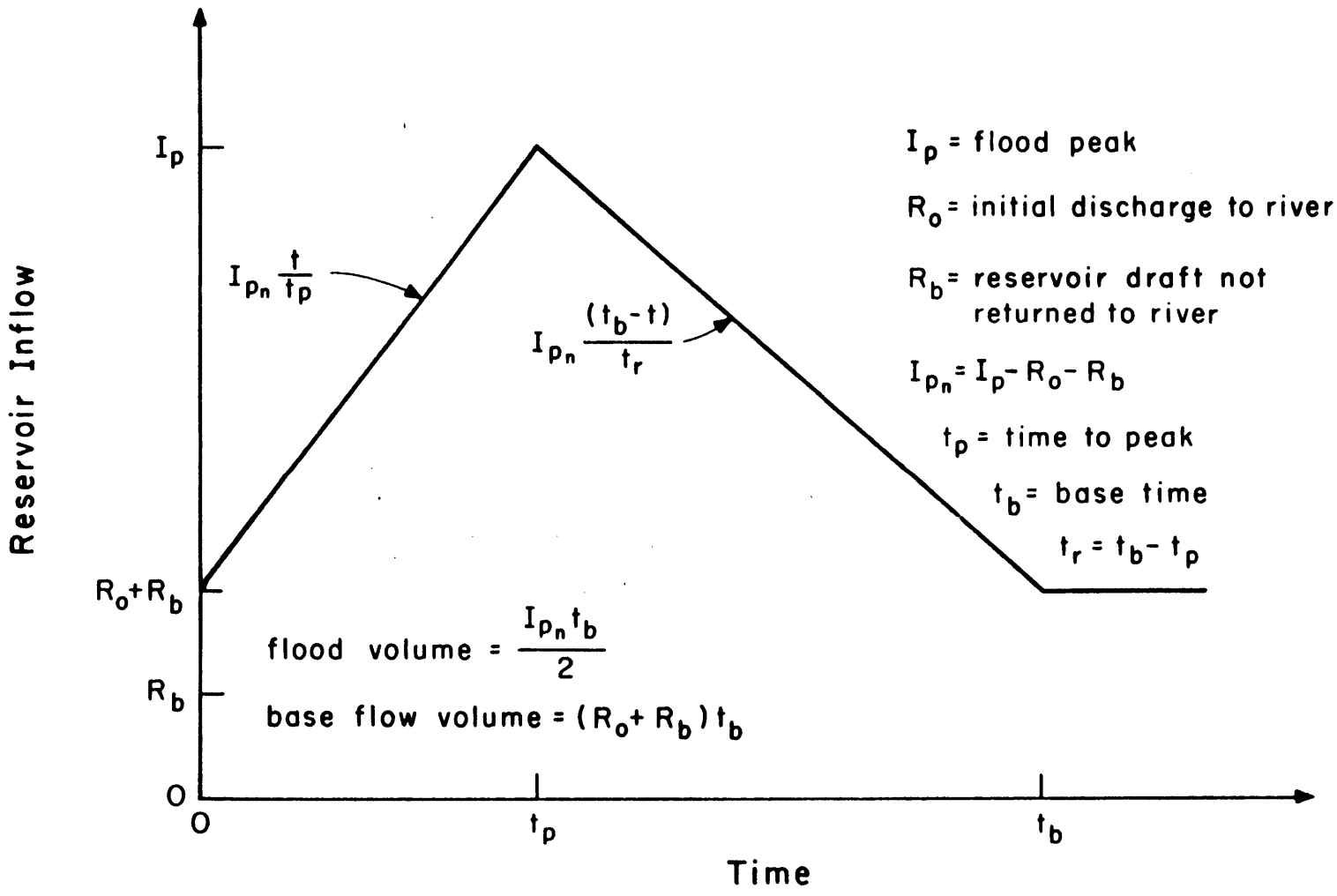

Figure 2.1: Reservoir Inflow Hydrograph

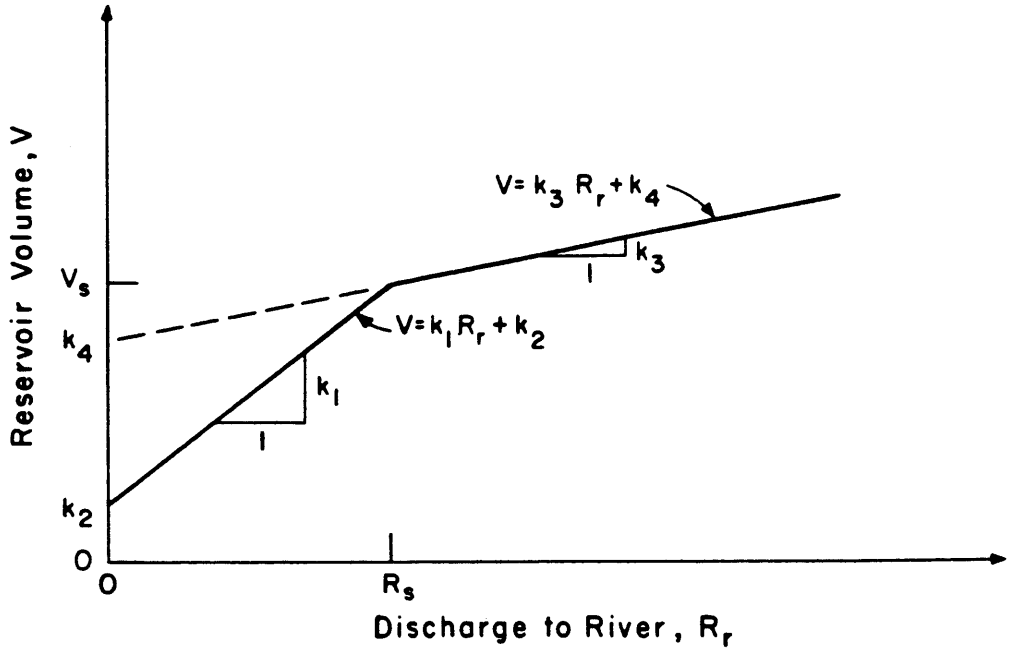

Figure 2.2: Reservoir Discharge Function

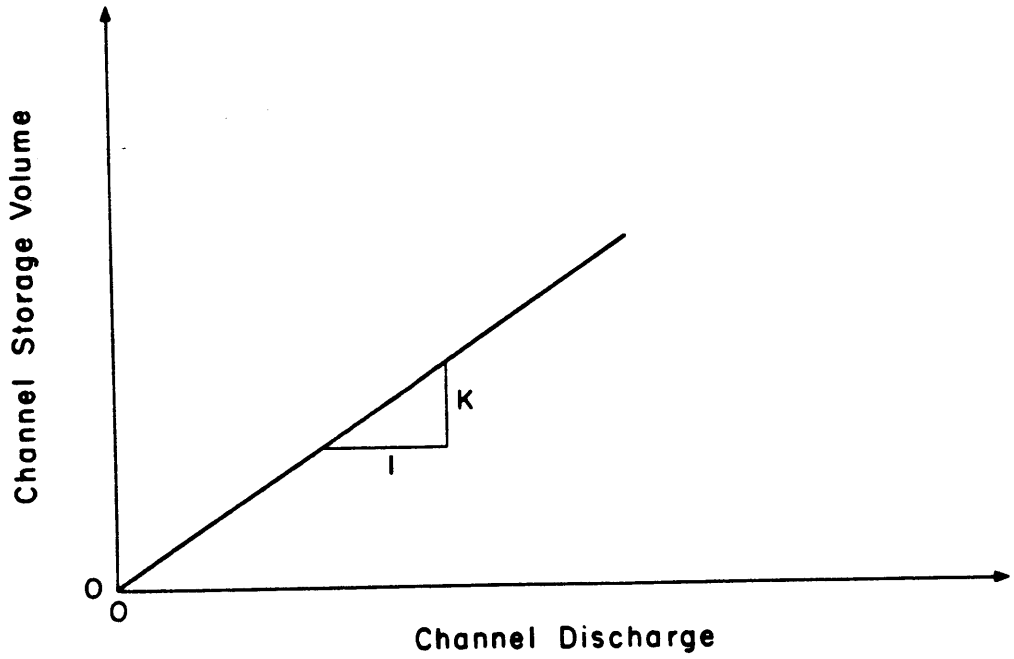

Figure 2.4: Channel Discharge Function

stage. As the reservoir terrain gets extremely flat or approaches being a gorge, or as the outlet works are more regulated, this relation becomes less accurate. The point of discontinuity (R_s,V_s) represents either the crest of a spillway or the top of the dam.

Volume and stage are related by a simple power function, as shown in Figure 2.3. This function represents most reservoirs well. V_c and H_c are the volume and stage at the crest of the dam.

The equations that describe the system are initially written in dimensional terms. Then values characteristic of the reservoir are used to remove the dimensions from the equations. Table 2.1 lists the characteristic values. The underscore indicates dimensional variables. Section 2.2.4.1 discusses estimation of these values. Conversion between dimensional and dimensionless parameters is described in Appendix B, along with the rest of the model development.

2.2.3 Channel Routing

Like the reservoir routing model, the channel routing model consists of a mass conservation equation, an upstream boundary condition, a downstream boundary condition, and an initial condition. The upstream boundary condition is the reservoir discharge, and the downstream boundary condition is the linear relation between storage and discharge shown in Figure 2.4, a simple function which has been found to be adequate for many natural channels (Sauer, 1973). The initial condition is a steady state discharge equal to the inital reservoir discharge (see Figure 2.1).

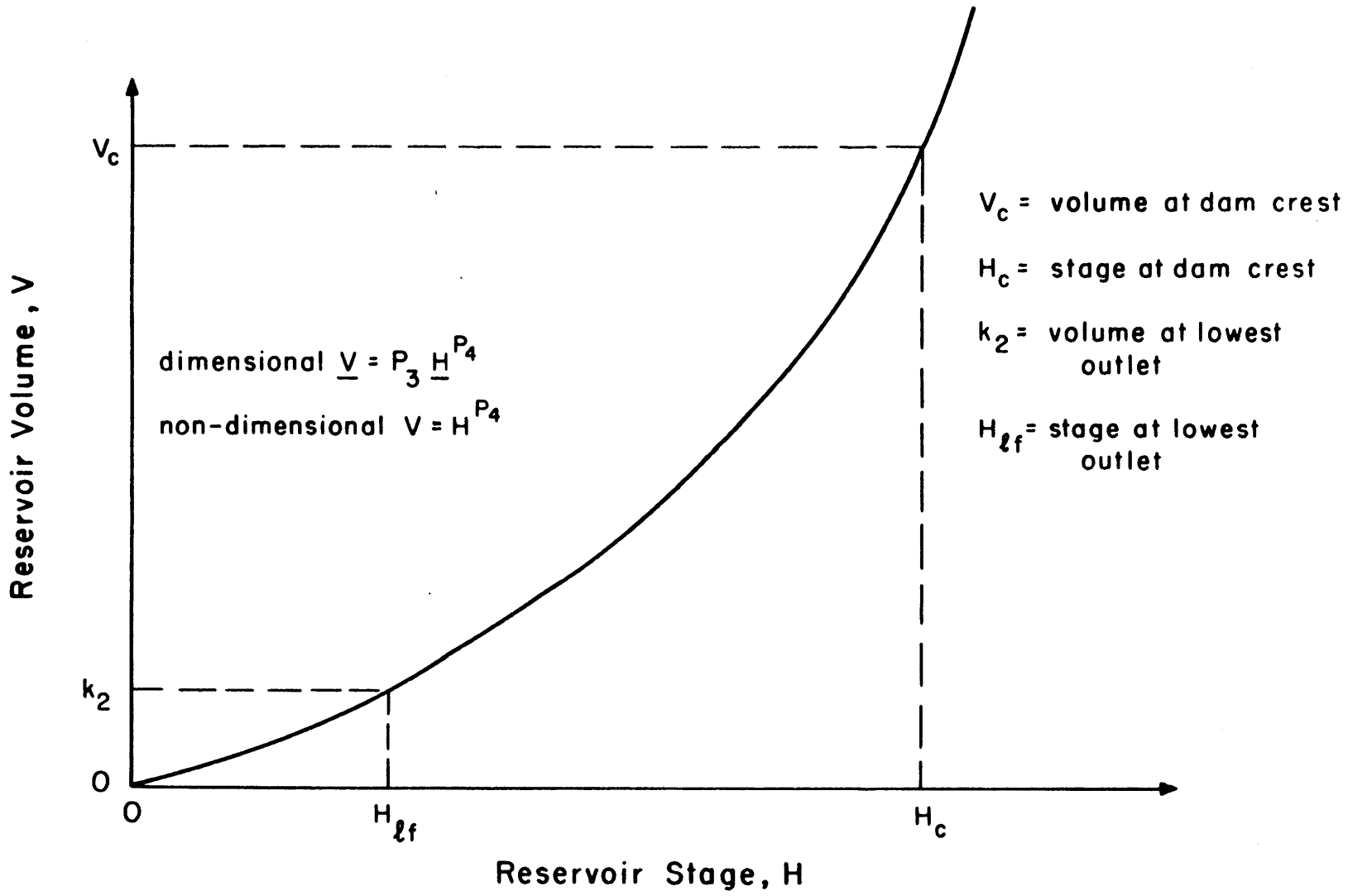

Figure 2.3: Reservoir Volume-Stage Function

Table 2.1

Characteristic Values for Reservoir

Values			Units
H_c	=	head on maximum depth breach (reservoir stage at crest of dam)	[length]
V_c	=	volume at crest of dam	[volume]
R_c	=	discharge at crest of dam	[discharge]
t_c	=	$\frac{V_c}{R_c}$	[time]

The channel routing model described here will not predict the discharge timing correctly, because wave travel time is not included in the model. This timing error generally increases with increasing channel length. Correct timing information, however, is not needed in this work because the damage model used in this work is a function of peak discharge, independent of the time at which that peak occurs. Were correct timing information needed, a correction factor could be added to the computed times. This correction factor is the lag time in what are known as lag and route models (see Linsley et al., 1975, or Dooge, 1973).

The discontinuities at t_p and t_b in the upstream boundary condition, and at (R_s, V_s) in the downstream boundary condition for the resevoir define six different situations, each of which has a separate set of reservoir and channel discharge equations. The mathematical forms of the equations in each set are similar. Equations for resevoir discharge, peak resevoir discharge, and channel discharge are developed in Appendix B. Peak channel discharge must be found by a numerical procedure, also described in Appendix B.

2.2.4 Parameter Estimation

2.2.4.1 Characteristic Values -

The first three values listed in Table 2.1, $\underline{H}_c$, $\underline{V}_c$, and $\underline{R}_c$ must be estimated from the resevoir properties. $\underline{H}_c$ is the hydraulic head, when the reservoir stage is at the crest of the dam, on the deepest breach which can be expected to occur. For most dams, $\underline{H}_c$ is the difference in elevation between the crest and upstream toe of the dam. The elevation used as the datum for $\underline{H}_c$ should be used as the datum for all other

elevations. $\underline{V}_c$ is the reservoir volume between the stage datum and $\underline{H}_c$. For most dams, $\underline{V}_c$ is the entire reservoir volume when the stage equals $\underline{H}_c$. The most notable exceptions to this are dams used to raise the levels of existing lakes, for which there may be substantial storage volume below the upstream toe of the dam. $\underline{R}_c$ is simply the reservoir discharge when the stage equals $\underline{H}_c$. The characteristic time, $\underline{t}_c$, is the ratio $\frac{\underline{V}_c}{\underline{R}_c}$.

2.2.4.2 Reservoir Parameters -

The following seven parameters must be estimated for the reservoir routing model (see Figures 2.1, 2.2, and 2.3)

	$(P_3), P_4$	volume-stage function parameter
	k_1, k_2	reservoir discharge parameters, $R_r \leq R_s$
	k_3, k_4	reservoir discharge parameters, $R_r \geq R_s$
and	t_p, t_b	reservoir inflow hydrograph timing

The volume-stage function contains two parameters, P_3 and P_4, when in dimensional form and only one parameter, P_4, when in non-dimensional form. (The parameters may be estimated from either dimensional or non-dimensional information.) The volume-stage function parameters can be estimated either from volume-stage data for the reservoir or from general information about the topography in the area, such as that shown in Table 2.2 (taken from Defense Intelligence Agency,1963). Volume-stage data can be developed from topographic maps, and is normally computed as part of the design studies for an engineered dam.

Table 2.2

Estimation of P_4 from General Information about Terrain and Estimation of P_3 from One Data Point

(from DIA, 1963)

Terrain	P_4
lake	1.0 - 1.5
flood plain and foothill	1.5 - 2.5
hill	2.5 - 3.5
gorge	3.5 - 4.5

$$P_3 = \frac{A_1}{P_4 H_1^{P_4-1}}$$

where A_1 = reservoir surface area at stage H_1

or

$$P_3 = \frac{V_1}{H_1^{P_4}}$$

where V_1 = volume at H_1

Phase I dam safety studies frequently contain volume-stage data. The parameters can be estimated from this data with any of several methods. One point is sufficient to compute P_4 from non-dimensional data, and two points are sufficient to compute P_3 and P_4 from dimensional data. The parameter values computed from several points may be averaged, or linear regression may be used to estimate parameters from logarithms of volume and stage.

The reservoir discharge coefficients may be estimated from values of volume and discharge. The values may be developed from a stage-discharge function for the outlet works and volume-stage function for the reservoir. A stage-discharge function can usually be constructed from the discharge works geometry and hydraulic equations, a straightforward process when the outlet works have fixed geometry. When the geometry is not fixed, as in gated spillways or hydroelectric turbines, assumptions about operating policies are necessary.

t_p is a function of the particular rain or snowmelt event which produced the flood, and of the slope, soil and vegetation properties, shape, and maximum length of the catchment. t_b is a function of the the peak flood discharge, I_{pn} (see Figure 2.1), and the flood volume. Proper estimation of t_p and t_b for a single flood, let alone a representative variety of floods is a major task. Simplified methods, in which both t_p and t_b are treated as constants for a given catchment, are used in this work. Information about more elaborate procedures is available in the hydrologic literature. For example, Hiemstra et al. (1976) present a method for modeling the ratio between t_p and t_b as a function of the peak catchment discharge, and Hiemstra and Francis

(1981) present a method for developing a joint probability distribution of flood peak and volume, which two variables determine t_b. These refinements can be incorporated into the model if greater accuracy is desired and the information necessary to estimate the parameters is available.

Linsley et al. (1975) present a method for estimating the time between the centroid of mass of a rainstorm and the time to peak of the catchment discharge from the geometric properties of the catchment. This time, along with a representative storm length, can be used to estimate t_p.

Gray (1970) suggests that $t_b = 2.67(t_p)$ is reasonable for many catchments in Canada. Equating volumes of a representative unit hydrograph presented in Viessman et al. (1977) with a triangular hydrograph yields $t_b = 2.76(t_p)$. $t_b = 2.7(t_p)$ will be used in this work.

2.2.4.3 Channel Parameters -

One parameter, the storage coefficient K (see Figure 2.4), is needed for the channel routing model.

When flood records are available, K may be estimated from the graphical procedures suggested by Linsley et al. (1975), from the receding limb of the flood hydrograph, as suggested by Sauer (1973), or from the average slope of a plot of storage against discharge. Storage can be estimated from topographic maps of the channel and records of water surface elevation.

When flood records are not available, discharge can be estimated from steady flow equations, base flow information, channel slope and length, or estimates of wave travel time. The discharge can then be plotted against storage volume to estimate the storage coefficient K. Dooge (1973) gives a method for estimating K in rectangular channels from base flow information. This method will usually underestimate K for real channels, but may be useful as an initial guess. Sauer (1973) presents a graph, based on estimates of K by other methods at several sites, which gives very rough estimates of K from only the channel slope and length. This chart should be used only when no other information is available or when a quick estimate is needed. The travel time of the center of mass of the flood wave, minus the travel time of the leading edge of the flood wave, is frequently a reasonable estimate of K (Sauer, 1973). Estimates of the center of mass travel time are complicated by off-channel storage. Without off-channel storage, the center of mass travel time can be estimated using the kinematic wave speed and the leading edge travel time can be estimated using the dynamic wave speed (see Henderson, 1966). Off-channel storage, however, effectively increases the travel time of the center of mass by storing some of the water as the flood wave passes and releasing it later. This effect is difficult to quantify in the absence of flood records.

2.3 DAM BREACHES

A variety of methods for predicting floods which could result from dam breaches have been suggested. Section 2.3.1 reviews some of these methods, and Section 2.3.2 describes the methods used in this work. Section 2.3.3 discusses parameter estimation for the dam breach model.

2.3.1 Review Of Methods

Section 2.3.1.1 reviews some methods for describing breach development and hydraulics, and Section 2.3.1.2 describes three examples of dam breach models.

2.3.1.1 Elements Of Dam Breach Models -

Physically, breach development cannot be separated from the reservoir, breach, and river channel hydraulics. In practice, modeling this interdependence has proved difficult, and breach development and flow hydraulics are usually modeled independently. The large uncertainty about how a given dam breach will form makes the choice of a modeling method as much a policy decision as a choice of the technically correct model (see Gundlach and Thomas, 1977, and Fread, 1981a).

Even the most accurate dam breach models do not always represent a given event accurately. Land (1980) presents a quantitative comparison of four dam breach models in three cases for which data are available. The large discrepancies between measured and predicted values and between the four models show the difficulty of modeling dam breaches accurately. Fread (1981a) discusses several difficulties of modeling dam breaches, even with the most sophisticated methods.

Breach development has been studied through examination of historical data, theoretical analysis, and experimentation. Johnson and Illes (1976) examined data from approximately 100 dam breaches and suggested that overtopping breaches in earth dams tend to develop as triangles whose top widths are three to four times their depth, and then expand to trapezoids. Non-overtopping breaches were thought to begin

with a hole in the embankment, but eventually reach the same shape as overtopping breaches. Ponce and Tsivloglou (1981), Cristofano (1973), and Harris and Wagner (1967) used sediment transport theory to develop coupled models of breach development and hydraulics, given that a breach has started. Brown and Rogers (date unknown) used the method developed by Harris and Wagner (1967) to model the Teton Dam failure. These models all require assumptions about the breach shape and pose difficult parameter estimation problems. Grzywienski (1971) performed laboratory experiments on breach erosion in an overtopped dam and developed an equation relating vertical erosion rates in model and prototype dams. Tinney and Hsu (1961) performed laboratory experiments of breach erosion in a fuse plug spillway and developed an equation relating lateral erosion rates in model and prototype fuse plug spillways. They also performed a half-scale field test in which the laboratory results were confirmed. The details of rates and duration of overtopping required to initiate breaches have not been reported.

There are three basic methods of modeling the hydraulics of the reservoir, dam breach, and river channel. The first method is to treat the breached dam as an internal point in a routing scheme that extends both upstream into the reservoir and downstream into the channel. The second method is to separate the reservoir and channel routing, with a breach discharge equation as the downstream boundary condition for the reservoir and the computed reservoir discharge as the upstream boundary condition for the channel. The third method is to develop the breach discharge hydrograph independently of the reservoir routing, and use that hydrograph as the upstream boundary condition for the channel routing. The three models described in Section 2.3.1.2 illustrate these

three methods. The relative accuracy of the three methods has not been firmly established because of the difficulty of determining what really happened in a given breach.

The first method is the most accurate, but sometimes the most difficult to implement, of the three methods. The method is difficult because dynamic wave, or some even more general routing method, must be used for the reservoir, breach, and channel. When the reservoir and channel have the same geometry and flow resistance, and the breach is complete and instantaneous, this method works well. The classic solution to the dam breach problem (see Henderson, 1966, or Stoker, 1957) uses this method. Sakkas (1980) develops a set of non-dimensional graphs for dam breach flood routing using this method (discussed further in Section 2.3.1.2). However, reservoirs and channels rarely have the same geometry and flow resistance, and breaches are rarely complete and instantaneous. Numerical solutions of the dynamic wave equations can handle variable geometry and flow resistance and can handle partial breaches, as demonstrated by Price et al. (1977), but have not yet been used for breaches which develop gradually, when the dam is treated as an internal point in the routing.

The second method is more versatile then the first method because the reservoir routing, breach discharge function, and channel routing may all be chosen independently. With this method, storage routing is usually used for the reservoir routing, though dynamic wave routing can be used, even with gradually developing breaches (Fread, 1982). Broad-crested weir equations and time dependent breach development are normally used to describe flow through the breach in this method. Any

channel routing method can be used to route the breach hydrograph downstream; dynamic wave and storage routing are the most commonly used. The primary problem when routing a dam breach flood wave (hydrograph) is the lack of data from which to estimate parameters. Parameters estimated from natural floods may not be appropriate for use with dam breach flood waves. This problem is discussed further in Section 2.3.3.

The third method is the simplest of the three. The complete discharge hydrograph is usually developed from estimates of the peak discharge, flow volume, and general shape of the hydrograph.

Peak discharge through a breach may be estimated from historical data, hydraulic principles, or experimental data. The simplest method is to use historical data. The Bureau of Reclamation has gathered data from several dam breaches and plotted peak discharge against stage at failure (Kirkpatrick,1976). Using these data avoids concern with breach geometry or hydraulics. Henderson (1966) and Stoker (1957) describe the development of an equation for peak discharge from the complete instantaneous removal of a rectangular dam in a dry frictionless channel. Dressler (1952) and Whitham (1954) considered the affect of friction on a dam breach wave. Su and Barnes (1970) developed equations for various breach shapes. Modifications to the theoretical equation for rectangular breaches, which account for breaches which do not extend to the full depth or width of the dam, were developed from a series of experiments performed by the Waterways Experiment Station (WES) of the Army Corps of Engineers (1960,1961). (Earlier experiments by Dressler, Eguiazaroff, and Schoklitsch are mentioned in WES (1960,1961) and Chow

(1959)). Wetmore and Fread (1981) present a simple equation for peak discharge from a breach which develops gradually. The equation was derived from broad-crested weir flow, an instantaneous rectangular breach, and a constant area reservoir.

The breach discharge hydrograph flow volume is estimated from storage volume in the reservoir and the reservoir inflow flood volume. The hydrograph shape is usually assumed to be either linear or exponential. As in the second method, any channel routing model can be used to route the breach hydrograph through the channel.

2.3.1.2 Examples Of Dam Breach Models -

Section 2.3.1.2 describes three dam breach models, one for each of the basic methods described in Section 2.3.1.1. The first, in which the dam is treated as an internal point in the routing model, is a set of dimensionless graphs developed from the solutions to a numerical model. The second, in which the breach discharge hydrograph is developed from the reservoir routing model, is a numerical model for use on digital computers. The third, in which the breach discharge hydrograph is developed independently of the reservoir routing model, is a solution of a numerical model presented in graphical form. Section 2.3.1.2 is not an exhaustive review of all dam breach models. A more complete summary of several dam breach models may be found in Water Resources Council (1977).

Sakkas (1980) developed a set of dimensionless curves for time of wave front arrival, maximum flood depth, and time of maximum flood depth for a wave from a sudden total failure of a dam in a dry prismatic

channel. The curves are developed from a method of characteristics solution of the dimensionless dynamic wave equations. It is not necessary to specify a special equation for breach discharge in this method, as the former location of the dam becomes simply an internal point in the channel once the dam is removed. The advantage of this method is that the depth and velocity for a given position and time are functions of just three parameters, the characteristic Froude number and two parameters of channel geometry. The primary disadvantage of this method is that dry prismatic channels and sudden complete breaches bear little resemblance to real situations. The effects on the breach flood wave of partial breaches, channel obstructions, flood inflow to the reservoir, tributary inflow along the channel, or base flow in the stream are not represented. Thus a model of this type is useful when only approximate information is needed or when few resources are available.

DAMBRK, developed by Fread (1982), is typical of, though perhaps more versatile than most, numerical models of dam breaches. DAMBRK can simulate breaches caused by either overtopping or piping type failures. For Overtopping Failures, breach geometry is trapezoidal, with side slopes, bottom width, and vertical erosion rate specified by the user. For piping (Non-Overtopping) failures, breach geometry is circular at first and then changes to trapezoidal as the breach enlarges. Broad-crested weir or orifice equations are used to describe breach discharge. Dynamic wave equations, solved with an implicit finite difference scheme, are used for the channel routing. Either dynamic wave or storage routing can be used for the reservoir. Geometric and flow resistance information for the routing must be supplied by the user.

DAMBRK can simulate a wider variety of situations than the other two models reviewed here. For example, rivers with several dams and even multiple dam failures may be modeled. Tributary flows and obstructions in the river, such as bridges, may also be represented easily. Various flow regimes, such as tailwater submergence at the dam and the occurrence of critical flow, are handled by DAMBRK. This is not a complete list of the model features, but serves to illustrate its versatility. This versatility is due in part to the basic method used and in part to the extensive development and testing of this particular model. DAMBRK was recommended by Land (1980) as the most suitable dam breach model for general use by the United States Geological Survey and has been used by the United States Army Corps of Engineers for inundation mapping.

Brevard and Theuer (1979) developed a dam breach model from simpler methods than those used by Fread (1982) or Sakkas(1980). This model can represent a wider variety of conditions than the model by Sakkas (1980), but is not as versatile as Fread's. Brevard and Theuer (1979) define the breach discharge hydrograph by estimating the peak from historical data, assuming a hydrograph shape, and computing the hydrograph volume.

The historical data was gathered by the Bureau of Reclamation (see Kirkpatrick, 1977 and Figure 2.7). The breach hydrograph function can be either linear or exponential. The linear function is used when the flow just below the dam is supercritical and the exponential function is used when that flow is subcritical. Flow in the stream prior to the breach is not considered. The slope of the linear function, or decay

parameter of the exponential function, is computed from the volume of flow through the breach. The flow volume is computed from the reservoir volume for Non-Overtopping failure and from the reservoir volume plus the total runoff from the catchment for Overtopping Failure. For Overtopping Failure, the breach is assumed to occur at the maximum stage reached during passage of a reservoir inflow flood. The breach hydrograph is routed through the channel with a method called the Attenuation-Kinematic (Att-Kin) model, developed by Brevard and Theuer (1977). The Att-Kin model is a combination of storage and kinematic wave routing in which the storage routing determines peak attenuation and the kinematic routing determines timing and distortion of the flood wave.

2.3.2 Development Of Dam Breach Model

Of the models reviewed, that of Brevard and Theuer (1979) is the most suited for this work. A model similar to DAMBRK (Fread, 1982) is not used here for the same reasons that simpler models were chosen for routing successfully passed floods (see Section 2.1). The model by Sakkas (1980) is enticing because of the small number of parameters, but it does not represent overtopping breaches or the effects of spillway size, and is thus not appropriate for this work.

The model developed by Brevard and Theuer (1979), however, also has some drawbacks for the purposes of this work. First, the Overtopping Failure condition and breach size are independent of the embankment characteristics. The dam is assumed to fail at the maximum reservoir stage caused by a given flood, and the breach size is not explicitly

represented. In the model developed here, the dam fails when the water in the reservoir reaches a specified stage, and the breach size is a function of that stage. Second, the peak discharge is not dependent on the stage at the time of failure. The peak breach discharge is a function of the stage at time of failure in the model developed here. Third, the breach discharge hydrograph volume is not dependent on the time of failure, and thus on the amount of water which has already been discharged from the reservoir. The breach discharge hydrograph volume is a function of the time of failure in the model developed here. Fourth, the Att-Kin routing model adds unecessary complexity to the model. In this work, damages are modeled as a function of peak flow, and thus only the peak attenuation, and not the timing or distortion, of the flood wave is needed. The model developed here uses storage routing. There are numerous other differences, but these four are the most important.

The dam breach discharge hydrograph is represented by a triangle superimposed on a constant base flow, as shown in Figure 2.5. The triangle is defined by the peak discharge and base width. The base flow is the initial steady state discharge from the dam (see Figure 2.1). Peak flow through the breach is given by equation 2.1, developed from experiments by WES (1960,1961).

$$R_{pb} = 0.29 g^{0.5} H_b^{1.5} B_b \left(\frac{B_d H_f}{B_b H_b}\right)^{0.28} \qquad (2.1)$$

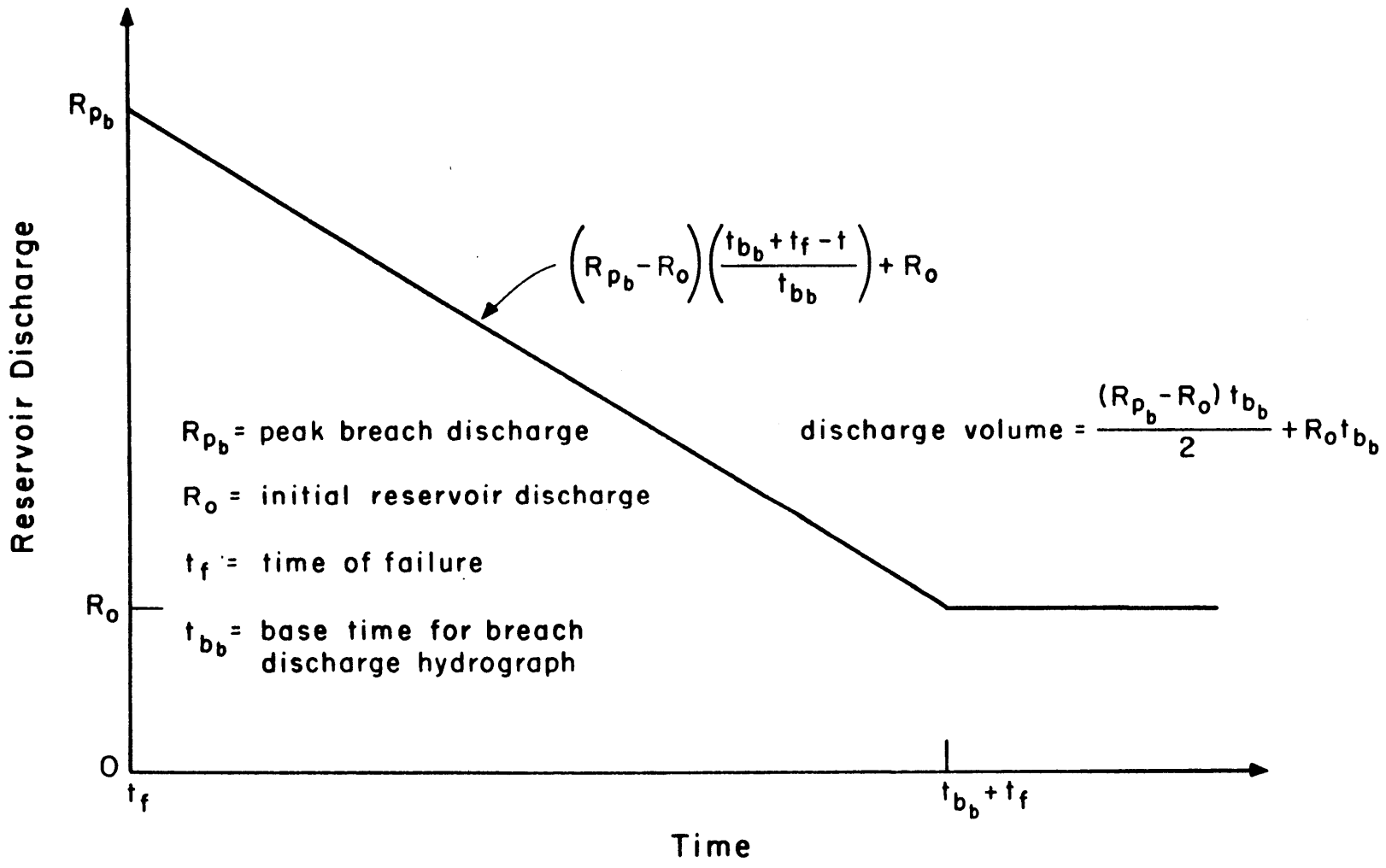

Figure 2.5: Reservoir Discharge after Breach

where: H_b = breach depth

B_b = breach width

H_f = water depth at time of breach

B_d = dam length

and g = acceleration of gravity

A sketch of the breach geometry from which Equation 2.1 was developed is shown in Figure 2.6. The breach depth and width are both modeled as functions of reservoir stage. Though there is no direct evidence for such a relation, it seems physically plausible. If we let H_b and B_b be linear functions of H_f, and remove the dimensions from Equation 2.1 with the characteristic values given in Table 2.1, the peak breach discharge is given by,

$$R_{pb} = B_{pg} B_1 H_f^{2.22} \tag{2.2}$$

where:
$$B_{pg} = \frac{g^{0.5} \underline{H_c}^{2.5}}{\underline{R_c}} \tag{2.3}$$

$$B_1 = 0.29 P_1^{1.22} P_2^{0.72} B_d^{0.28} \tag{2.4}$$

$$P_1 = \frac{H_b}{H_f} \tag{2.5}$$

and
$$P_2 = \frac{B_b}{H_f} \tag{2.6}$$

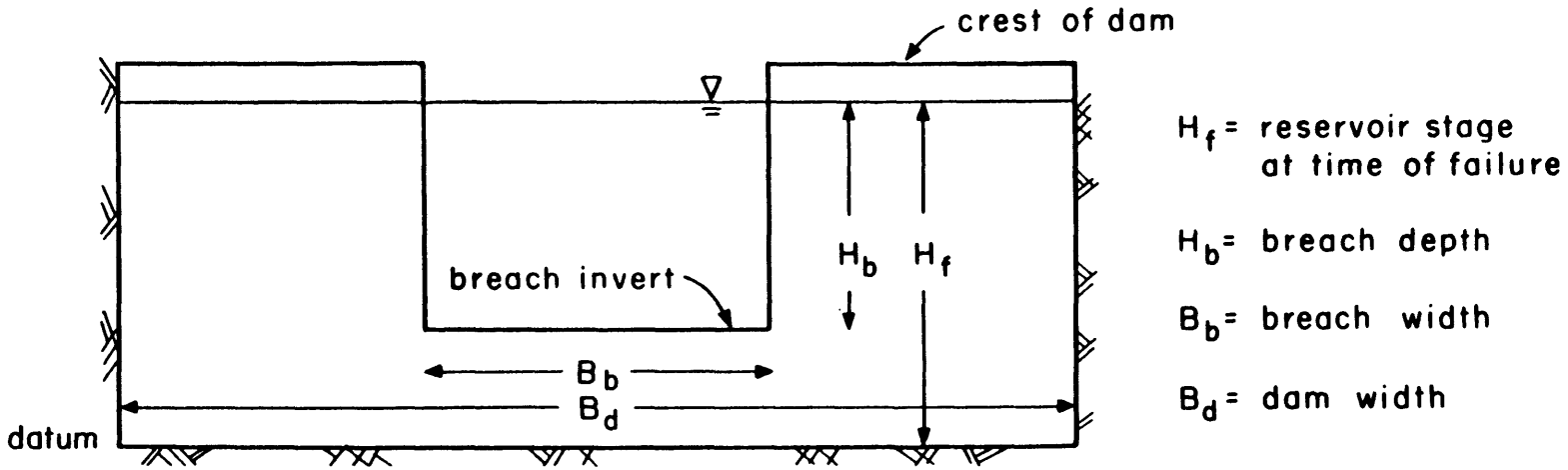

Figure 2.6: Idealized Breach Geometry

Failure during reservoir inflow floods (Overtopping Failure) is assumed to occur when the water reaches a stage specified by the user. The failure stage is treated as a stochastic variable in the derivation of the probability distribution. Failure during times of normal reservoir inflow (Non-Overtopping failure) occurs with a probability, specified by the user, which is allowed to vary with stage. The failure stage for Overtopping Failure and probability of Non-Overtopping Failure are discussed further in Section 2.5.3.

The peak of the discharge hydrograph (Figure 2.5) is determined only by the flow through the breach. The discharge works of a dam could still function following a breach and thus influence the peak discharge and time to empty, t_{bb}, but this possibility is not included in the model. As shown in Figure 2.7, the peak breach discharge computed from Equation 2.1 is reasonable relative to the estimated total peak discharge from real dam failures, except at very high dams, where it appears that Equation 2.1 may overestimate the peak discharge. Several curves which have been suggested to fit the data in Figure 2.7 are shown. Note that the hypothetical peak discharges are generally higher than the observed peak discharges.

At a low dam, such as a run of the river hydroelectric dam, below a large drainage area, the peak reservoir discharge during large natural floods that cause Overtopping Failure could be larger than the peak breach discharge. In some cases, the spillway discharge at the failure stage may already be larger than the breach discharge. Also, if the breach occurs before the time to peak of the reservoir inflow flood, the peak reservoir discharge may occur after the breach. Dynamic wave

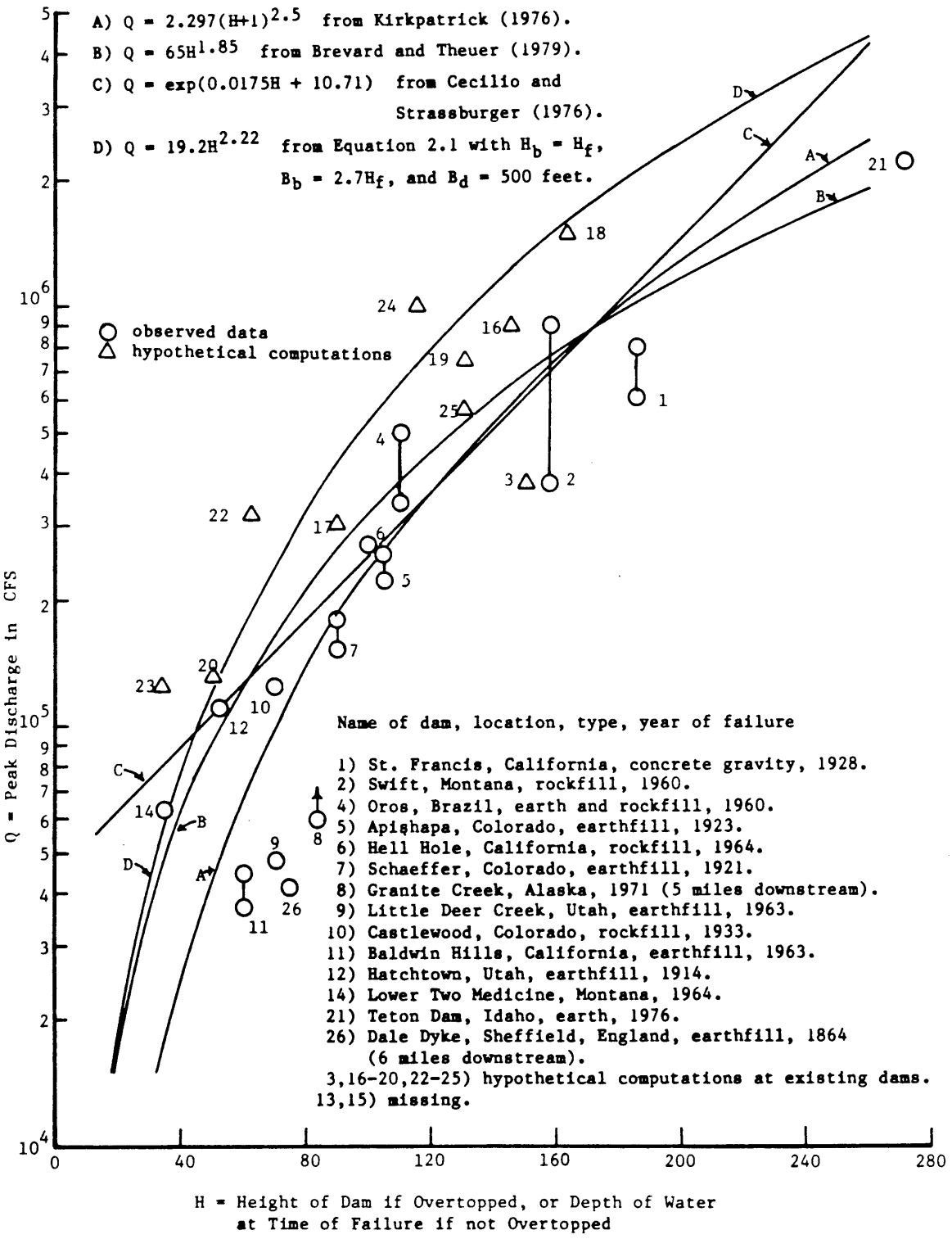

Figure 2.7: Peak Discharges From Dam Breaches (after Kirkpatrick, 1976)

routing methods would be required to model this situation accurately. For such cases, the model developed here may underestimate the flood damages and should be used cautiously, if at all.

Overtopping Failures are clearly not significant at such dams, and the primary dam safety issue is Non-Overtopping Failure, the analysis of which is more dependent on geotechnical and structural investigations than on models such as that developed here. These situations can be discovered by comparing some low probability flood peaks with the peak breach discharge when the reservoir stage is at or near the crest of the dam. A low value of B_{pg} (see Equation 2.3) also indicates the potential existence of this situation.

In the model, when the computed peak breach discharge is less then the pre-breach discharge at the failure stage, the pre-breach discharge at the failure stage is used as the peak breach discharge, R_{pb}.

The base time of the breach discharge hydrograph, t_{bb}, is computed by equating the volume of the discharge hydrograph to the volume of water available for passage through the breach. The available volume is the sum of the volume stored in the reservoir when the breach occurs and the volume which flows into the reservoir after the breach has formed. The volume stored in the reservoir may be computed from the volume-stage function shown in Figure 2.3. The volume of base flow is the product of R_o and t_{bb}. This quantity will usually be negligible relative to the stored volume and flood inflow. The time of failure depends on the failure stage, initial stage, and flood peak. It is computed with a numerical procedure which is described in Appendix B. The flood inflow volume can be computed easily once the time of failure is known.

For Overtopping Failures, the reservoir flood inflow may continue for some time after the reservoir is mostly drained, causing the tail of the hydrograph to depart from the triangular shape. This problem will be neglected because more accurate simulation of the situation would require the use of a dynamic wave model.

The discharge hydrograph is routed downstream using the same method used for successfully passed floods (see Section 2.2.2).

2.3.3 Parameter Estimation

The parameters described in Section 2.2.4 for Successful Passage floods are also needed for the dam breach model. Reservoir parameters estimated for use with Successful Passage floods are suitable for use with the dam breach model. The channel routing parameter may not be as satisfactory, for two reasons. First, the accuracy of storage routing, which works well for slowly varying flood waves, when applied to rapidly varying dam breach flood waves, is not clear. Second, even if storage routing is a reasonable method, the parameters estimated for Successful Passage flood routing may not be appropriate for dam breach flood routing. Land (1980) has shown, however, that a storage routing method using parameters estimated from channel geometry can perform reasonably well for routing dam breach floods.

In addition to the parameters for Successful Passage flood routing (see Section 2.2.4), the following three parameters for dam breaches must be estimated.

B_d = dam length

P_1, P_2 = breach size parameters

The dam length, B_d, is simply the distance from one end of the dam to the other. If the ends of the embankment slope steeply, it may be best to use a value between the top and bottom lengths.

The breach size parameters are estimated from a combination of data and judgement about the erodibility of the dam. Little guidance for estimating P_1 is available. P_1 will normally not exceed 1. When the dam does not contain erosion retarding layers and is made of easily erodable material, P_1 should be close to 1. The reservoir volume may also influence P_1. For example, small reservoirs may not contain enough water to erode a full depth breach, in which case P_1 should be reduced.

Some guidance for estimating P_2 may be developed as follows. Johnson and Illes (1976) suggest that a typical shape for a breach in an earth dam, at the time the breach reachs its maximum depth, was a triangle with a top width between 3 and 4 times its depth. An equivalent rectangle may be computed from the breach discharge equations developed by Su and Barnes (1970), shown in Figure 2.8. Using $z = 3.5$ with Equation 2.7, $P_2 = 2.7$. P_2 may be adjusted from 2.7 according to embankment condition or reservoir volume. Like P_1, P_2 will be higher for easily erodable material and lower for smaller reservoir volumes.

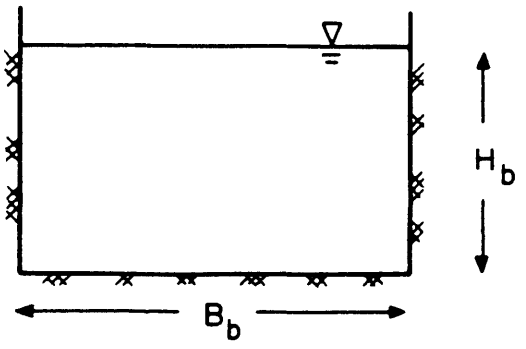

$$Q_p = 0.3\, B_b g^{0.5} H_b^{1.5}$$

(Su and Barnes, 1970)

Rectangular Breach

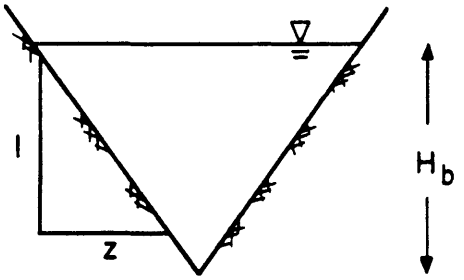

$$Q_p = 0.23\, g^{0.5} H_b^{2.5} z$$

(Su and Barnes, 1970)

Triangular Breach

Q_p = peak breach discharge

g = acceleration of gravity

Computation of Equivalent Breach size:

let $B_b = p_2 H_b$

then, equating peak discharges

$$Q_p = 0.3\, p_2 H_b g^{0.5} H_b^{1.5} = 0.23\, g^{0.5} H_b^{2.5} z$$

and $p_2 = 0.77\, z$ (2.7)

Figure 2.8: Equivalent Rectangular and Triangular Breaches

2.4 DAMAGE MODEL

2.4.1 Description

Flood damages are modeled as a power function of peak flow at the damage site, as shown in Figure 2.9. Two curves, both with the same functional form, are shown. One is for Successful Passage flood damages, and the other is for dam breach flood damages, from both Overtopping Failures and Non-Overtopping failures. L_d is the value of the damage to the dam caused by a breach. Qualitatively, dam breach flood damages are expected to be higher, for a given peak discharge, than Successful Passage flood damages, because the water velocity in dam breach flood waves is usually higher than in natural flood waves, and there may be less warning for a breach than for a natural flood. Little else is known. The main advantage of this damage model is flexibility. Damages estimated from any of several methods can be described accurately by these functions. The main disadvantage of this model is that the parameters can not be estimated directly from the primary data used to develop damage estimates.

When damage estimates are used in a cost-benefit analysis, both the time dependent value of money and possible changes in the damage areas should be considered. Methods for doing so are described by Bhavnagri and Bugliarello (1965).

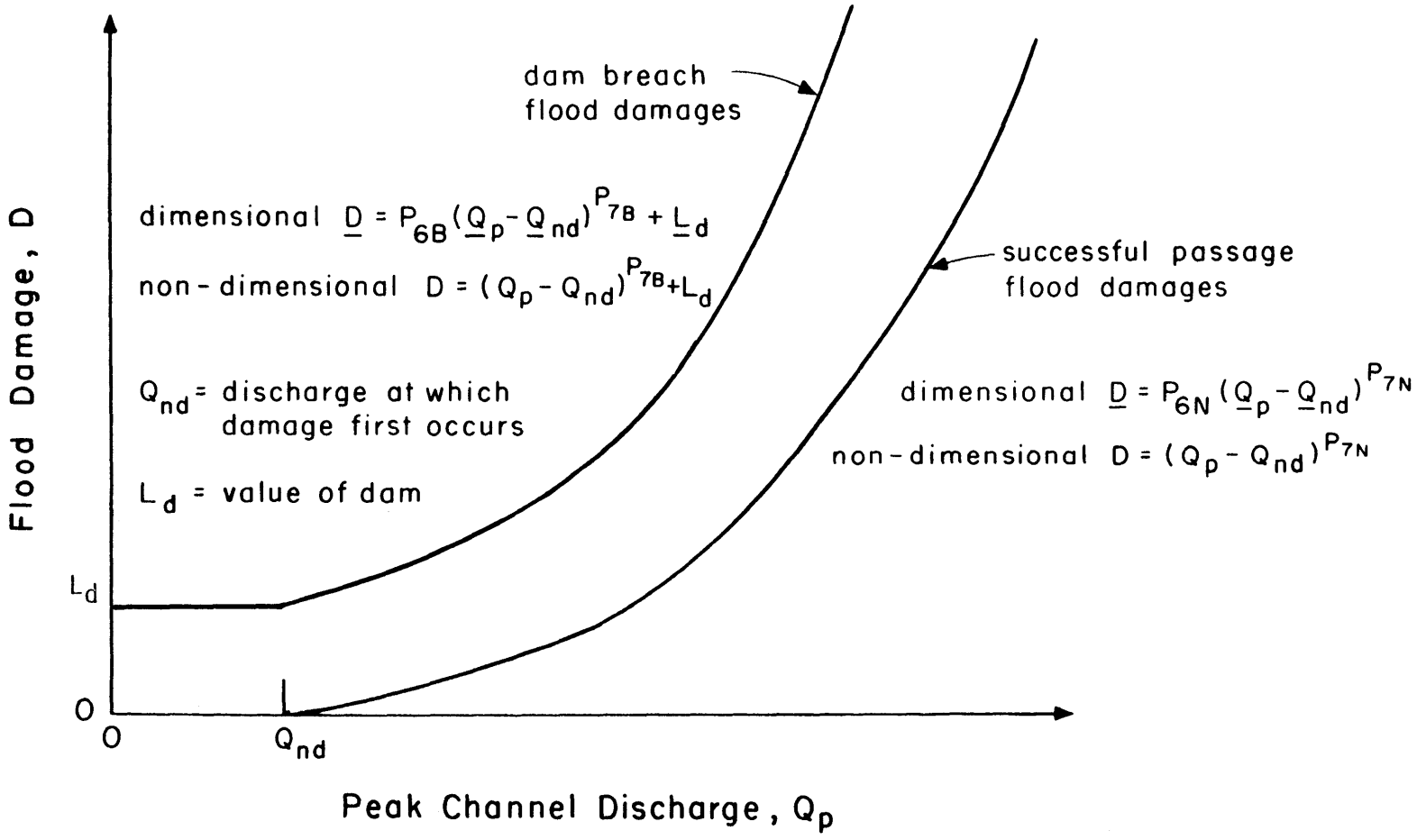

Figure 2.9: Damage Function

2.4.2 Parameter Estimation

The damage function parameters, P_6 and P_7 (see Figure 2.9), may be estimated from values of damages and peak flow. Linear regression on the logarithms of the values, or other curve fitting methods, can be used. The discharge at which damage first occurs, Q_{nd}, can be estimated from channel geometry and maps of development.

Damages which are caused by a given peak flow may be estimated in several ways. Damage estimation for concentrated damage centers is described by Grigg and Helweg (1975), Bhavnagri and Bugliarello (1965), and James and Lee (1971), among others. Damage estimation for distributed damage sites, such as agricultural lands, is more difficult, and no set procedures are recommended here. However, approximate damage estimates may be derived by relating flood peaks at one location to flood peaks elsewhere along the river. Estimated gage relations (see Linsley et al., 1975) may be adequate for this purpose.

Estimation of damages caused by dam breach flood waves is a special problem. The literature cited in the preceeding paragraph deals with damage from Successful Passage flood waves, and few data from which damages caused by dam breach flood waves can be estimated are available.

The value of the loss of the dam, L_d, can be measured as either the cost of rebuilding the dam or as the value of the benefits which the dam was expected to provide in the future. The parameter L_d is not used in this work, and detailed consideration of its computation is beyond the scope of this work. L_d is included in this model only for possible use in future work. More information about valuing dams can be found in

Baecher et al. (1979) or Pate (1981).

2.5 STOCHASTIC VARIABLES

Probability distributions of the reservoir flood inflow size, reservoir stage, and failure stage must be specified by the model user. Section 2.5 describes some methods for estimating these probability distributions and describes their representation in the present computer implementation of this model. All of the probability distributions can be specified either through parameters of a distribution function or as a table of values. The computer program can be changed to use distribution functions other than those currently programmed without affecting the operation of the rest of the program.

2.5.1 Flood Size

Flood frequency has been studied extensively. Chow (1964) presents a review of the theoretical background, commonly used frequency distributions, and parameter estimation methods for flood size frequency analysis. Discussions of flood frequency can also be found in most hydrology texts (see, for example, Linsley et al., 1975 or Viessman et al., 1977).

Flood frequency is usually defined in terms of peak flow. However, the nature of reservoirs and the mathematics of storage routing make the flood volume as, if not more, important than the flood peak. (This was discussed briefly in Sections 2.2.4.1 and 2.3.2.) Thus, when flood volume frequencies can be estimated, volume can replace peak discharge as the stochastic variable, with only a small change in the model. The

reservoir inflow flood peak, instead of being chosen directly, would be computed as a function of the flood volume and base time. Even better, when sufficient information is available, the joint probability distribution of peak and volume may be estimated (Heimstra and Francis, 1981). This would add one stochastic variable, but determine the parameter t_b (see Section 2.2.4.1). Peak discharge is used in this work because peak discharge data is more commonly available than volume data.

Unless extensive streamflow records are available, regional flood frequency estimates, such as those published by the United States Geological Survey, should be used to estimate the probability distribution of flood peaks. Unfortunately, even regional flood frequency information rarely deals with floods larger than that with a 100 yr. return period. Because we want to explicitly measure the flood damage risk from floods of the magnitude which are frequently used for spillway design floods, the probability distribution for flood peaks must be extended well beyond the 100 year flood, preferably out to floods of the size associated with the term probable maximum flood (PMF) (see Section 1.2.1). This could be done by extrapolating from the distribution for smaller floods, but there are few data with which to judge the validity of this approach. There is also no reason to assume that a function which describes the occurence of more frequent floods also describes the occurence of extremely rare floods. Chow (1964) states,

> From a practical point of view, the frequency analysis is only a procedure to fit the hydrologic data to a mathematical model of distribution. It is only experience and verification of data that decide the use of a certain distribution.

There are even some physical arguments against assuming that the same function describes both low and extremely high return period floods. The physical phenomena which cause the extreme floods may be different than those which cause the more common floods. For example, on a large catchment in New England, thunderstorms may dominate the low return period floods, and large tropical storms may dominate the extremely high return period floods. The reverse may be true for small catchments, because of the small chance, but extreme consequence, of a severe thunderstorm centering itself on the catchment.

Another method of extending the distribution, the method which will be used in Chapter 3 for the case studies, is to fit different functions to the low and high return period floods. The only restriction on the functions is that together they satisfy the properties of a legitimate probability distribution.

Since the concept of the PMF is frequently used for spillway design, it will be used here as a parameter of the floods frequency distribution. The distribution will be extended beyond the 100 year flood by interpolating between the 100 year flood and an estimate of the PMF size with a specified return period. Section 1.2.1 discussed the lack of concensus on a definition of the PMF. Also, because of both the vague definition and lack of data, it is nearly impossible to estimate a return period for the PMF. (Research on regional flood frequency estimation for rare floods could help in this area.)

The term PMF will be used here simply as a parameter of the flood distribution, a large flood with an extremely small probability of occurrence. Chapter 3 (Section 3.2) describes the particular method of interpolation between the 100 yr. flood and the PMF used in this work, and Chapter 4 examines the sensitivity of flood damage estimates to the selection of the PMF size and return period.

When the PMF is considered to be the largest flood which can occur, (a view not shared by the author), all of these methods are deficient because they do not have maximum values, and the PMF is not assigned an infinite return period. When the probability distribution is continuous, this problem can be fixed by simply ending the distribution at the PMF and adjusting the function so that the cumulative probability at the PMF equals one. This method gives the PMF an infinite return period. The use of distributions which vary between definite limits, such as the beta distribution (see Benjamin and Cornell, 1970), could also be investigated.

When the flood peak probability distribution is specified as a table of values, rather than as a continuous function, the upper tail of a lambda distribution (see Stedinger and Henriques, 1979) is used to interpolate between points. The lambda distribution is given by:

$$x = aF^b - c(1-F)^d + e \qquad (2.8)$$

where: x = the stochastic variable

F = the cumulative probability

and a,b,c,d,e = parameters

The upper tail, which is given by:

$$x = e - c(1-F)^d \tag{2.9}$$

approximates Equation 2.8, the complete distribution, when F is greater than 0.5. Since the important floods for this work will all be greater than the mean annual flood, the lower tail, for F less than 0.5, is not needed.

When b=d=0.135, the lambda distribution is a good approximation to the log-normal distribution (see Benjamin and Cornell, 1970); d is set equal to 0.135 in this work. With d=0.135, e and c, the other parameters of the upper tail, can be estimated from two points, making the lambda distribution ideal for interpolating between points.

The largest reservoir inflow flood during a given time period, usually one year, is assumed to determine the flood damages during that period. When there is more than one flood season during a year, it may be appropriate to divide the year and consider separate flood size frequency distributions for each period. In any case, the frequency distribution should be for the largest flood during the chosen time period.

2.5.2 Initial Reservoir Condition

The probability distribution of reservoir stage is used to specify the probability of initial conditions for reservoir inflow floods and the stage probability for Non-Overtopping Failure. It can be derived either from mathematical models or estimated directly from data. Chow (1964) describes the derivation of stage probability from reservoir inflow-outflow models. Langbein (1958) presents a sample computation of a reservoir storage frequency distribution in which the volume-discharge function shown in Figure 2.3 is used. When data are available, reservoir stage frequencies may be estimated from those data with considerably less effort than is required to derive the frequencies from physical models. Data can be used either to define frequencies of stage intervals directly or to estimate the parameters of a probability distribution. Some reservoir stage probability distributions for dams in New England are shown in Appendix F.

The reservoir stage probability distribution is modeled as a beta distribution (see Benjamin and Cornell, 1970). The beta distribution was chosen because it can assume a variety of shapes. It may be specified either through a mean and variance, the two parameters of the distribution, or a mean and one of the two parameters of the distribution.

The desired frequency distribution of initial stage applies to the stage which might be expected at the beginning of a flood. Thus, if we assume that only one flood occurs at a time, the stages which occur during floods should be removed from the data record before estimating the frequency distribution.

2.5.3 Overtopping Failure Stage And Non-Overtopping Failure Probability

Little is known about either the stage at which a dam will fail when overtopped or the probability of Non-Overtopping Failure, either in total or as a function of stage.

The probability distribution of Overtopping Failure stage is modeled as a beta distribution (see Benjamin and Cornell, 1970), though current knowledge does not justify using anything more elaborate than a uniform distribution between the lowest stage at which it is believed that failure could occur and the highest stage which the embankment is believed to be able to withstand. (The beta distribution can take the form of a uniform distribution.)

Probabilities of Non-Overtopping failure, given reservoir stage, are represented by the following function,

$$P_{f/H_o} = P_{min}+(P_{max}-P_{min})\left(\frac{H_o-H_{min}}{H_{max}-H_{min}}\right)^{P_8} \qquad (2.10)$$

where: P_{f/H_o} = Non-Overtopping Failure Probability, given H_o

P_{min}, P_{max} = bounds on P_{f/H_o}

H_{min}, H_{max} = bounds on H_o

H_o = reservoir stage at time of failure

P_8 = shape parameter

Quantitatively sound estimation procedures for the parameters of Equation 2.10 are not known. However, judicious guesses allow qualitatively correct representation of failure probabilities. For example, P_g could equal 1 and P_{min} and P_{max} could be equally spaced on either side of a value thought to represent the overall Non-Overtopping Failure probability. The total Non-Overtopping Failure probability may be estimated using a procedure developed by Bohnenblust and Vanmarcke (1982), which is described in Appendix A.

2.6 COMPUTATION OF DISTRIBUTION AND MOMENTS OF FLOOD DAMAGE

Integration, stochastic simulation (also called Monte Carlo method), and enumeration are commonly used to derive probability distributions of dependent variables from probability distributions of independent variables. These three methods are described by Benjamin and Cornell (1970). Direct integration over all three stochastic variables is mathematically intractable for this model. Stochastic simulation is most needed when the number of stochastic variables is so large that systematic variation of one variable at a time leads to an excessive computational burden. With only three stochastic variables, this model is well suited to the use of direct enumeration.

The three stochastic variables in this model may be reasonably assumed to be independent. Thus, joint probabilities can be computed as the products of marginal probabilities. The frequency distribution of each variable may be discretized by dividing the range of interest into intervals and assigning the probability mass of that interval to a representative value in the interval. Once the frequency distributions

have been discretized, computation of a cumulative probability function is straightforward. Damage values for every possible combination of the representative values of the three stochastic variables are computed and associated with the product of the probabilty masses of those variables. The damage values are then arranged in order of increasing value and the associated probability masses summed. The moments of the distribution may be computed from the damage values and associated probabilities.

Chapters 4 and 5 examine the variation of damage potential with variation of several of the less certain model parameters and with variation of the spillway size and initial reservoir stage. For this purpose it is useful to divide the total damage into several components. The total damage may be divided into two basic components, the damage caused by reservoir inflow floods, both those which do not cause failure and those which do cause failure, and the damage caused by Non-Overtopping Failures. The damage caused by reservoir inflow floods may be divided in two ways, both of which are described below. Also, it is useful to examine the Natural Flood damages, in the absence of the dam. These divisions define the following seven measures of the damage.

1) Successful Passage damage

2) Overtopping Failure damage

3) Non-Overtopping Failure damage

4) total damage

5) No-Failure damage

6) marginal Overtopping Failure damage

7) Natural damage, without dam

The model computes the mean and variance of these seven measures of damage potential, though only the mean values are examined in Chapters 4 and 5. The probability of Overtopping Failure is also computed. Appendix B5 describes the computations.

Successful Passage damage is the damage caused by reservoir inflow floods which do not cause the dam to fail. Thus, only reservoir inflow floods up to the size which causes overtopping contribute to this quantity.

Overtopping Failure damage is the damage caused by reservoir inflow floods which cause the dam to fail. Only reservoir inflow floods which cause Overtopping Failure contribute to this quantity.

Non-Overtopping Failure damage is the damage caused by failures from all causes other than overtopping during a reservoir inflow flood, such as excessive seepage, foundation weakness, or earthquakes.

Total damage is the sum of the Successful Passage, Overtopping Failure, and Non-Overtopping Failure damages.

No-Failure damage is the damage caused by reservoir inflow floods when the dam is assumed to not fail. This quantity differs from Successful Passage damage in that the full range of floods (through the PMF) contributes.

Marginal Overtopping Failure damage is the difference between the Overtopping Failure damage and the No-Failure damage, for those reservoir inflow floods which cause Overtopping Failure. Marginal Overtopping Failure damage is thus the damage which can be attributed directly to the Overtopping Failure, the damage which would not have occurred if the dam had not failed.

The sum of Successful Passage damage and Overtopping Failure damage equals the sum of No-Failure damage and marginal Overtopping Failure damage. The same total, all the damage caused by reservoir inflow floods, is simply split in two different ways. For example, assume the PMF causes the dam to fail, given a failure stage. Then Successful Passage damage equals zero; Overtopping Failure damage equals the damage computed by routing the PMF through the reservoir without allowing the dam to fail; and marginal Overtopping Failure damage equals the difference between Overtopping Failure damage and No-Failure damage.

Though the mean Successful Passage damage is always smaller than the mean No-Failure damage, the difference between these two is frequently small. The model always computes all seven measures of flood damages. However, not all seven are presented in the results that appear in later chapters. The mean No-Failure and mean marginal Overtopping Failure damage are always shown; the mean Successful Passage and mean Overtopping Failure damage are shown only when there are qualitative differences which can be illustrated by doing so. The mean No-Failure and marginal Overtopping Failure damage were chosen as the primary results because they are conceptually more significant for

economic analysis than the other quantities. Resources applied to reducing the chances of Overtopping Failure should be weighed against the marginal damage caused by Overtopping Failures.

In the model, the total damage is computed as the sum of the Successful Passsage and Overtopping Failure damages, plus, of course, the Non-Overtopping Failure damage. The total damage could just as easily have been computed from the No-Failure and marginal Overtopping Failure damages. The particular choice that was made is based on the historical development of the model and does not usually affect the results. It can, however, affect the results for very low dams at which the discharge following a breach may not be represented well by the model. This problem was discussed briefly in Section 2.3.2.2 and will be discussed further, for a dam at which this problem applies, in Section 4.1.

The Natural Flood damage, without dam, is the damage caused by the reservoir inflow flood wave routed to the damage site without first passing through the reservoir. The difference between the mean Natural Flood damage and the mean total damage shows the change in flood damage potential caused by the presence of the dam. Because of the contribution of failure damages, this difference is not always positive. The difference between the mean Natural Flood damage and the mean No-Failure damage shows the reduction in flood damage potential caused by the dam if the dam never failed. This difference is always positive.

The Overtopping Failure probability is the probability that a reservoir inflow flood will be greater than or equal to the smallest reservoir inflow flood which causes an Overtopping Failure, for given initial and failure stages. When the initial or failure stages are given as probability distributions, rather than as single values, the mean Overtopping Failure probability is computed. The total failure probability is plotted with the Overtopping Failure probability in this work, and the vertical distance between the two curves equals the Non-Overtopping Failure probability. The Non-Overtopping Failure probability is constant except when it is varied in Section 4.3.3.

Table 2.3

Parameter Summary

Catchment Parameters	(see Figure 2.1)
t_p = time to peak	
t_b = base time	
I_p = peak reservoir inflow	
(Probability distribution of I_p)	
Reservoir Parameters	
k_1, k_2, k_3, k_4 (discharge)	(see Figure 2.2)
B_d = dam length	(see Figure 2.6)
P_3,P_4 (volume-stage function)	(see Figure 2.3)
H_o = initial reservoir stage	
(Probability distribution of H_o)	
Breach Parameters	
P_1,P_2 (breach size)	(see Equations 2.5 and 2.6 and Figure 2.6)
B_{pg} = breach parameter group	(see Equation 2.3)
$_pNOF$ = probability of non-overtopping failure	
(Variation of $_pNOF$ with reservoir stage)	
H_f = overtopping failure stage	(see Equations 2.1 and 2.2 and Figure 2.6)
(Probability distribution of H_f)	
Channel Parameter	
K = storage coefficient	(see Figure 2.4)
Damage Function Parameters	(see Figure 2.9)
Q_{nd} = discharge at which damage first occurs	
P_{6N}, P_{6B} = scale parameters	
P_{7N}, P_{7B} = shape parameters	
L_d = value of dam	

Chapter 3

Parameter Estimation for Case Studies

Chapter 3 describes estimation of parameters of the model described in Chapter 2 for the four dams which will be examined in Chapters 4 and 5. The four dams were selected to present a variety of dam designs. They were not chosen either to be representative of any classes of dams, or to span the complete range of dam designs. Dams vary too much to be representative or all encompassing with four examples. The four dams were chosen primarily on the basis of their height; a range of heights was desired. They were not screened for behavior from a longer list. The four dams presented here are the same four which were initially selected.

The primary interest in this work is the behavior of the dam, reservoir, and catchment. The characteristics of a particular damage site at a particular place on a particular channel are of lesser interest and, in this work, would only cloud the differences between the dams. To help clarify the differences between the behavior of the four dams, the same non-dimensional values of the downstream channel and damage site parameters (see Sections 2.2.3 and 2.4) are used for all four dams.

Using the same channel and damage site for each dam allows qualitative comparison of the behavior of different dams, but, because all the numbers are non-dimensional, care must be exercised when making

those comparisons. While the parameters used in this work were derived from real dams, once non-dimensionalized, the parameters represent a dam of any size whose geometry and natural setting (upstream catchment) are similar to the dam from which the parameters were estimated. Thus, if the non-dimensional damage caused by dam A is larger than that caused by dam B, the real damage potential below dam A is not necessarily greater than that below dam B. Rather, if the dam, reservoir and catchment of dams A and B were scaled so that their real peak spillway discharges were equal, and their non-dimensional parameters were not changed, the real damage potential below dam A would then be greater than that below dam B, for identical downstream channels and damage sites. This is an example of why the term damage potential, rather than just damage, has been used thus far. From here on the terms damage and damage potential will both be used to mean damage potential.

Section 3.1 gives general information about the dams, and Sections 3.2 through 3.6 describe the parameter estimation. Tables 3.2 and 3.3, found at the end of this chapter, summarize the parameter values. Table 2.3 gave a complete list of the parameters which must be estimated.

3.1 General Information

The four dams, named Miles Pond Dam (MPD), Gale Meadows Dam (GMD), Springfield Reservoir Dam (SRD), and Knightville Dam (KVD), are

located in New England; three in Vermont and one in Massachusetts. Figure 3.1 shows their location. MPD is 10 feet high and is used to raise the level of an existing lake, primarily to enhance recreation on the lake. GMD is 30 feet high and is used to create a fishing impoundment. SRD is 50 feet high and is used to impound an emergency water supply for the town of Springfield, Vermont. KVD is 150 feet high and is used for flood control. All four dams are earth embankments with fixed crest spillways. Some further information about the four dams is given in Table 3.1.

The parameters for MPD, GMD, and SRD are estimated from information contained in Phase I safety inspection reports (Corps, 1980a, 1980b, 1980c). The parameters for KVD are estimated from information contained in Appendix H of the Westfield River Watershed Master Manual of Water Control (Corps, 1978).

The Phase I report for MPD reported that the dam was in good condition, but that the spillway could not pass the required test flood, the PMF, without overtopping. MPD was classified as intermediate size and high hazard (see Figure 1.1 and Table 1.2).

The Phase I report for GMD reported that the dam was in only fair condition, having some problems with erosion and seepage, but that the spillway could pass the test flood, half the PMF, without overtopping. GMD was classified as intermediate size and significant hazard.

The Phase I report for SRD reported that the dam was in very poor condition, and that the spillway could not pass the test flood,

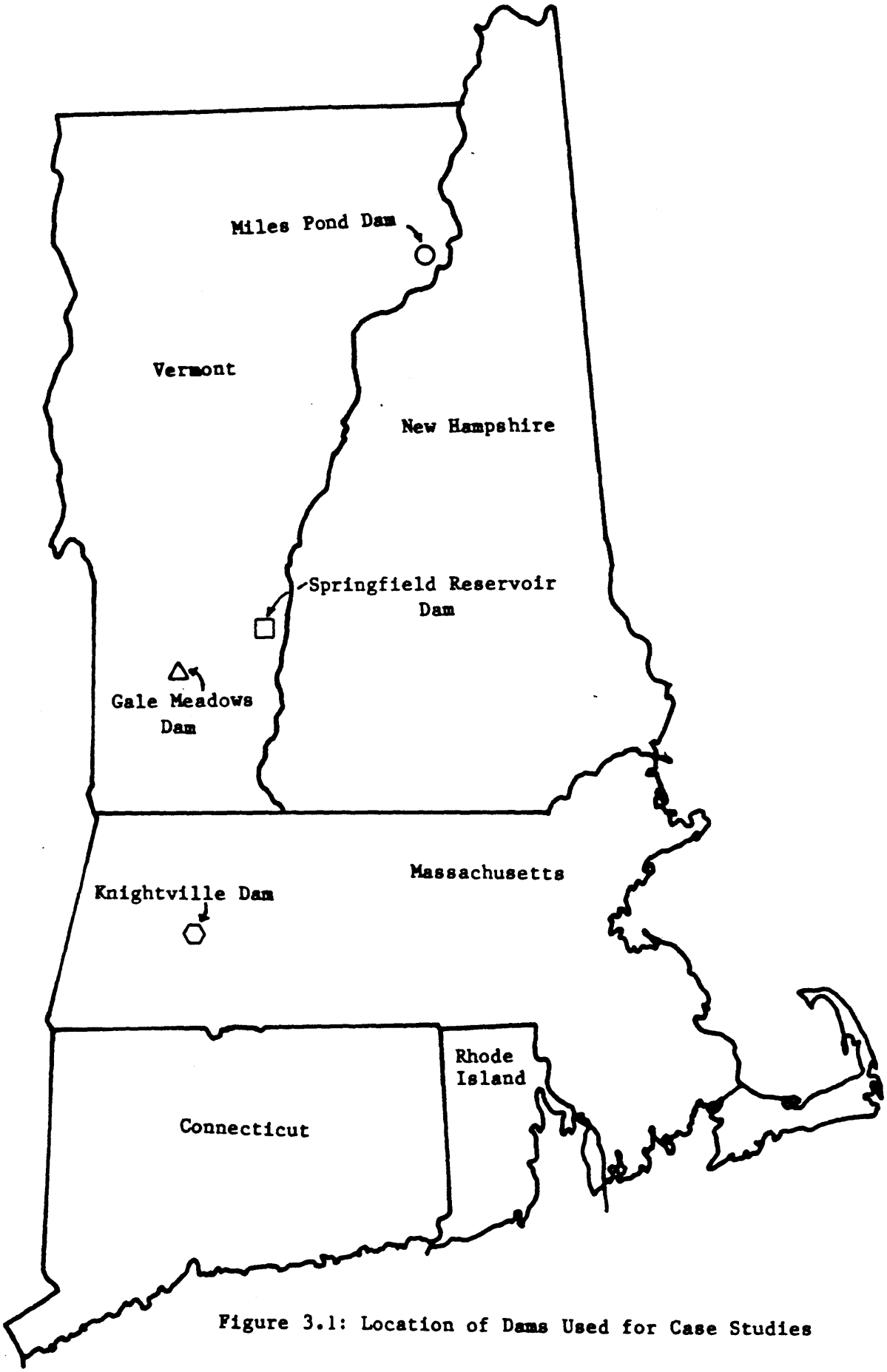

Figure 3.1: Location of Dams Used for Case Studies

Table 3.1

General Information about MPD, GMD, SRD, and KVD

	MPD	GMD	SRD	KVD
Owner	Vermont Dept. of Water Res.	Vermont Dept. of Fish & Game	Springfield, Vermont	U.S. Army Corps of Engineers
Purpose	Recreation	Fishing	Water Supply	Flood Control
Construction	Earth Embankment	Earth Embankment, Clay Core	Earth Embankment, Concrete Core	Hydraulic Earthfill
Year Built	Unknown	1965	1903	1941
River	Miles Pond Brook	Mill Brook	Unnamed Tributary to Black River	Westfield River
Hydraulic Height (ft)	10.4	27	47	150
Crest Length (ft)	400	300	320	1,200
Volume (af):				
Winter Pool	946	-	-	-
Normal Pool	1,370	1,338	174	22
Spillway Crest	1,500	1,734	174	49,000
Dam Crest	2,200	2,942	240	71,000
Discharge (cfs):				
Spillway Crest	120	239	0	14,500
Dam Crest	2,353	5,300	1,040	143,365
Spillway Type	Fixed Crest	Fixed Crest	Fixed Crest	Fixed Crest
Catchment Area (m_i^2)	6.7	10.0	2.6	162

half the PMF, without overtopping. The reservoir level was lowered ten feet because of the condition of the embankment. SRD was classified as intermediate size and significant hazard.

KVD was not inspected as part of the Phase I inspection program.

3.2 Catchment Parameters

The catchment parameters are the time to peak, t_p, base time, t_b, and probability distribution of the peak, I_p, for the reservoir inflow hydrograph shown in Figure 2.1.

The Phase I inspection reports used Snyders method, given by Equation 3.1 (see Linsley et al., 1975), to estimate the time between the centroid of rainfall and the reservoir inflow hydrograph peak (the basin lag) for MPD, GMD, and SRD.

$$t_\ell = C_t(LL_c)^{0.3} \tag{3.1}$$

where

t_ℓ = basin lag

C_t = catchment coefficient

L = length of main stem from dam to catchment divide

L_c = length of main stem from dam to point nearest the catchment centroid

C_t was assumed to equal 2.0, the value suggested by Chow (1964) for use in the Appalachian Highlands, for all three catchments.

The time to peak, t_p, can then be found by assuming a storm duration, t_s. The relation

$$t_s = t_\ell / 5.5 \qquad (3.2)$$

was used here. This relation implies a short storm duration. These three catchments are small, and the critical storms are likely to be short, intense, localized thunderstorms.

If the centroid of the storm is approximated by the midpoint of the storm,

$$t_p = t_\ell + t_s/2 \qquad (3.3)$$

using Equation 3.2 in 3.3 gives

$$t_p = 1.09\ t_\ell \qquad (3.4)$$

The base time, t_b, was computed as 2.7 t_p, as discussed in Section 2.2.4.2.

The base time for the reservoir inflow hydrograph at KVD was computed from the volume and peak for the spillway design flood, using the relation implied by a triangular hydrograph

$$t_b = 2V/I_{pn} \qquad (3.5)$$

where

V = flood volume

I_{pn} = flood peak

t_b was divided by 2.7 to compute t_p.

The probability distribution of reservoir inflow peak, I_p, was developed in four parts.

First, floods with return periods of 2, 5, 10, 25, 50, and 100 years were computed from regional equations developed by the United States Geological Survey. Equations from Johnson and Tasker (1974) were used for the three dams in Vermont and equations from Wandle (1982) were used for KVD.

Second, the magnitude of the PMF was estimated from the graph shown in Figure 3.2. Figure 3.2 was developed by the New England Division Corps of Engineers to assist those doing Phase I inspections. In Fig. 3.2, maximum probable flood is the same as probable maximum flood, NED stands for New England Division, and SPF stands for standard project flood. Lines have been fit to the data for three types of terrain.

Third, a return period was chosen for the PMF.

Fourth, the gap between the PMF and 100 yr. flood was filled by interpolation using the upper tail of a lambda distribution with d=0.135 (see Section 2.5.1). This is equivalent to drawing a straight line on log-normal probability paper.

Figure 3.3 shows the floods estimated from the USGS equations and the PMF computed from Figure 3.2, plotted on log-normal probability paper, for each of the four dams. The PMF has been plotted at a return period of 10^5 years.

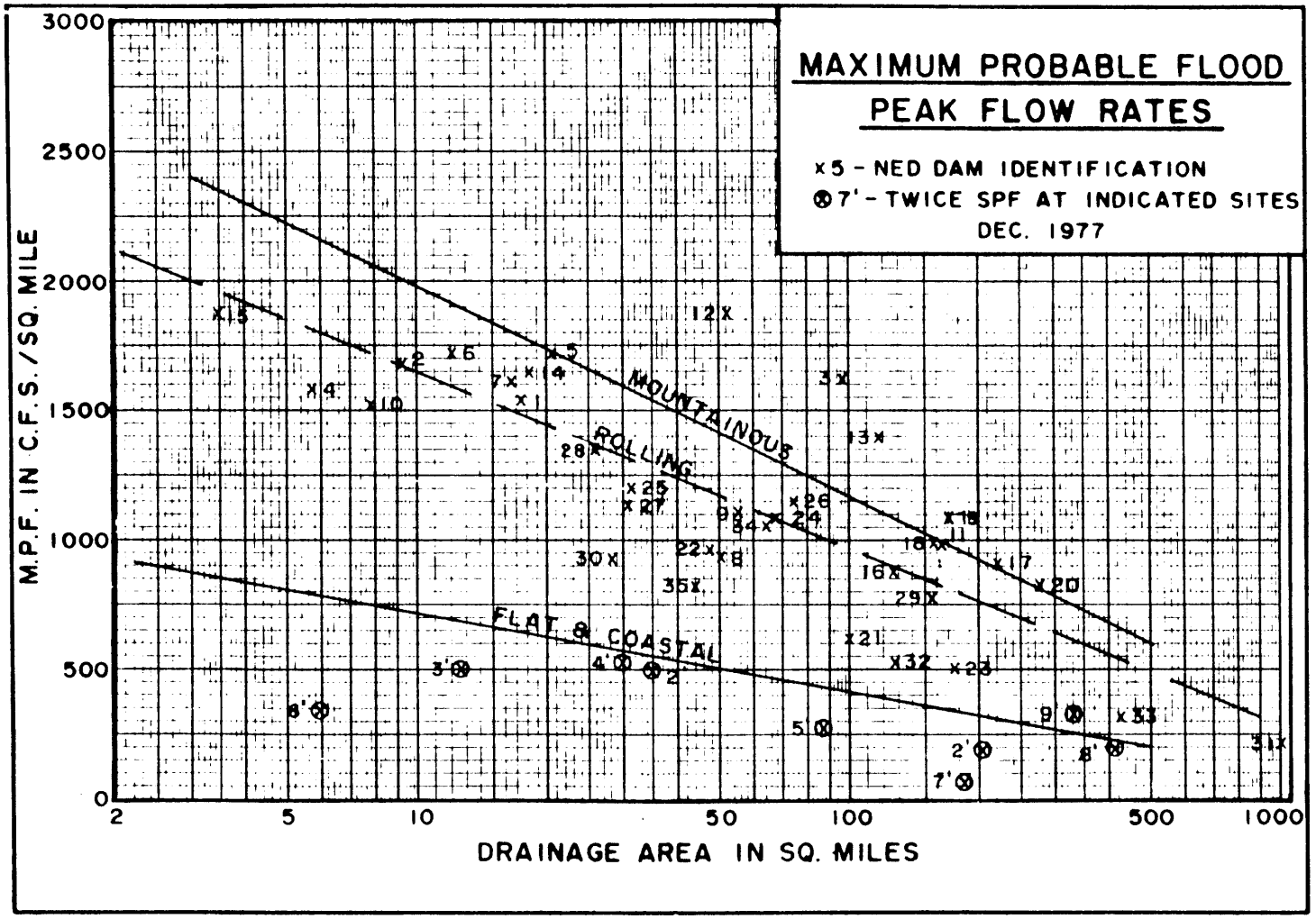

Figure 3.2: Guidelines for Computing the Probable Maximum Flood in Phase I Dam Inspections (New England Division, U.S. Army Corps of Engineers)

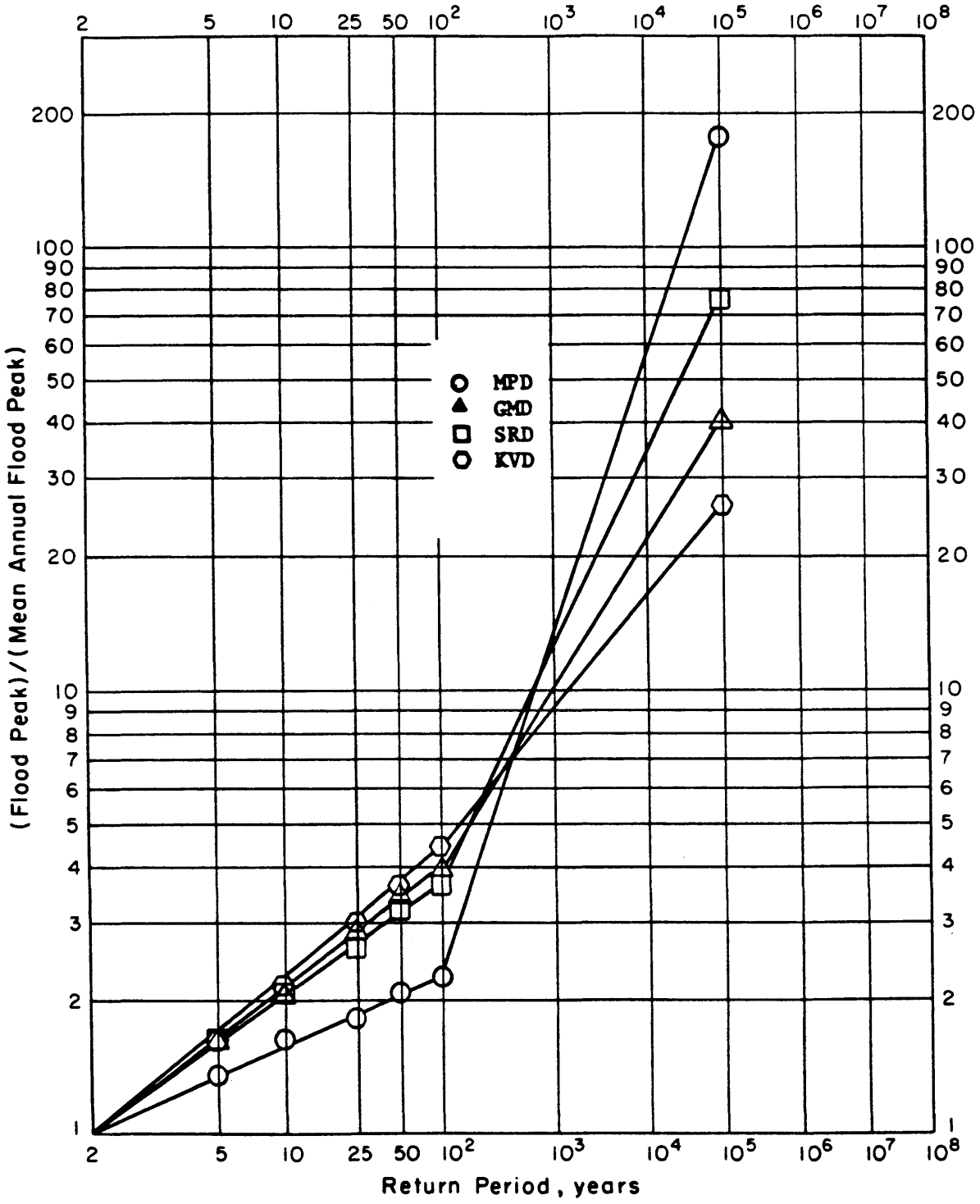

Figure 3.3: Flood Peak Probability Distributions for MPD, GMD, SRD, and KVD

This method is far from perfect. The kink in the distribution at the 100 yr. flood is certainly unrealistic. When different functions are used in different regions, the transitions should be smooth. Also, there is still a need to specify the return period of the PMF. Further, the appropriate line for extending the distribution past the 100 yr. flood may be skewed more or less than the straight line implies (a straight line implies the logarithms of the flood peaks have zero skew, greater skew causes upward curvature and lesser skew causes downward curvature).

Connecting the 100 yr. flood and PMF with a straight line has two advantages over other methods of interpolation. First,the effect of changing the distribution for only the higher frequency floods can be examined because the flood frequency distribution below the 100 yr. flood can be left unchanged while the distribution above the 100 yr. flood is varied. (This advantage would apply even if the 100 yr. flood and PMF were connected with a curved line.) Second, as discussed in Section 2.5.1, a straight line on log normal paper may be represented with a lambda distribution, which is mathematically explicit, and the procedure described in Section 2.5.1 may be used to estimate the lambda distribution parameters from the 100 yr. flood and the PMF with a specified return period. Floods having the desired return period can then be computed from the lambda distribution.

The probability distribution of flood frequency is specified as a table of values for the computer program. The points given are the 2,

5, 10, 25, 50, and 100 yr. floods computed from the USGS equations and the 200, 500, 1000, 2000, 5000, 10000, 20000, 50000, and 100000 yr. floods computed from the lambda distribution. The 100,000 yr. flood is the PMF. Section 4.1.1 examines the sensitivity of the results to the choice of PMF return period.

3.3 Reservoir Parameters

The reservoir parameters are the length of the dam, B_d (see Figure 2.6), the reservoir shape parameter, P_4 (see Figure 2.3), the probability distribution of initial stage, H_o, and the coefficients of the volume-discharge function k_1, k_2, k_3, and k_4 (see Figure 2.2).

The length of the dam, B_d, was taken directly from the data source for each dam.

The reservoir shape parameter, P_4, is estimated by plotting volume against stage on log-log paper, fitting a line through the points, and computing the slope of the line. The slope, in terms of logarithms, equals P_4. Figure 3.4 shows data for MPD, GMD, SRD, and KVD. The lines were fit by eye.

A single representative value of the initial reservoir stage, H_o, equal to the mean stage, is used in this work. This is done to clarify the influence of a given initial stage and of changes in the initial stage.

The reservoir discharge parameters, k_1, k_2, k_3, and k_4, are estimated by plotting volume against discharge, fitting lines through

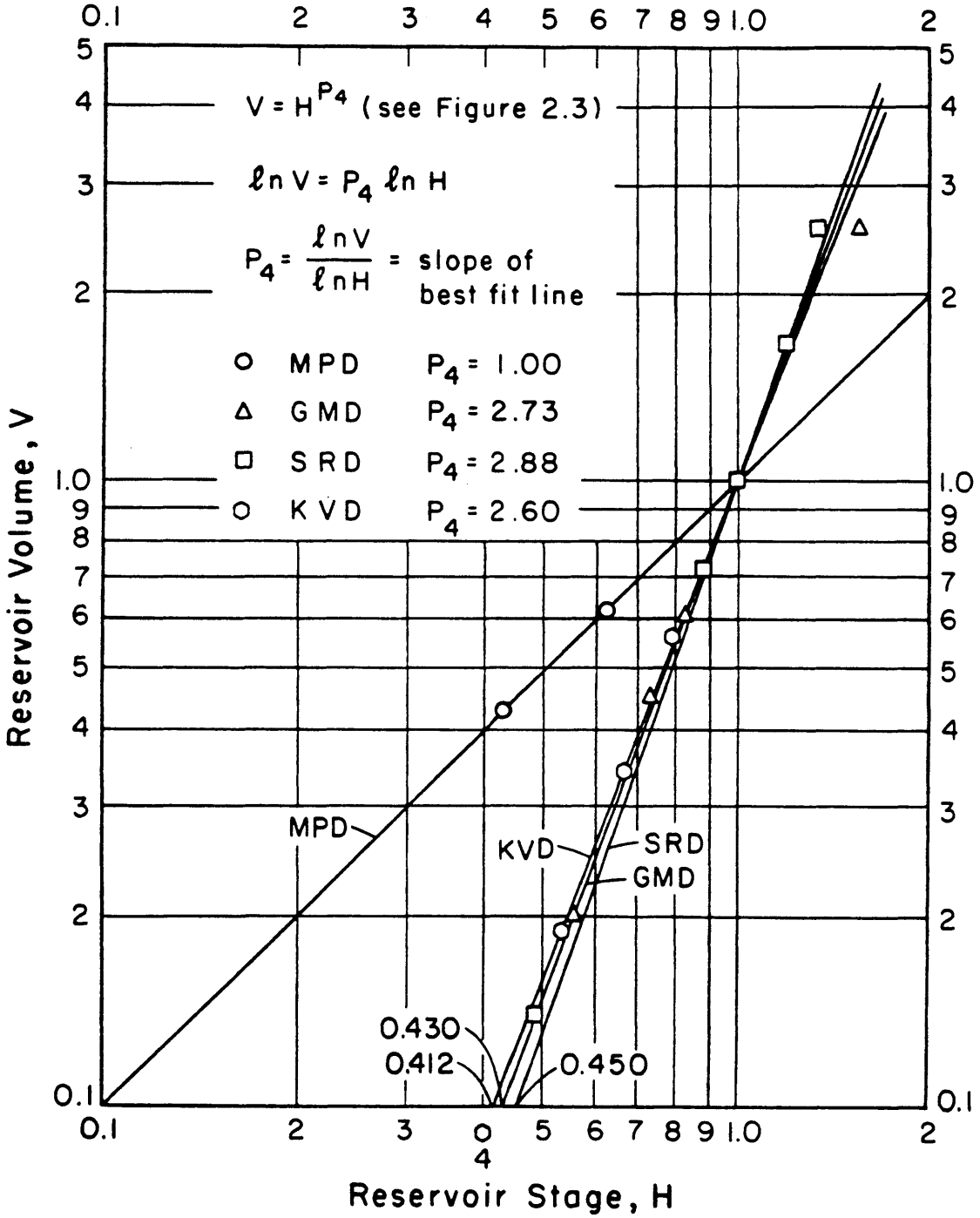

Figure 3.4: Estimation of Reservoir Shape Parameter

the points, and computing the slopes and intercepts of the lines. Figure 3.5 shows data and parameter estimates for MPD, GMD, SRD and KVD. The lines were fit by eye.

The outlet works at GMD and SRD are normally left in the same configuration all year. At MPD, some stoplogs are removed from the outlet works to lower the reservoir by two feet during the winter and spring. The parameters used here are for the winter and spring conditions. The outlet works at KVD are operated according to an elaborate schedule which includes consideration of not only the reservoir stage at KVD, but also the amount of precipitation and the river and reservoir stages elsewhere in the watershed. No attempt was made to duplicate this operating schedule. We assume here only that the outlet works are fully open when the reservoir stage is at the spillway crest.

The breakpoint in the reservoir discharge function may be at either the crest of the emergency spillway, neglecting the change at the crest of the dam, or at the crest of the dam, neglecting the change at the crest of the discharge works. The first way is called "upper limb as spillway" and the second is called "lower limb as spillway" in Figure 3.5 and Table 3.2. The appropriate choice depends on both the characteristics of the dam and the purpose of the analysis. The outlet works on SRD are so small that they may be neglected. The outlet works and emergency spillway on KVD are so large that the change in discharge function at the crest of the dam may be neglected. MPD

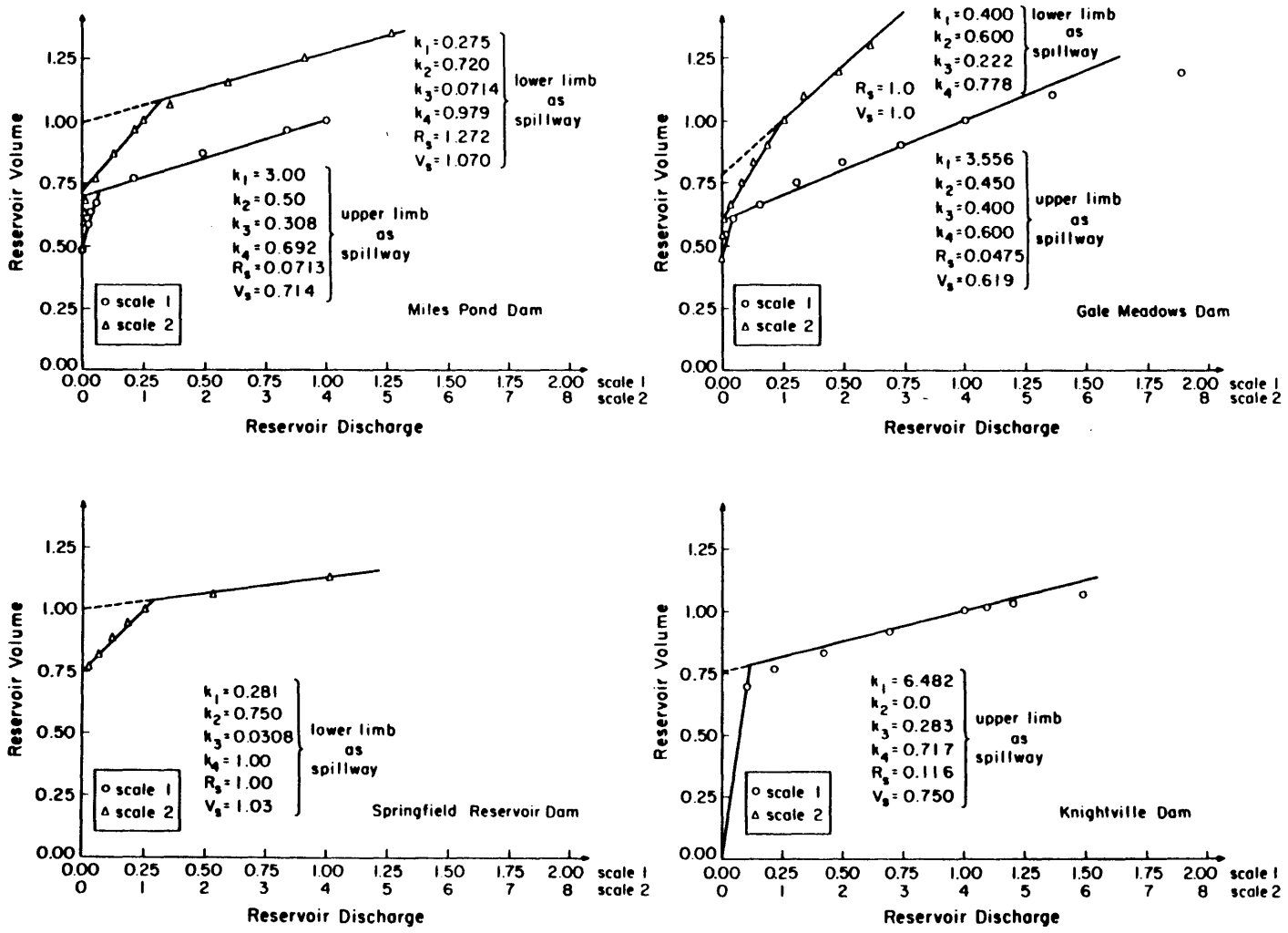

Figure 3.5: Estimation of Reservoir Discharge Parameters

and GMD are intermediate situations. When the details of the reservoir outlet works are of interest, as when modeling changes in the crest height of the spillway or outlet works, flow over the crest of the dam must be neglected. The outlet works may be neglected for most other purposes.

The reservoir discharge parameters which neglect the outlet works will be used except where stated otherwise.

3.4 Breach Parameters

The breach parameters are the width and depth ratios, P_1 and P_2 (see Figure 2.6 and Equations 2.5 and 2.6), the probability distribution of the reservoir stage at which failure occurs, H_f (see Figure 2.6), and probability of non-overtopping failure, P^{NOF}. The probability of overtopping failure is computed in the model (see Appendix B5).

Typical values of the width and depth ratios, P_1 and P_2, were discussed in Section 2.3.3. The values chosen for the four dams used here are based on those values, with modifications for the condition and characteristics of each dam. $P_1 = 0.9$ and $P_2 = 2.7$ were selected for GMD and KVD. Somewhat smaller values, $P_1 = 0.8$ and $P_2 = 2.5$, were selected for MPD because the dam is so low, and still smaller values, $P_1 = 0.7$ and $P_2 = 2.0$, were selected for SRD because the volume of water impounded by the dam is so small. The particular values chosen for MPD and SRD are quantitatively arbitrary, but qualitatively reasonable.

For MPD, GMD, and SRD, the failure stage, H_f, was specified as a single value, equal to the height of the dam, with probability equal to one. These three dams are normally kept nearly full and have probably experienced floods which require use of the emergency spillway.

A failure probability of one when the water reaches the dam crest is not strictly correct. These dams can probably withstand some overtopping. SRD was overtopped in 1969. The overtopping caused severe erosion, but did not cause a breach. In absence of good information about how much overtopping the dams can withstand, however, the dams are assumed to fail when overtopped.

KVD is normally nearly empty. It filled to the spillway crest in 1949, to within two feet of the spillway crest in 1955, to within twenty three feet of the spillway crest in 1960, and has not filled to within thirty feet below the spillway crest since. Since these extreme floods are separated by several years, and the dam has never been filled above the spillway crest, the failure probabilities appropriate for use when the dam fills above the spillway crest are those for a first filling. Baecher et al. (1980) suggested that the annual average failure probability for first filling and the first five years after construction is 10^{-3}. This 10^{-3} chance of failure was spread over the top ten feet of the dam by assigning a $(3)10^{-4}$ probability of failure at ten feet below the dam crest, an additional $(7)10^{-4}$ probability of failure at five feet below the crest of the dam, and an additional 0.999 probability of failure, which brings the cumulative probability

to one, at the crest of the dam.

10^{-3} may be too high for estimating overtopping failure probabilities, because it was developed as an annual failure probability for all types of failure. The real first filling failure probability, however, without also including the first five years after construction, is probably higher than 10^{-3}, at least for rapid unmonitored fillings, so 10^{-3} was used.

For MDP, GMD, and SRD, P^{NOF} was estimated using the method proposed by Bohnenblust and Vanmarcke (1982). This method translates qualitative information about the condition of the dam, as is contained in Phase I inspection reports, into quantitative information about failure probabilities. Appendix A describes the general method and computations for these three dams.

For KVD, P^{NOF} was not estimated using the method proposed by Bohnenblust and Vanmarcke (1982) because no inspection reports were available. KVD was assumed to be in generally good condition. Baecher et al. (1980) suggested that the annual average non-overtopping failure probability for dams over five years old in good condition was around $(3.5)10^{-5}$ (see Appendix A, Table A5). This value was reduced to $(1)10^{-6}$ for KVD because the normal reservoir stage is so low.

3.5 Channel Parameter

The channel parameter, K, is the slope of the volume-discharge curve (see Figure 2.4). As discussed in Section 3.1, the same non-

dimensional value of K is used for each dam in the parameter variation studies presented in Chapters 4 and 5, though the common value used is varied to examine the influence of channel storage. Equating the non-dimensional, rather than dimensional, values of K makes the channels similar with respect to the characteristic time of the dam (see Tables 2.1 and B1.1).

As a channel reach becomes longer or wider, the channel storage for a given discharge increases and K increases. As K increases the attenuation of the inflow peak increases. The relative attenuation of different shapes of flood waves also varies with K. Sharp transients, flood waves with high peaks and low volumes, are only slightly attenuated in short or narrow channels, but are severly attenuated in long or wide channels. On the other hand, broad transients, flood waves with low peaks and high volumes, are hardly attenuated in any channel. Appendix C describes and illustrates this behavior in greater detail.

Thus, while an increase in K causes a general decrease in the channel flood peaks, the importance of different types of flood events (natural floods, overtopping failures, or non-overtopping failures) may change as the character of the stream, reflected in the constant K, changes.

All of the parameter variation studies were run at two values of K, 0.001 and 1.0. K=0.001 represents a short or narrow channel, and K=1.0 represents a long or broad channel. Results are shown for

K=0.001 in most cases. Results are shown for K=1.0 when they are qualitatively different or illustrate a point better, as for example, when the relative importance of different types of flood events changes substantially with K.

3.6 Damage Function Parameters

The damage function parameters are the base discharge below which no damage occurs, Q_{nd}, the scale factors in the damage function, P_{6N} and P_{6B}, the exponents in the damage function, P_{7N} and P_{7B}, and the value of the dam, L_d, (see Figure 2.9). The values selected for these parameters are not chosen to represent any particular damage site, but rather to represent damage sites which could exist. Two further simplifications are that the value of the dam, L_d, will be neglected, and the same parameter values will be used for both failure and no-failure floods.

It would be interesting, and could be useful, to examine the effect on damage potential of variations between the failure and no-failure flood damage functions, and even variations between overtopping and non-overtopping failure damage functions. Also, as discussed briefly in Section 1.3, the use of utility functions to reflect the non-linear relation between the dollar value of damage and the effect on the community could be explored. Within the time and space limitations of this work, however, it is more important to examine the differences between various dams, rather than differences in the damage sites.

Only variations in the exponent of the damage function P_7, will be examined in Chapters 4 and 5.

The base flow below which no damage occurs, Q_{nd}, is set equal to the peak of the flood with a two year return period. This choice is somewhat arbitrary, but is a reasonable lower bound. Development in the channel required to carry the mean annual flood is rare.

The real size of Q_{nd} varies with location because channel geometry and economic development vary with location. Also, the size of the two year flood varies with location, usually increasing in the downstream direction. In spite of these considerations, the two year flood at the dam is appropriate for use in this work because additions to the river flow between the dam and damage site are not considered, and only damage attributable to the catchment upstream of the dam is of interest.

P_{6N} and P_{6B} are linear scale factors which will not affect the results qualitatively. P_{6N} and P_{6B} are both set equal to one.

P_{7N} and P_{7B} are probably the most significant damage parameters for the purposes of this work. P_{7N} and P_{7B} determine the relative importance of different size floods. As P_{7N} and P_{7B} increase,larger floods become relatively more significant. P_{7N} and P_{7B} will always have the same value in this work.

The flood plain model proposed by Bhavnagri and Bugliarello (1965), simplified by neglecting the base values below which no damage occurs and by linearizing the damage functions, can be used to help

define the possible range of P_7. Assume that damage to an individual structure is given by:

$$d = C_1(S_p - h) \tag{3.6}$$

where

d = damage to an individual structure

C_1 = constant

S_p = peak river stage

h = elevation of base of structure

Then specify the development density as a power function of stage.

$$V(h) = h^{C_2} \tag{3.7}$$

where

$V(h)$ = total value of development at ground elevation h

C_2 = constant

The total damage due to a flood with peak S_p can then be found by integrating

$$D(S_p) = \int_0^{S_p} h^{C_2} C_1(S_p - h)dh = C_3 S_p^{C_2+2} \tag{3.8}$$

where

$$C_3 = \frac{C_1}{C_2+1} - \frac{C_1}{C_2+2}$$

and

$D(S_p)$ = total damage due to flood with peak stage S_p. If the rating curve at the damage site is then given by

$$Q_P = C_4 S_p^{C_5} \tag{3.9}$$

The damage may be written as

$$D(S_p) = C_3 \left(\frac{Q_p}{C_4}\right)^{\frac{C_2+2}{C_5}} \tag{3.10}$$

The term $(C_2+2)/C_5$ in Equation 3.10 is approximately equal to P_7. C_2 can vary substantially, depending on the type of development. Bhavnagri and Bugliarello (1965) suggest that C_2 can range at least -1 to 2. C_5 depends on the river geometry. From Mannings equation (Henderson, 1966), C_5 is approximately 1 2/3 for a rectangular channel, 2 1/3 for a parabolic channel, and 2 2/3 for a triangular channel with 10 to 1 side slopes. C_5 increases as the side slopes of the channel get flatter. Varying C_2 from -1 to 2 and C_5 from 2 to 3 gives a range for P_7 of 1/3 through 2.

$P_7 = 2$ and $P_7 = 1$ are used in this work. When P_7=2, larger floods are relatively more important than when P_7=1. Results are usually shown for $P_7 = 2$, and results are shown for $P_7 = 1$ when they are qualitatively different than for $P_7 = 2$.

Table 3.2

Parameter Values Part A: Non-Stochastic Parameters

	MPD	GMD	SRD	KVD
H_c (ft)	10.4	27.0	47.0	150.0
V_c / $\underline{V}_c$ (ft^3) / (af)	9.58E7 / 2,199	1.28E8 / 2,942	1.05E7 / 240	3.09E9 / 71,016
R_c / $\underline{R}_c$ (cfs)	2,355	5,300	1,040	143,365
t_c / $\underline{t}_c$ (s) / (hr)	4.07E4 / 11.3	2.42E4 / 6.7	1.01E4 / 2.8	2.16E4 / 6.0
B_{pg}	0.8	4.1	82.6	10.9
t_p / $\underline{t}_p$ (hr)	0.366 / 4.14	0.813 / 5.45	1.013 / 2.83	1.67 / 10.0
t_b / $\underline{t}_b$ (hr)	0.988 / 11.18	2.195 / 14.72	2.735 / 7.64	4.51 / 27.0
	Upper Limb as Spillway			
k_1 / $\underline{k}_1$ (hr)	3.00 / 33.9	3.560 / 23.9	-	6.480 / 38.9
k_2 / $\underline{k}_2$ (af)	0.500 / 1,100	0.450 / 1,324	-	0.000 / 0
k_3 / $\underline{k}_3$ (hr)	0.308 / 3.48	0.400 / 2.68	-	0.283 / 1.70
k_4 / $\underline{k}_4$ (af)	0.692 / 1,522	0.600 / 1,765	-	0.717 / 50,918
R_S / $\underline{R}_S$ (cfs)	0.0713 / 168	0.0475 / 252	-	0.116 / 16,630
V_S / $\underline{V}_S$ (af)	0.714 / 1,570	0.619 / 1,821	-	0.752 / 53,404
	Lower Limb as Spillway			
k_1 / $\underline{k}_1$ (hr)	0.275 / 3.11	0.400 / 2.68	0.281 / 0.787	-
k_2 / $\underline{k}_2$ (af)	0.720 / 1,583	0.600 / 1,765	0.750 / 180	-
k_3 / $\underline{k}_3$ (hr)	0.0714 / 0.807	0.222 / 1.49	0.0308 / 0.0862	-
k_4 / $\underline{k}_4$ (af)	0.979 / 2,153	0.778 / 2,289	1.00 / 240	-
R_S / $\underline{R}_S$ (cfs)	1.272 / 2,993	1.0 / 5,300	1.00 / 1,040	-
V_S / $\underline{V}_S$ (af)	1.070 / 2,353	1.0 / 2,942	1.03 / 247	-
P_3	9.21E6	1.58E4	1.61E2	6.79E3
P_4	1.0	2.73	2.88	2.60
H_o / $\underline{H}_o$ (ft)	0.50 / 5.2	0.746 / 20.1	0.894 / 42.0	0.044 / 6.6
B_c / $\underline{B}_c$ (ft)	38.5 / 400	11.1 / 300	6.7 / 315	8.0 / 1,200
P_1	0.8	0.9	0.7	0.9
P_2	2.5	2.7	2.0	2.7
H_f / $\underline{H}_f$ (ft)	1.0 / 10.4	1.0 / 27.0	1.0 / 47.0	See Table 3.3
P^{NOF}	8.0E-6	3.5E-5	1.7E-4	1.0E-6

Note: EN = 10^N e.g. E-5 = 10^{-5}

Table 3.3

Parameter Values Part B: Stochastic Parameters
(Reservoir Inflow Flood Peak for all Four Dams and
Overtopping Failure Stage for KVD)

Peak Reservoir Inflow, I_p / $\underline{I}_p$ (cfs)		MPD	GMD	SRD	KVD
Return Period	2	0.0282 / 66	0.0534 / 283	0.0569 / 59	0.0382 / 5,344
	5	0.0385 / 91	0.0861 / 456	0.0916 / 95	0.0620 / 8,631
	10	0.0454 / 107	0.113 / 600	0.119 / 123	0.0816 / 11,329
	25	0.0527 / 124	0.153 / 809	0.150 / 156	0.112 / 15,485
	50	0.0580 / 137	0.182 / 964	0.181 / 189	0.138 / 19,041
	100	0.0646 / 152	0.222 / 1,178	0.216 / 224	0.173 / 23,830
PMF		5.11 / 12,035	2.16 / 11,440	4.54 / 4,720	1.02 / 145,800

Failure Stage Probability
Distribution for KVD

Failure Stage H_f / $\underline{H}_f$ (ft)	Cumulative Probability
0.9333 / 140	3E-4
0.9667 / 145	1E-3
1.0 / 150	1

Note: EN = 10^N e.g. E-5=10^{-5}

Chapter 4

VARIATION OF UNCERTAIN PARAMETERS

Chapter 4 examines the sensitivity of damage potential to variations in several model parameters, concentrating on parameters which are difficult to estimate accurately. Chapter 5 will consider variations in parameters which reflect the design of the spillway and operation of the dam. Chapter 3 described the physical characterisics of and parameter estimates for the four dams which will be examined.

Several of the model parameters are difficult to estimate and are at best highly uncertain. The PMF size and return period are selected to define several possible probability distributions of large floods. There is no way, at present, to determine which choice is closest to reality (see Section 2.5.1). Using a single volume/peak ratio for reservoir inflow floods of all sizes is a gross approximation at best. There are no established procedures for estimating the breach size parameters and Overtopping Failure stage, though historical data provide some guidance. The procedure used to estimate the Non-Overtopping Failure probability (see Appendix A) has not yet been tested, and the parameters used within the procedure are only preliminary conjectures.

Yet all these parameters must be estimated to begin progressing towards usable methods of risk analysis for spillway evaluation, and, as a first step, it is useful to examine sensitivity of the results to variations in these parameters.

Chapter 4 examines variations of the following seven parameters: In Section 4.1, three parameters of catchment hydrology:

1) PMF size

2) PMF return period

3) reservoir inflow flood volume-peak relation

and in Section 4.2, four parameters of dam breaches:

4) breach depth

5) breach width

6) Overtopping Failure stage

7) Non-Overtopping Failure probability.

Section 4.3 discusses some conclusions which may be drawn from the results.

The significance of the results shown in Chapter 4 is not in the general trends shown, the general trends are as expected in all cases, but is rather in the changes in relative contributions of the several components of total damage potential (see Section 2.6) and in how much the damage potential and failure probabilities change with the parameter changes. Overtopping Failure probabilities increase with increasing PMF size, increasing reservoir inflow flood volume, decreasing failure stage, and decreasing PMF return period. Total damage potential increases with increasing PMF size, reservoir inflow flood volume, breach depth or width, and probability of Non-Overtopping Failure. Total damage potential decreases with increasing PMF return period. Total damage potential decreases with increasing failure stage in all the results shown here. Total damage potential, however, could either increase or decrease with increasing failure stage, because the damage given failure will increase and the probability of failure will decrease. The balance between the

two terms determines the net trend.

The parameter variation studies presented here do not tell the correct values for the parameters. Rather, they indicate which parameters influence the results the most, and thus where the most effort towards refining the parameter estimates, or the model formulation, should be applied.

The four combinations of channel and damage site parameters described in Chapter 3, $(K,P_7) = (0.001,2)$, $(1,2)$, $(0.001,1)$, and $(1,1)$, were examined for each of the parameter variation studies. The results for $K = 0.001$, a short or narrow channel, with $P_7 = 2$, damage proportional to the square of peak discharge, are shown for most cases. Results for the other channel and damage parameter combinations are shown when they either illustrate a point better than or differ qualitatively from the results for $(K,P_7) = (0.001,2)$ as, for example, when the relative balance between No-Failure and Overtopping Failure damages changes. The failure probabilities are independent of K and P_7.

The magnitudes of the non-dimensional damage computed with different values of P_7 can not be compared directly. Non-dimensional damage is multiplied by the factor $P_6\underline{R}_c^{P7}$ (see Equation B4.3) to compute dimensional damage, which then can be compared directly. Table 3.2 lists the values of $\underline{R}_c$ for each dam.

The results shown in this work are non-dimensional damage. This eases comparisons among different dams for a given value of P_7, though the absolute values of damage still can not be compared directly, because $\underline{R}_c$ varies among the dams, but complicates comparison among different values of P_7 at the same dam. The relative variations in damage with

variations in parameter values and the relative contributions of damage from different sources (No-Failure, marginal Overtopping Failure, and Non-Overtopping Failure) are emphasized here. The variation of dimensional damage below a given dam as P_7 changes is not discussed.

Special Note About MPD

Results for damage potential variations at MPD are shown only in Sections 4.1.1 and 4.2.3. These results illustrate the insignificance of marginal Overtopping Failure and Non-Overtopping Failure damage relative to No-Failure damage. The results for MPD, however, are not sufficiently accurate for drawing further conclusions, because MPD is in the class of low dams for which this model may not predict the peak reservoir discharge during an overtopping failure accurately. (See Section 2.3.2.2.)

The low value of B_{pg} (see Equation 2.3) for MPD signals the potential existence of this problem. B_{pg} is a measure of the size of the peak reservoir discharge from Overtopping Failure floods, relative to that from Successfully Passed floods.

The peak discharge from a breach of MPD, when failure occurs with reservoir stage at the crest of the dam, with $P_1 = 0.8$, and $P_2 = 2.5$, is 2,250 cfs (see Equation 2.1). The discharge from the spillway and outlet works when the reservoir stage is at the crest of the dam is 2,350 cfs. To claim that the peak reservoir discharge during an Overtopping Failure is determined primarily by the breach is clearly wrong for this situation. The peak could easily be determined either by the pre-breach reservoir discharge or, if the breach occurs before the time to peak of a large flood, the reservoir inflow flood routed through the now existing breach.

This problem is partially corrected by letting R_{pb}, the peak

failure discharge (see Figure 2.5), equal the larger of the reservoir discharge at the failure stage or the peak discharge through the breach. Thus, for example, R_{pb} is increased to 2,350 for the conditions described above. This solution is far from exact, but at least avoids the problem of having a breach cause a reduction in flood damages.

The reservoir inflow peaks for the very large floods at MPD are much larger than either the peak spillway or breach discharge. Thus, the real peak reservoir discharge is probably larger than either the spillway discharge at the time of failure or the peak breach discharge. Because of this, the No-Failure damage is a better estimate of the total damage caused by reservoir inflow floods than is the sum of the Successful Passage and Overtopping Failure damages. Also, the computed Overtopping Failure damage is too low.

Mathematically, as computed in this model, the marginal Overtopping Failure damage is negative, because the Overtopping Failure damage is less than the No-Failure damage. These negative values are displayed as zeroes in the results shown in Chapters 4 and 5.

The marginal Overtopping Failure damage should be a small positive number; the primary effect of Overtopping Failure at MPD is to reduce the attentuation of the flood as it passes through the reservoir (because the effective spillway size has been increased). Thus, the Overtopping Failure damage will be slightly larger than the No-Failure damage. This effect is not represented by the model.

Computation of the Overtopping Failure probability is not affected by these problems.

4.1 Catchment Hydrology Parameters

4.1.1 Probability Distribution of Large Floods

The difficulty of defining the probability distribution of extremely large floods was discussed in Sections 1.2.1 and 2.5.1. Variation of the PMF size and return period is used to define a variety of probability distributions for large floods. The probability distribution below the 100 year flood is not changed.

ASCE (1973) suggested that 10^4 years was probably lower than the real return period for a PMF. The study by Hershfield (1961), discussed in Section 1.2.1, confirms this guess, assuming that the return periods of the PMP and PMF are similar. No upper limit on the PMF return period is known. The return period of the PMF is varied here from 10^4 through 10^8 years. As will be seen later in this section, estimates of the damage potential become insensitive to the PMF return period as it approaches 10^8 years.

The PMF size is varied from 60 to 120 percent of the original estimate. This variation was chosen arbitrarily. Since the PMF size is used primarily as a parameter of the flood peak distribution for large floods, the estimates of the PMF developed in Chapter 3 have little intrinsic meaning, except as the largest flood for which spillways are designed.

Figures 4.1 through 4.4, plotted on log-probability paper, show the range of probability distributions of peak reservoir inflow defined by these ranges of PMF size and return period.

The probability distributions of flood peaks used for the computations are defined by the 2, 5, 10, 25, 50, and 100 year floods computed from regional flood frequency estimates developed by the USGS (see Section

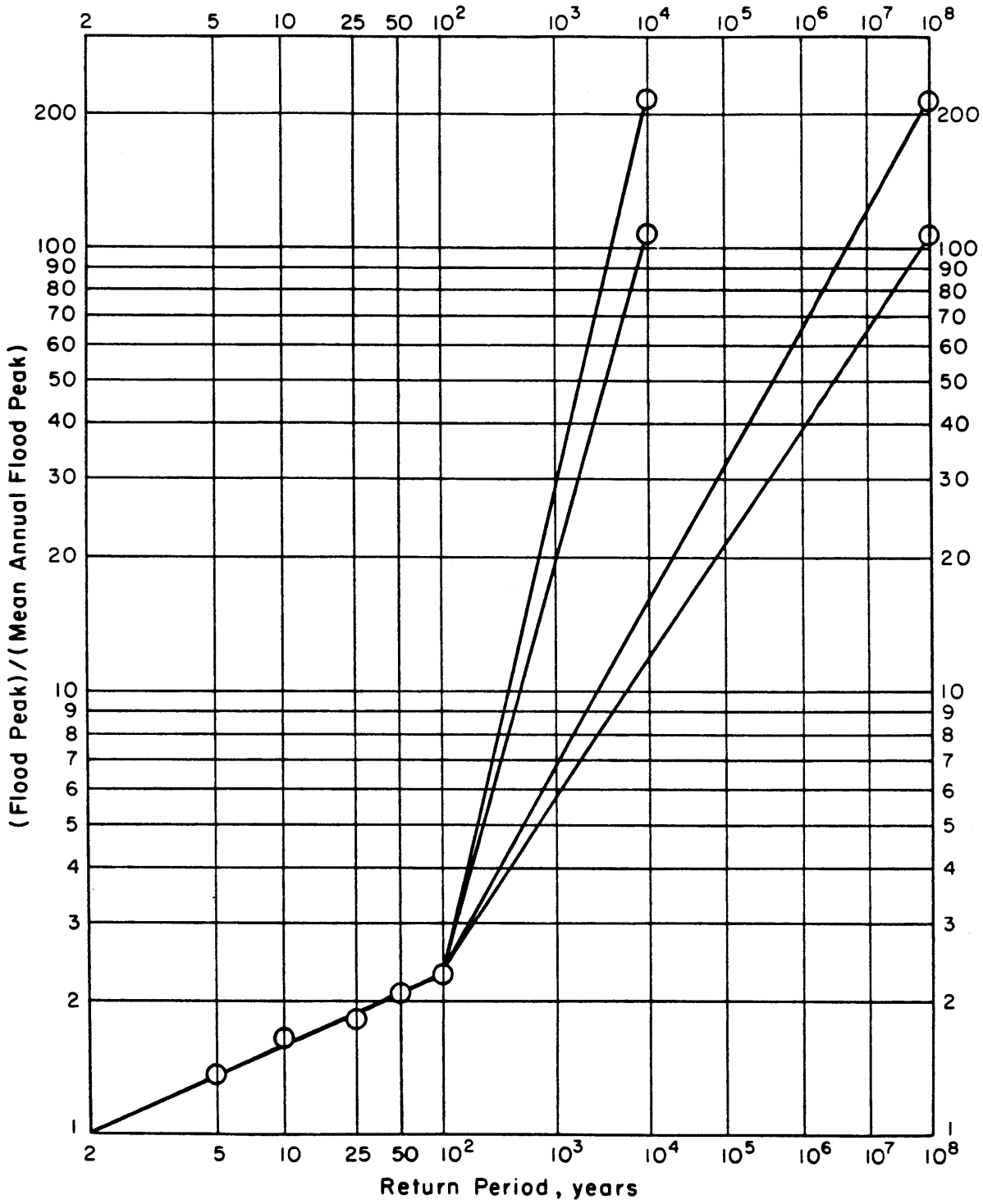

Figure 4.1: Range of Flood Peak Probability Distributions for Miles Pond Dam

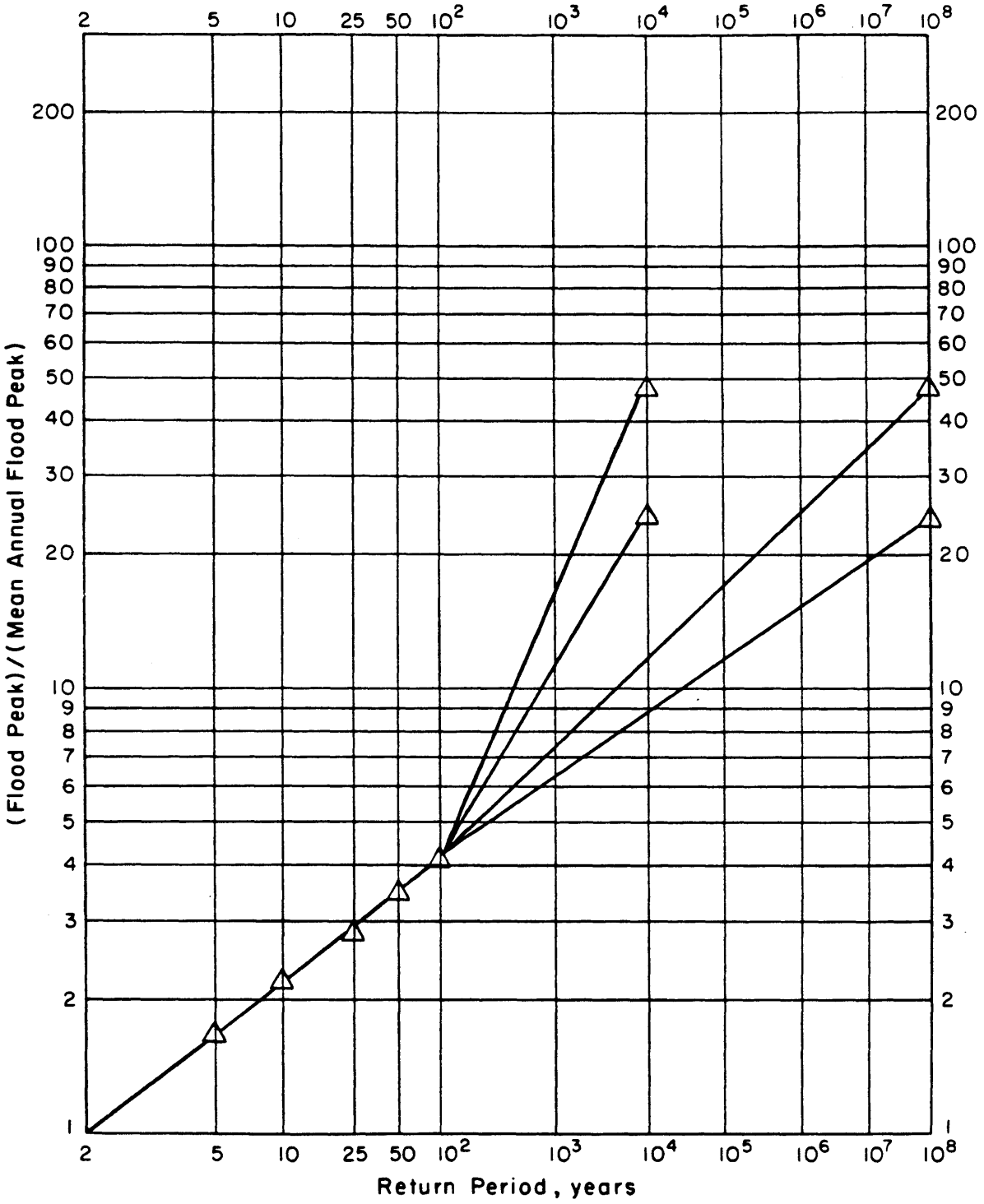

Figure 4.2: Range of Flood Peak Probability Distributions for Gale Meadows Dam

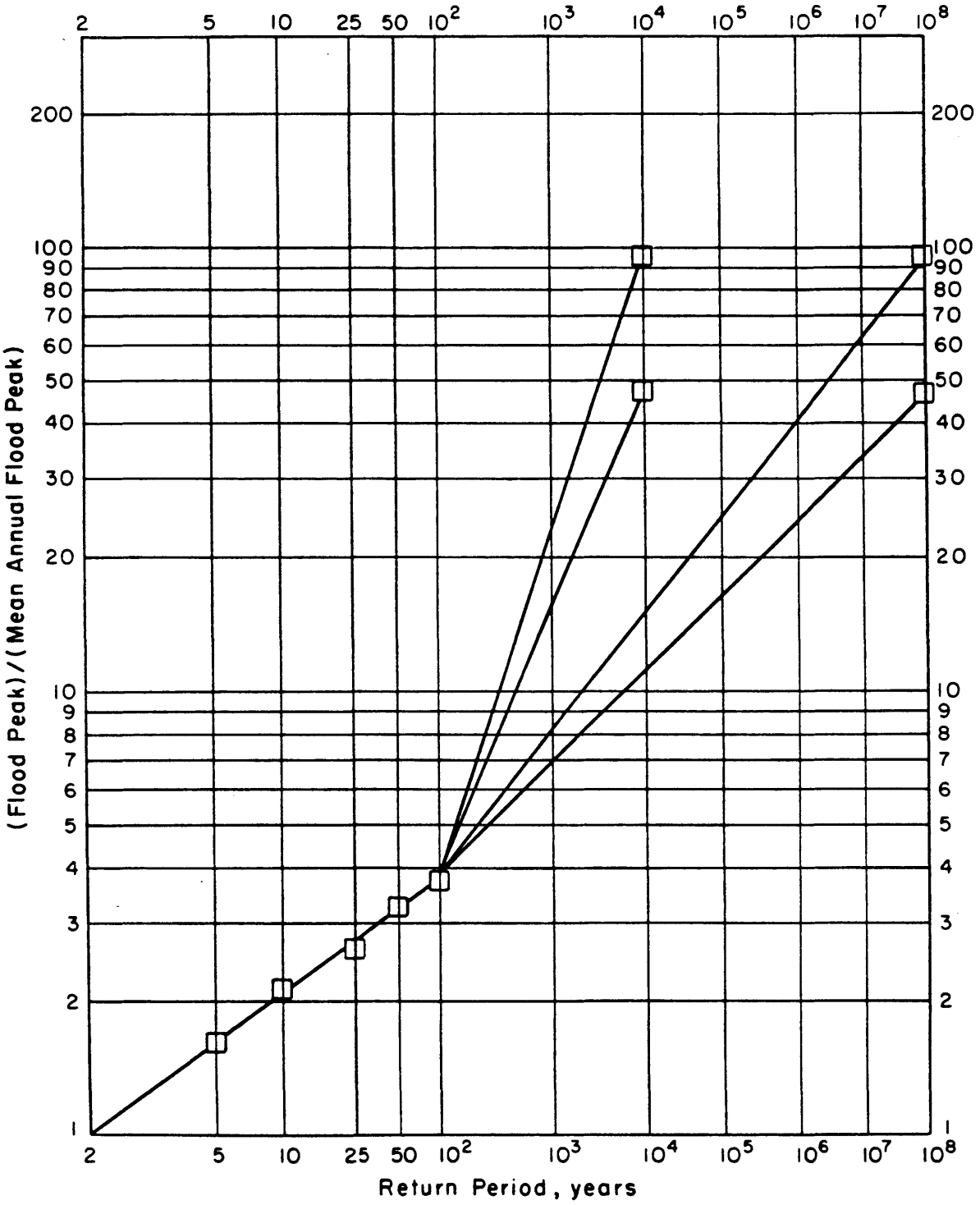

Figure 4.3: Range of Flood Peak Probability Distributions for Springfield Reservoir Dam

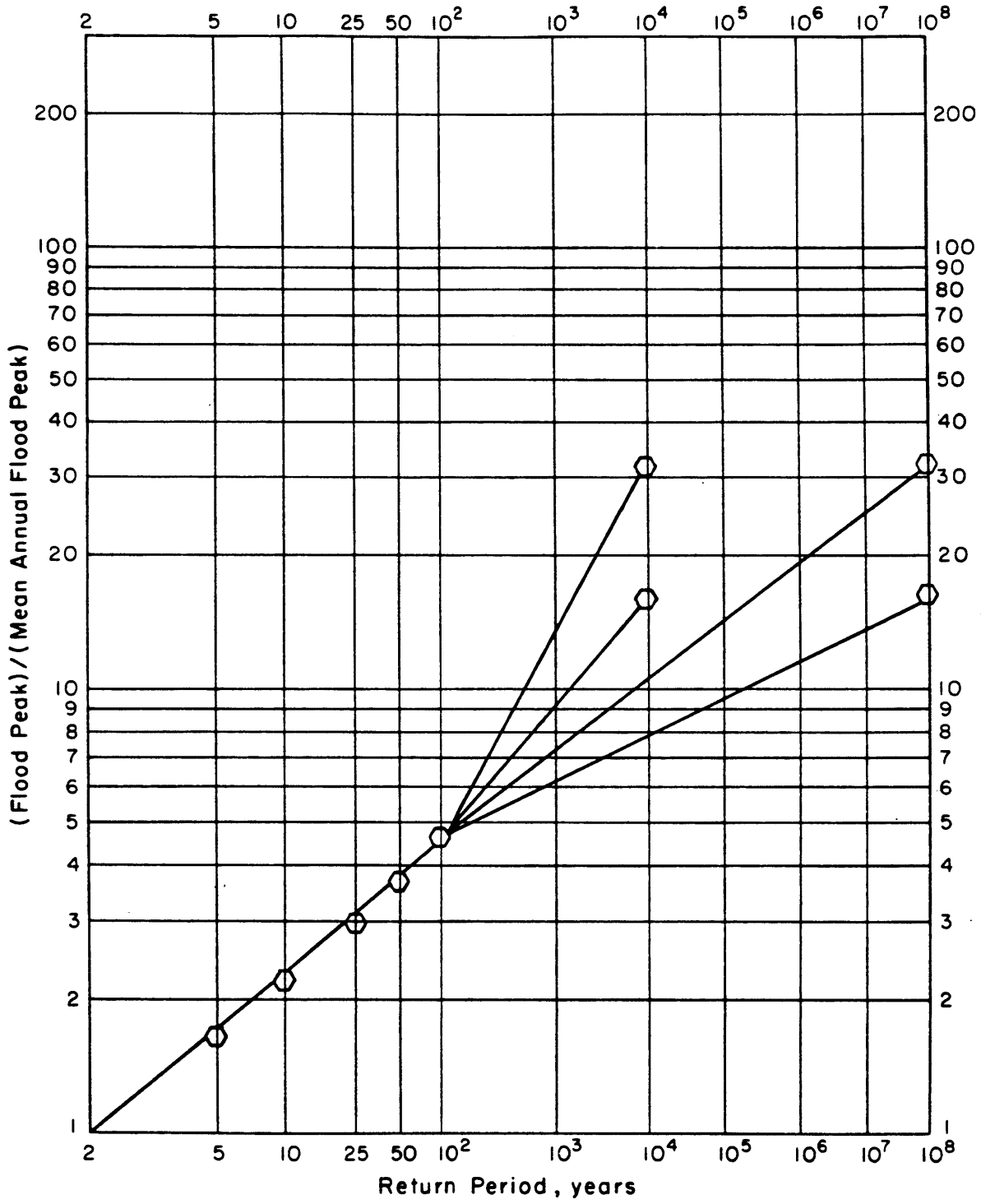

Figure 4.4: Range of Flood Peak Probability Distributions for Knightville Dam

3.2.2), and floods of selected return periods up to the return period chosen for the PMF. The return periods selected between the 100 year flood and PMF are the powers of 10, that is 10^3, 10^4, and so on, and the two tenths and five tenths points between the powers of ten, that is, 200, 500, 2000, 5000, and so on.

The PMF size and return period are varied together, with the results shown in three dimensional figures. The horizontal axes are the ratio of the PMF size to the original estimate of the PMF size and the logarithm of the PMF return period. Thus, for example, PMF size = 1.2 means that the size of the PMF is twenty percent larger than the original estimate, and log (PMF Return Period) = 5 means that the PMF return period is 10^5 years.

Figure 4.5 shows the failure probabilities for all four dams. The vertical scales vary among the plots, but all four start at zero. The dashed lines show the Overtopping Failure probability, and the solid lines show the total failure probability. Thus, the vertical distance between the dashed and solid lines equals the Non-Overtopping Failure probability (see Table 3.2 for values of P^{NOF}).

The Overtopping Failure probabilities all vary as expected, increasing as PMF size increases and decreasing as the PMF return period increases. The sensitivity of failure probability to PMF size increases as the return period decreases. The Overtopping Failure probabilities range from nearly 0 to $(4.5)10^{-4}$ for MPD, from 0 to $(4.2)10^{-4}$ for GMD, from $(3)10^{-5}$ to $(1.5)10^{-3}$ for SRD, and from 0 to $(1.0)10^{-4}$ for KVD.

KVD was designed to pass the PMF without overtopping. Figure 4.5 shows that the Overtopping Failure probability does indeed equal zero, unless the estimate of the PMF used for the design was low. The Overtopping

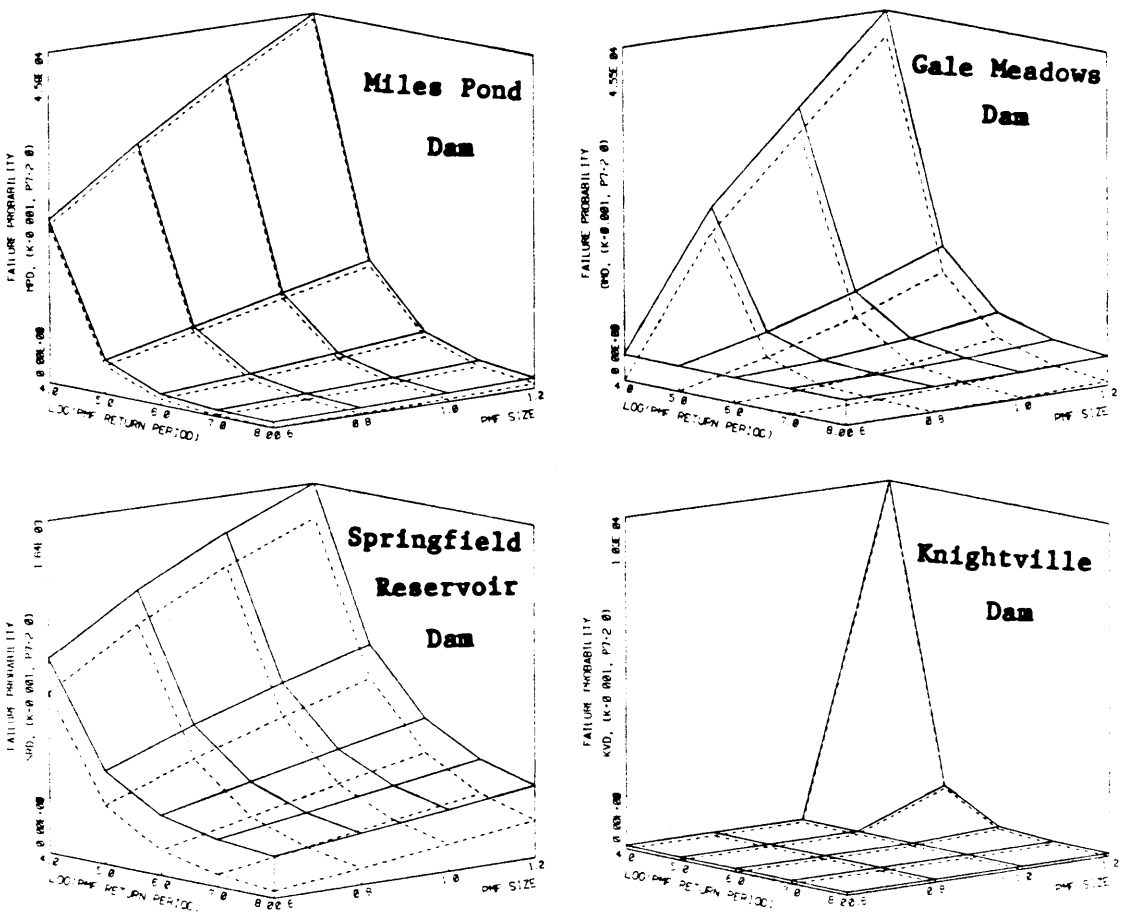

Figure 4.5: Variation of Failure Probability with Variation of PMF Size and Return Period

— — — Overtopping Failure Probability
——— Total Failure Probability

Failure probability for KVD when the PMF size is twenty percent larger than estimated is approximately equal to the probability of occurence for the PMF (the reciprocal of the return period).

Figures 4.6 through 4.15 show the variations in damage potential with variations in PMF size and return period. The mean No-Failure plots show two curves. The solid curves are natural flood damage, without the dam. The dashed curves are damage with the dam in place, assuming the dam never fails. Thus, the vertical distance between the dashed and solid curves equals the flood damage reduction due to the presence of the dam, assuming the dam never fails. This is similar to current practice for determining flood damage attenuation by a dam, differing in that the range of flood sizes considered here is much larger than normally used in flood damage studies.

Figure 4.6 shows the results for MPD with $(K,P_7) = (0.001,2)$. The results do not vary qualitatively for the other channel and damage parameters. As discussed in the introduction to this chapter the mean total damage, Successful Passage damage, and Overtopping Failure damage plots should be neglected. They are shown only to illustrate the model computations. The No-Failure damage curves show that MPD reduces flood damages substantially, as long as it does not fail. The marginal Overtopping Failure probability should probably be slightly larger than shown, because a breach acts like a large spillway, but is likely still small. This result is reasonable for such a low dam. Thus, for MPD, the primary flood damage potential is from the natural flood regime of the river.

The MPD spillway was inadequate under the Phase I inspection guidelines and was thus subject to a Phase II inspection in which the PMF

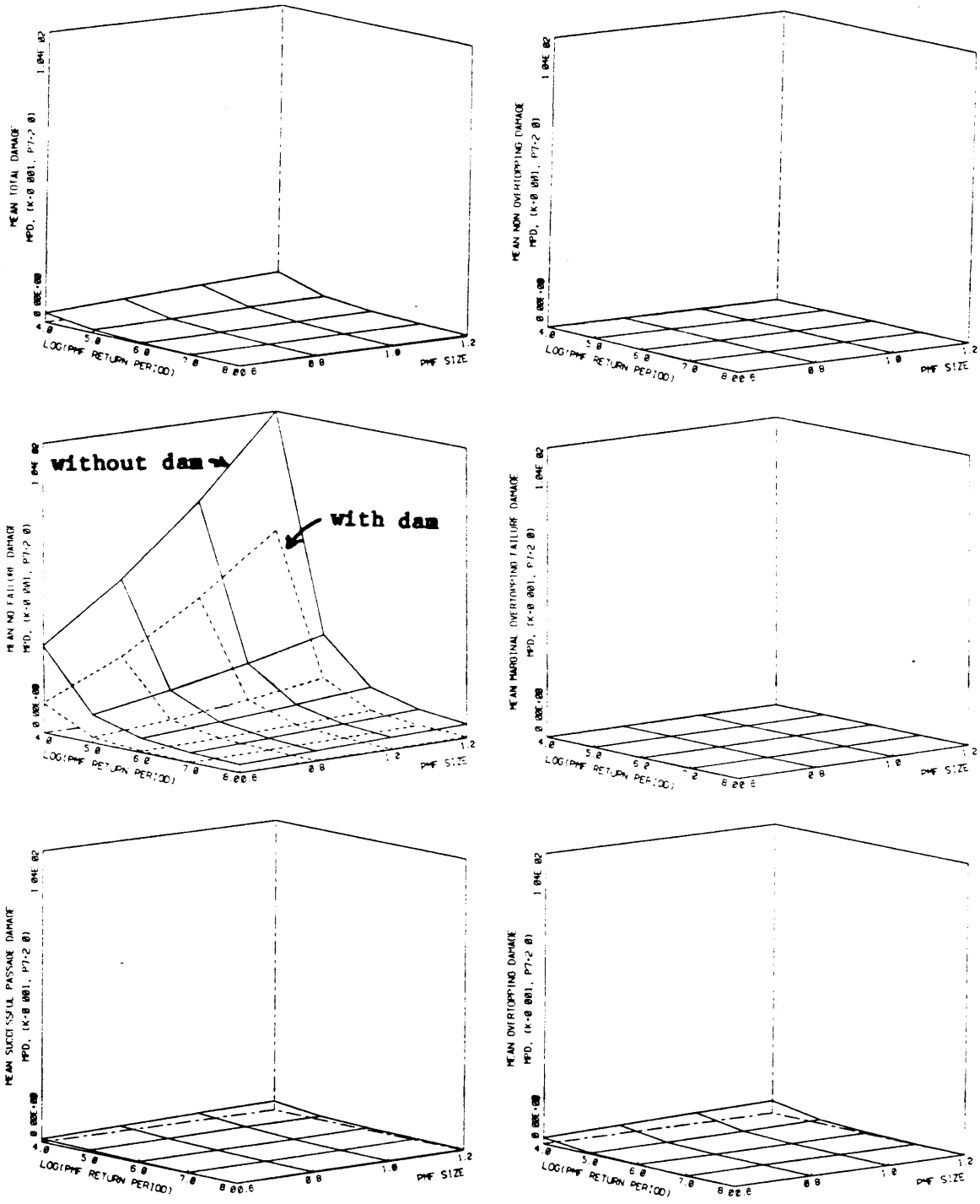

Figure 4.6: Variation of Damage Potential with Variation of PMF Size and Return Period for Miles Pond Dam with $(K,P_7) = (0.001,2)$

would be more carefully computed and routed. The results shown here suggest that sound economic analysis, and a careful investigation of the hydraulic effects of a larger spillway, not a refined estimate of the PMF, is needed to assess the need for a larger spillway. A larger spillway will likely increase the total expected flood damage.

Figures 4.7 and 4.8 show the results for GMD with $(K,P_7) = (0.001,2)$ and $(0.001,1)$. The results did not change qualitatively when K was increased to 1.0.

When $P_7 = 2.0$, Overtopping Failure damage contributes substantially to the total damage when the PMF return period is less than 10^6 or the PMF size is greater than one. If the PMF return period is 10^4 and the PMF size is twenty percent greater than estimated, the marginal damage due to Overtopping Failure is larger than the original damage potential without the dam. If the PMF return period is 10^5 and the PMF size is twenty percent greater than estimated, the total damage potential, with the dam, is nearly equal to the damage potential without the dam.

When $P_7 = 1.0$, failure damages are no longer very significant. The relative flood damage reduction caused by the dam is much higher than for $P_7 = 2.0$, and the marginal Overtopping Failure damages is a small portion of the total damage potential.

Thus, damage estimates for GMD are very sensitive to the probability distribution of extremely large floods when $P_7 = 2$, but relatively insensitive when $P_7 = 1$.

Figures 4.9 through 4.12 show the damage potential variations for SRD with $(K,P_7) = (0.001,2)$, $(0.001,1)$, $(1,2)$, and $(1,1)$. Because SRD is relatively high for its low volume, failures produce high peak discharges which will attenuate rapidly as the flood wave encounters

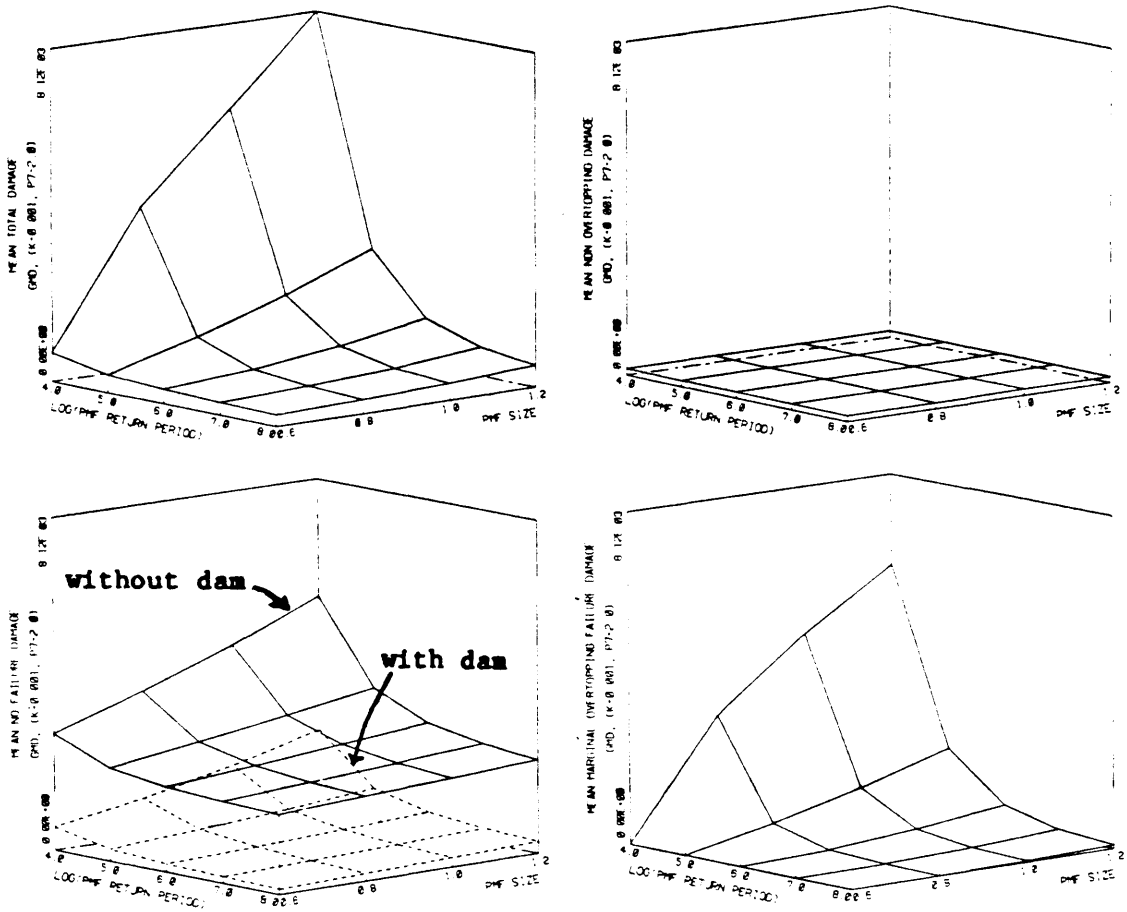

Figure 4.7: Variation of Damage Potential with Variation of PMF Size and Return Period for Gale Meadows Dam with $(K,P_7) = (0.001,2)$

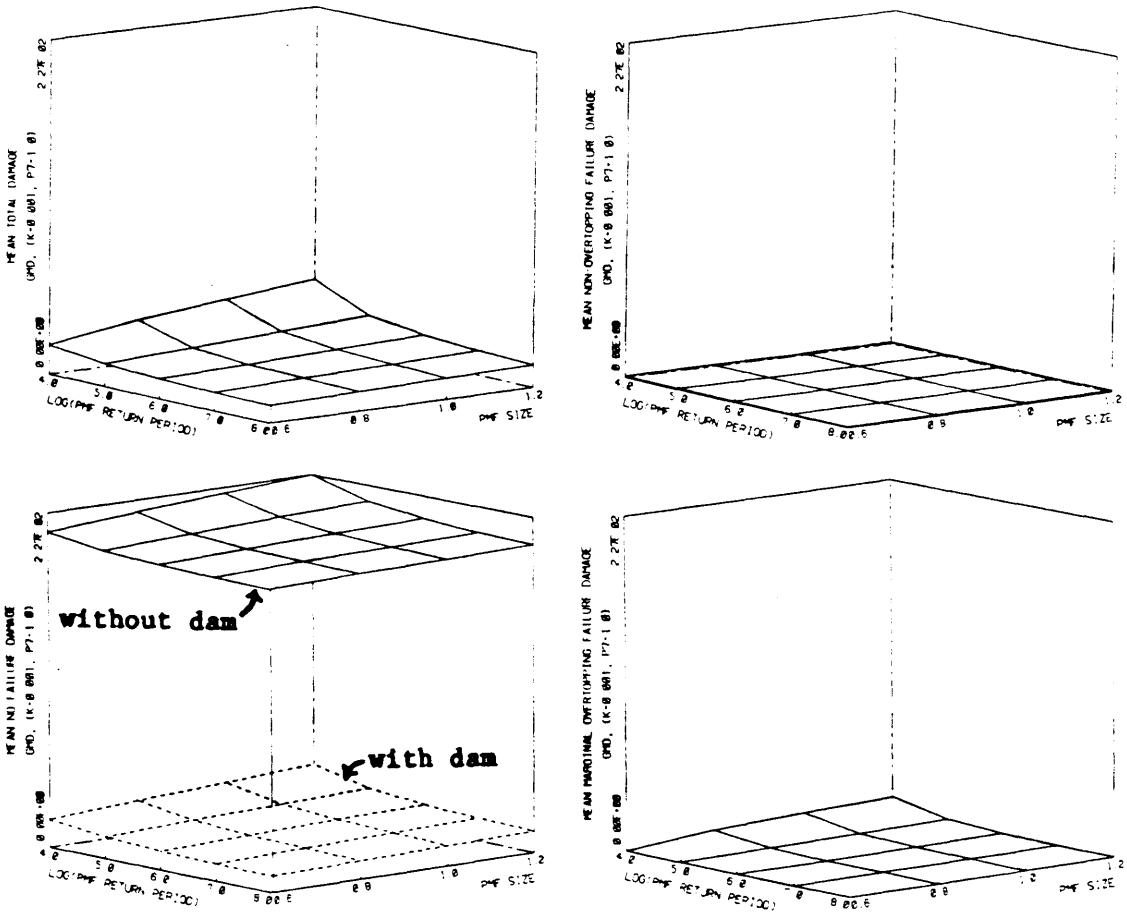

Figure 4.8: Variation of Damage Potential with Variation of PMF Size and Return Period for Gale Meadows Dam with $(K,P_7) = (0.001,1)$

channel storage. Thus, while failure damages may be significant near the dam, they will lose significance rapidly as the channel gets longer or wider. Results are shown for all four combinations of channel and damage parameters to illustrate these changes.

When $(K,P_7) = (0.001,2)$ (Figure 4.9), SRD provides relatively little natural flood damage attenuation, and Overtopping Failure damage dominates the total damage potential. Non-Overtopping Failure damage becomes more important than Overtopping Failure damage only when the PMF return period is high and PMF size is small.

When P_7 is changed to 1 (Figure 4.10), SRD provides relatively more natural flood damage attenuation, and the No-Failure flood damage becomes more significant. The marginal Overtopping Failure damage is still large, and it dominates the total damage potential if the PMF size is high and return period is low. The relative significance of the Non-Overtopping Failure damage does not change much.

When $(K,P_7) = (1,2)$ (Figure 4.11), the situation is very similar to $K = 0.001$ and $P_7 = 2$ (Figure 4.9), except that No-Failure damage is now more important when the PMF size is large and return period is small. The Successful Passage and mean Overtopping Failure damages are shown here, and in Figure 4.12, to illustrate the difference between total damage when Overtopping Failure occurs and the marginal damage which can be attributed directly to the failure. Successful Passage damage is nearly constant in Figures 4.11 and 4.12, while the No-Failure damage increases with increasing PMF size and decreasing return period.

When $(K,P_7) = (1,1)$ (Figure 4.12), the No-Failure damage potential dominates the total over the entire range of PMF sizes and return periods, though Overtopping Failure damage is also significant for low PMF return

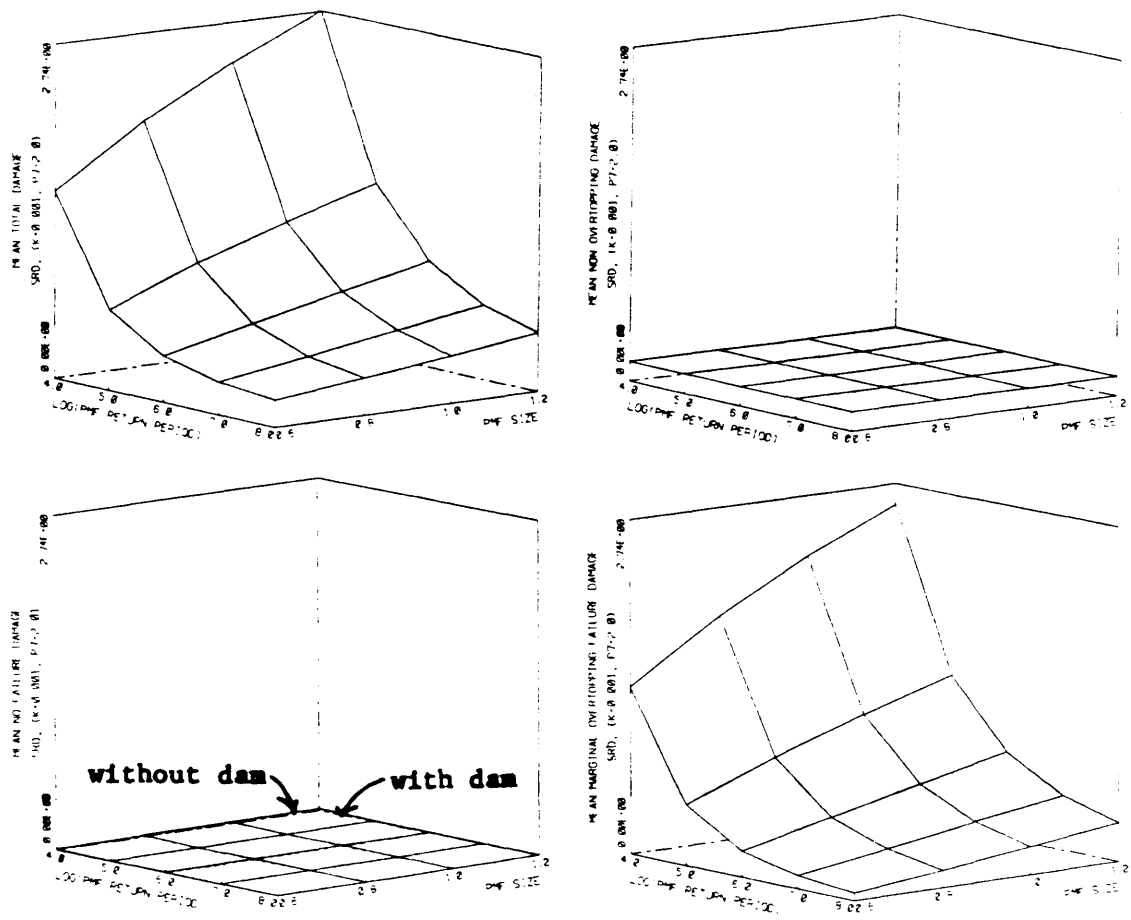

Figure 4.9: Variation of Damage Potential with Variation of PMF Size and Return Period for Springfield Reservoir Dam with $(K,P_7) = (0.001,2)$

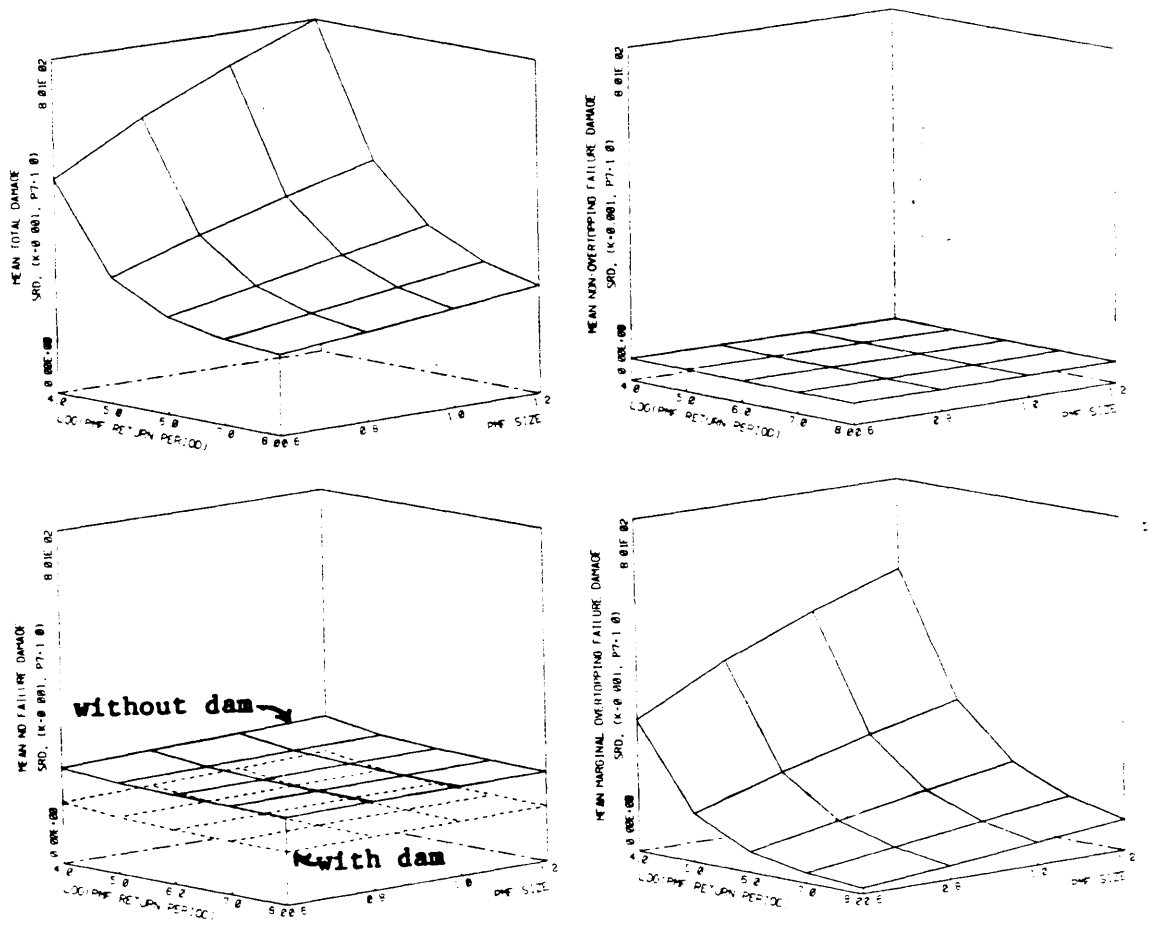

Figure 4.10: Variation of Damage Potential with Variation of PMF Size and Return Period for Springfield Reservoir Dam with $(K,P_7) = (0.001,1)$

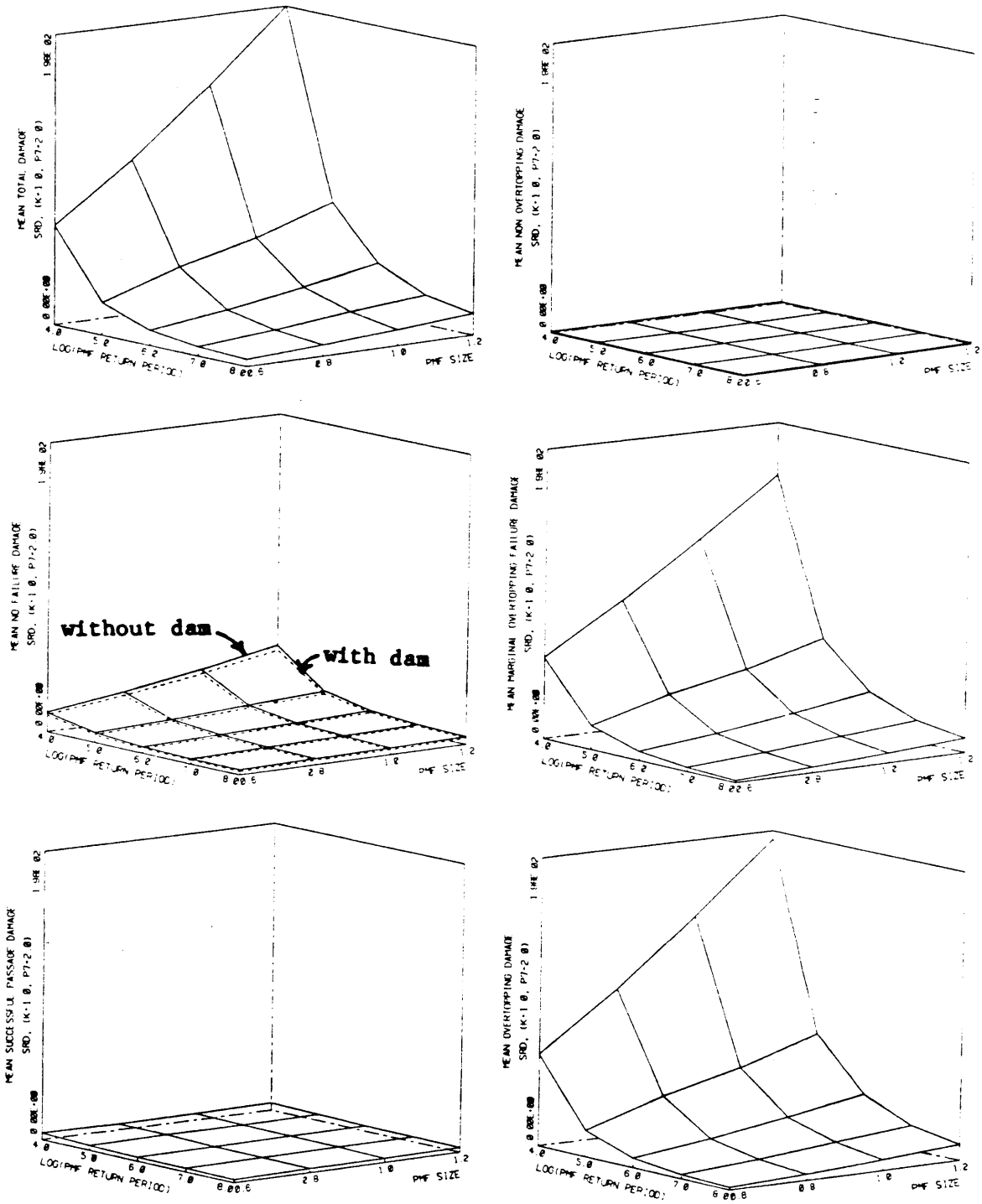

Figure 4.11: Variation of Damage Potential with Variation of PMF Size and Return Period for Springfield Reservoir Dam with $(K,P_7) = (1,2)$

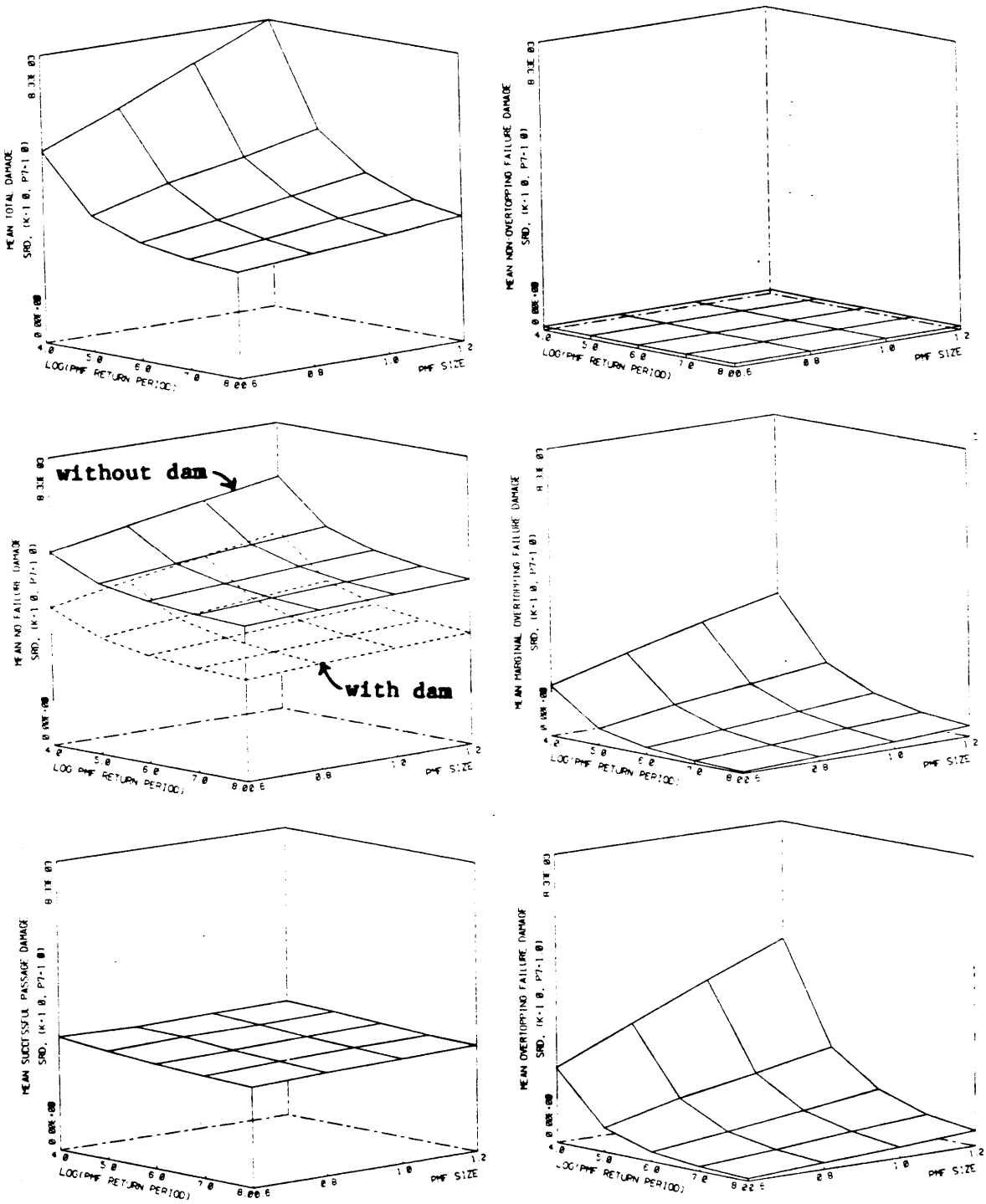

Figure 4.12: Variation of Damage Potential with Variation of PMF Size and Return Period for Springfield Reservoir Dam with $(K,P_7) = (1,1)$

periods and high PMF sizes.

The general dominance of Overtopping Failure damage potential shows that construction of SRD greatly increased the damage potential near the dam for most of the probability distributions of extreme floods considered here. The small spillway contributes to this problem. Chapter 5 examines the effect of spillway size on the damage potential.

There is little development between SRD and North Springfield Reservoir, a large U.S. Army Corps of Engineers flood control dam downstream of SRD. Thus, the threat posed by SRD is small. These results show, however, that a dam designed like SRD would have to provide substantial benefits through other functions, such as water supply, before its construction could be justified economically.

Figures 4.13, 4.14, and 4.15 show the results for KVD with (K,P_7) = (0.001,2), (1,2), and (0.001,1). Results for (K,P_7) = (1,1) are similar to the results for (K,P_7) = (0.001,1). The Non-Overtopping Failure damage is insignificant in all cases because the normal reservoir stage is so low. The primary loss in a Non-Overtopping Failure would be the value of the dam itself, a loss which is not included in this analysis (see Section 2.4.2).

When $(K,P_7$ = (0.001,2) (Figure 4.13), KVD provides substantial flood damage reduction, unless the PMF is larger than estimated. If the PMF is 20 percent larger than estimated, the marginal Overtopping Failure damage approximately equals the no-dam damage when the PMF return period is 10^5 and far outweighs the no-dam damage when the PMF return period is 10^4.

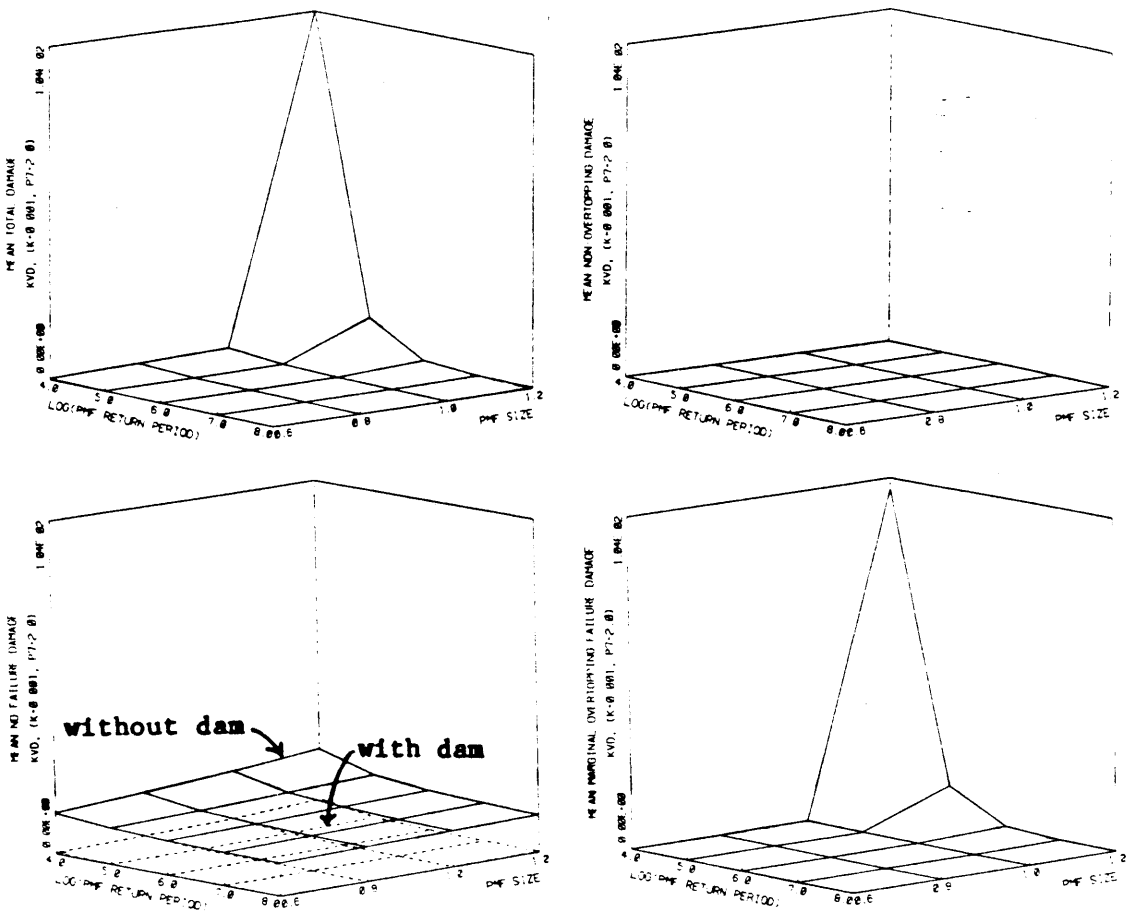

Figure 4.13: Variation of Damage Potential with Variation of PMF Size and Return Period for Knightville Dam with $(K,P_7) = (0.001,2)$

When K is changed to 1 (Figure 4.14), KVD provides even greater natural flood damage attenuation, and the Overtopping Failure damage is no longer as dominant for low PMF return periods, though it is still significant.

When $(K,P_7) = (0.001,1)$ (Figure 4.15), the relative natural flood damage attenuation provided by KVD is extremely large. No-Failure flood damage dominates the total for the PMF return periods greater than 10^4. When the PMF return period equals 10^4, Overtopping Failure damage is about half of the total damage.

KVD clearly provides substantial flood protection, and, as long as the estimate of the PMF size is accurate, there is negligible chance of an Overtopping Failure. If the estimate of the PMF size is low, however, the damage potential caused by Overtopping Failure could outweigh the reduction in natural flood damage provided by the dam, possibly changing the dam from a provider of flood protection to a public menace.

Thus, proper choice of the spillway design flood is a crucial element in the overall safety of KVD. In 1975, the spillway design flood for KVD was reevaluated and the peak inflow was increased by twenty-eight percent from the original value of 113,200 cfs. Thus, changes of twenty percent in the spillway design flood for a given dam and catchment, whether caused by changing spillway design criteria or by improved hydrologic techniques, are possible. As described in Section 1.2.1, the initial reservoir conditions and operating assumptions were changed at the same time the spillway design flood was reevaluted. The spillway was thus judged adequate for both spillway design floods.

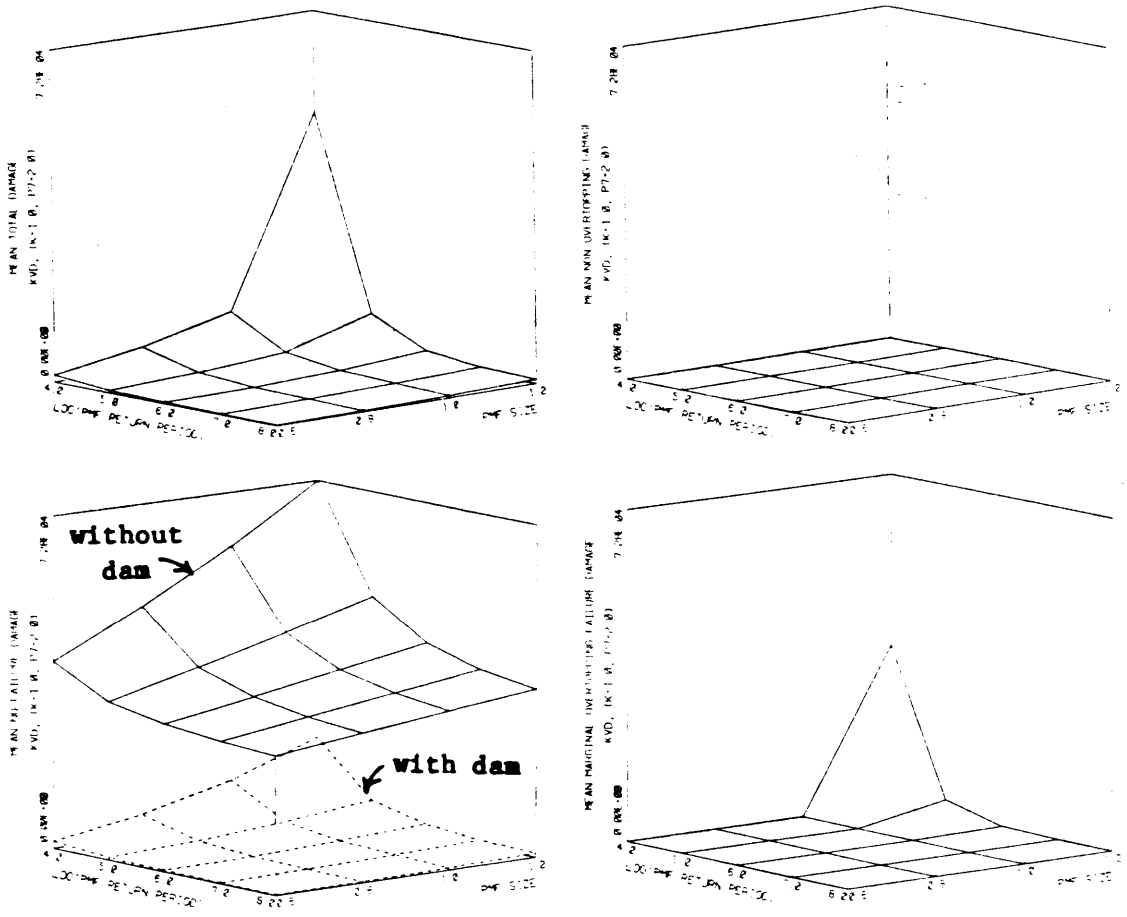

Figure 4.14: Variation of Damage Potential with Variation of PMF Size and Return Period for Knightville Dam with $(K,P_7) = (1,2)$

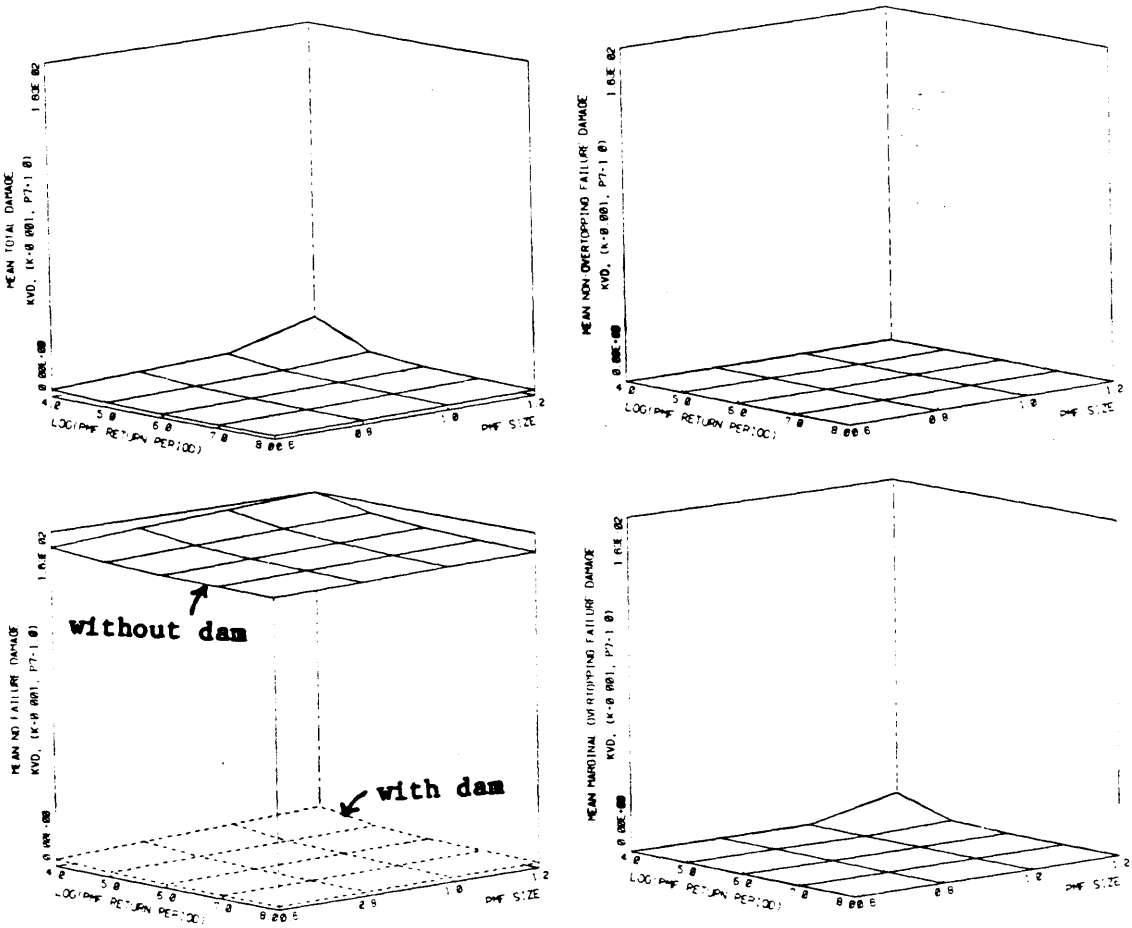

Figure 4.15: Variation of Damage Potential with Variation of PMF Size and Return Period for Knightville Dam with $(K,P_7) = (0.001,1)$

These results show that the PMF return period of 10^4 used by ASCE (1973) does, as intended, give great prominence to Overtopping Failure damage. It is currently impossible, however, to determine if this prominence is realistic.

A PMF return period must be chosen for use in the rest of this work. 10^5 years was chosen, not as the correct value, since there is no way of knowing the correct value, but as a value which is high enough so that Overtopping Failure damage does not always dominate the analysis and low enough so that Overtopping Failure damage is not always negligible.

All further results shown in this work use a 10^5 year return period for the PMF.

4.1.2 Volume-Peak Relation

Figure 2.1 shows that the volume/peak ratio for the reservoir inflow flood equals $t_b/2$. Thus, the volume/peak ratio can be varied by varying t_b.

For MPD, GMD, and SRD, t_b was estimated by using Snyders method to estimate t_p, a gross approximation at best, and then multiplying t_p by 2.7, a further large approximation (see Section 3.2.2). These approximations are compounded by the inaccuracy of using a constant value of t_b for all flood peaks, or even a constant value for a given flood peak (see Section 2.2.4.2). The value of t_b estimated for KVD is probably more accurate than for the other dams, at least for large floods, because it was based, indirectly, on more sophisticated hydrologic procedures; though it also suffers from the approximation of being constant for all floods.

Section 4.1.2 examines the sensitivity of flood damage potential to variations in the estimate of t_b, but does not consider the improvements to the catchment model which were discussed in Section 2.2.4.2.

t_b, and thus the ratio between the reservoir inflow flood volume and peak, is varied from a half to one and a half times the original estimate. This range was chosen because the direction of the errors for MPD, GMD, and SRD are not known. The original estimate for KVD is probably near the high end of reasonable estimates, and one and a half times the original value may be unrealistically high. t_p is also varied to preserve the relation $t_b = 2.7t_p$.

The horizontal axis in Figures 4.16 through 4.20 is the ratio of t_b to the original estimate of t_b, and is equal to the ratio of the flood volume to the flood volume derived from the original estimate of t_b.

Figure 4.16 shows the variation in failure probability with the volume/peak ratio. The vertical scales are different for each graph in Figure 4.16, though all begin at zero. The lower line in each curve is the Overtopping Failure probability. The total Overtopping Failure probability variations shown in Figure 4.16 are $(9.8)10^{-5}$ for MPD, $(8.5)10^{-5}$ for GMD, $(2.7)10^{-4}$ for SRD, and $(1.0)10^{-7}$ for KVD. Those variations, when divided by the original Overtopping Failure probabilities (horizontal axis = 1), are 1.0 for MPD, 1.3 for GMD, 0.5 for SRD, and 2.0 for KVD. Thus, for these four dams, the relative variation of Overtopping Failure probability with reservoir inflow volume varies inversely with the size of the absolute variation. For MPD, GMD, and SRD, the rate of change of failure probability seems to be decreasing with increasing volume/peak ratio.

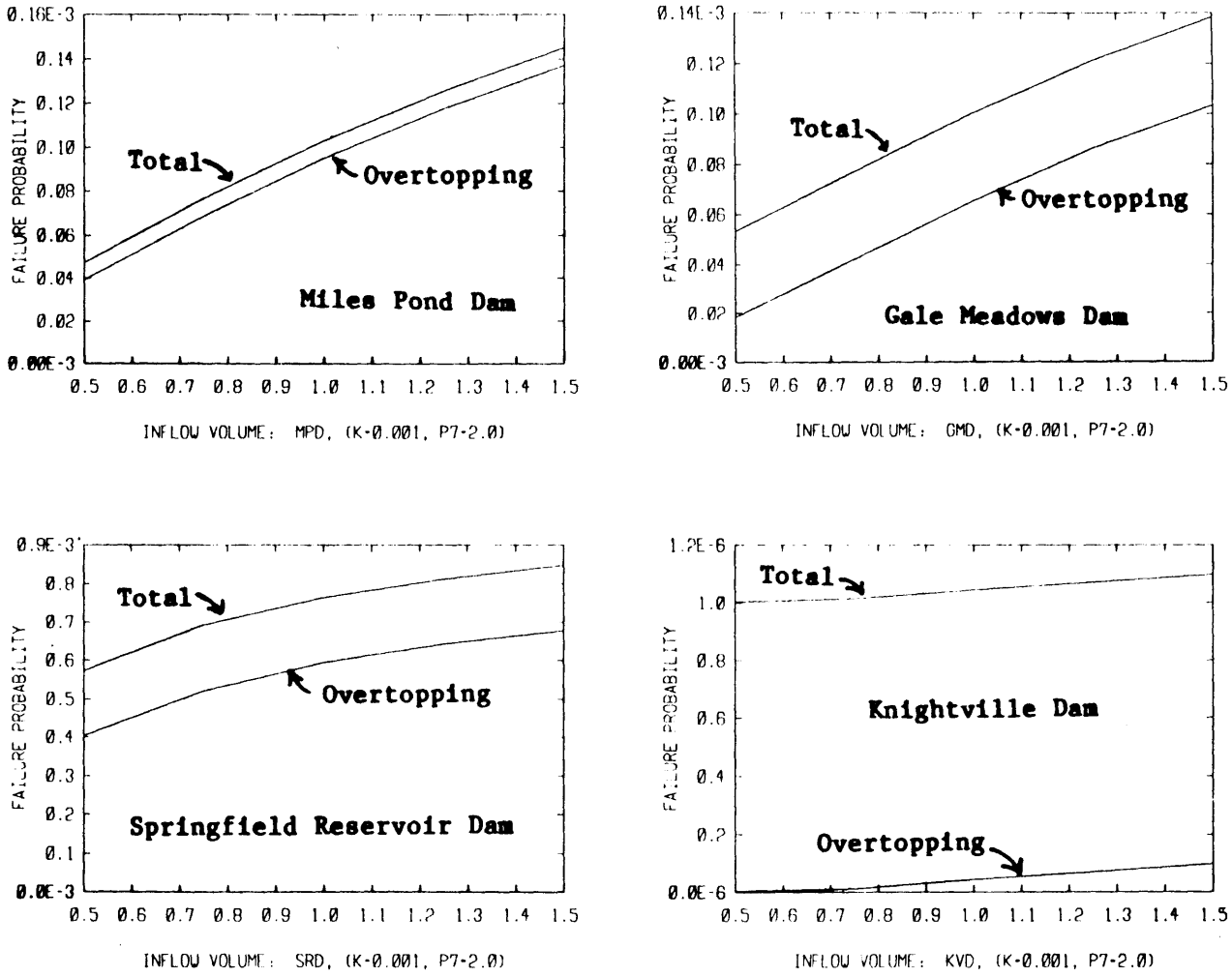

Figure 4.16: Variation of Failure Probability with Variation of the Reservoir Flood Inflow Volume

Figure 4.17 shows the results for GMD, with $(K,P_7) = (0.001,2)$ and $(0.001,1)$. Results for K = 1 are qualitatively similar to those for K = 0.001. The total damage variations divided by the total damages at the original value of t_b are 1.2 for $P_7 = 2$ and 1.8 for $P_7 = 1$. The normalized variations increase when K = 1. Thus, the reservoir inflow flood volume has a strong influence on the damage potential, an influence that increases when P_7 decreases. Also, the marginal Overtopping Failure damage is greater than the No-Failure damage when $P_7 = 2$, but the reverse is true when $P_7 = 1$.

Figure 4.18 shows the results for SRD with $(K,P_7) = (0.001,2)$ and $(1,2)$, and Figure 4.19 shows the results for SRD with $(K,P_7) = (0.001,1)$ and $(1,1)$. The total damage variations, divided by the total damage at the original value of t_b, are 0.4 for $(K,P_7) = (0.001,2)$, 1.5 for $(K,P_7) = (1,2)$, 0.5 for $(K,P_7) = (0.001,1)$, and 1.4 for $(K,P_7) = (1,1)$. Thus the sensitivity to reservoir inflow flood volume increases as K increases (the stream channel gets larger or wider). The difference between the marginal Overtopping Failure damage and the total Overtopping Failure damage is greater for K = 1 than for K = 0.001, for both values of P_7.

When $P_7 = 2$ (Figure 4.18), the No-Failure damage is insignificant with K = 0.001. When K = 1, with P_7 still equal to 2, the No-Failure damage is more significant, and the Non-Overtopping Failure damage becomes insignificant. The Overtopping Failure damage increases more rapidly with increasing inflow volume than does the No-Failure damage. The Non-Overtopping Failure damage becomes less significant when K increases because the storage volume in SRD is so low.

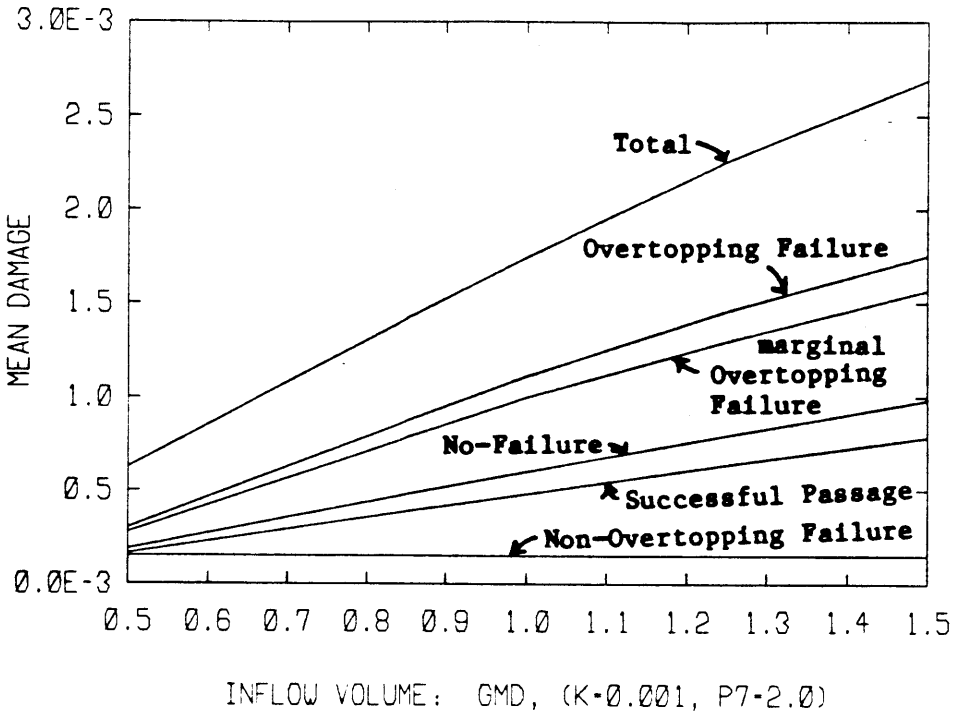

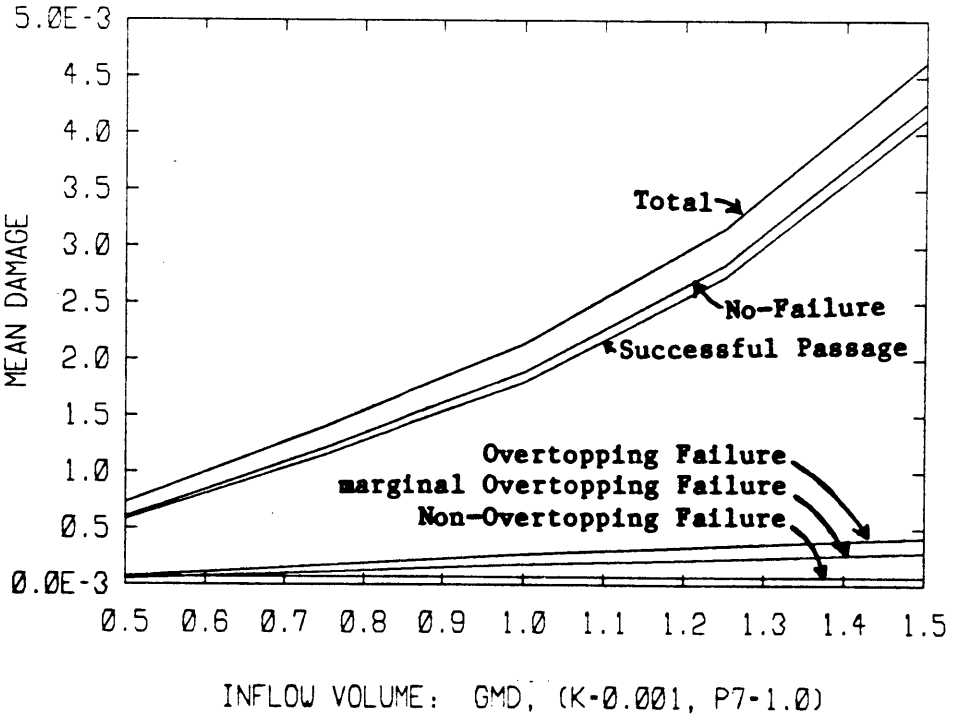

Figure 4.17: Variation of Damage Potential with Variation of Reservoir Flood Inflow Volume for Gale Meadows Dam with $(K,P_7) = (0.001,2)$ and $(0.001,1)$

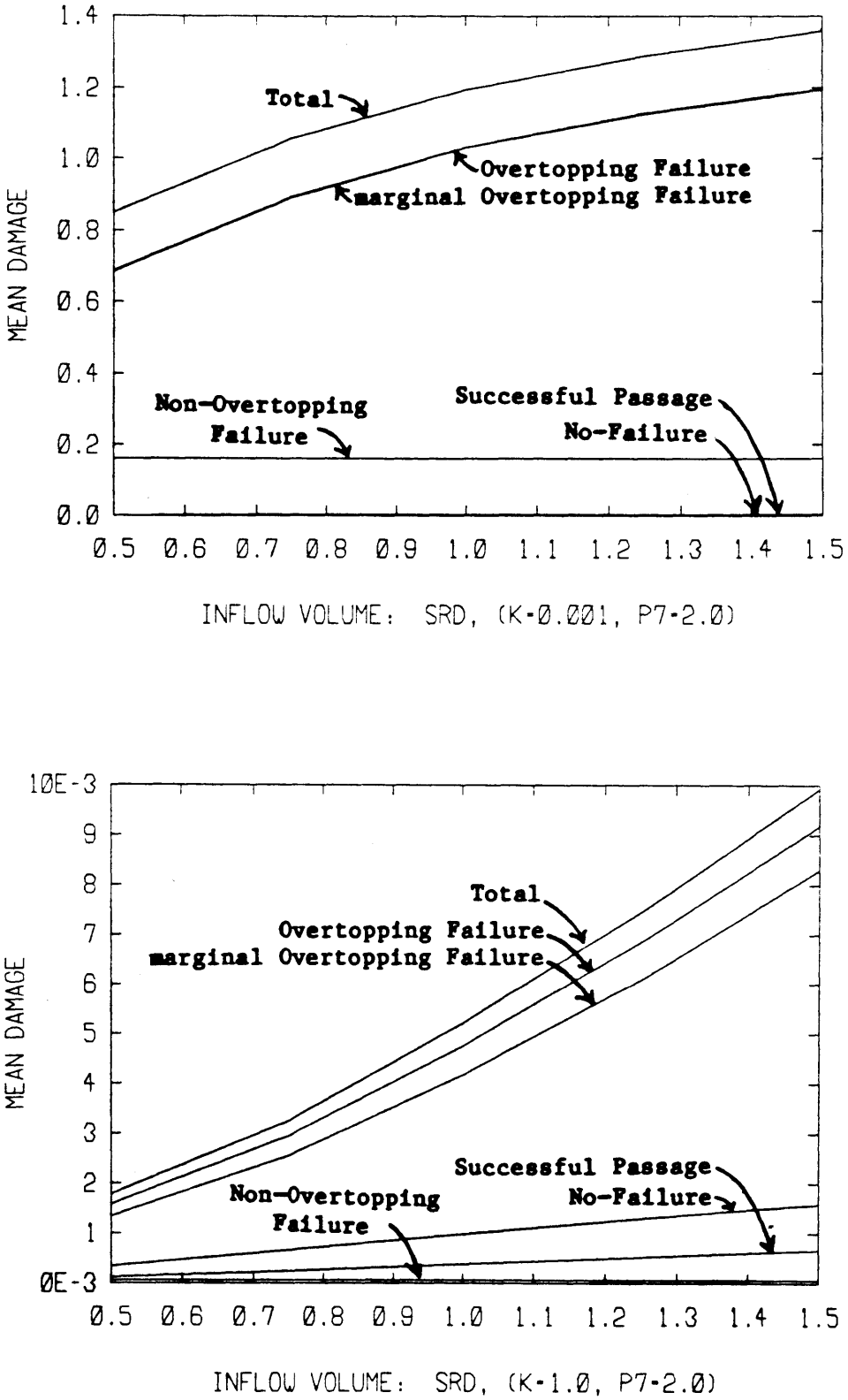

Figure 4.18: Variation of Damage Potential with Variation of Reservoir Inflow Flood Volume for Springfield Reservoir Dam with (K,P_7) = (0.001,2) and (1,2)

When P_7 = 1 (Figure 4.19), the No-Failure and Overtopping Failure damages show similar increases with inflow volume with K = 0.001, the Overtopping Failure damage still dominating the No-Failure damage. When K = 1, with P_7 still equal to 1, the No-Failure damage increases with inflow volume much more rapidly than the Overtopping Failure damage, and even dominates the Overtopping Failure damage, a reversal from the other situations.

Figure 4.20 shows the results for KVD with $(K,P_7) = (0.001,2)$. The results were similar for all four combinations of channel and damage parameters. The total damage variation, normalized by the total damage at the original value of t_b, is 2.4. Failure damages are insignificant.

The no-dam damage was computed, but is not shown here. The variation in no-dam damage over the range of t_b considered here, divided by the value at the original value of t_b, was approximately 0 with K = 0.001 and approximately 1 with K = 1 for all four dams.

4.2 Failure Parameters

4.2.1 Breach Size

Section 2.3.3 discusses some general guidelines for the breach size parameters, P_1 and P_2, and Table 3.2 lists the values of P_1 and P_2 chosen for the dams examined in this work. Recall that P_1 is the ratio of breach depth to water depth and P_2 is the ratio of breach width to water depth (see Equations 2.5 and 2.6). P_1 and P_2 are varied through a range of values that should encompass most breaches, from 0.5 through 1 for P_1, and from 1 through 4 for P_2. Failure probability does not vary with breach size, and is thus not presented in this section.

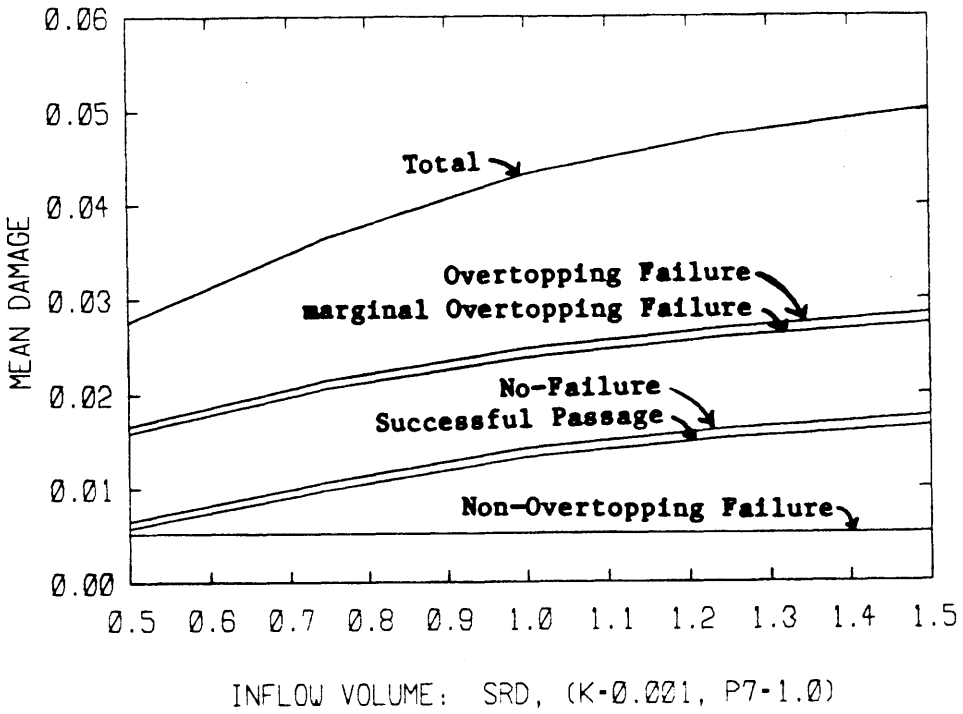

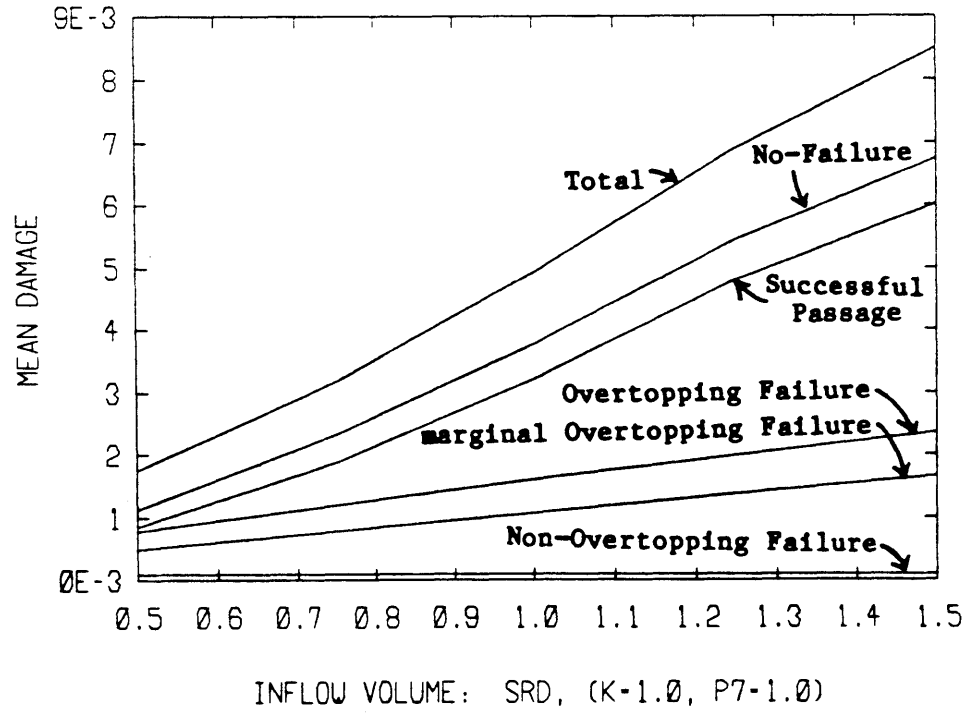

Figure 4.19: Variation of Damage Potential with Variation of Reservoir Inflow Flood Volume for Springfield Reservoir Dam with $(K,P_7) = (0.001,1)$ and $(1,1)$

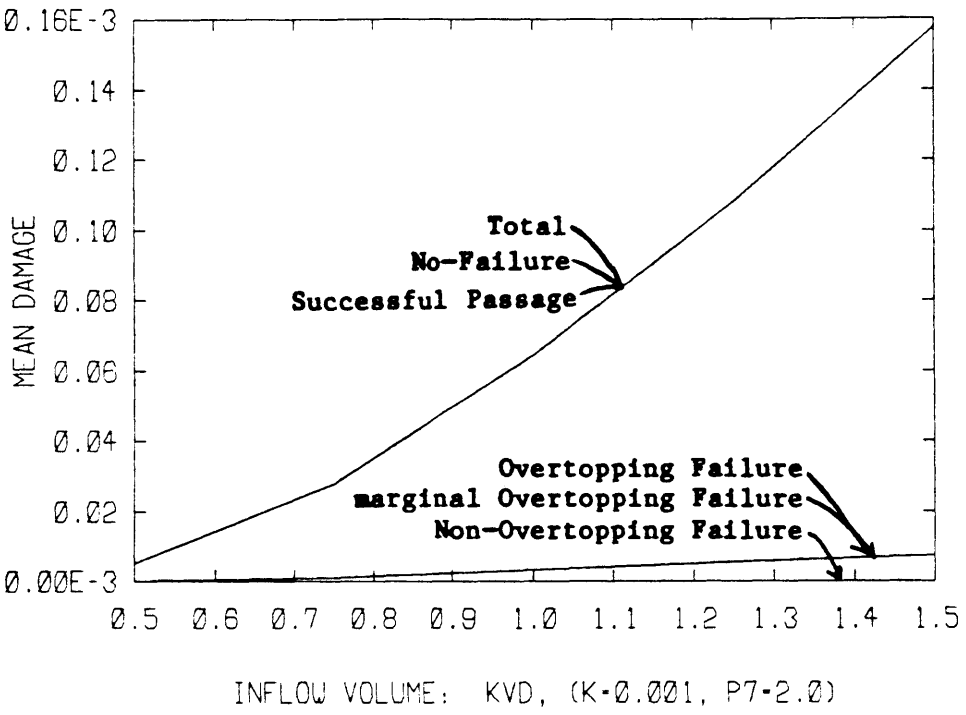

Figure 4.20: Variation of Damage Potential with Variation of Reservoir Inflow Flood Volume for Knightville Dam with $(K,P_7) = (0.001,2)$

Figures 4.21 and 4.22 show the results for GMD with $(K,P_7) = (0.001,2)$ and $(0.001,1)$. The general variations in the relative importance of different components of the total damage potential with variation in K and P_7 which have been noted in the previous results were noted again here. For example, failure damages become more prominent as P_7 increases, and floods with greater volumes become more prominent as K increases. Also, variation of the damage potential with variation of breach size is greater when $P_7 = 2$ than when $P_7 = 1$ because the relative importance of large floods, floods from dam failures in particular, increases as P_7 increases.

Figures 4.23 and 4.24 show the results for SRD with $(K,P_7) = (0.001,2)$ and $(1,1)$. The remarks in the previous paragraph, for GMD, apply equally to these figures.

No results are shown for KVD because the failure damage is such a small proportion of the total that varying the breach size does not cause any significant changes.

4.2.2 Overtopping Failure Stage

The failure stage was varied from a few feet below to a few feet above the crest of the dam for each of the four dams. The non-dimensional variation in failure stage is different for each dam. The dimensional variations in failure stage, relative to the crest of the dam, which correspond to the non-dimensional variations shown in the figures in this section are $\pm$ 2.1 feet for MPD, $\pm$ 2.7 feet for GMD, $\pm$ 2.4 feet for SRD, and $\pm$ 3.8 feet for KVD.

The meaning of failure stage in this section is the stage at which the cumulative probability of failure equals one. For MPD, GMD, and SRD

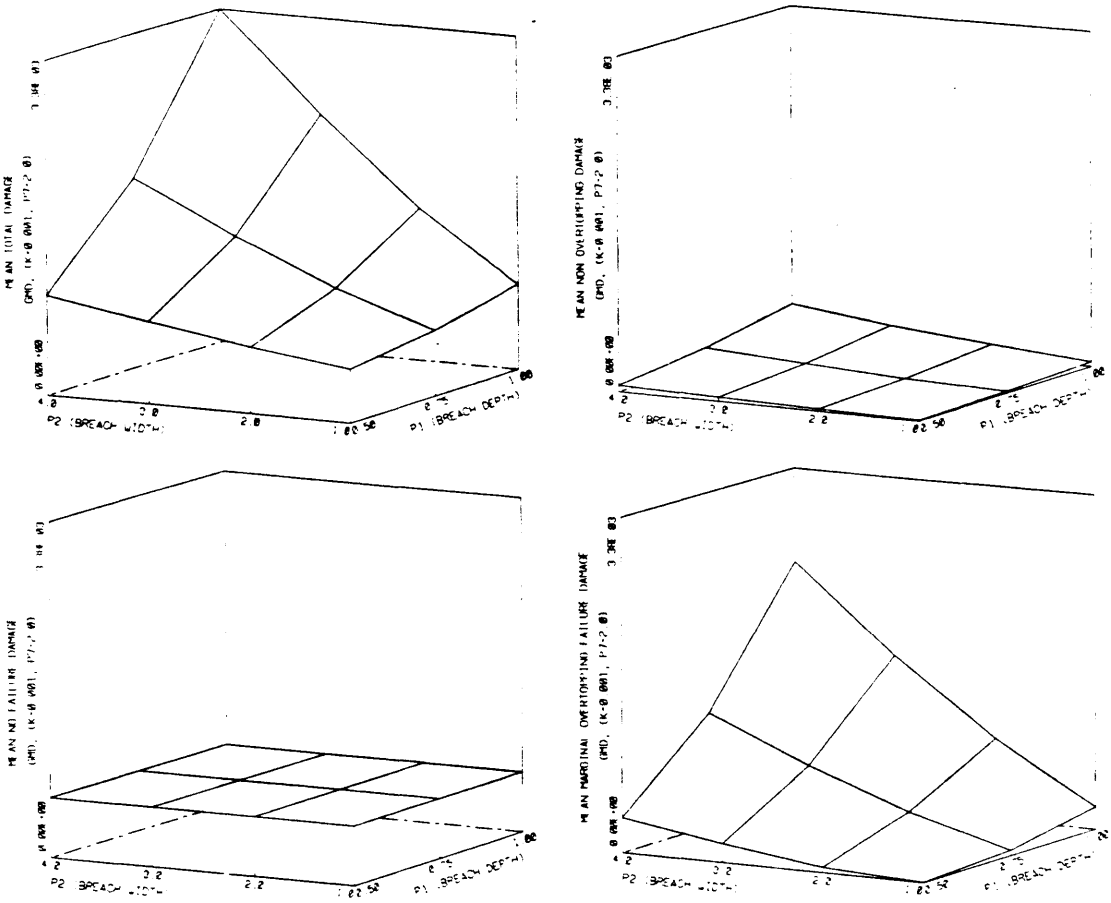

Figure 4.21: Variation of Damage Potential with Variation of Breach Size Parameters for Gale Meadows Dam with $(K,P_7) = (0.001,2)$

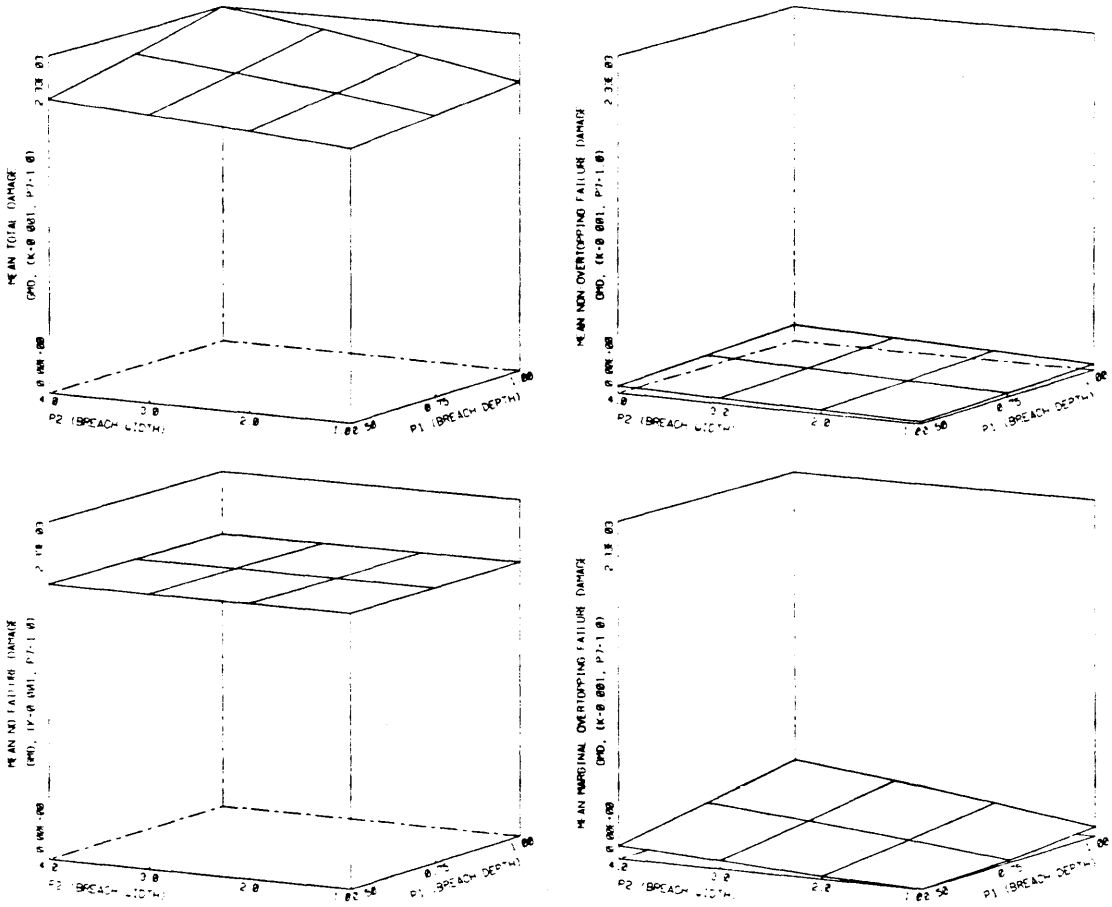

Figure 4.22: Variation of Damage Potential with Variation of Breach Size Parameters for Gale Meadows Dam with $(K,P_7) = (0.001,1)$

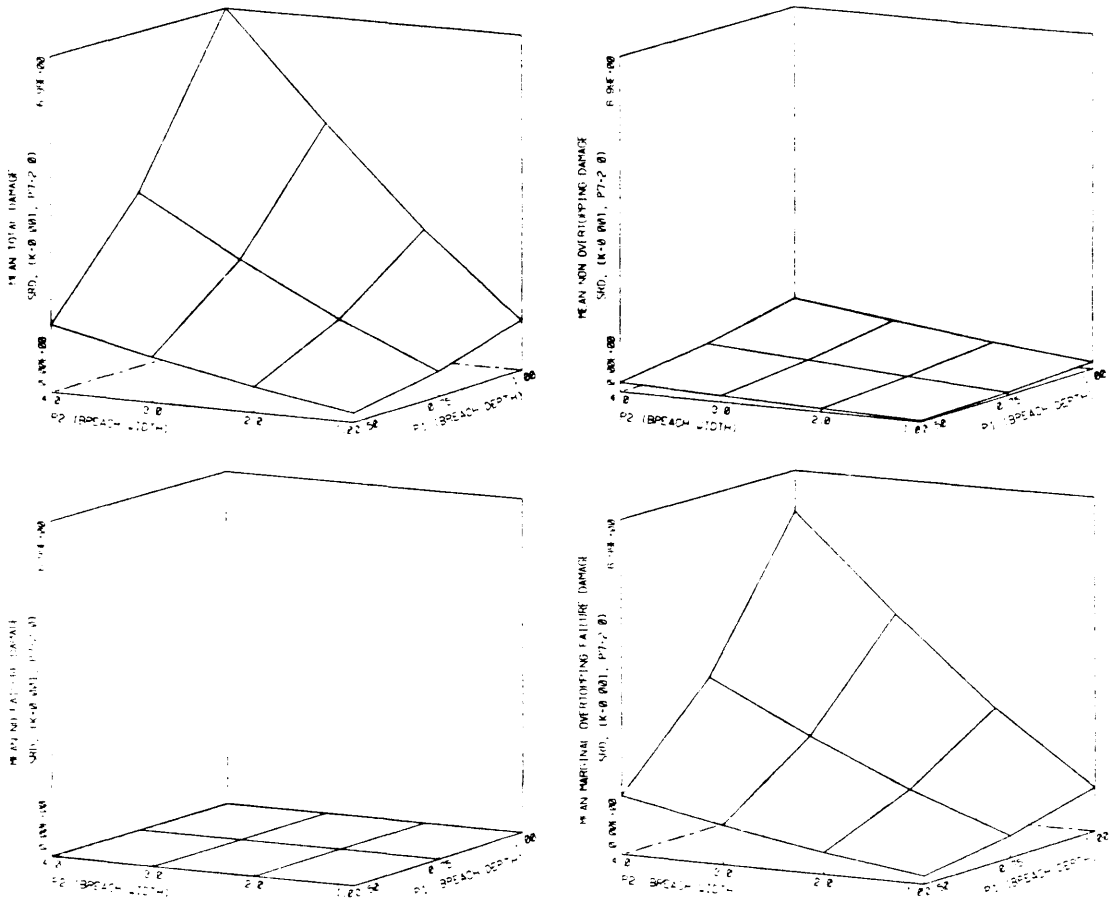

Figure 4.23: Variation of Damage Potential with Variation of Breach Size Parameters for Springfield Reservoir Dam with $(K,P_7) = (0.001,2)$

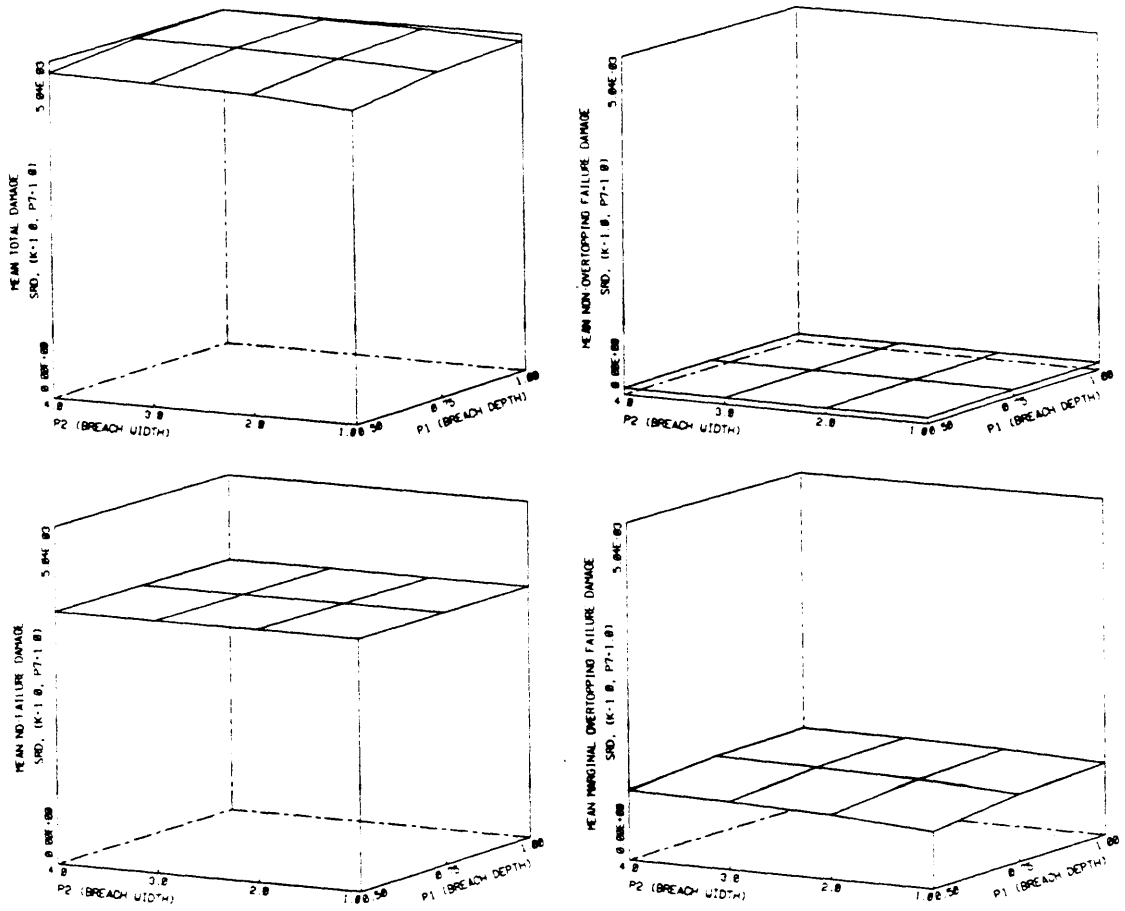

Figure 4.24: Variation of Damage Potential with Variation of Breach Size Parameters for Springfield Reservoir Dam with $(K,P_7) = (1,1)$

this is simply the stage at which failure is assumed to occur. For KVD it is the highest stage in the probability distribution of failure stage (see Table 3.3). The lower points in the distribution are not changed.

Figure 4.25 shows the variation of failure probability with failure stage. There appears to be an approximately exponential decline in failure probability as the failure stage increases, until the failure probability reaches zero.

Figure 4.26 shows the results for GMD with $(K,P_7) = (1,2)$ and $(1,1)$. The results for $K = 0.001$ are qualitatively similar. Results for $K = 1$ are shown because the lines are spread out more than when $K = 0.001$, and thus are easier to view. For both $P_7 = 1$ and $P_7 = 2$, the Overtopping Failure damage decreases as the failure stage increases. The difference between $P_7 = 1$ and $P_7 = 2$ is primarily in the failure stage at which No-Failure damage becomes more important than the marginal Overtopping Failure damage.

The results for SRD and KVD are qualitatively similar to those shown for GMD. As the failure stage increases, the No-Failure damage is constant, as it should be, the total damage approaches the No-Failure damage from above, the Successful Passage damage approaches the No-Failure damage from below, and the Overtopping Failure damage and mean marginal Overtopping Failure damage decline and approach zero. The differences between the results for the different dams and different channel and damage parameters are in the relative significance of the failure and No-Failure damages, and in how that relative significance changes with the failure stage. Figures 4.27 and 4.28, which show results for SRD with $(K,P_7) = (1,2)$ and $(1,1)$ and for KVD with $(K.P_7) = (0.001,2)$ and $(1,2)$,

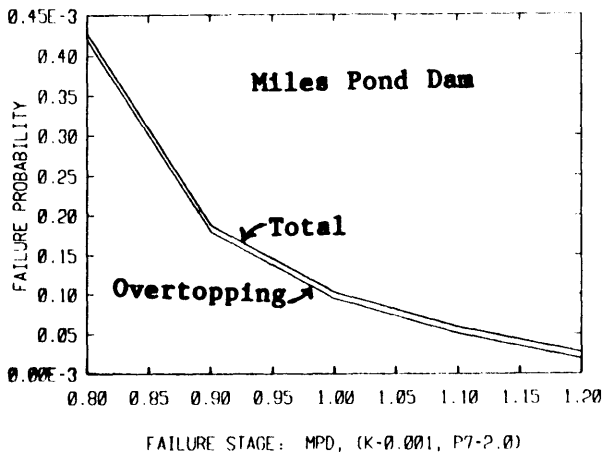

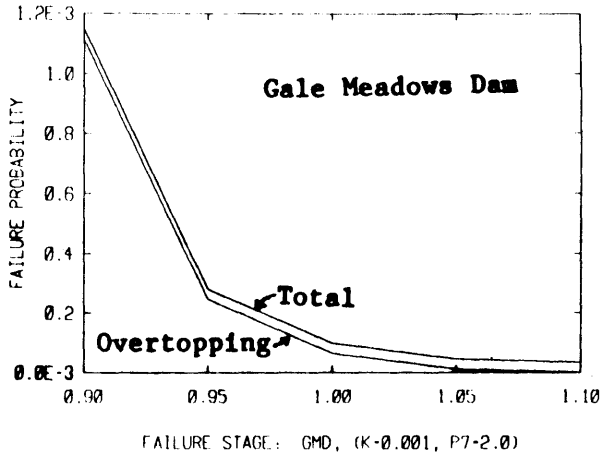

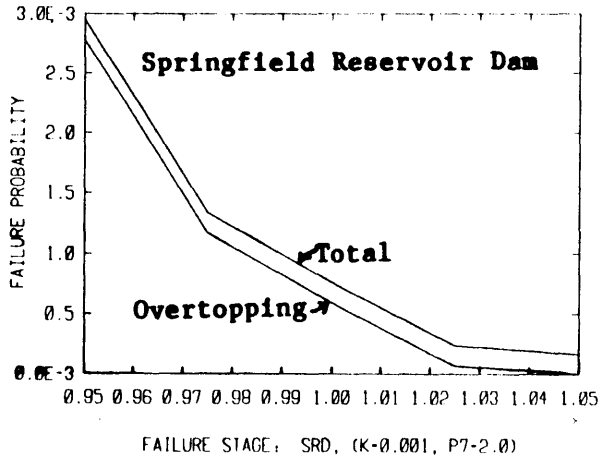

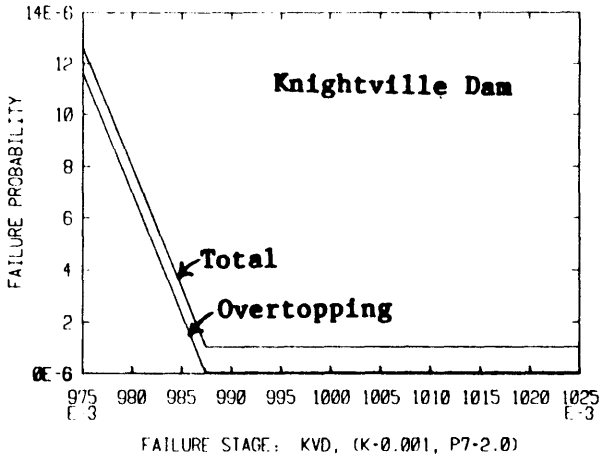

Figure 4.25: Variation of Failure Probability with Variation of Overtopping Failure Stage

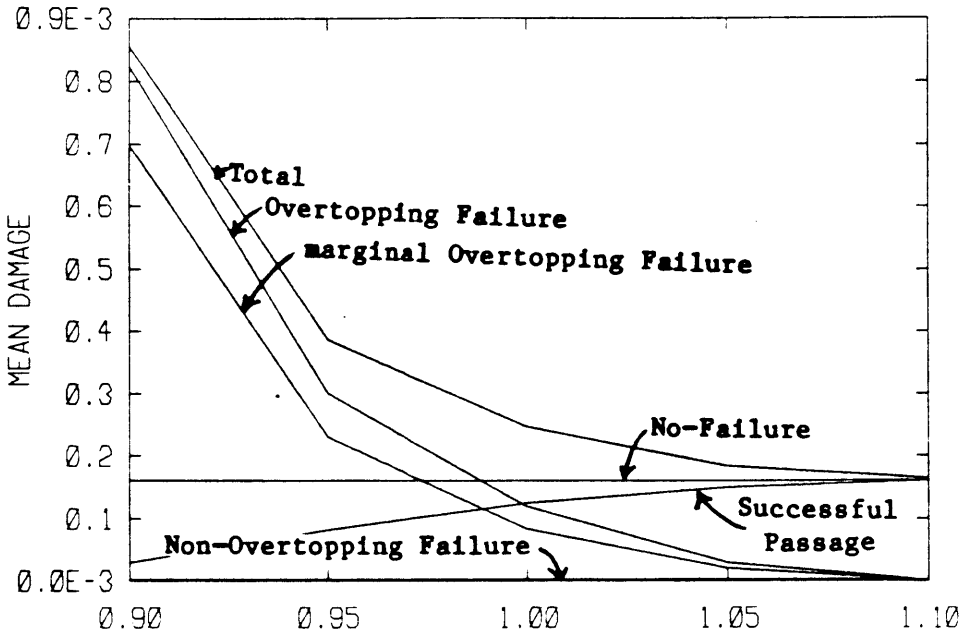

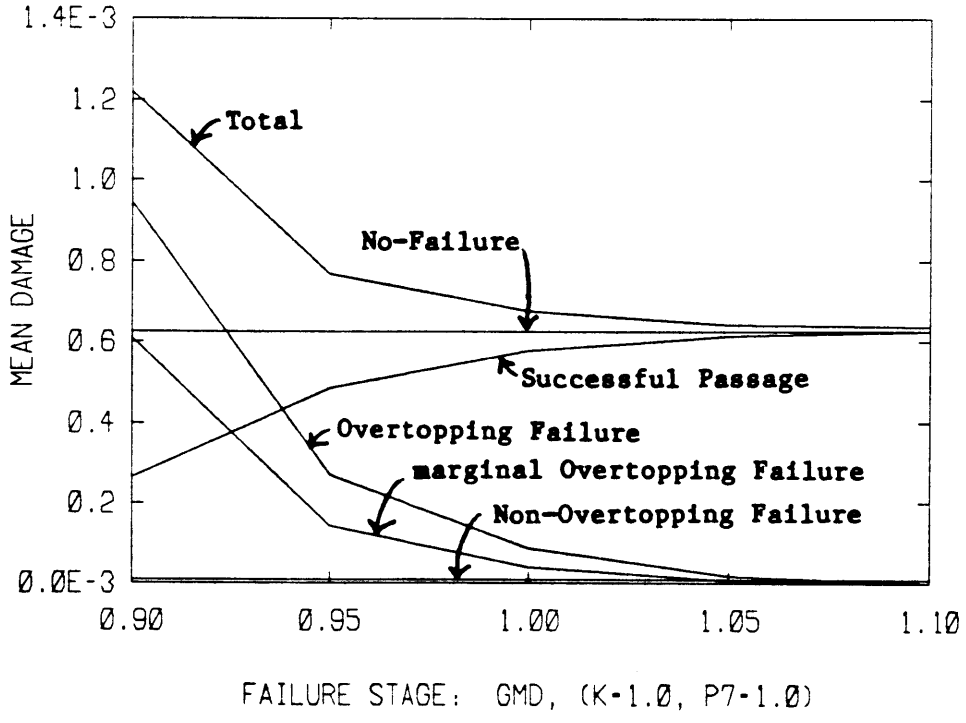

Figure 4.26: Variation of Damage Potential with Variation of Overtopping Failure Stage for Gale Meadows Dam with (K,P_7) = (1,2) and (1,1)

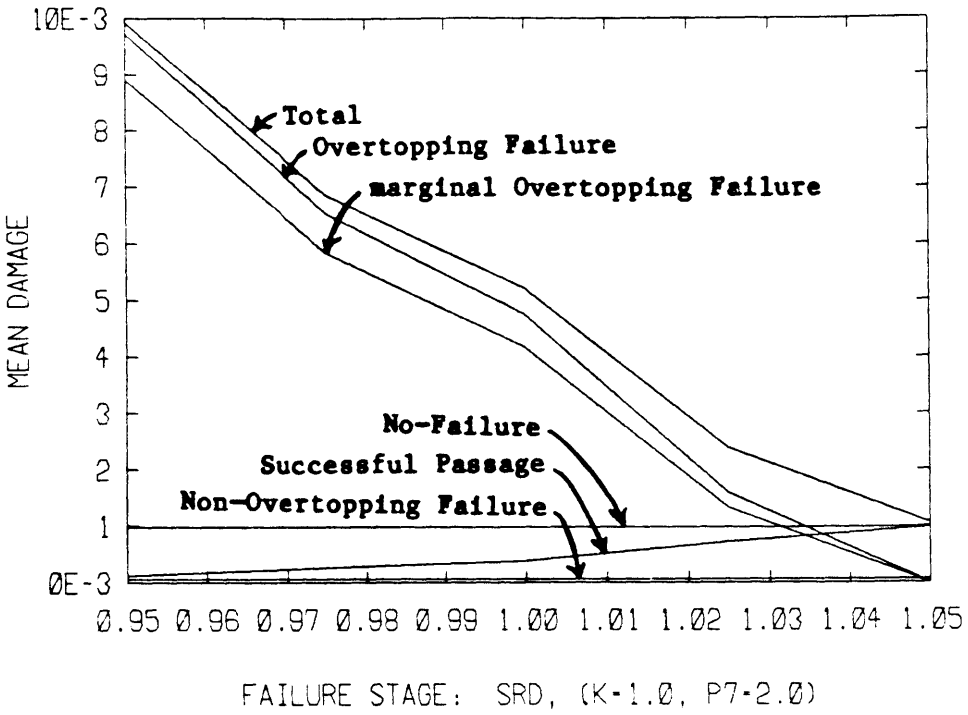

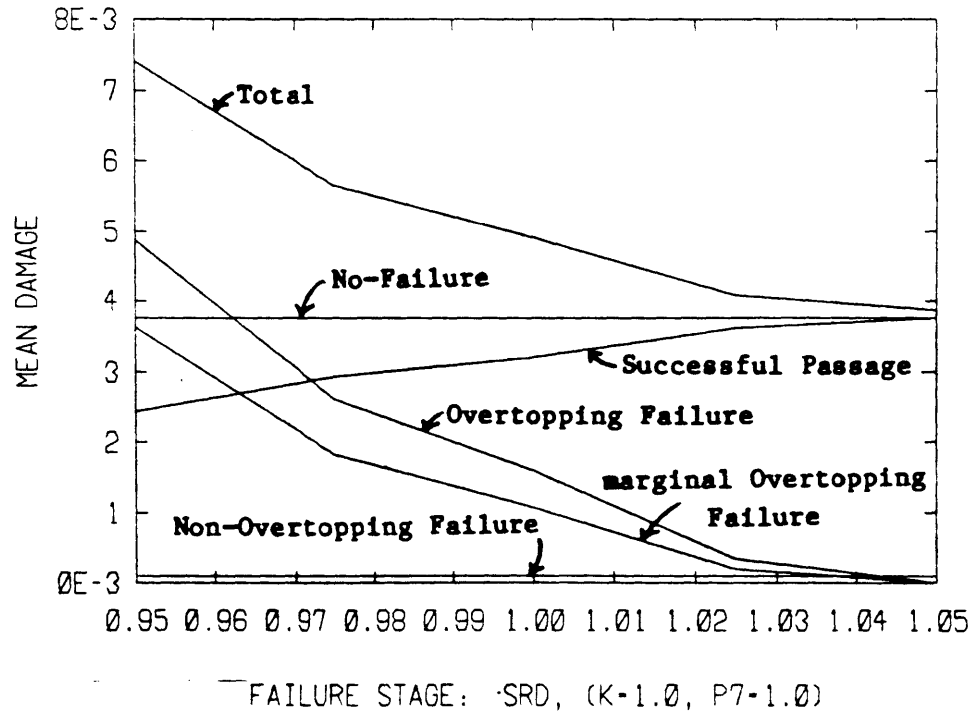

Figure 4.27: Variation of Damage Potential with Variation of Overtopping Failure Stage for Springfield Reservoir Dam with $(K,P_7) = (1,2)$ and $(1,1)$

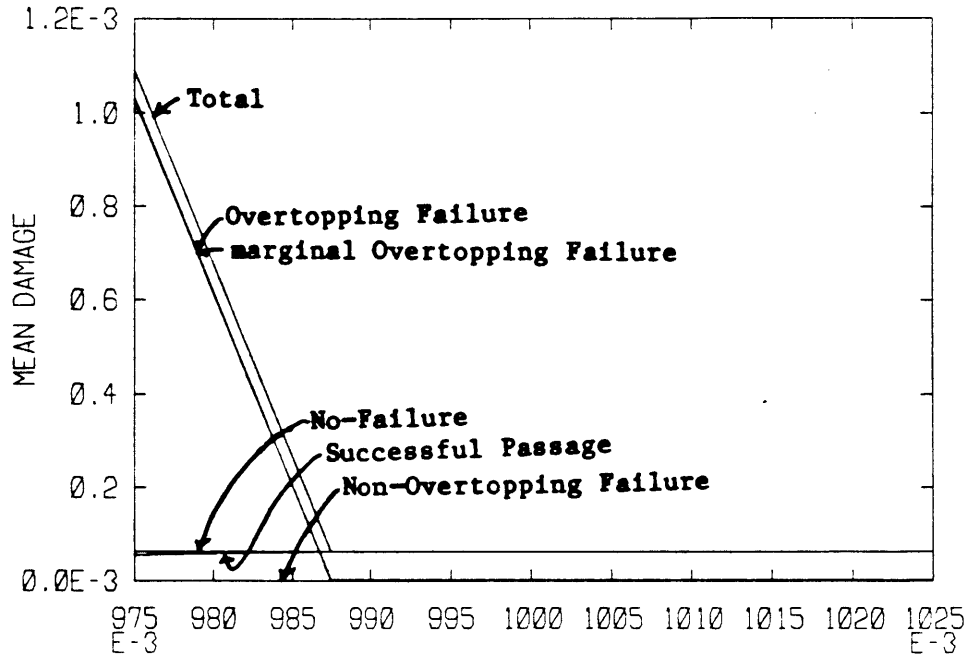

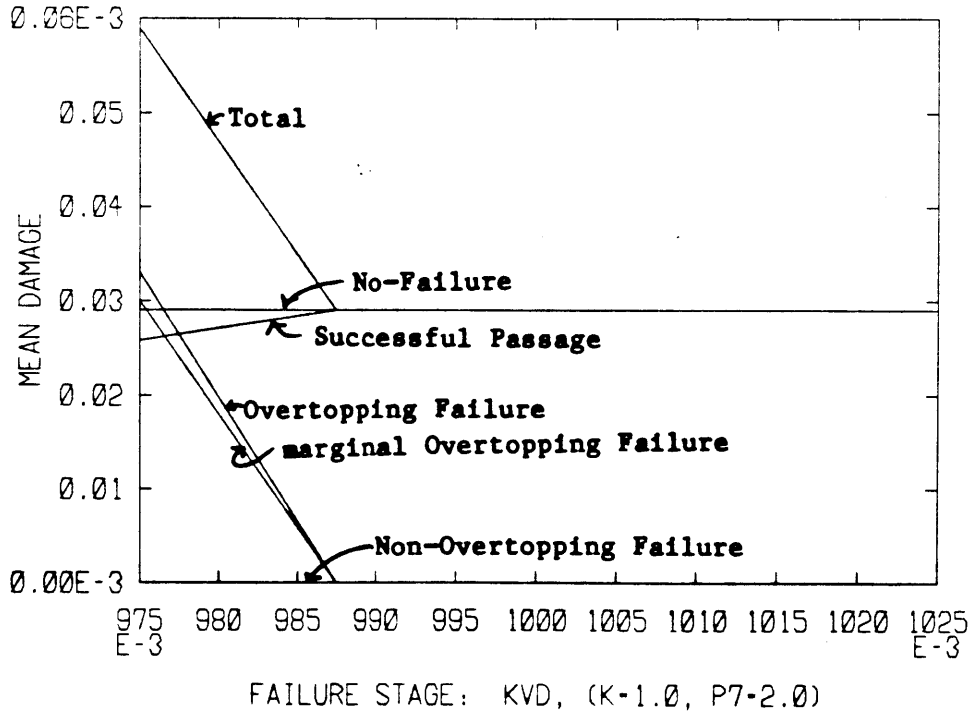

Figure 4.28: Variation of Damage Potential with Variation of Overtopping Failure Stage for Knightville Dam with (K,P_7) = (0.001,2) and (1,2)

illustrate these variations.

4.2.3 Non-Overtopping Failure Probability

The Non-Overtopping Failure probabilities, P^{NOF}, estimated in Section 3.2.4 are $(8)10^{-6}$ for MPD, $(3.5)10^{-5}$ for GMD, $(1.7)10^{-4}$ for SRD, and $(1)10^{-6}$ for KVD (see Table 3.2). P^{NOF} is varied from 10^{-7} through 10^{-3} in this section. 10^{-7} is probably lower than could be expected for any dam, and 10^{-3} is probably higher than would be tolerated for an engineered dam.

The initial reservoir stage is also varied in this section, because the importance of Non-Overtopping Failure varies substantially with [illegible] reservoir stage. For MPD, GMD, and SRD, the initial reservoir [illegible] varied from approximately the mean value down to a nearly empty [illegible]r. KVD is normally nearly empty. For KVD, the reservoir stage is varied from empty to 25 feet below the spillway crest, a non-dimensional stage of 0.7. This range of initial stage is worth considering because KVD was planned with the possibility of someday adding a hydropower installation, which would benefit from maintenance of a higher reservoir stage.

The reservoir stage at MPD, GMD, and SRD, varied here without varying any of the other parameters. The parameters of the lower limb of the reservoir discharge curve, k_1 and k_2, need to be changed when the initial reservoir stage at KVD is changed because otherwise the initial discharge would be unrealistically high. Section 5.1 discusses the methods by which the initial reservoir stage can be changed and the implications of those methods for the model parameters.

The No-Failure damage is nearly constant as P^{NOF} changes. It changes slightly because the probability of not having a Non-Overtopping Failure,

$1 - P^{NOF}$, changes. (See Appendix B5.5.) Only results for (K,P_7) = (0.001,2) are shown in this section. Results for other values of (K,P_7) do not show variations which have not been noted before.

Figure 4.29 shows the variation of failure probability with P^{NOF} and initial stage. All four dams show approximately the same behavior. The Overtopping Failure probability rises as the initial stage rises, though the overtopping probability is still zero for KVD at the top of the reservoir stage range considered here, and P^{NOF} begins to dominate the total failure probability as P^{NOF} reaches values of 10^{-4} and 10^{-3}.

Figure 4.30 shows the results for MPD with (K,P_7) = (0.001,2). As before, the No-Failure damage is a better estimate of the total damage than is the curve labeled total damage, and the Overtopping Failure damage curve is much too low. Figure 4.30 shows that variations in P^{NOF} do not affect the total damage potential below MPD very much, regardless of initial reservoir stage.

Figure 4.31 shows the results for GMD with (K,P_7) = (0.001,2). Non-Overtopping Failure damage becomes significant when the initial stage is greater than about 0.6 for $P^{NOF} = 10^{-4}$ and when the initial stage is greater than about 0.3 for $P^{NOF} = 10^{-3}$. The mean initial stage under current operation is 0.75 (see Table 3.2).

Figure 4.32 shows the results for SRD with (K,P_7) = (0.001,2). The results are similar to those for GMD, except that the marginal Overtopping Failure damage is relatively more important.

After the Phase I inspection, the water level in SRD was lowered ten feet because the embankment was in such poor condition; the non-dimensional stage was lowered from 0.89 to 0.68. Lowering the water level not only reduced the size of the flood wave which would result from a Non-Overtopping

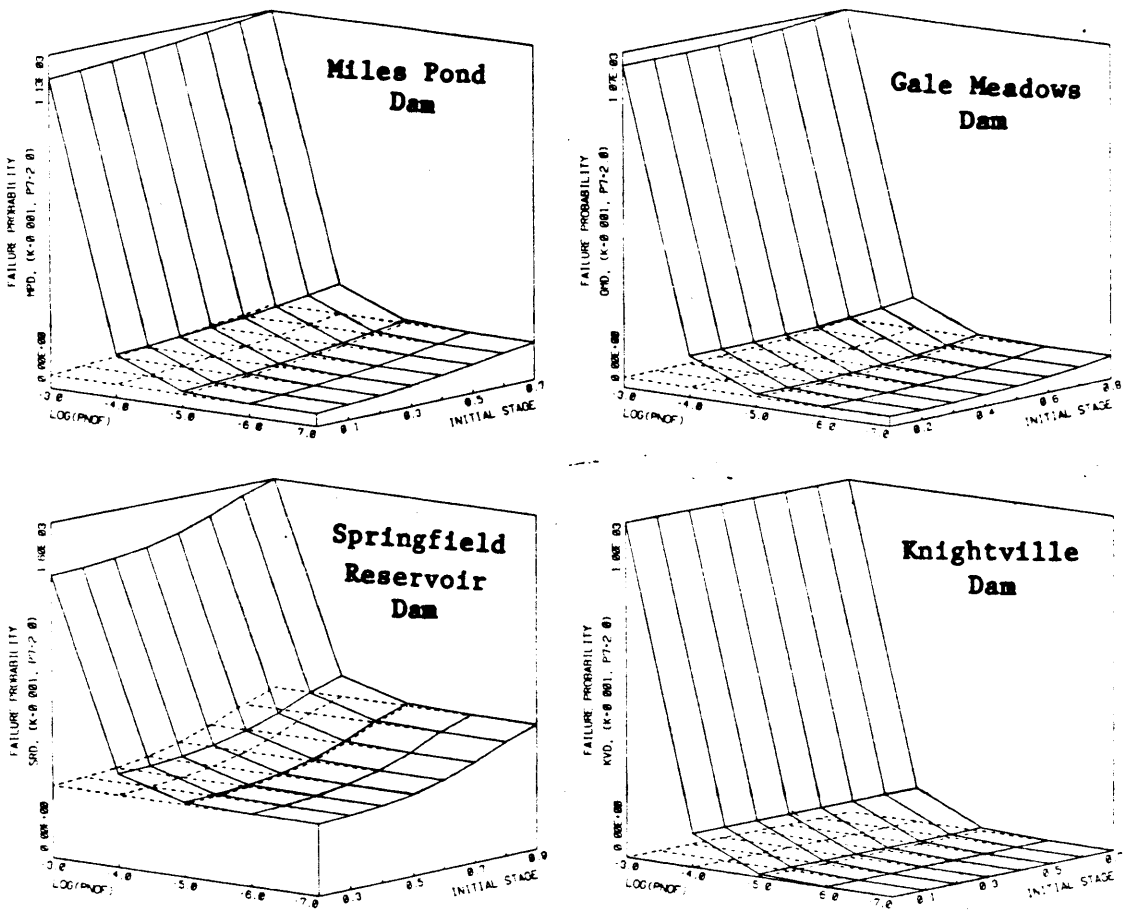

Figure 4.29: Variation of Failure Probability with Variation of Non-Overtopping Failure Probability and Initial Reservoir Stage

— — — Overtopping Failure Probability
——— Total Failure Probability

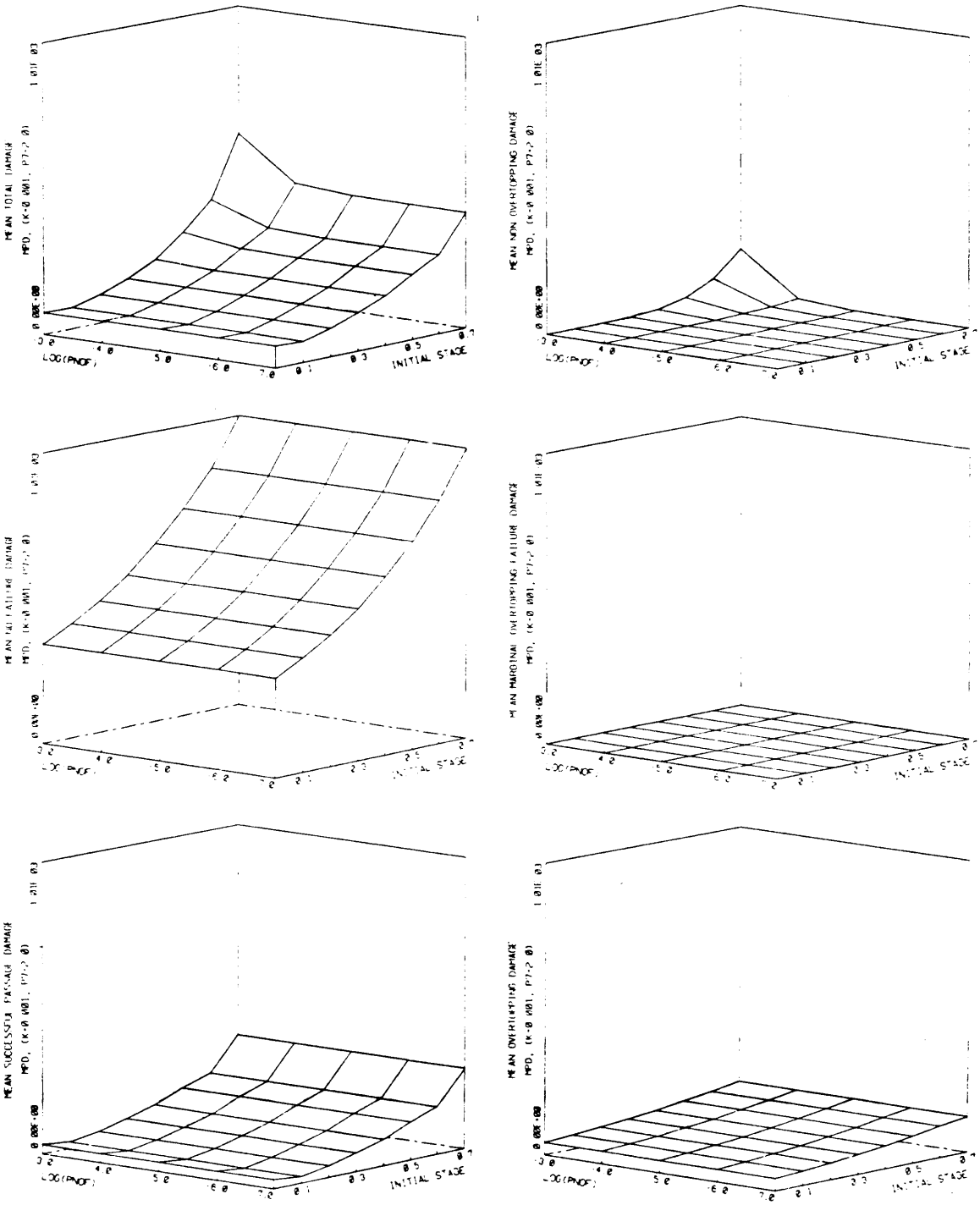

Figure 4.30: Variation of Damage Potential with Variation of Non-Overtopping Failure Probability and Initial Reservoir Stage for Miles Pond Dam with $(K,P_7) = (0.001,2)$

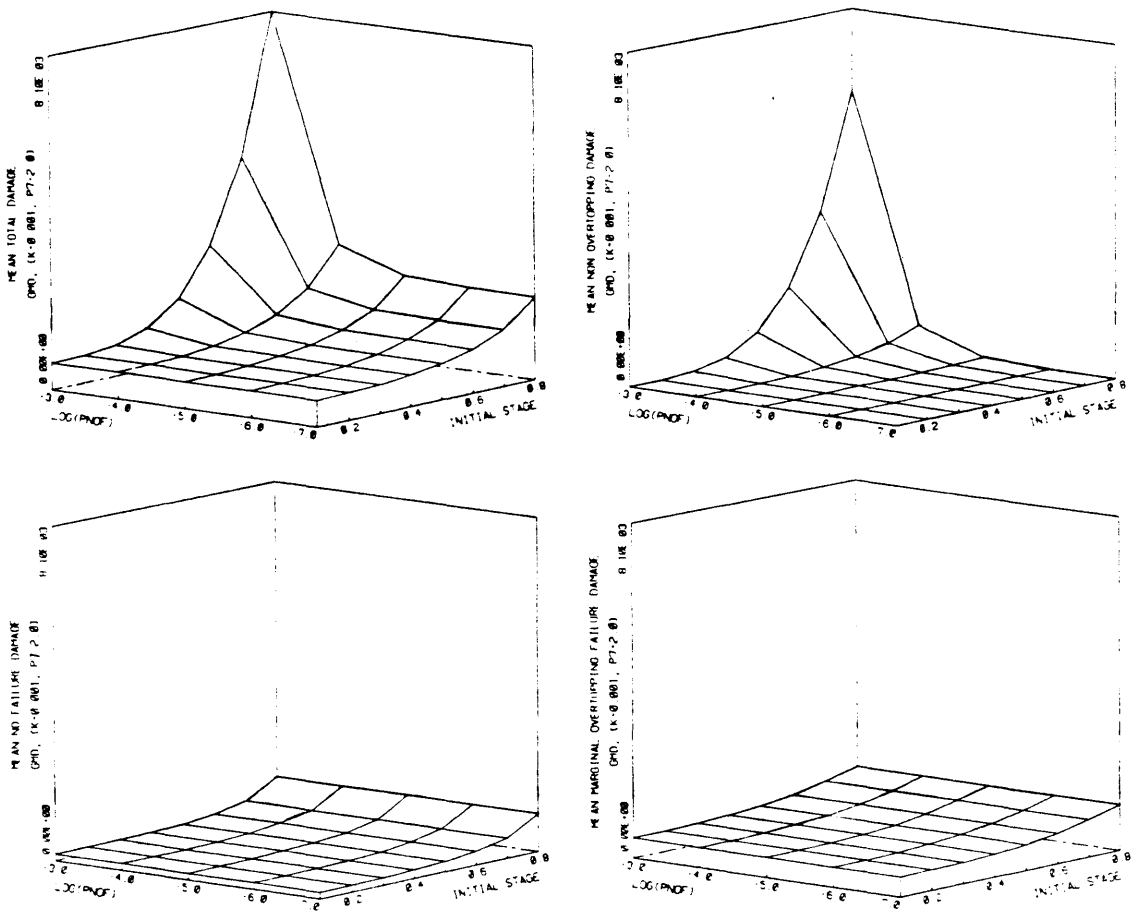

Figure 4.31: Variation of Damage Potential with Variation of Non-Overtopping Failure Probability and Initial Reservoir Stage for Gale Meadows Dam with $(K,P_7) = (0.001,2)$

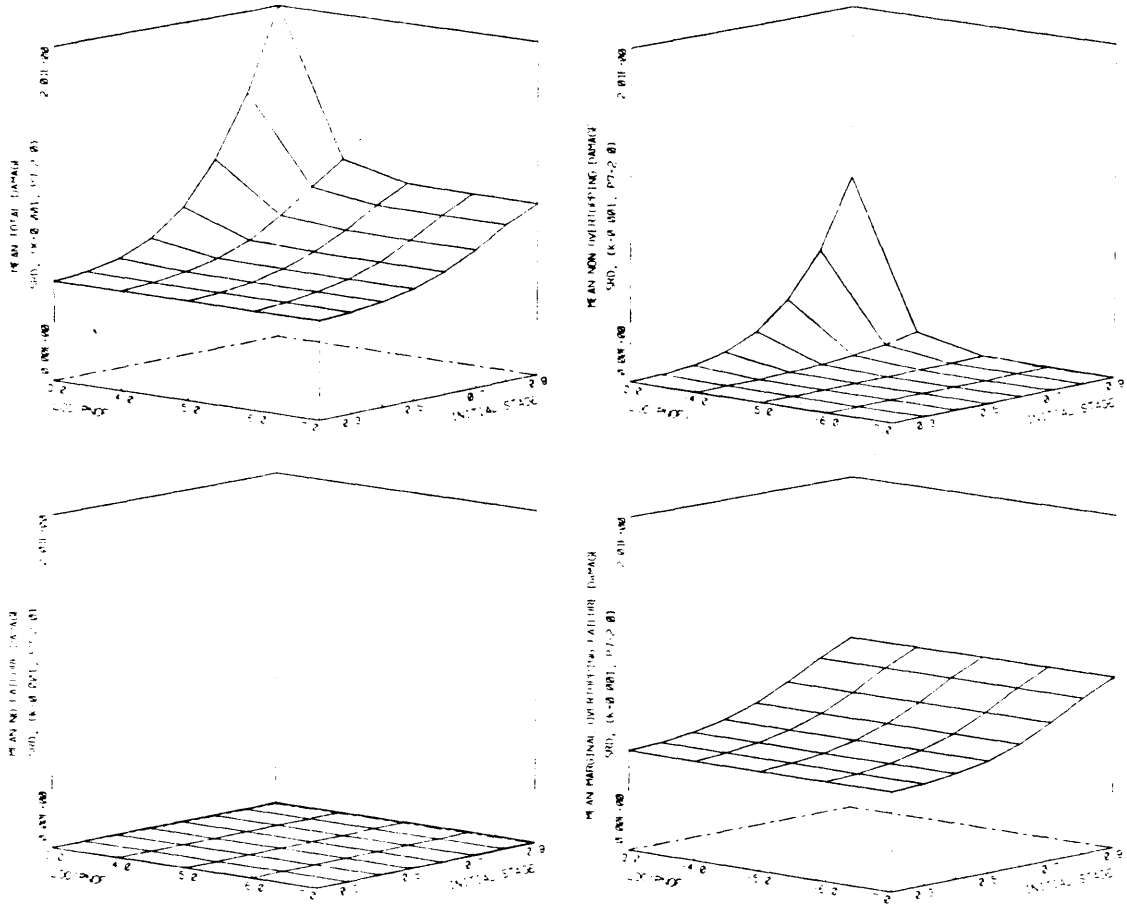

Figure 4.32: Variation of Damage Potential with Variation of Non-Overtopping Failure Probability and Initial Reservoir Stage for Springfield Reservoir Dam with (K,P_7) = (0.001,2)

Failure, but probably also reduced the probability of Non-Overtopping Failure and definitely reduced the probability of Overtopping Failure (see Figure 4.29). Figure 4.32 shows that lowering the initial stage from 0.89 to 0.68 can produce a substantial reduction in total damage potential, depending of course on the damage site, even if the probability of Non-Overtopping Failure is not reduced. However, even with the lower stage and at $P^{NOF} = 10^{-4}$, the Overtopping Failure damage potential dominates the total. (SRD was overtopped in 1969.)

Figure 4.33 shows the results for KVD with $(K,P_7) = (0.001,2)$. The damage potential for high P^{NOF} and high stages dominates the total damage potential. If the initial stage is 0.7, Non-Overtopping Failure damage would be a significant portion of the total damage potential, even at $P^{NOF} = 10^{-5}$, a low value. (The estimate of $P^{NOF} = 10^{-6}$, used as the base value in this work, was based on an extremely low initial reservoir stage.)

4.3 Conclusions

Section 4.1.1 showed that accurate estimation of the PMF had moderate significance when estimating the damage potential of GMD and SRD, but that an error of twenty percent in the PMF size for KVD could totally alter the damage potential by introducing the possibility of overtopping failure. Thus, accurate knowledge of the probability distribution of extremely large floods can be crucial when evaluating the safety of a dam. Unfortunately, current methods of estimating the probability distribution of large floods, or even of just estimating the PMF, can easily be in error by twenty percent or more.

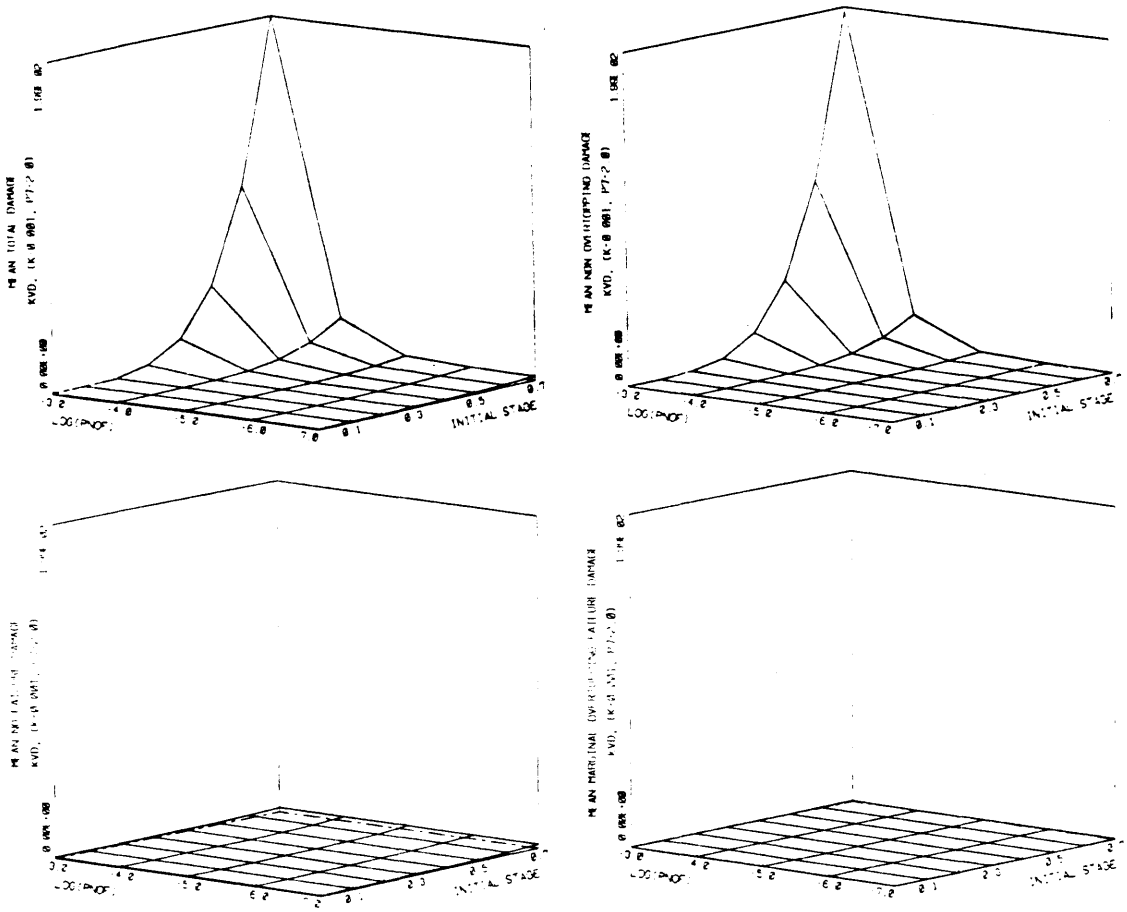

Figure 4.33: Variation of Damage Potential with Variation of Non-Overtopping Failure Probability and Initial Reservoir Stage for Knightville Dam with $(K,P_7) = (0.001,2)$

Section 4.1.2 showed that the failure probability for MPD and GMD varies substantially with reservoir flood inflow volume, the failure probability for SRD varies a little, and the failure probability for KVD hardly varies at all. Total damage, however, varies substantially with reservoir inflow volume for all four dams. This indicates that modeling the upstream catchment with greater acuracy is important.

Section 4.2.1 showed that the significance of modeling the breach size accurately can vary substantially with the damage site characteristics.

Section 4.2.2 showed that all the results were sensitive to the failure stage. This indicates that further knowledge about or control of the failure stage could be significant.

Section 4.2.3 showed how the Non-Overtopping Failure damage can dominate the total damage potential when the Non-Overtopping Failure probability and initial reservoir stage are high.

These results show that parameter uncertainties can have a strong influence on estimates of the damage potential. The strength of that influence, however, varies substantially among dams and among different combinations of channel and damage site characteristics. This indicates that the damage estimates derived from a risk analysis approach to spillway analysis should not be used without an examination of the sensitivity of the results to variations in the uncertain parameters.

Further research is needed to reduce the uncertainties in most of these parameters. The confidence which can be placed in the results of this model can be increased most readily by modeling the volume/peak ratio for reservoir inflow floods more accurately. For example, a distribution of base times, t_b, could be used with each value of the peak inflow, I_f (see Section 2.2.4.2). Given current knowledge, the

immediate solution for the other parameters is simply to vary them within a reasonable range for the particular situation being examined.

Chapter 5

VARIATION OF DESIGN PARAMETERS

Chapter 5 examines how the damage potential below the four dams described in Chapter 3 changes as the spillway size and initial reservoir stage change. Enlarging the spillway and lowering the reservoir level are two of the most commonly suggested methods of increasing dam safety. Both of these actions obviously decrease the probability of a dam breach, and lowering the reservoir level reduces the size of the flood wave should a breach still occur. However, enlarging the spillway increases the severity of flood damage when the dam does not fail, counteracting the decrease in overtopping failure damage. Also, lowering the reservoir usually, except at purely flood control dams, may reduce the value of the reservoir.

As discussed in Section 1.3, the direct costs of changing a spillway or lowering the reservoir stage, the construction costs and foregone benefits, are not examined in this work. The cost of damage to the dam itself and of foregone benefits from the dam after failure are also not in the analysis (see Section 3.2.6). These omissions tend to counteract each other, but when considering these results the reader should remember that this is an examination of only the downstream damage potential, not a complete economic analysis.

Section 5.1 shows the results of varying the spillway size and initial reservoir stage. Spillway size can be increased either by lengthening the spillway or by lowering the spillway crest elevation; it is varied by lengthening the spillway for the results shown in Section 5.1. Some results not shown in this work indicate that, for a given spillway

size, variation of the spillway crest elevation within a reasonable range does not greatly affect the damage potential for MPD, SRD, and KVD. Thus, the results shown in Section 5.1 are fairly general, even though they apply strictly only to changing spillway length. Section 5.2 shows results for the exception, GMD. Section 5.3 summarizes the results of this chapter.

As in Chapter 4, the PMF return period equals 10^5 years. Tables 3.2 and 3.3 list the parameter values used in this work. The special note about MPD in the introduction to Chapter 4 applies with equal force to the results shown in this chapter.

5.1 Spillway Size and Initial Reservoir Stage

Results are shown in three dimensional figures, with spillway size and initial stage as the horizontal axes. The spillway size is varied from half of the current design to a size at least large enough to pass the PMF without overtopping. The lower end of this range, half the existing size, is included to show what the damage potential would have been, had the spillway been built smaller; it is unlikely that anyone would propose reducing the spillway size on an existing dam, but two situations shown here indicate that the total damage potential could be reduced by reducing the spillway size. The upper end of this range, safe passage of the PMF, is normally the most stringent requirement ever placed on a spillway; also, some results not shown here indicate that damage potential does not vary much when the spillway size is increased beyond that necessary to pass the PMF without overtopping. The initial stage is varied through the same ranges described in Section 4.2.3.

The axis labeled spillway size is the ratio of the reservoir discharge when the reservoir stage is at the crest of the dam, $\underline{R}_c$, to the original value of $\underline{R}_c$. (R_c, the non-dimensional value always equals one.) For example, a value of two means that the reservoir discharge capacity, with the reservoir stage at the crest of the dam, is twice that of the existing design.

Both the spillway and the outlet works contribute to $\underline{R}_c$. In this work, however, only the spillway is changed when $\underline{R}_c$ is changed. The outlet works are not changed. Thus, when $\underline{R}_c$ is doubled (spillway size equals 2 in the figures), the spillway size itself is actually slightly more than doubled because the portion of the increase due to doubling the outlet works contribution to $\underline{R}_c$ is attributed to the spillway.

When $\underline{R}_c$ is changed, the non-dimensional values of several parameters must change if the real values of those parameters are to remain constant. Appendix D describes the necessary adjustments.

The axis labeled initial stage is the non-dimensional initial reservoir stage. The initial reservoir stage is normally determined by the outlet works of a dam. The outlet works for MPD, GMD, and SRD are fixed crest weirs, and the mean reservoir stage for these dams is approximately equal to the outlet works crest elevation. The outlet works for KVD are gated conduits with inverts near the base of the dam. (See Section 3.3) The initial stage at KVD is thus changed by changing the gate opening.

Changing the initial stage can also require parameter changes, depending on how the total discharge is modeled and how the initial stage is changed. When the outlet works are not explicitly represented in the

reservoir discharge curves, the effect on the total discharge curve of changing the outlet works depends on how the outlet works are changed. If the outlet works are changed by changing the crest elevation, the contributions of the outlet works to the total discharge could change substantially. If they are changed by adding a small outlet pipe at a low elevation, the contribution of the outlet works to the total discharge would change only slightly.

The outlet works are not represented explicitly in the reservoir discharge functions used here for MPD, GMD, and SRD. The initial stages for those dams are changed without changing the reservoir discharge function. This approach is most accurate for SRD, because the only low level outlet is a small pipe, and less accurate for GMD and MPD. At GMD, the reservoir can be lowered a few feet by lowering the outlet works crest; the reservoir can then be lowered further through a gated drain port at the base of the outlet structure. At MPD the reservoir can be nearly completely drained by lowering the outlet works crest.

The primary reason, however, for not changing the reservoir discharge function when the initial stage is changed is to clarify the source of changes in the results. For example, in Section 5.2, the total reservoir discharge at the crest of the dam, $\underline{R}_c$, is varied along one axis and the initial reservoir stage is varied along the other axis. If $\underline{R}_c$ were also changing as the initial stage changed, the effects of changing the two variables being examined would become intermingled and difficult to interpret. This way, changing the initial stage affects only the available storage volume and the stage at which Non-Overtopping Failures occur.

KVD is a different situation. The lower limb of the reservoir discharge curve for KVD represents the outlet works explicitly. The

outlet gates are operated to produce the desired initial reservoir stage. We assume here that the gates are always fully open when the reservoir stage is at the spillway crest. Thus, changing the initial stage by operating the outlet gates will not change $\underline{R}_c$. However, changing the initial stage without changing the parameters of the lower limb of the discharge function will change the initial discharge. The parameters of the lower limb of the discharge function are changed to preserve the correct discharge at the spillway crest and preserve the correct initial discharge for the specified initial stage. Appendix D2 describes the computations.

Figure 5.1 shows the variation in failure probability. As in Chapter 4, the dashed lines show the Overtopping Failure probability and the solid lines show the total failure probability. All four dams show the expected increase in failure probability with increasing initial stage and decreasing spillway size. The results show that the sensitivity of failure probability to initial stage variations increases as the spillway size decreases. Similarly, the sensitivity of failure probability to spillway size variations increases as the initial stage increases.

After the Phase I inspection, the reservoir stage at SRD was ordered to be lowered by ten feet because of the poor condition of the embankment; the non-dimensional stage was changed from 0.89 to 0.68. From Figure 5.1, this change lowered the overtopping failure probability only slightly, from $(5)10^{-4}$ to $(3.5)10^{-4}$, a change of $(1.5)10^{-4}$. If the spillway were half as large as it is, the overtopping failure probability would have changed from $(1.7)10^{-3}$ to $(1)10^{-3}$, a change of $(7)10^{-4}$. This example is not meant to advocate reducing the spillway size at SRD, but

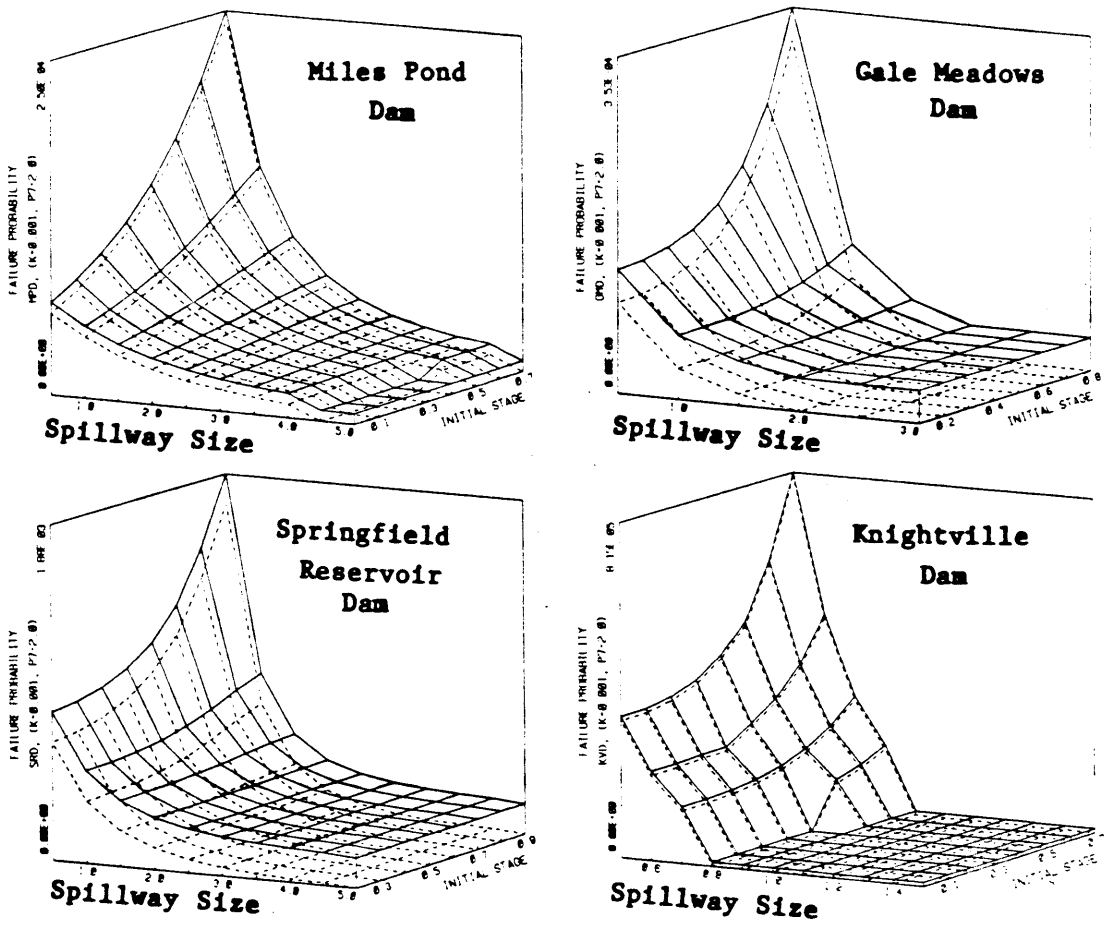

Figure 5.1: Variation of Failure Probability with Variation of Spillway Size and Initial Reservoir Stage

— — — Overtopping Failure Probability
——— Total Failure Probability

rather simply to illustrate the variation of sensitivity with spillway size.

Figure 5.2 shows the results for MPD with $(K,P_7) = (0.001,2)$. While the results for MPD must be interpreted carefully (see the Special Note about MPD in the introduction to Chapter 4), they can still be used. As before, the mean No-Failure damage curve is a better measure of the total damage than the total damage curve. The real total damage curve should be slightly higher than the No-Failure damage curve because breaches will increase the damage slightly.

The peak breach discharge, when the reservoir stage is at the crest of the dam, is approximately 95 percent of the existing spillway discharge at that stage. As the spillway gets larger, the size of the peak breach discharge relative to the peak spillway discharge will decrease, and the importance of breaches will decrease from their already low level. This means that the primary effect of increasing the spillway size will be to increase the damage potential downstream of the dam. Standard practice guidelines for spillway evaluation do not consider this possibility. For example, The Phase I inspection criteria suggest that the spillway size at MPD should be increased.

Figures 5.3, 5.4, and 5.5 show the results for GMD with $(K,P_7) = (0.001,2)$, $(0.001,1)$, and $(0.001,1.5)$. The results for GMD with $K = 1$ were similar to those for $K = 0.001$, though the No-Failure damage was relatively more significant when $K = 1$.

When $P_7 = 2$ (Figure 5.3), the total damage decreases as the spillway size increases, primarily due to the decrease in Overtopping Failure damage. That decrease is countered in part by the increasing No-Failure

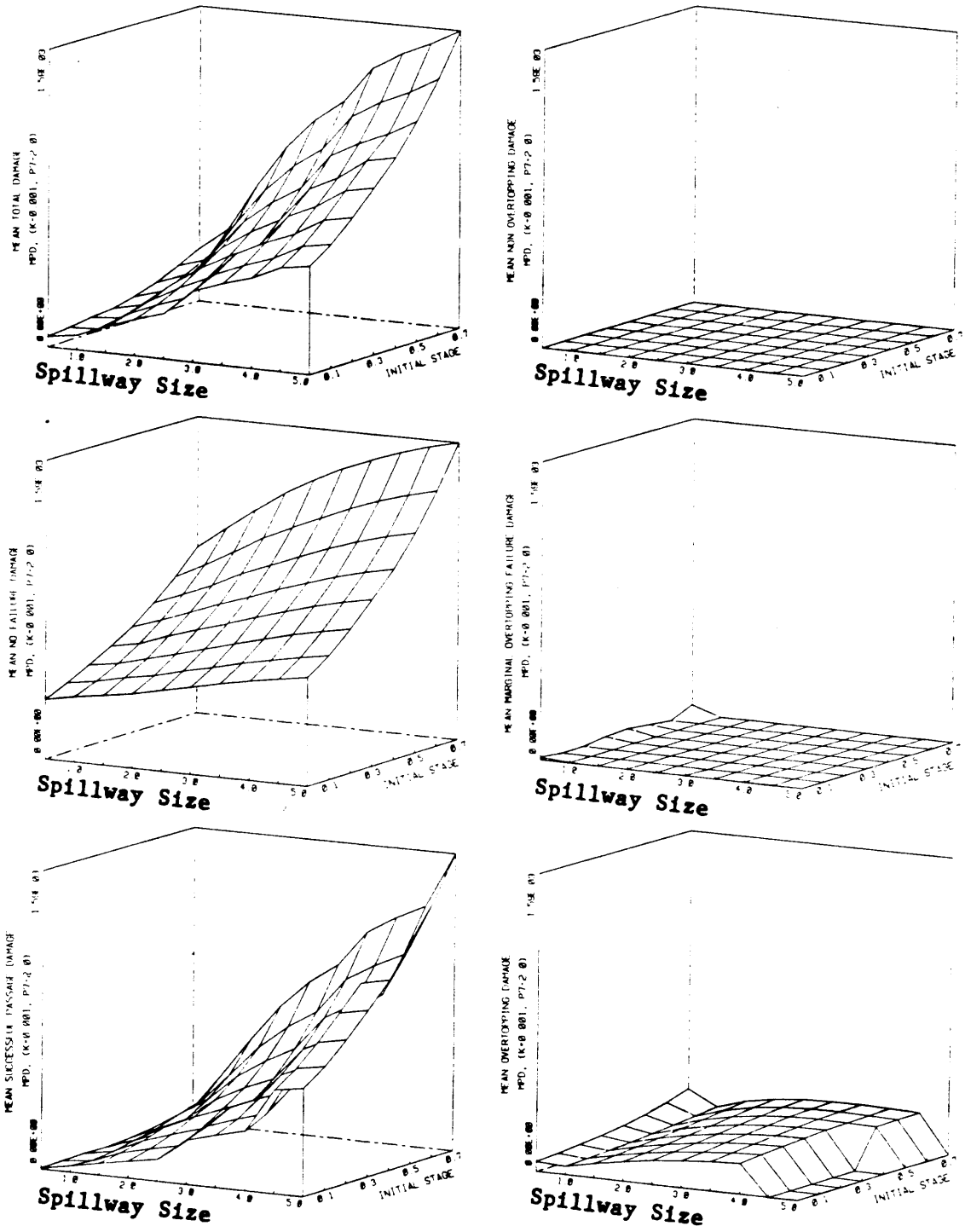

Figure 5.2: Variation of Damage Potential with Variation of Spillway Size and Initial Reservoir Stage for Miles Pond Dam with $(K,P_7) = (0.001,2)$

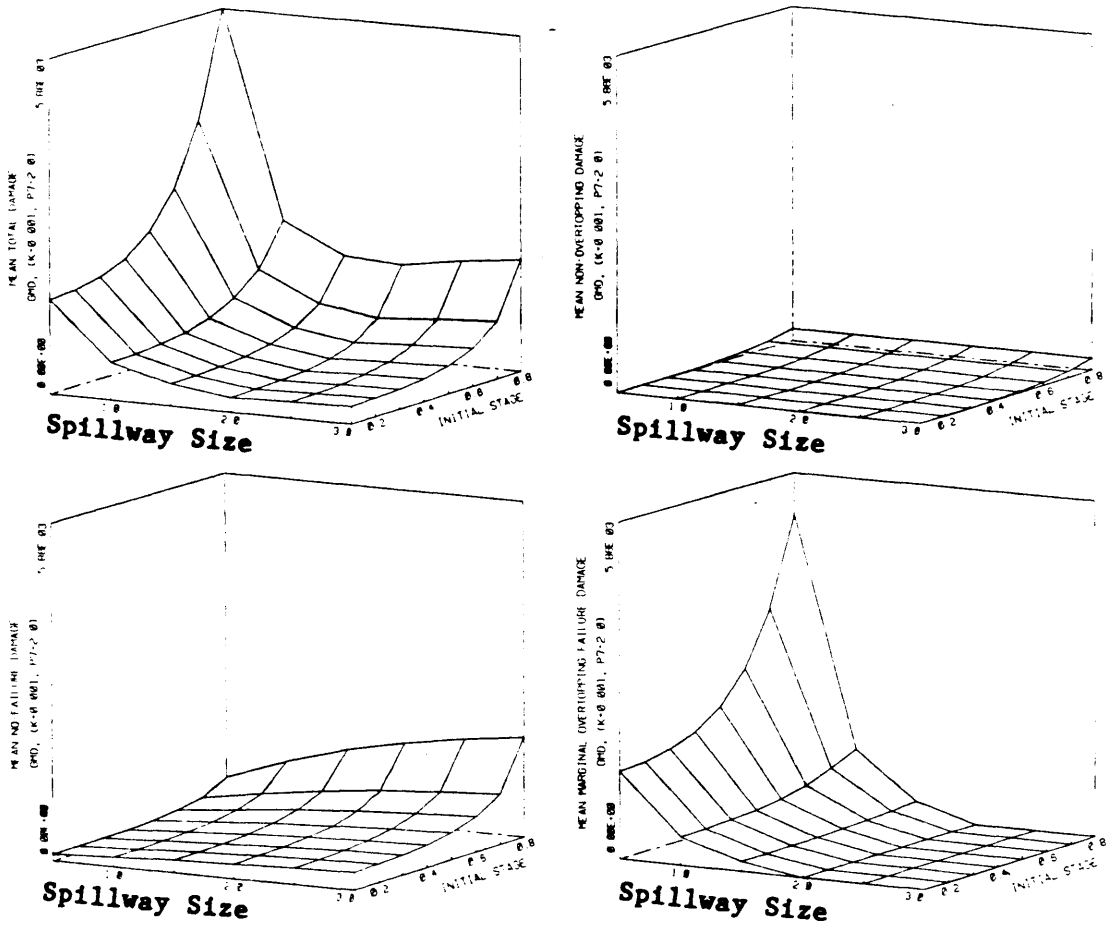

Figure 5.3: Variation of Damage Potential with Variation of Spillway Size and Initial Reservoir Stage for Gale Meadows Dam with $(K,P_7) = (0.001,2)$

damage, causing the total damage to increase slightly as the spillway is enlarged beyond twice the original size.

When P_7 = 1 (Figure 5.4), the total damage increases as the spillway size increases, for initial stages above 0.7, primarily due to the large increase in No-Failure damage. When the initial stage is below 0.7, the total damage is approximately constant as the spillway is enlarged from its present size and increases slightly when the spillway size is reduced.

When P_7 = 1.5 (Figure 5.5), the total damage starts high and passes through a minimum as the spillway size is increased, as first the Overtopping Failure and then the No-Failure damage dominates the total. For the current mean initial stage, 0.75, the minimum is near the existing spillway size. As the initial stage decreases, the spillway size at which the minimum total damage occurs increases.

Figure 5.6 shows the results for SRD when $(K,P_7) = (0.001,1)$. The total damage decreases as the spillway size increases, primarily due to the decrease in Overtopping Failure damage. No-Failure damage is not sensitive to spillway size variations. Results for the other combinations of K and P_7 are qualitatively similar to the results shown.

Figures 5.7 and 5.8 show the results for KVD when $(K,P_7) = (0.001,2)$ and $(0.001,1)$. When P_7 = 2, the total damage curve follows the shape of the failure probability curve (see Figure 5.1), being dominated by Overtopping Failure damage. When P_7 = 1, the total damage is dominated by the No-Failure damage and does not vary substantially with spillway size. The total damage varies substantially with initial reservoir stage for both values of P_7.

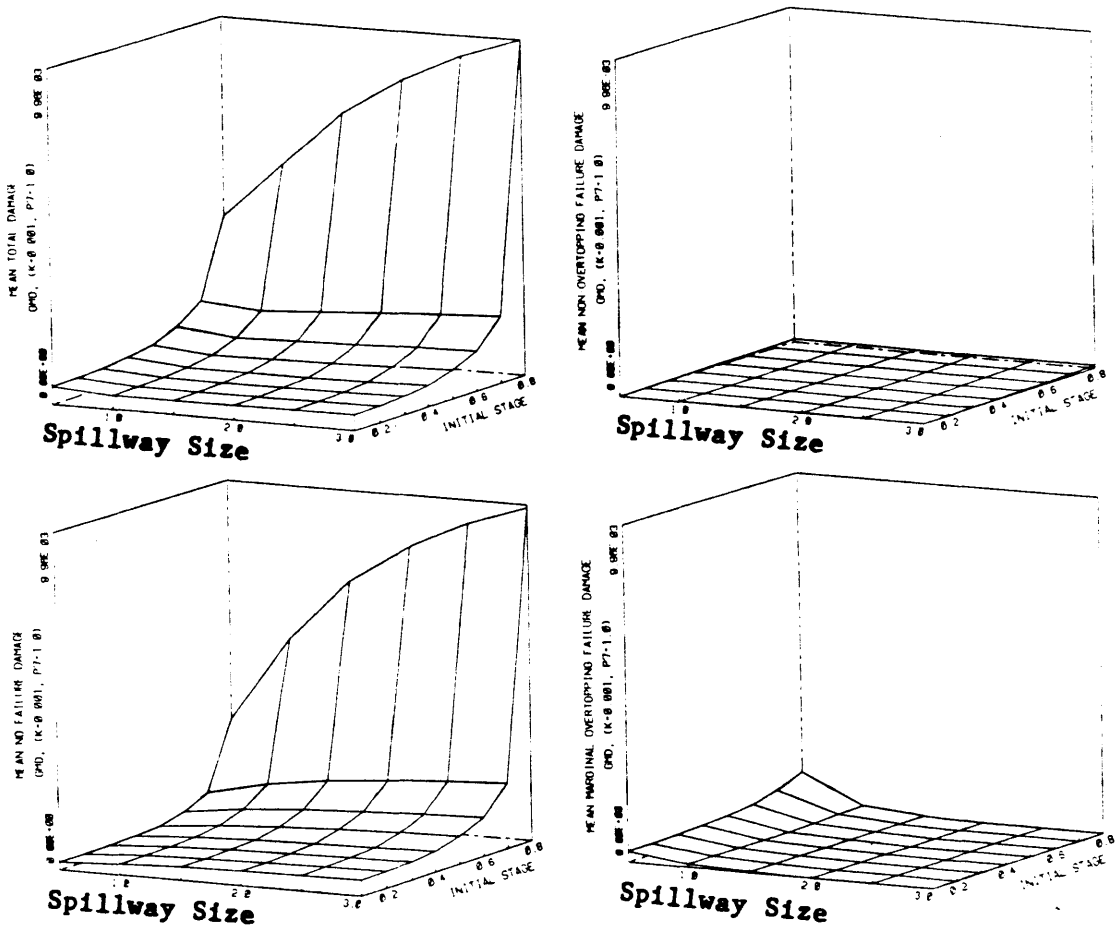

Figure 5.4: Variation of Damage Potential with Variation of Spillway Size and Initial Reservoir Stage for Gale Meadows Dam with $(K,P_7) = (0.001,1)$

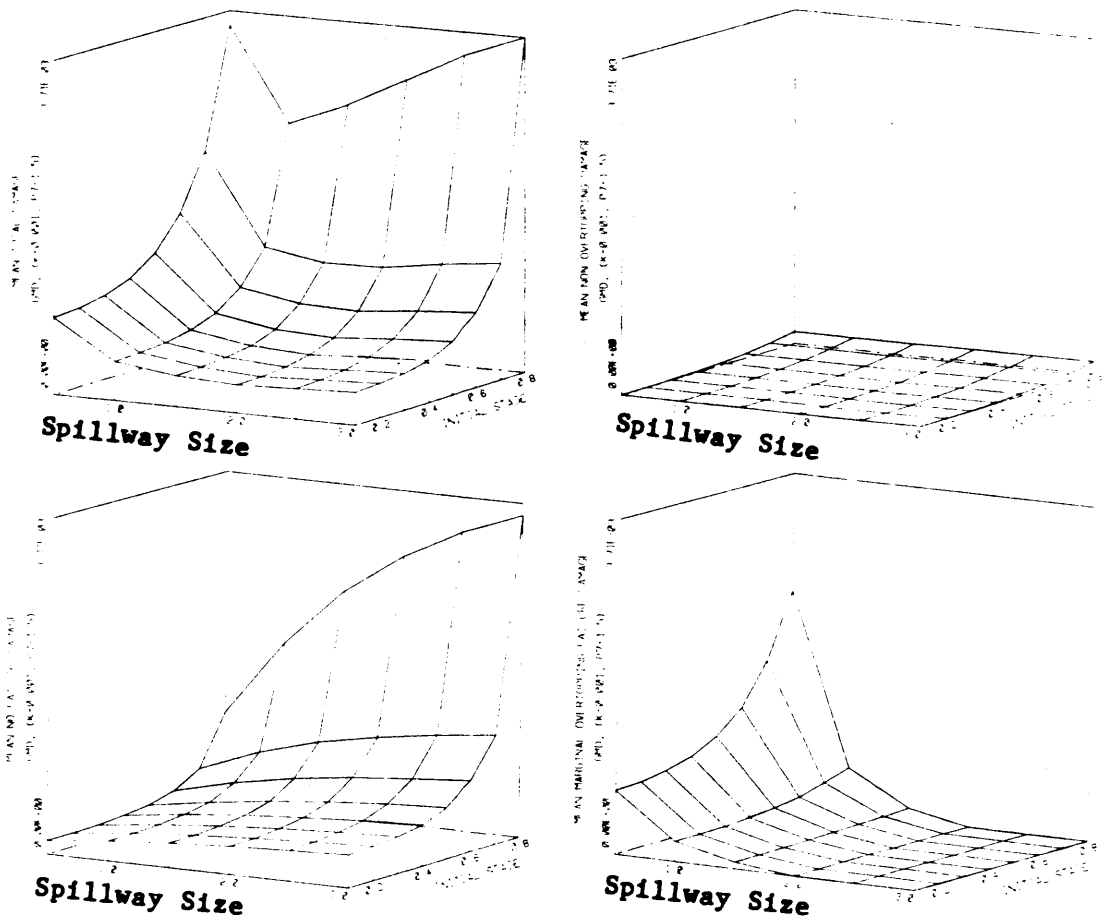

Figure 5.5: Variation of Damage Potential with Variation of Spillway Size and Initial Reservoir Stage for Gale Meadows Dam with $(K,P_7) = (0.001,1.5)$

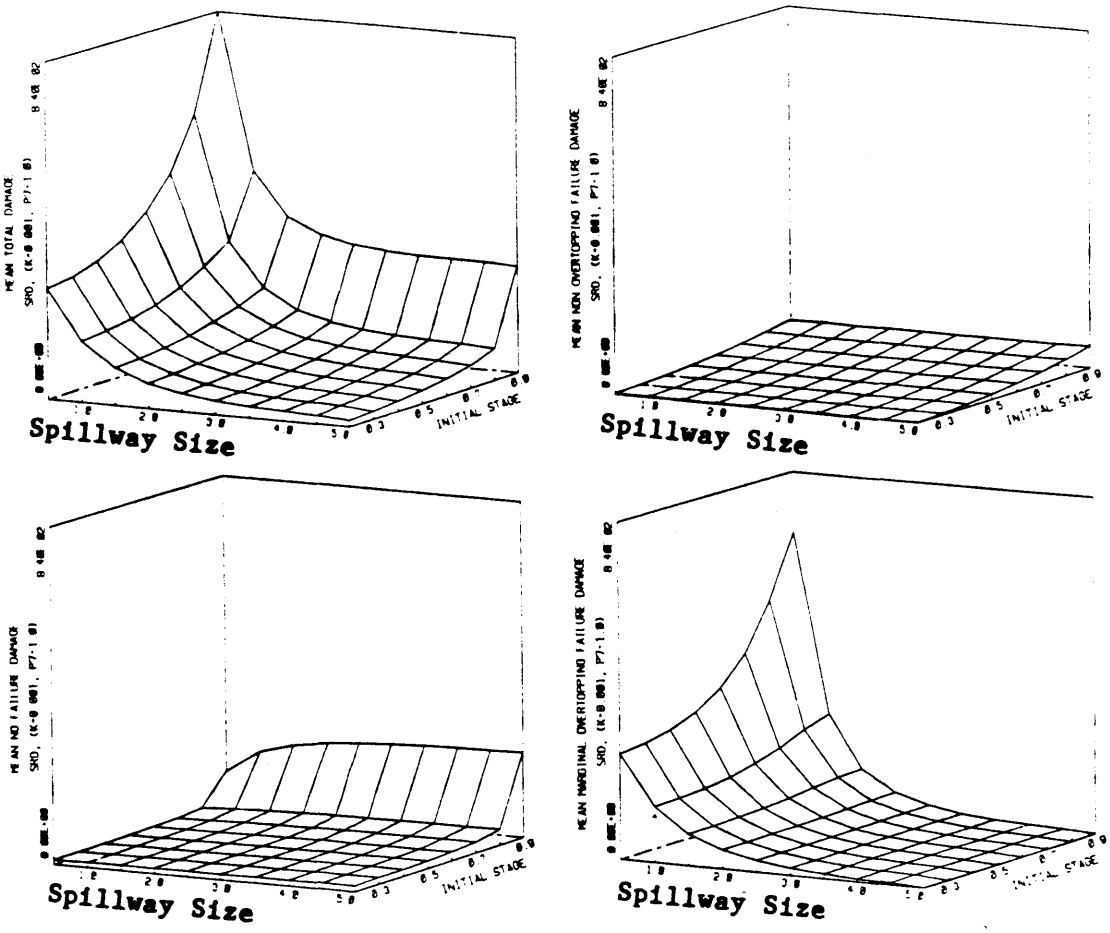

Figure 5.6: Variation of Damage Potential with Variation of Spillway Size and Initial Reservoir Stage for Springfield Reservoir Dam with $(K,P_7) = (0.001,1)$

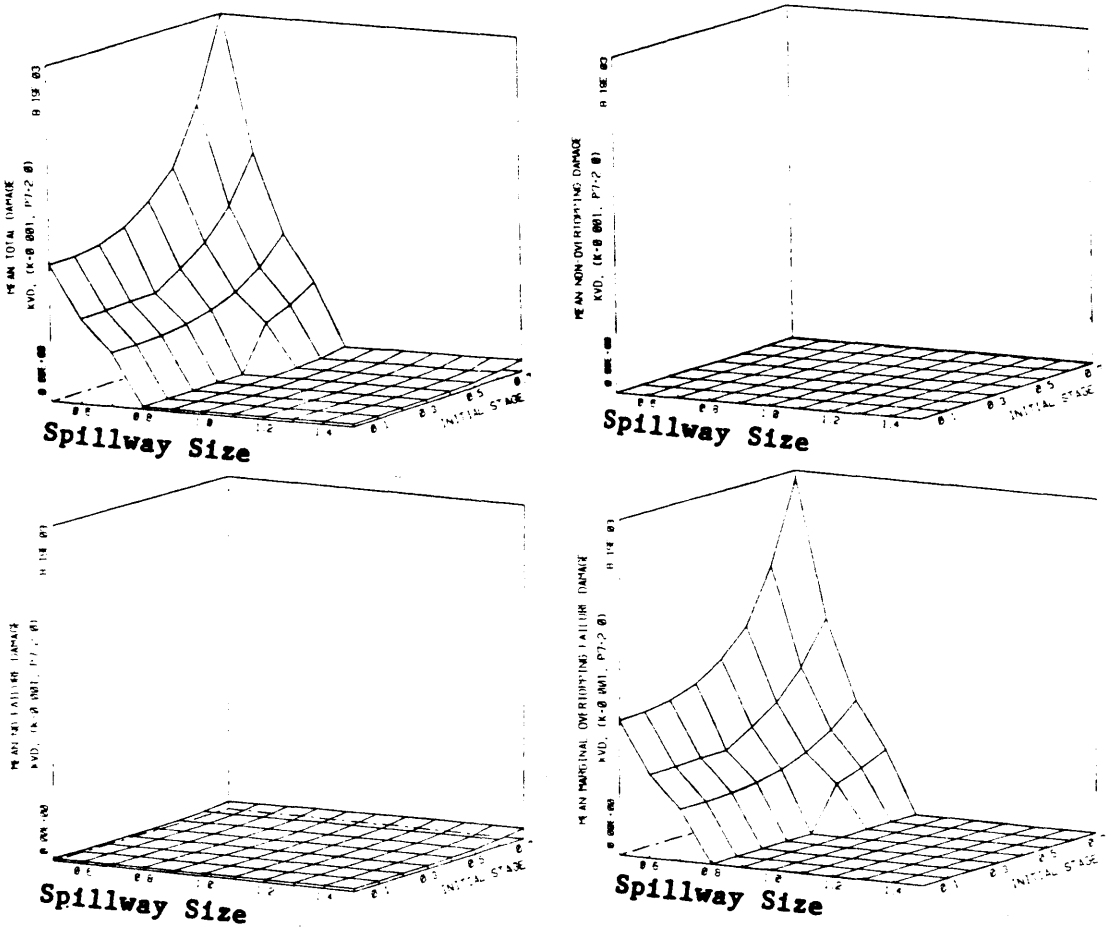

Figure 5.7: Variation of Damage Potential with Variation of Spillway Size and Initial Reservoir Stage for Knightville Dam with $(K,P_7) = (0.001,2)$

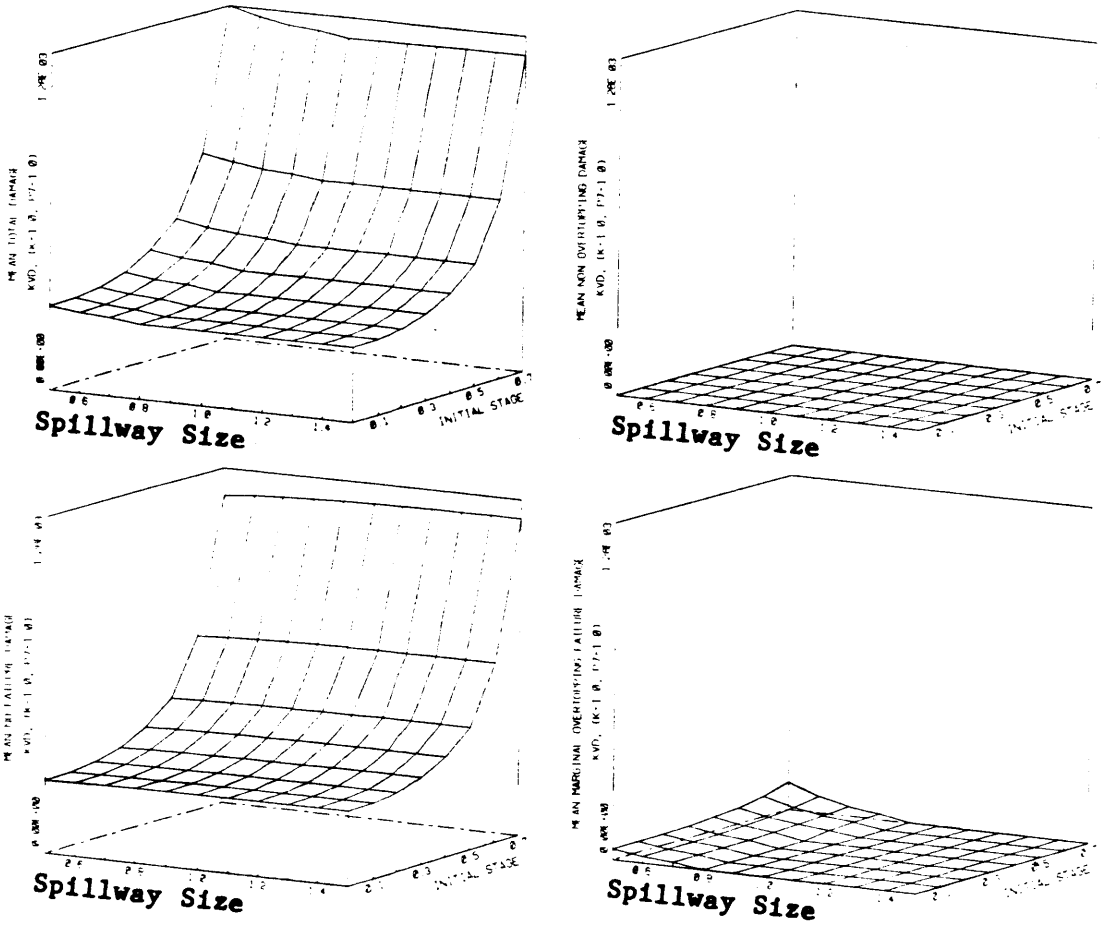

Figure 5.8: Variation of Damage Potential with Variation of Spillway Size and Initial Reservoir Stage for Knightville Dam with $(K,P_7) = (1,1)$

These results for KVD are caused by large flood attenuation capacity of KVD, without encroaching on the spillway, and the extremely large breach discharge when KVD does fail.

5.2 Spillway Size and Spillway Crest Elevation.

The results in this section are also shown in three dimensional figures with spillway size and spillway crest elevation as the horizontal axes. For a constant spillway size (measured by discharge at the crest of the dam), the spillway length must increase as the spillway crest height increases, and for a constant spillway crest height, the spillway length must increase as the spillway size increases. The spillway size is varied through the same range as in Section 5.1. The spillway crest elevation is varied from 0.9 to 1.05 times the current elevation. This small range of variation was chosen because crest elevations for fixed crest spillways are highly constrained by freeboard requirements and normal operation of the dam. The crest should be low enough to prevent wind generated waves from overtopping the dam during passage of the spillway design flood. The crest is normally higher than the highest normal operating level for the reservoir and is never lower than the crest of the outlet works.

When the lower limb of the reservoir discharge curve applies for all reservoir elevations below the crest of the dam, the spillway crest is usually not explicitly represented in the reservoir discharge function, and spillway crest elevation changes are not accurately represented by parameter changes. SRD is an exception to this because the outlet works are so small. The spillway crest is represented explicitly when the lower limb of the reservoir discharge function applies only to elevations below the

spillway crest. Figure 3.5 and Table 3.2 show two sets of reservoir discharge parameters for MPD and GMD. The parameters labeled upper limb as spillway were used in this section. The parameters labeled lower limb as spillway were used everywhere else. The outlet works at SRD are so small that the one set of parameters, for the lower limb as spillway, represents the spillway crest accurately. The outlet works at KVD are so large that the parameters for the upper limb as spillway, which represent the spillway crest explicitly, are always used.

When the spillway crest elevation is varied while $\underline{R_c}$ remains constant, the reservoir discharge function parameters must change. Appendix D describes the necessary changes.

The damage potential and failure probabilities for MPD, SRD, and KVD varied only slightly with changes in spillway crest elevation. These results are not shown. The damage potential, though not the failure probability, for GMD varied substantially with spillway crest elevation. These results are shown.

Figures 5.9 and 5.10 show the results for GMD with $(K,P_7) = (0.001,2)$ and $(0.001,1)$. The real variation in spillway crest height at GMD which corresponds to the non-dimensional variation of 0.9 through 1.05 shown in Figures 5.9 and 5.10 is -2.2 through +1.1 feet.

The variation with spillway discharge shown in Figures 5.9 and 5.10 is similar to that shown in Figures 5.3 and 5.4.

The total damage varies with spillway crest height primarily because of the No-Failure damage variation. The rate of change of No-Failure damage with spillway crest height changes substantially with spillway size, being larger for larger spillways. This variation, combined with

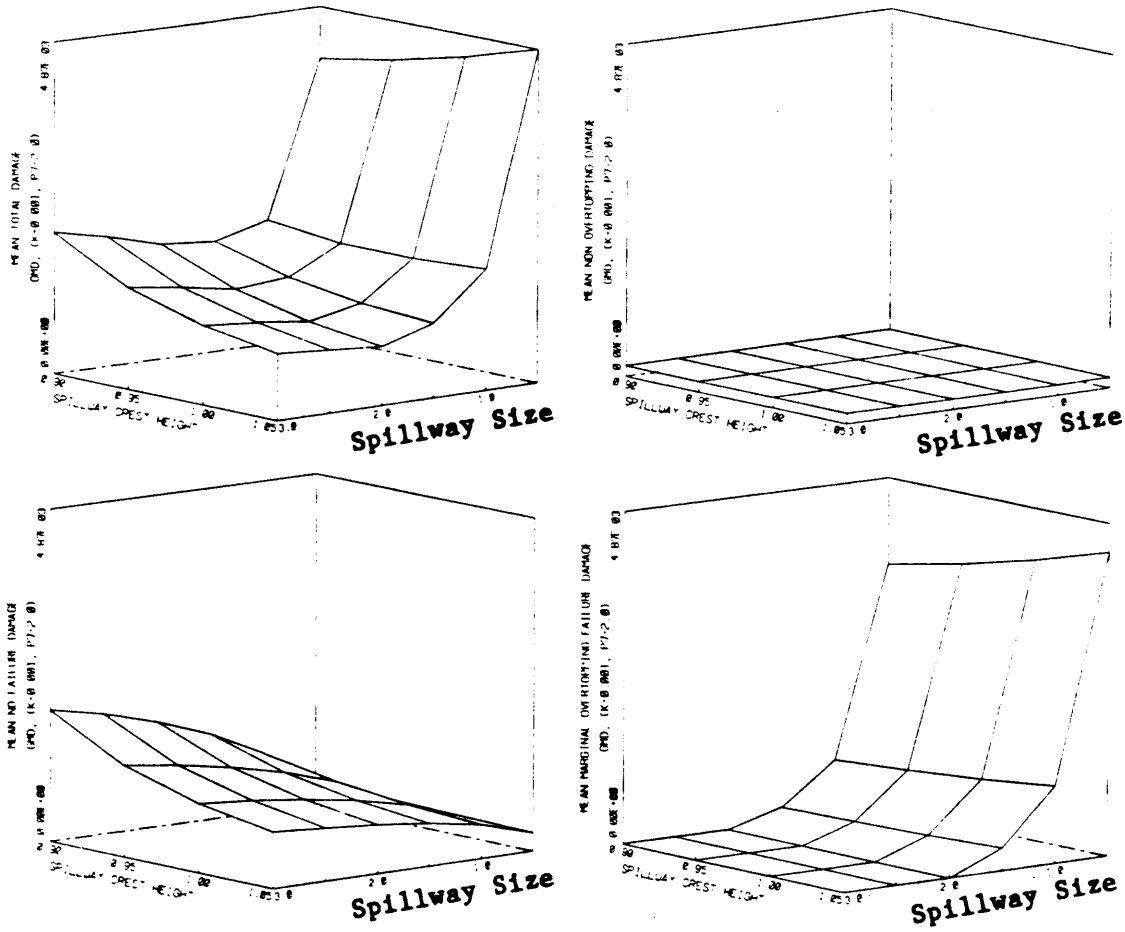

Figure 5.9: Variation of Damage Potential with Variation of Spillway Size and Spillway Crest Height for Gale Meadows Dam with $(K,P_7) = (0.001,2)$

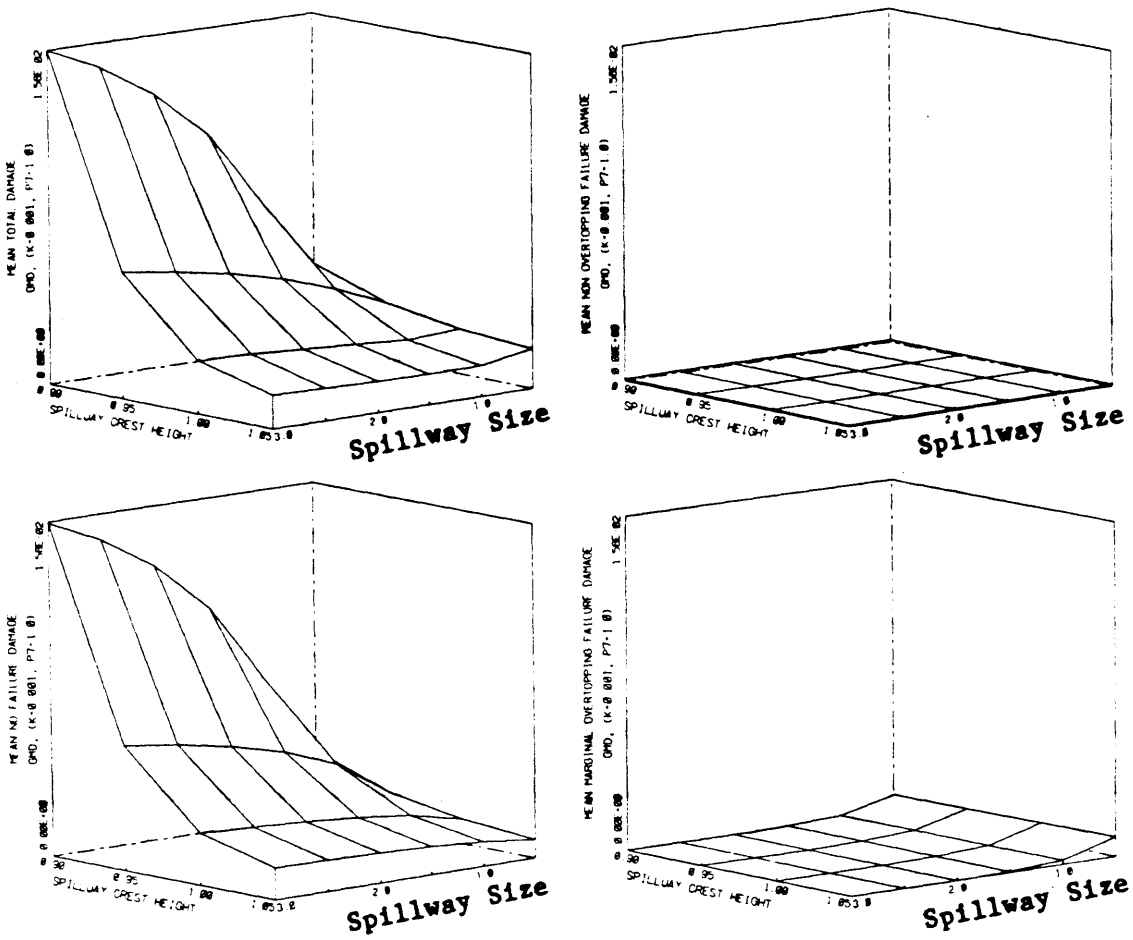

Figure 5.10: Variation of Damage Potential with Variation of Spillway Size and Spillway Crest Height for Gale Meadows Dam with $(K,P_7) = (0.001,1)$

a slight trend in the other direction for Overtopping Failure damage, causes direction of the change in total damage with spillway crest height to change as the spillway size changes, when $P_7 = 2$. This effect is not seen when $P_7 = 1$ because the No-failure damage dominates the total damage over the entire range of spillway sizes and crest heights considered here.

5.3 Conclusions

These results show that total expected damage can increase, decrease, pass through a minimum, or hardly change as the spillway size is increased. At MPD, enlarging the spillway will increase total expected damage. At GMD, the change in total expected damage with spillway size depends on the characteristics of the damage site. At SRD, enlarging the spillway will decrease the total expected damage. At KVD, total expected damage decreases with increasing spillway size (until the spillway is sufficiently large to prevent overtopping) when $P_7 = 2$, but hardly changes with changing spillway size when $P_7 = 1$.

Standard practice in spillway design does not require examination of the variations in flood damage caused by variations in spillway design within the requirement that the spillway design flood be passed without exceeding a maximum reservoir stage. Section 5.2 showed that the spillway crest elevation can affect the damage potential below a dam, though the damage potential below three of the four dams examined here was not sensitive to spillway crest height variations.

Chapter 6

SUMMARY, CONCLUSIONS, AND RECOMMENDATIONS

6.1 Summary

This work developed, tested, and applied a non-dimensional flood damage model which explicitly included the possibility of both overtopping and non-overtopping dam failures. The model represented the catchment upstream of the dam, the reservoir and dam, the channel downstream of the dam, and a damage site. Peak reservoir inflow, initial reservoir stage, and Overtopping Failure stage were represented as stochastic variables.

The model computed the mean and variance of the total downstream flood damage, and also separately computed the mean and variance of several components of that total. Those components measured the damage attributable to natural causes (Successful Passage or No-Failure floods), Overtopping Failures, and Non-Overtopping Failures. Only the mean damage was examined in this work. The model also computed Overtopping Failure probability.

Four dams in New England were selected as case studies. These dams were not selected as representatives of groups of dams, but rather to simply illustrate four different cases. Chapter 3 described parameter estimation for those four dams. The parameters of the catchment, reservoir, and dam were estimated from real data for the dams. The channel and damage site parameters were selected to represent channels and damage sites which could exist.

Chapter 4 examined sensitivity of model results to variations of model parameters. The parameters chosen for study were

Three parameters of the upstream catchment:

1) probable maximum flood (PMF) size

2) PMF return period

3) reservoir inflow flood volume-peak relation

and four parameters of dam failures:

1) breach depth

2) breach width

3) Overtopping Failure stage

4) Non-Overtopping Failure probability.

These seven parameters are hard to estimate accurately, and, for some, there is no way of knowing when an estimate is accurate. The PMF size and return period were used as parameters of the probability distribution for large floods. The true nature of this distribution is unknown. The reservoir inflow flood volume/peak ratio is extremely variable in nature, but was represented as a constant in this work. The dam failure parameters are difficult to estimate because there are few data from which to work and, until recently, little effort towards developing good estimates for these parameters.

The downstream channel and damage site parameters were also varied, not as uncertain parameters, but rather as parameters which vary from place to place.

Chapter 5 examined the changes in expected damage below the dams caused by changes in the spillway size, spillway crest height, and initial reservoir stage.

6.2 Conclusions

Two primary conclusions can be drawn from the results of this work.

First, from the results shown in Chapter 4, estimates of expected flood damage downstream from a dam can vary substantially as parameters which are difficult to estimate accurately are varied within reasonable ranges. Since the senstitivity to parameter variations varied among different dams and among different channels and damage sites below a given dam, this implies that the sensitivity to parameter variations should be examined before the results of a risk analysis are used for design decisions. This conclusion should not be construed to imply that the results of a risk analysis that includes dam failures and consideration of extremely large floods is any less accurate than traditional flood damage estimates. Traditional flood damage estimates simply ignore the sources of flood damage which have been shown here to be difficult to model accurately.

Second, from the results shown in Chapter 5, traditional thinking about spillways does not capture the full complexity of the influence of spillways on dam safety. Traditional thought assumes that a larger spillway produces a safer dam. Even ASCE (1973), when proposing risk analysis for spillway reevaluation, suggested that increasing spillway size always increases safety. The results shown in Chapter 5 show that the interplay between Overtopping Failure damage and Successful Passage damage (Overtopping Failure damage is expected to decrease and Successful Passage damage is expected to increase when the spillway size is increased) can cause the total expected damage to increase, decrease, pass through a minimum, or remain fairly constant as the spillway size increases. The behavior depends on the whole system, the catchment,

reservoir, dam, channel, and damage site, not on just the spillway design. Also, the effect of changing the spillway size depends on the initial reservoir stage. This suggests that the operation of the dam should also be considered when evaluating spillways.

These two conclusions taken together suggest that each situation must be examined for its own peculiarities when evaluating how spillway design and reservoir operation affect downstream flood damage. They further suggest that traditional flood damage evaluation methods sometimes ignore the dominant components of flood damage and that traditional spillway evaluation methods may not fully capture the influence of spillway design on dam safety. Using a risk analysis approach to spillway evaluation, and considering extreme floods and the possibility of dam failure, even when the procedures and parameters are uncertain, at least shows when the traditional methods may be deficient or misleading.

6.3 Recommendations

Risk analysis is not yet ready to replace current practice procedures for spillway analysis, but its development and use should be accelerated beyond the current pace. Risk analysis methods for spillway design need to be developed further, applied to several complete case studies, and then reexamined before they can be either embraced for tentative use or put aside in favor of other methods.

The particular model developed here would benefit substantially from improved representation of the catchment. One improvement, suggested in Chapter 4, would be to model the base time of the reservoir inflow hydrograph as a probability distribution. That distribution, or perhaps

just its mean and variance, could vary with the flood peak. Some data from which these distributions could be estimated are available (Hiemstra and Francis, 1981) and more should become available as hydrologic records are increasingly computerized. This would add substantially to the computational burden of the model, but also add substantially to the confidence which could be placed in the results. The computational burden of the current model is low, and adding this feature would not make it excessive.

Regional data analysis, perhaps along the lines of Hershfield's (1961,1965) studies of probable maximum precipitation, could perhaps provide better definition of the probability distribution of extreme floods. Also, as for the problem of the reservoir inflow flood volume-peak relation, the increasing amount of flood data and the increasing use of computers to store and retrieve that data should facilitate research in this area.

Improved information about breach formation would, of course, also be useful. Suggestions for specific improvements in these areas are, however, outside the scope of this work.

The next thing that should be done is to use the model for complete economic analyses of several case studies. These analyses would include estimation of the value of the dam, changes in the value of the dam when the reservoir stage is changed, construction costs for the spillway, and downstream damage. It might also include speculation about future development below the dam and consideration of the potential for human death, both from dam failures and from other causes such as drowning in the reservoir, drowning during floods, and construction related deaths. These analyses could be used to chose the minimum cost spillway design and should then be used as a vehicle to reexamine the sensitivity of the

results to parameter variations.

It would be possible, of course, to make the model more accurate by using numerical solutions of the dynamic wave equations for all the flood routing, including for the dam breach flood routing. Such a step would be desirable when preparing plans that will really be implemented. The increased accuracy would come at the cost of considerably increasing the computational burden of the analysis. The increased accuracy is probably not sufficiently important for research purposes to justify the increased expense.

This work was aimed primarily at the reevaluation of existing spillways at small to medium size dams, but the extension of these methods to the design of spillways for new dams and the reevaluation of existing spillways at large dams can not be ignored. The underlying principles are the same in all cases. The spillway should cost no more than the benefits it provides and the dam must meet any socially or politically imposed standards of public safety. Even at new dams or at large dams, risk analysis can provide information about the costs and benefits of different spillway designs. The costs of meeting any standards of public safety can then be made public. This information could help improve public decision making.

Risk analysis for spillway design is likely to have the greatest impact on spillway designs in the areas at which this work was initially directed, because the incremental costs of spillway enlargement are higher at existing dams that at new dams, and because the author suspects that a complete risk analysis for most large dams would probably show that large spillways are economically justified, if for no other reason than

that the value of the dam is so high. The higher incremental cost of spillway enlargement for existing dams may also lead to more serious consideration of nonstructural means, such as warning systems, to improve dam safety. Increased spillway size is particularly susceptible to being traded off against warning systems because methods to provide flood warning are available and are currently being improved through the use of remote sensing devices and microprocessors.

Some may argue that the uncertainties in risk analysis and the difficulty of estimating the parameters make it unsuitable for use where public safety is concerned. Others may argue that economic considerations are simply not sufficient for designing structures when public safety is at stake. Dorfman (in Maass et al., 1962), in a review of economic analysis applied to water resource projects, stated

> In the first place, it is clear that in a comparison between two decisions the one that gives rise to the higher expected value is not invariably to be preferred. Expected value, after all, is only a mathematical artifact; there is nothing compelling about it.

The first objection can be answered though further development and examination of risk analysis procedures. Most of the uncertainties that directly affect risk analysis for spillway design can be reduced at least to statements about reasonable ranges of values for the parameters. This level of knowledge is really no different than that in any other branch of engineering practice. The second objection can be answered through use of the variety of methods available today for assessing the influence on public decisions of uncertain and extreme events. Some of these were mentioned by Baecher et al. (1980). While these methods are far from perfect, they can still be used to illustrate the effects on economic analyses of different decision criteria. Also, few, if any, persons

advocate blind use of risk analysis to dictate public decisions.

Finally, the primary answer to these, and most other, objections to the use of risk analysis for spillway evaluation is that the parameters which are hard to estimate and the decisions about how to value uncertain or extreme events that are hard to make explicitly are all made implicitly in current practice. These difficult problems do not go away just because they are buried in a set of commonly accepted guidelines. The real value of risk analysis is that it forces careful explicit attention to at least some of the many considerations which influence decisions.

REFERENCES

Arrow, K.J., and R.C. Lind, Uncertainty and the evaluation of public investment decisions, American Economic Review, v.60, 364-378, 1970.

ASCE, Task Committee on the Reevaluation of the Adequacy of Spillways of Existing Dams, Reevaluating spillway adequacy of existing dams, J. Hyd. Div., Amer. Soc. Civil Eng., 99(HY2), proc. p. 9571, 337-372, Feb. 1973.

Baecher, G.B., M.-E. Patė, and R. de Neufville, NED cost determination for probability of dam failure, report, U.S. Water Resources Council, Wash., D.C., 1979.

Baecher, G.B., M.-E. Patė, and R. de Neufville, Risk of dam failure in benefit-cost analysis, Water Resources Res., 16(3), 449-456, June 1980.

Banks, H.O., Hydrology of spillway design: Introduction, J. Hyd. Div., Amer. Soc. Civil Eng., 90(HY3), proc. p. 3912, 235-237, May 1964.

Benjamin, J.R., and C.A. Cornell, Probability, Statistics, and Decision for Civil Engineers, McGraw-Hill, New York, 1970.

Bhavnagri, V.S., and G. Bugliarello, Mathematical representation of an urban flood plain, J. Hyd. Div., Amer. Soc. Civil Eng., 91(HY2), proc. p. 4265, 149-173, March 1965.

Bohnenblust, H., and E.H. Vanmarcke, Decision Analysis for Prioritizing Dams for Remedial Measures: A Case Study, Massachusetts Institute of Technology, Dept. of Civil Engineering, Research Report R82-12, May 1982.

Brevard, J.A., and F.D. Theurer, Simplified Dam Break Routing Procedure, Technical Release No. 66, U.S. Dept. Agr., Soil Conservation Service, Engr. Div., March 1979.

Brown, R.J., and D.C. Rogers, A Simulation of the Hydraulic Events During and Following the Teton Dam Failure, Bur. Rec., Denver, Colo., date unknown.

Buehler, B., Reevaluating spillway adequacy of existing dams, Proc., Engineering Foundation Conference on Inspection, Maintenance and Rehabilitation of Old Dams, Amer. Soc. Civil Eng., 23-28 Sept. 1973.

Buehler, B., Reevaluating spillway adequacy of existing dams, Proc., Engineering Foundation Conference on Safety of Small Dams, Amer. Soc. Civil Eng., Henniker, New Hampshire, 4-9 Aug. 1974.

Buehler, B., Dams in relation to balanced public safety, Proc., Engineering Foundation Conference on Responsibility and Liability of Public and Private Interests on Dams, Amer. Soc. Civil Eng., Pacific Grove, Calif., 28 Sept. - 3 Oct., 1975.

Buehler, B., Unit curves for judging spillway adequacy, Proc., Engineering Foundation Conference on the Evaluation of Dam Safety, Amer. Soc. Civil Eng., 28 Nov. - 3 Dec., 1976.

Bureau of Reclamation, Design of Small Dams, 2nd ed., U.S. Govt. Printing Office, Wash., D.C. 1973.

Carnahan, B., H.A. Luther, and J.O. Wilkes, Applied Numerical Methods, John Wiley & Sons, New York, 1969.

Chen, B.C., and W.H. Tang, Hydraulic and hydrologic aspects of dam safety, Proc., 3rd Engineering Mechanics Division Specialty Conference, Amer. Soc. Civil Eng., Austin, Texas, 17-19 Sept. 1979.

Chow, V.T., Open Channel Hydraulics, McGraw-Hill, New York, 1959.

Chow, V.T., ed., Handbook of Applied Hydrology, McGraw-Hill, New York, 1964.

Corps, U.S. Army Corps of Engineers, Office of the Chief of Engineers, Recommended guidelines for the safety inspection of dams, (appendix D of National Program of Inspection of Dams), May 1975.

Corps, U.S. Army Corps of Engineers, New England Division, Westfield, River Watershed: Master Manual of Water Control, (Appendix H), Jan. 1978.

Corps, U.S. Army Engineers, Office of the Chief of Engineers, Inspection of Non-Federal Dams: First Years Progress, Volume I (summary) and Volume II (appendices), 1 Dec. 1978a.

Corps, U.S. Army Corps of Engineers, New England Division, Phase I Inspection Report, National Inspection Program, Miles Pond Dam, VT 00062, Dec. 1980a.

Corps, U.S. Army Corps of Engineers, New England Division, Phase I Inspection Report, National Dam Inspection Program, Gale Meadows Dam, VT 00115, March 1980b.

Corps, U.S. Army Corps of Engineers, New England Division, Phase I Inspection Report, National Dam Inspection Program, Springfield Reservoir Dam, VT 00159, Feb. 1980c.

Cristofano, E.A., Method of Computing Erosion Rate for Failure of Earthfill Dams, Bur. Rec., Denver, Colo., Apr. 1965.

Defense Intelligence Agency, Computation of Outflow From Breached Dams, B-147-63, June 1963.

Dooge, J.C.I., Linear Theory of Hydrologic Systems, Technical Bulletin No. 1468, Agricultural Research Service, U.S. Dept. Agr., 1973.

Dressler, R.F., Hydraulic resistance effect upon the dam-break functions, J. Research, Nat. Bur. Standards, 49(3), res. pap. 2356, 217-225, Sept. 1952.

Engineering News Record, Dam safety: No national answer, 10-11, 8 May 1980.

FCCSET, Ad Hoc Interagency Committee on Dam Safety of the Federal Coordinating Council for Science Engineering and Technology, Federal Guidelines for Dam Safety, Wash. D.C., 25 June 1979.

Fread, D.L., Some limitations of dam-breach flood routing models, Preprint, Amer. Soc. Civil Eng. Fall Convention, St. Louis, Missouri, 26-30 Oct. 1981a.

Fread, D.L., Flood routing: A synopsis of past, present, and future capability, Proc., International Symposium on Rainfall-Runoff Modeling, Mississippi State, Mississippi, 18-22 May 1981b.

Fread, D.L., DAMBRK: The NWS Dam-Break Flood Forecasting Model, Office of Hydrology, National Weather Service, 30 Jan. 1982.

Gray, D.M., ed., Handbook on the Principles of Hydrology, National Resource Council of Canada, 1970 (published by Water Information Center, Inc., Huntington, New York, 1973).

Grigg, N.S., and O.J. Helweg, State-of-the-art of estimating flood damage in urban areas, Water Resources Bull., 11(2), 379-390, April 1975.

Grzywienski, A., Failure of conventional dams by overtopping, Proc., Institution of Civil Eng., v.48, 35-50, Jan. 1971.

Gundlach, D.L., and W.A. Thomas, Guidelines for Calculating and Routing a Dam-Break Flood, U.S. Army Corps of Engineers, Hydrologic Eng. Center, Research Note No. 5, Jan. 1977.

Harris, G.W. and D.A. Wagner, Outflow From Breached Dams, University of Utah, 1967.

Hawkins, E.F., Discussion of ASCE (1973) in J. Hyd. Div, Amer. Soc. Civil Eng., 100(HY1), 251-252, Jan. 1974.

Henderson, F.M., Open Channel Flow, Macmillan, New York, 1966.

Hershfield, D.M., Estimating the probable maximum precipitation, J. Hyd. Div., Amer. Soc. Civil Eng., 87(HY5), proc. p. 2933, 99-116, Sept. 1961.

Hershfield, D.M., Method for estimating probable maximum rainfall, Amer. Water Works Assoc. Journal, v.57, 965-972, 1965.

Hiemstra, L.A.V., and D.M. Francis, Run hydrograph for prediction of flood hydrographs, J. Hyd. Div., Amer. Soc. Civil Eng., 107(HY6), proc. p. 16324, 759-775, June 1981.

Hiemstra, L.A.V., W.S. Zucchini, and G.G.S. Pegram, A method of finding the family of runhydrographs for given return periods, J. Hydrology, v.30, 95-103, 1976.

Institution of Civil Engineers, Floods and Reservoir Safety, London, 1978.

James, D.L., and R.R. Lee, Economics of Water Resources Planning, McGraw-Hill, New York, 1971.

Jansen, R.B., Dams and Public Safety, U.S. Dept. Interior, Water and Power Resources Service, U.S. Govt. Printing Office, Wash., D.C., 1980.

Jennings, M.E., and V.B. Sauer, Flow routing models for stream system studies, Water Resources Bull., 8(5), 948-956, Oct. 1972.

Johnson, C.G., and G.D. Tasker, Progress Report on Flood Magnitude and Frequency of Vermont Streams, U.S. Geol. Sur., Open-File Report 74-130, March 1974.

Johnson, F.A., and P. Illes, A classification of dam failures, Int. Water Power and Dam Constr., 28(12), 43-45, Dec. 1976.

Keefer, T.N., Comparison of linear systems and finite difference flow-routing techniques, Water Resources Res., 12(5), 997-1006, Oct. 1976.

Keeney, R.L., and H. Raiffa, Decisions with Multiple Objectives: Preferences and Value Tradeoff, Wiley, New York, 1976.

Kirkpatrick, G.W., Evaluation guidelines for spillway adequacy, Proc., Amer. Soc. Civil Eng. Conf. on the Evaluation of Dam Safety, Pacific Grove, Calif., 28 Nov. - 3 Dec., 1976.

Koelzer, V.A. and M. Bitoun, Hydrology of spillway design floods: Large structures - limited data, J. Hyd. Div., Amer. Soc. Civil Eng., 90(HY3), proc. p. 3913, 261-293, May 1964.

Lambe, W.T., W.A. Marr, and F. Silva, Safety of a constructed facility: Geotechnical aspects, J. Geo. Eng. Div., Amer. Soc. Civil Eng., 107(GT3), proc. p. 16107, 339-352, March 1981.

Land, L.F., Evaluation of Selected Dam-Break Flood-Wave Models by Using Field Data, U.S. Geol. Sur., Water Res. Div., report WRI-80-44 (also numbered WRI-80/060), 54pp., Aug 1980.

Langbein, W.B., Queuing theory and water storage, J. Hyd. Div., Amer. Soc. Civil Eng., 84(HY5), proc. p. 1811, 1811/1 - 1811/24, Oct. 1958.

Linsley, R.K., M.A. Kohler, and J.L. Paulhus, Hydrology for Engineers, 2nd ed., McGraw-Hill, New York, 1975.

Maass, A., M.M. Hufschmidt, R. Dorfman, H.A. Thomas, Jr., S.A. Marglin, and G.M. Fair, Design of Water Resource Systems, Harvard University Press, Cambridge, 1962.

Ogrosky, H.O., Hydrology of spillway design: Small structures - limited data, J. Hyd. Div., Amer. Soc. Civil Eng., 90(HY3), proc. p. 3914, 295-310, May 1964.

OSTP, Office of Science and Technology Policy, Federal Dam Safety: Report of the OSTP Independent Review Panel, Wash., D.C., 6 Dec. 1978.

Pape, M.B., A Framework for Dam Safety Analysis, Master of Science Thesis, Dept. of Civil Engineering, Massachusetts Institute of Technology, Sept. 1980.

Paté, M.-E, Risk-Benefit Analysis for Construction of New Dams: Sensitivity Study and Real Case Applications, Massachusetts Institute of Technology, Dept. of Civil Engineering, Research Report No. R81-26, July 1981.

Ponce, V.M., and A.J. Tsivoglou, Modeling gradual dam breaches, J. Hyd. Div., Amer. Soc. Civil Eng., 107(HY7), proc. p. 16372, 829-838, July 1981.

Price, R.K., Flood Routing Methods for British Rivers, Hydraulics Research Station, Wallingford, England, Report No. INT 111, March 1973.

Price, J.T., G.W. Lowe, and J.M. Garrison, Unsteady flow modeling of dam-break waves, Proc., Dam-Break Flood Routing Workshop, U.S. Water Resources Council, Bethesda, Maryland, 18-20 Oct 1977, (NTIS No. PB 275 437).

Sakkas, John G., Dimensionless Graphs of Floods from Ruptured Dams, U.S. Army Corps of Engineers, Hydrologic Eng. Center Research Note No. 8, April 1980.

Sauer, V.B., Unit-response method of open channel flow routing, J. Hyd. Div., Amer. Soc. Civil Eng., 99(HY1), proc. p. 9499, 179-193, Jan. 1973.

Shah, H.C., and J.P. Franzini, Dam failure risk analysis, Proc., 3rd Engineering Mechanics Division Specialty Conference, Amer. Soc. Civil Eng., Austin, Texas, 17-19 Sept. 1979.

Snyder, F.F., Hydrology of spillway design: Large structures - adequate data, J. Hyd. Div., Amer. Soc. Civil Eng., 90(HY3), proc. p. 3915, 239-259, May 1964.

Stedinger, J.R. and A.N.F.G. Henriques, On the flexibility of Lambda and Wakeby distributions: A comparison, manuscript, Cornell University, March 1979.

Stoker, J.J., Water Waves, Interscience, New York, 1957.

Su, S., and A.H. Barnes, Geometric and frictional effects on sudden releases, J. Hyd. Div., Amer. Soc. Civil Eng., 96(HY11), proc. p. 7650, 2185-2200, Nov. 1970.

Taylor, A.E., and W.R. Mann, Advanced Calculus, 2nd ed., Xerox College Publishing, Lexington, Massachusetts, 1972.

Tinney, E.R., and H.Y. Hsu, Mechanics of washout of an erodible fuse plug, J. Hyd. Div., Amer. Soc. Civil Eng., 87(HY3), proc. p. 2808, 1-29, May 1961.

Vanmarcke, E.H., Decision Analysis in dam safety monitoring, Proc., Engineering Foundation Conference on Safety of Small Dams, Amer. Soc. Civil Eng., Henniker, New Hampshire, 4-9 Aug. 1974.

Vanmarcke, E.H., Safety, risk analysis, and insurance, Proc., Conference on Applications of Probability and Statistics to Soil and Structural Engineering, Sidney, Australia, Jan. 1979.

Viessman, W., Jr., J.W. Knapp, G.L. Lewis, and T.E. Harbaugh, Introduction to Hydrology, 2nd ed., IEP, New York, 1977.

Wandle, S.W., Jr., Estimating Peak Discharges of Small, Rural Streams in Massachusetts, U.S. Geol. Sur., Open-File Report 80-676, 1982.

Water Resources Council, Guidelines for Determining Flood Flow Frequency, Bull. No. 17A of the Hydrology Committee, U.S. Water Resources Council, June 1977.

Water Resources Council, Proceedings of Dam-Break Flood Routing Model Workshop, Bethesda, Maryland, 18-20 October 1977, (NTIS No. PB 275 437).

Weather Bureau, U.S., and U.S. Army Corps of Engineers, Seasonal Variation of the Probable Maximum Precipitation East of the 105th Meridian for Areas from 10 to 1000 Square Miles and Durations of 6, 12, 24 and 48 Hours, Hydrometeorological Report No. 33, Wash., D.C., April 1956.

Weather Bureau, U.S., Generalized Estimates of Probable Maximum Precipitation for the United States West of the 105th Meridian, Technical Paper No. 38, Wash. D.C., 1960.

Weather Bureau, U.S., and U.S. Army Corps of Engineers, Probable Maximum Precipitation Estimates, United States East of the 105th Meridian, Hydrometeorological Report No. 51, Wash., D.C., June 1978.

Weiss, H.W., and D.C. Midgley, Suite of mathematical flood plain models, J. Hyd. Div., Amer. Soc. Civil Eng., 104(HY3), proc. p. 13604, 361-376, Mar. 1978.

WES, U.S. Army Corps of Engineers Waterways Experiment Station, Floods Resulting from Suddenly Breached Dams, Hydraulic Model Investigation, Miscellaneous Paper No. 2-374, Report 1, Feb. 1960, and Report 2, Nov. 1961, Corps of Engineers, Vicksburg, Mississippi.

Wetmore, J.N., and D.L. Fread, The NWS simplified dam-break flood forecasting model, Proc., 5th Canadian Hydrotechnical Conference, Fredericton, New Brunswick, Canada, 26-27 May 1981.

Whitham, G.B., The effects of hydraulic resistance in the dam-break problem, Proc., Royal Society of London, Series A, v.227, 399-407, 1955.

Yevdjevich, V.M., Bibliography and Discussion of Flood Routing Methods and Unsteady Flow In Channels, U.S. Geol. Sur. Water-Supply Paper 1690, 235pp., 1964.

Appendix A

COMPUTATION OF NON-OVERTOPPING FAILURE PROBABILITY

A1 General Method

Bohnenblust and Vanmarcke (1982) suggested that Bayes Theorem (see Benjamin and Cornell, 1970) may be used to adjust prior information about failure probabilities for the conditions observed at a particular dam. For this purpose Bayes Theorem may be written:

$$p_j^F = \frac{p_j^{*F} \; p^{Z/F}}{p^Z} \qquad \text{(A1.1)}$$

where:

p_j^F = posterior probability of failure type j

p_j^{*F} = prior probability of failure type j

Z = an indicator for the condition of the dam

$p^{Z/F}$ = probability of observing condition Z given that the dam will fail

p^Z = total probability of observing condition Z

p^Z may be written as:

$$p^Z = p_j^{*F} \; p^{Z/F} + p_j^{*NF} \; p^{Z/NF} \qquad \text{(A1.2)}$$

where:

$p_j^{*NF} = 1 - p_j^{*F}$ = prior probability that failure type j will not occur

$p^{Z/NF}$ = probability of observing condition Z, given that the dam will not fail

Prior information about failure probabilities, p_j^{*F}, may be estimated from historical failure data. Baecher, et al. (1980) divided failure mechanisms into four categories and computed the frequency of occurrence for these mechanisms. Five different data sources were used. The four categories of failure mechanisms and average frequency of occurrence from the five data sets are shown in Table A1.

Table A1

OBSERVED FREQUENCY OF OCCURRENCE FOR FAILURE MECHANISMS
(from Baecher, et al., 1980)

Mechanism	Frequency
1) Spillway or Overtopping	0.30
2) Piping or Seepage	0.40
3) Slides	0.10
4) Miscellaneous	0.20

p_j^{*F} can be estimated by multiplying the frequencies in Table A1 by an estimate of the total failure rate. An example of the computation is shown in Table A5 in Section A2.

Estimating $p^{Z/F}$ and $p^{Z/NF}$ is more difficult. For now, these parameters can be estimated only through expert judgement. Bohnenblust and Vanmarcke (1982) suggested the scheme shown in Tables A2, A3, and A4 for use with Phase I inspection reports. These tables translate qualitative information, such as a statement that the dam is in fair condition, into quantitative information which can be used to estimate failure probabilities. Tables A2, A3, and A4 can be difficult to use because they are qualitative. For example, to use Table A2 one must decide if the seepage is or is not excessive; to use Table A3 one must decide if there are or are not stability problems; and to use Table A4 one must decide if there are special problems. These questions may be easy to answer for extreme cases, but no guidelines are offered here. Lambe et al. (1981) address these issues.

A2 Computation for Miles Pond Dam, Gale Meadows Dam, and Springfield Reservoir Dam

p^{NOF} for Miles Pond Dam (MPD), Gale Meadows Dam (GMD), and Springfield Reservoir Dam (SRD) is estimated using the frequency of occurrence for failure mechanisms shown in Table A1, the scheme for estimating $p^{Z/F}$ and $p^{Z/NF}$ shown in Tables A2, A3, and A4, the qualitative information contained in the Phase I inspection reports, and

Table A2

VALUES OF INDICATOR Z AND FUNCTIONS $p^{Z/F}$ AND $p^{Z/NF}$ FOR NON-OVERTOPPING FAILURE CAUSED BY INTERNAL EROSION

Values of Indicator Z +, 0, -, or --		Construction					
		Core		Zoned		Homogeneous	
		Excessive Seepage					
		No	Yes	No	Yes	No	Yes
General Condition	good	+	+	+	0	+	0
	fair	+	0	+	0	0	-
	poor	+	0	0	-	-	--
	very poor	0	-	0	--	-	--

	Z			
	+	0	-	--
$p^{Z/F}$	0.1	0.4	0.3	0.2
$p^{Z/NF}$	0.39	0.4	0.2	0.01

Table A3

VALUES OF INDICATOR Z AND FUNCTIONS $p^{Z/F}$ and $p^{Z/NF}$ FOR NON-OVERTOPPING FAILURE CAUSED BY SLIDES

Values of Indicator Z +, 0, -, or --		Indications of Stability Problems: No	Yes
General Condition	good	+	0
	fair	+	-
	poor	0	-
	very poor	-	--

	Z: +	0	-	--
$p^{Z/F}$	0.1	0.3	0.4	0.2
$p^{Z/NF}$	0.39	0.3	0.3	0.01

Table A4

VALUES OF INDICATOR Z AND FUNCTIONS $p^{Z/F}$ AND $p^{Z/NF}$ FOR MISCELLANEOUS NON-OVERTOPPING FAILURE MECHANISMS

Values of Indicator Z +, 0, -, or --		Indication of Special Problems: No	Yes
General Condition	good	+	0
	fair	+	-
	poor	0	-
	very poor	-	--

	Z: +	0	-	--
$p^{Z/F}$	0.05	0.35	0.4	0.2
$p^{Z/NF}$	0.3	0.35	0.3	0.05

the estimate of the total failure probability from historical data given by Baecher, et al. (1980).

Baecher, et al. (1980) suggested that the average annual failure probability over the lifetime of an average well-built dam was approximately 10^{-4}. They further noted that about half of all failures occur during the first five years after construction. Then, assuming a 100-year life span, the total failure probability is 10^{-2}, and the annual failure probability is 10^{-3} for the first five years and $(5)10^{-5}$ for the remaining ninety-five years. MPD, GMD, and SRD are all more than five years old. The relative frequencies for failure mechanisms shown in Table A1 are thus multiplied by $(5)10^{-5}$ to compute the average annual failure probabilities for these dams. Table A5 shows the computations and results.

Table A5

AVERAGE PROBABILITY OF OCCURRENCE FOR FAILURE MECHANISMS: DAMS OVER FIVE YEARS OLD

1)	Spillway or Overtopping	$p_1^{*F} = (0.3)(5)10^{-5} = (1.5)10^{-5}$
2)	Piping or Seepage	$p_2^{*F} = (0.4)(5)10^{-5} = (2)10^{-5}$
3)	Slides	$p_3^{*F} = (0.1)(5)10^{-5} = (5)10^{-6}$
4)	Miscellaneous	$p_4^{*F} = (0.2)(5)10^{-5} = (1)10^{-5}$

The failure probabilities for the non-overtopping failure mechanisms are then computed from Equation A1.1, using the parameter values shown in Tables A5, A6, and A7. The information in Table A6 is from the Phase I inspection reports. Table A7 was developed by applying Tables A2, A3, and A4 to the information in Table A6. P^{NOF} is the sum of the p_j^F for the three non-overtopping failure mechanisms.

Table A6

SUMMARY OF CONDITION OF MPD, GMD, AND SRD

	General Condition	Construction	Excessive Seepage	Stability Problem	Special Problems
MPD	Good	Unknown	No	No	No
GMD	Fair	Clay Core	Yes	No	Yes
SRD	Very Poor	Concrete Core	Yes	Yes	Yes

Table A7

INDICATOR Z AND FUNCTIONS $p^{Z/F}$ AND $p^{Z/NF}$
FOR MPD, GMD, AND SRD

MPD	Internal Erosion	Slides	Misc.
Z	+	+	+
$p^{Z/F}$	0.1	0.1	0.05
$p^{Z/NF}$	0.39	0.39	0.3
p_j^F	$(5.0)10^{-6}$	$(1.3)10^{-6}$	$(1.7)10^{-6}$

$p^{NOF} = (8.0)10^{-6}$

GMD	Internal Erosion	Slides	Misc.
Z	0	+	-
$p^{Z/F}$	0.4	0.1	0.4
$p^{Z/NF}$	0.4	0.39	0.3
p_j^F	$(2.0)10^{-5}$	$(1.3)10^{-6}$	$(1.4)10^{-5}$

$p^{NOF} = (3.5)10^{-5}$

SRD	Internal Erosion	Slides	Misc.
Z	-	--	--
$p^{Z/F}$	0.3	0.2	0.2
$p^{Z/NF}$	0.2	0.01	0.05
p_j^F	$(3.0)10^{-5}$	$(1.0)10^{-4}$	$(4.0)10^{-5}$

$p^{NOF} = (1.7)10^{-4}$

Appendix B

MODEL DEVELOPMENT

B1 Reservoir Routing

B1.1 Equation Development

The continuity equation is:

$$\underline{I} - \underline{R} = \frac{d\underline{V}}{d\underline{t}} \qquad \text{(B1.1)}$$

where:

$\underline{I}$ = reservoir inflow

$\underline{R}$ = reservoir discharge

$\underline{V}$ = reservoir volume

$\underline{t}$ = time

The underscore, here and throughout this work, indicates dimensional variables. All other variables are non-dimensional.

The upstream boundary condition (reservoir inflow), shown in Figure 2.1, is given by:

$$\underline{I} = \underline{I}_{pn} \frac{\underline{t}}{\underline{t}_p} + \underline{R}_0 + \underline{R}_b \qquad 0 \leq \underline{t} \leq \underline{t}_p \qquad \text{(B1.2A)}$$

$$= \underline{I}_{pn} \left(\frac{\underline{t}_b - \underline{t}}{\underline{t}_r}\right) + \underline{R}_0 + \underline{R}_b \qquad \underline{t}_p \leq \underline{t} \leq \underline{t}_b \qquad \text{(B1.2B)}$$

$$= \underline{R}_0 + \underline{R}_b \qquad \underline{t} \leq 0,\ \underline{t}_b \leq \underline{t} \qquad \text{(B1.2C)}$$

where:

$$\underline{I}_{pn} = \underline{I}_p - \underline{R}_0 - \underline{R}_b \qquad \text{(B1.3)}$$

$\underline{t}_p$ = time to peak

$\underline{t}_b$ = base time

$$\underline{t}_r = \underline{t}_b - \underline{t}_p \qquad \text{(B1.4)}$$

$\underline{R}_0$ = initial discharge to channel

$\underline{R}_b$ = reservoir draft not discharged to channel

The downstream boundary condition (reservoir discharge), shown in Figure 2.2, is given implicitly by:

$$\underline{V} = \underline{k}_1 \underline{R}_r + \underline{k}_2 \qquad \underline{R}_r \leq \underline{R}_s, \underline{V} \leq \underline{V}_s \qquad \text{(B1.5A)}$$

$$= \underline{k}_3 \underline{R}_r + \underline{k}_4 \qquad \underline{R}_r \geq \underline{R}_s, \underline{V} \geq \underline{V}_s \qquad \text{(B1.5B)}$$

where:

$\underline{k}_1, \underline{k}_2, \underline{k}_3, \underline{k}_4$ = constants

$\underline{R}_r$ = reservoir discharge to channel

$\underline{R}_s, \underline{V}_s$ = point of discontinuity in volume-discharge function

Total reservoir discharge is given by:

$$\underline{R} = \underline{R}_r + \underline{R}_b \qquad \text{(B1.6)}$$

The volume-stage function, shown in Figure 2.3, is given by:

$$\underline{V} = p_3 \underline{H}^{p_4} \qquad \text{(B1.7)}$$

This function is not used directly in the equations for natural flood routing, but is used, along with Equation B1.5, to compute reservoir discharge from reservoir stage. Equation B1.7 will also be used in the dam break model, described in Sections 2.3 and B3.

Dimensions are removed from each variable through division by the characteristic value from Table 2.1 which has the correct units. Dimensions are then removed from Equations B1.1 - B1.7 through substitution of the resulting expression. For example:

$$R_r = \frac{\underline{R}_r}{\underline{R}_c}$$

where:

R_r = dimensionless discharge to channel

$\underline{R}_r$ is then replaced by $R_r \underline{R}_c$ in all equations.

This procedure does not change Equations B1.1 through B1.6, except that all variables are replaced by their dimensionless counterparts. Equation B1.7 becomes:

$$V = H^{p_4} \qquad \text{(B1.8)}$$

because of the relation:

$$\underline{V}_c = p_3 \underline{H}_c^{p_4} \qquad \text{(B1.9)}$$

which comes from the definition of $\underline{V}_c$ as the volume at $\underline{H}_c$.

Substituting the non-dimensional forms of Equations B1.2 through B1.6 in B1.1 gives:

$$0 = \frac{dR_r}{dt} \qquad t \leq 0 \qquad \text{(B1.10A)}$$

$$I_{pn} \frac{t}{t_p} + R_0 - k_{[1,3]} R_r - k_{[2,4]} = k_{[1,3]} \frac{dR_r}{dt} \qquad 0 \leq t \leq t_p \qquad \text{(B1.10B)}$$

$$I_{pn}\left(\frac{t_b - t}{t_r}\right) + R_0 - k_{[1,3]} R_r - k_{[2,4]} = k_{[1,3]} \frac{dR_r}{dt} \qquad t_p \leq t \leq t_b \qquad \text{(B1.10C)}$$

$$R_0 - k_{[1,3]} R_r - k_{[2,4]} = k_{[1,3]} \frac{dR_r}{dt} \qquad t_b \leq t \qquad \text{(B1.10D)}$$

where:

$$k_{[1,3]} = k_1 \text{ when } R_r \leq R_s \qquad \text{(B1.11)}$$
$$k_3 \text{ when } R_r \geq R_s$$

$$k_{[2,4]} = k_2 \text{ when } R_r \leq R_s \qquad \text{(B1.12)}$$
$$k_4 \text{ when } R_r \geq R_s$$

Each part of Equation B1.10 is a first order linear differential equation, the general solutions of which are:

$$R_r = R_0 \qquad 0 \leq t_d \qquad \text{(B1.13A)}$$

$$R_r = I_{pn}\left[\frac{t - k_{[1,3]}}{t_p} + g_a \exp\left(\frac{-t}{k_{[1,3]}}\right)\right] + R_0 \qquad t_d \leq t \leq t_p \qquad \text{(B1.13B)}$$

$$R_r = I_{pn}\left[\frac{t_b + k_{[1,3]} - t}{t_r} + g_b \exp\left(\frac{-t}{k_{[1,3]}}\right)\right] + R_0$$

$$\max(t_d, t_p) \leq t \leq t_b \qquad \text{(B1.13C)}$$

$$R_r = I_{pn}\left[g_c \exp\left(\frac{-t}{k_{[1,3]}}\right)\right] + R_0 \qquad t_b \leq t \qquad \text{(B1.13D)}$$

where:

$g_{[a,b,c]}$ = constants determined by initial conditions

t_d = time at which reservoir discharge begins

When R_0 is greater than zero, t_d equals zero. When R_0 equals zero, the initial reservoir stage is at or below the invert of the outlet works and the reservoir must fill to that invert before discharging. When $t_d > t_p$, Equation B1.13B does not apply, and when $t_d > t_b$, there is no reservoir discharge.

t_d may be calculated by letting $R_r = R_0 = 0$ and solving the dimensionless version of Equation B1.1 for volume. The resulting equation may be solved for the time at which the reservoir volume equals k_2, the volume at which discharge begins. Substituting the

dimensionless version of Equation B1.2A into the dimensionless version of Equation B1.1 and letting $R_r = R_0 = 0$ gives:

$$I_{pn} \frac{t}{t_p} = \frac{dV}{dt} \tag{B1.14}$$

Solving for V, and letting $V = V_0$ at $t = 0$,

$$V = \frac{I_{pn}}{2t_p} t^2 + V_0 \quad t \leq t_d \leq t_p \tag{B1.15}$$

Letting $V = k_2$, and solving for t gives:

$$t_d = \left[(k_2 - V_0) \frac{2t_p}{I_{pn}}\right]^{\frac{1}{2}} \tag{B1.16}$$

When t_d computed from Equation B1.16 is greater than t_p, the dimensionless version of Equation B1.2B must be used to describe the reservoir inflow. Equation B1.14 is then replaced by:

$$I_{pn}\left(\frac{t_b - t}{t_r}\right) = \frac{dV}{dt} \quad t_p \leq t \leq t_d \tag{B1.17}$$

Solving Equation B1.17 and taking the initial condition from Equation B1.15 at $t = t_p$:

$$V = \frac{I_{pn}}{t_r}\left(t_b t - \frac{t^2}{2}\right) - \frac{I_{pn}\, t_b\, t_p}{2t_r} + V_0 \tag{B1.18}$$

Solving Equation B1.18 for t_d:

$$t_d = t_b \pm (t_b^2 - 2a)^{\frac{1}{2}} \tag{B1.19}$$

where:

$$a = (k_2 - V_0) \frac{t_r}{I_{pn}} + \frac{t_p t_b}{2} \tag{B1.20}$$

The negative sign in the right-hand side of B1.19 should be used. When $2a > t_b^2$ (no real root to Equation B1.18) there is no reservoir discharge anytime during the passage of the flood.

The solutions for routing floods through the reservoir must be considered in several separate cases because the upstream boundary condition changes form at $t = t_p$ and $t = t_b$, and the downstream boundary condition changes form at ($V = V_s$, $R = R_s$). These changes define the six cases, divided into four major cases, two of which have sub-cases, listed in Table B1.1. Each of the six cases has a separate set of equations, though some equations are common to more than one case. Also, within the cases listed there are further sub-cases which depend on the value of t_d. These further sub-cases are not listed.

Table B1.2 summarizes the reservoir discharge equations. The first column indicates the sub-cases for $0 < t_d < t_p$ and $t_p < t_d < t_b$ within cases 1, 2, and 3. The letters NA indicate that the value of t_d does not matter. The second and third columns list the base equation and time interval over which the solution applies. The fourth column lists the reservoir discharge at the beginning of the time interval. The constants determined by the initial reservoir discharge change when the discharge passes through the point (R_s, V_s)

Table B1.1

CASES DEFINED BY BOUNDARY CONDITION DISCONTINUITIES

Case 1:

$R_0 < R_s$ $\qquad$ $R_p \leq R_s$

Case 2:

$R_0 < R_s$ $\qquad$ $R_p \geq R_s$ $\qquad$ $R_r < R_s$ at $t = t_p$

Case 2a: $\qquad$ $R_r < R_s$ at $t = t_b$

Case 2b: $\qquad$ $R_r > R_s$ at $t = t_b$

Case 3:

$R_0 < R_s$ $\qquad$ $R_p \geq R_s$ $\qquad$ $R_r > R_s$ at $t = t_p$

Case 3a: $\qquad$ $R_r < R_s$ at $t = t_b$

Case 3b: $\qquad$ $R_r > R_s$ at $t = t_b$

Case 4:

$R_0 \geq R_s$

where R_p = peak reservoir discharge

Table B1.2

RESERVOIR DISCHARGE EQUATIONS

Time of Initial Discharge t_d	Equation B1.13	Time Interval	Initial Discharge	Constant Determined by Initial Discharge	
				Name	Expression
Case 1					
$0 < t_d$	A	$0 \leq t \leq t_d$	$R_0 = 0$	--	
$0 \leq t_d \leq t_p$	B	$t_d \leq t \leq t_p$	R_0	g_{1a}	$\frac{k_1 - t_d}{t_p} \exp(\frac{t_d}{k_1})$
	C	$t_p \leq t \leq t_b$	-	g_{1b}	$g_{1a} - \frac{k_1 t_b}{t_p t_r} \exp(\frac{t_p}{k_1})$
$t_p \leq t_d \leq t_b$	C	$t_d \leq t \leq t_b$	$R_0 = 0$	g_{1b}	$\frac{t_d - t_b - k_1}{t_r} \exp(\frac{t_d}{k_1})$
NA	D	$t_b \leq t$	-	g_{1c}	$g_{1b} + \frac{k_1}{t_r} \exp(\frac{t_b}{k_1})$

Table B1.2 (Cont'd)

Time of Initial Discharge t_d	Equation B1.13	Time Interval	Initial Discharge	Constant Determined by Initial Discharge	
				Name	Expression
Case 2					
$0 < t_d$	A	$0 \leq t \leq t_d$	$R_0 = 0$	--	
$0 \leq t_d \leq t_p$	B	$t_d \leq t \leq t_p$	R_0	g_{2a}	$\frac{k_1 - t_d}{t_p} \exp(\frac{t_d}{k_1})$
	C	$t_p \leq t \leq t_{s1}$	-	g_{2b}	$g_{2a} - \frac{k_1 t_b}{t_p t_r} \exp(\frac{t_p}{k_1})$
$t_p \leq t_d \leq t_b$	C	$t_d \leq t \leq t_{s1}$	$R_0 = 0$	g_{2b}	$\frac{t_d - t_b - k_1}{t_r} \exp(\frac{t_d}{k_1})$

Table B1.2 (Cont'd)

Time of Initial Discharge t_d	Equation B1.13	Time Interval	Initial Discharge	Constant Determined by Initial Discharge	
				Name	Expression
Case 2a					
NA	C	$t_{s1} \leq t \leq t_{s2}$	R_s	g_{2c}	$(\frac{R_s - R_0}{I_{pn}} - \frac{t_b + k_3 - t_{s1}}{t_r}) \exp(\frac{t_{s1}}{k_3})$
	C	$t_{s2} \leq t \leq t_b$	R_s	g_{2d}	$(\frac{R_s - R_0}{I_{pn}} - \frac{t_b + k_1 - t_{s2}}{t_r}) \exp(\frac{t_{s2}}{k_1})$
	D	$t_b \leq t$	-	g_{2e}	$g_{2d} + \frac{k_1}{t_r} \exp(\frac{t_b}{k_1})$
Case 2b					
NA	C	$t_{s1} \leq t \leq t_b$	R_s	g_{2c}	$(\frac{R_s - R_0}{I_{pn}} - \frac{t_b + k_3 - t_{s1}}{t_r}) \exp(\frac{t_{s1}}{k_3})$
	D	$t_b \leq t \leq t_{s2}$	-	g_{2f}	$g_{2c} + \frac{k_3}{t_r} \exp(\frac{t_b}{k_3})$
	D	$t_{s2} \leq t$	R_s	g_{2g}	$\frac{R_s - R_0}{I_{pn}} \exp(\frac{t_{s2}}{k_1})$

Table B1.2 (Cont'd)

Time of Initial Discharge t_d	Equation B1.13	Time Interval	Initial Discharge	Constant Determined by Initial Discharge	
				Name	Expression
		Case 3			
$0 < t_d$	A	$0 \leq t \leq t_d$	$R_0 = 0$	--	
$0 \leq t_d \leq t_{s1}$	B	$t_d \leq t \leq t_{s1}$	R_0	g_{3a}	$\frac{k_1 - t_d}{t_p} \exp(\frac{t_d}{k_1})$
	B	$t_{s1} \leq t \leq t_p$	R_s	g_{3b}	$(\frac{R_s - R_0}{I_{pn}} - \frac{t_{s1} - k_3}{t_p}) \exp(\frac{t_{s1}}{k_3})$
		Case 3a			
NA	C	$t_p \leq t \leq t_{s2}$	-	g_{3c}	$g_{3b} - \frac{k_3 t_b}{t_p t_r} \exp(\frac{t_p}{k_3})$
	C	$t_{s2} \leq t \leq t_b$	R_s	g_{3d}	$(\frac{R_s - R_0}{I_{pn}} - \frac{t_b + k_1 - t_{s2}}{t_r}) \exp(\frac{t_{s2}}{k_1})$
	D	$t_b \leq t$	-	g_{3e}	$g_{3d} + \frac{k_1}{t_r} \exp(\frac{t_b}{k_1})$

Table B1.2 (Cont'd)

Time of Initial Discharge t_d	Equation B1.13	Time Interval	Initial Discharge	Constant Determined by Initial Discharge	
				Name	Expression
			Case 3b		
NA	C	$t_p \leq t \leq t_b$	-	g_{3c}	$g_{3b} - \frac{k_3 t_b}{t_p t_r} \exp(\frac{t_p}{k_3})$
	D	$t_b \leq t \leq t_{s2}$	-	g_{3f}	$g_{3b} + \frac{k_3}{t_r} \exp(\frac{t_b}{k_3})$
	D	$t_{s2} \leq t$	R_s	g_{3g}	$\frac{R_s - R_0}{I_{pn}} \exp(\frac{t_{s2}}{k_1})$

Table B1.2 (Cont'd)

Time of Initial Discharge t_d	Equation B1.13	Time Interval	Initial Discharge	Constant Determined by Initial Discharge	
				Name	Expression
Case 4					
NA	B	$0 \leq t \leq t_p$	R_0	g_{4a}	$\frac{k_1}{t_p}$
	C	$t_p \leq t \leq t_b$	-	g_{4b}	$g_{4a} - \frac{k_3 t_b}{t_p t_r} \exp(\frac{t_p}{k_3})$
	D	$t_b \leq t$	-	g_{4c}	$g_{4b} + \frac{k_3}{t_r} \exp(\frac{t_b}{k_3})$

and when time passes the points t_d, t_p, and t_b. Where no initial discharge is listed, the value is taken from the equation for the previous time period. The fifth and sixth columns list the symbols and expressions for the constants derived from the initial discharge.

t_{s1} and t_{s2} are the times at which $R_r = R_s$ on the rising and falling limbs of the reservoir discharge hydrograph. Section B1.3 discusses computation of the time at which a specified discharge occurs.

The case which applies for a given situation must be known before the correct set of equations from Table B1.2 can be chosen. Section B1.2 discusses the computation of boundaries between the cases.

Explicit expressions for the time and magnitude of peak reservoir discharge can be derived from the reservoir discharge equation by differentiating the equations, solving for the time at which the derivative equals zero, and substituting that time back into the original equation. The time of peak will always be between the larger of (t_p, t_s) and the smaller of (t_b, t_s). Only the equation which applies over this time interval need be considered. Table B1.3 gives expressions for the time and magnitude of peak reservoir discharge for each case.

Table B1.3

PEAK RESERVOIR DISCHARGE EQUATIONS

$$t_{rp1} = -k_1 \ln \left(\frac{-k_1}{g_{1b}\, t_r}\right) \qquad \text{(B1.21A)}$$

$$t_{rp2} = -k_3 \ln \left(\frac{-k_3}{g_{2c}\, t_r}\right) \qquad \text{(B1.21B)}$$

$$t_{rp3} = -k_3 \ln \left(\frac{-k_3}{g_{3c}\, t_r}\right) \qquad \text{(B1.21C)}$$

$$t_{rp4} = -k_3 \ln \left(\frac{-k_3}{g_{4b}\, t_r}\right) \qquad \text{(B1.21D)}$$

$$R_{pi} = I_{pn} \left(\frac{t_b - t_{rpi}}{t_r}\right) + R_0 \qquad \text{(B1.22)}$$

where:

t_{rpi} = time of peak, case i

R_{pi} = peak reservoir discharge, case i

B1.2 Boundaries Between Cases

Boundaries between cases are defined by values of the flood peak, for a given initial reservoir stage. The conditions which define the boundaries between the cases are given in Table B1.1. Case 4 applies whenever the initial discharge is greater than R_s. The boundaries between cases 1, 2, and 3 are functions of both the initial discharge and peak reservoir inflow. Case 1 applies whenever the peak reservoir discharge is less than R_s, and case 2 applies whenever the discharge at t_p is less than R_s. Thus, using Equation B1.22 with $R = R_s$ to define case 1:

$$I_{pn12} = \frac{(R_s - R_0)t_r}{t_b - t_{rp1}} \tag{B1.23}$$

where t_{rp1} is given by Equation B1.21A.

Using the case 1 equation for $t_d \leq t \leq t_p$, with $R_r = R_s$ at $t = t_p$ (see Table B1.2):

$$I_{pn23} = \frac{R_s - R_0}{(1 - k_{1/t_p} + g_{1a} \exp(-t_p/k_1))} \tag{B1.24}$$

where:

case 1 applies for $0 \leq I_{pn} \leq I_{pn12}$

case 2 applies for $I_{pn12} \leq I_{pn} \leq I_{pn23}$

and case 3 applies for $I_{pn23} \leq I_{pn}$

When t_d equals zero (initial reservoir stage at or above invert of outlet works), the case boundaries computed for an initial reservoir stage apply to the complete range of flood peaks, from zero to infinity. When t_d is greater than zero, the case boundaries are a function of the flood peak, and thus a flood peak must be specified before the applicable case can be computed. When t_d is greater than t_p, only case 1 or 2 may apply, and only I_{pn12} need be computed.

Cases 2a, 2b, 3a, and 3b can be determined by simply examining the reservoir discharge at t_b and using the criteria listed in Table B1.1. The boundaries between cases 1, 2, 3, and 4 are shown schematically in Figure B1.

B1.3 Solving for Time, t, Given Discharge, R_r

Equation B1.13D, for t greater than t_b, may be solved explicitly for t. Equations B1.13B and B1.13C, for t between 0 and t_b, cannot be solved explicitly for t. Two approximate methods of solving these equations for t are discussed here.

The first is an expansion of the exponential term using Taylor's series, and the second method is the regula falsi method (Carnahan, et al., 1969). The Taylor's series approximation produces a solution in one step, but the accuracy of the solution is unknown, and an initial estimate is required. The regula falsi method may converge slowly, but it always converges, and the maximum number of iterations required for a given accuracy may be computed in advance. The regula falsi

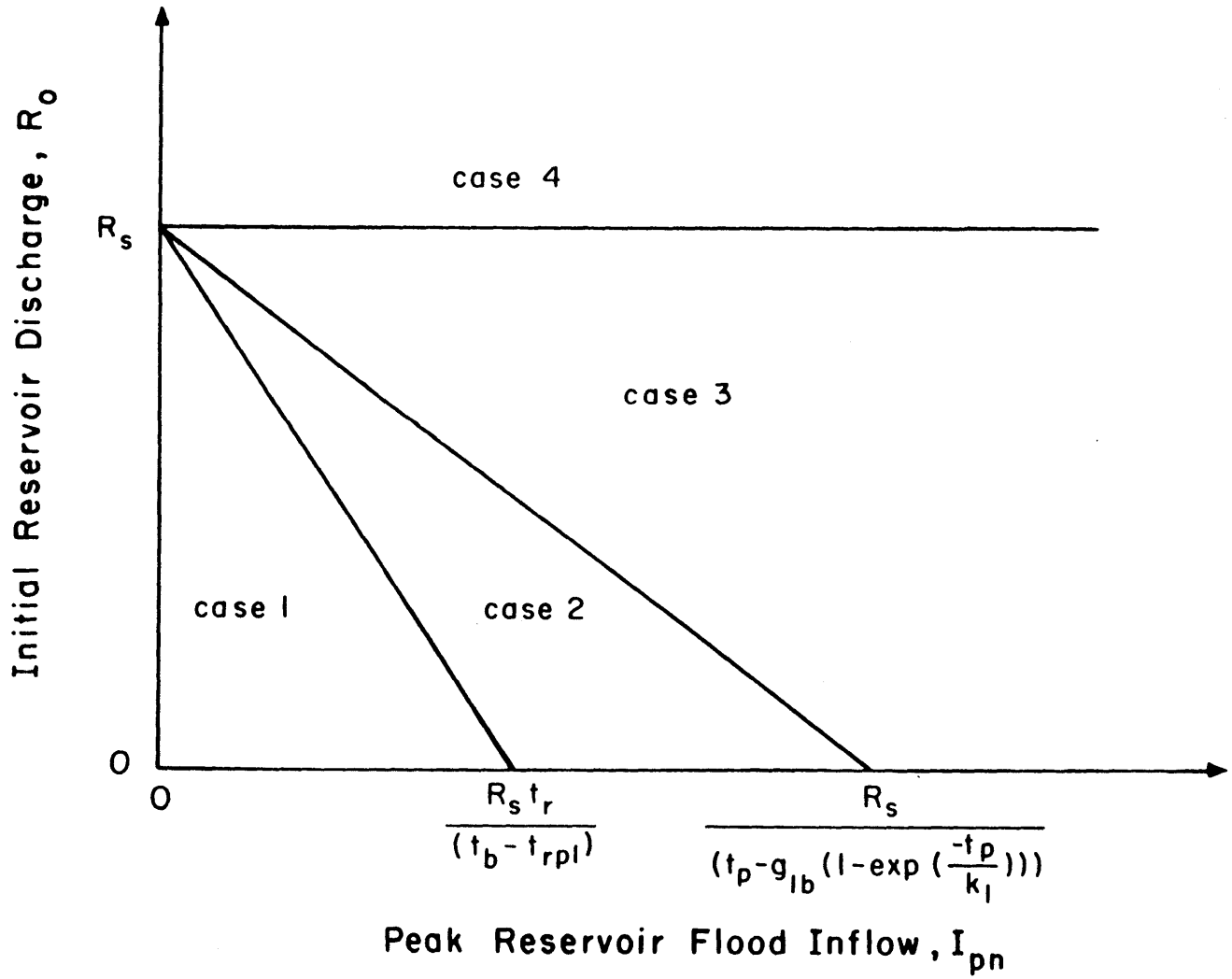

Figure B1: Boundaries Between Cases for Reservoir Routing

method is used in this work because it is more reliable over the wide range of situations encountered in the parameter variations studies of Chapters 4 and 5. The Taylor's series method is presented because it would be useful in situations where an explicit solution was required.

The second order Taylor's series expansion of the exponential term in Equations B1.13B and B1.13C is:

$$\exp\left(\frac{-t}{k_{[1,3]}}\right) \simeq \exp\left(\frac{-t_c}{k_{[1,3]}}\right) \left[\left(1 + \frac{t_c}{k_{[1,3]}} + \frac{t_c^2}{2k_{[1,3]}^2}\right)\right.$$

$$\left. - \left(\frac{1}{k_{[1,3]}} + \frac{t_c}{k_{[1,3]}^2}\right) t + \frac{1}{2k_{[1,3]}^2} t^2\right] \qquad \text{(B1.25)}$$

where t_c = an estimate of the desired value of t

Equations B1.13B and B1.13C may both be written as:

$$R_r = I_{pn}\left[A_1 + A_2 t + A_3 \exp\left(\frac{-t}{k_{[1,3]}}\right)\right] + R_0 \qquad \text{(B1.26)}$$

where the definitions of A_1, A_2, and A_3 for different situations can be seen by comparison with Equations B1.13[B,C] and Table B1.2.

Substituting Equation B1.25 for the exponential term, Equation B1.26 may be written:

$$R_r = I_{pn}\left[A_4 + A_5 t + A_6 t^2\right] + R_0 \qquad \text{(B1.27)}$$

where:

$$A_4 = A_1 + A_3 \left(1 + \frac{t_c}{k_{[1,3]}} + \frac{t_c^2}{2k_{[1,3]}^2}\right) \exp\left(\frac{-t_c}{k_{[1,3]}}\right) \tag{B1.28}$$

$$A_5 = A_2 - A_3 \left(\frac{1}{k_{[1,3]}} + \frac{t_c}{k_{[1,3]}^2}\right) \exp\left(\frac{-t_c}{k_{[1,3]}}\right) \tag{B1.29}$$

and:

$$A_6 = \frac{A_3}{2k_{[1,3]}^2} \exp\left(\frac{-t_c}{k_{[1,3]}}\right) \tag{B1.30}$$

which may be solved for t:

$$t = \frac{-A_5 \pm \left(A_5^2 - 4A_6\left(A_4 - \frac{R_r - R_0}{I_{pn}}\right)\right)^{\frac{1}{2}}}{2A_6} \tag{B1.31}$$

where the positive sign is used for the smaller root (time of occurrence less than t_{rp}) and the negative sign for the larger root (time of occurrence larger than t_{rp}).

The method of regula falsi is described well by Carnahan, et al. (1969), and the details of the solution technique will not be discussed here. It is necessary to choose upper and lower bounds for the solution when using the regula falsi method. When solving for t_{s1} and t_{s2}, these bounds may chosen as follows. For t_{s1}, some lower bounds are $t = t_p$ for case 2 and $t = 0$ for case 3. Some upper bounds are $t = t_p$ for case 2 and $t = t_{rp3}$ for case 3. For t_{s2}, some lower bounds are $t = t_{rp2}$ for case 2 and $t = t_{rp3}$ for case 3. An upper bound for cases 2A and 3A is $t = t_b$. This method is not needed for cases 2B and 3B because Equation B1.13D applies.

B2 Channel Routing

The continuity equation is:

$$\underline{R}_r - \underline{Q} = \frac{d\underline{V}_r}{d\underline{t}} \qquad \text{(B2.1)}$$

where:

$\underline{Q}$ = channel discharge at selected site

$\underline{V}_r$ = storage volume in the channel

The upstream boundary condition, R_r, is given by the reservoir discharge equations listed in Table B1.2. The downstream boundary condition (channel discharge), shown in Figure 2.4, is given implicitly by:

$$\underline{V} = \underline{K}\,\underline{Q} \qquad \text{(B2.2)}$$

Substituting Equation B2.2 into Equation B2.1 gives:

$$\underline{K}\,\frac{d}{d\underline{t}}\,\underline{Q} + \underline{Q} = \underline{R}_r \qquad \text{(B2.3)}$$

The dimensions may be removed from Equations B2.1 through B2.3 using the characteristic values given in Table 2.1 and the method described in Section B1 for the reservoir equations. As for the reservoir equations, the form of the equations does not change when written with dimensionless variables.

The non-dimensional form of Equation B2.3 could be integrated directly, as was done for the reservoir routing. However, because several equations are needed to describe the reservoir discharge, it is convenient to develop an impluse response function and use convolution integrals to solve for the channel discharge.

Taking the Laplace transform of Equation B2.3 yields:

$$Ks\ L[Q] + L[Q] = L[R_r] \tag{B2.4}$$

and

$$\frac{L[Q]}{L[R_r]} = \frac{1}{Ks + 1} \tag{B2.5}$$

where:

L[A] = Laplace transform of the function A

The inverse transform of the right-hand side of Equation B2.5 is the desired impulse response function.

$$h(t) = L^{-1}\left[\frac{1}{Ks + 1}\right] = \frac{1}{K}\ e^{-\frac{t}{K}} \tag{B2.6}$$

The reservoir discharge is then given by:

$$Q(t) = \int_0^t h(t - a)\ R_r(a)\ da \tag{B2.7}$$

For example, the channel discharge for $t > t_b$, when $t_d < t_p$, is given by:

$$Q(t) = \int_0^{t_d} h(t - a)(0)\, da + \int_{t_d}^{t_p} h(t - a)((\text{Eq. B1.13B}) - R_0)da$$

$$+ \int_{t_p}^{t_b} h(t - a)((\text{Eq. B1.13C}) - R_0)da$$

$$+ \int_{t_b}^{t} h(t - a)((\text{Eq. B1.13D}) - R_0)da + R_0 \qquad \text{(B2.8)}$$

where the particular forms taken by Equations B1.13 [B,C,D] are given by Table B1.2. Some of the integrals in Equation B2.8 may have to be further subdivided where the constant determined by the initial condition, changes.

Figure B2 illustrates Equation B2.8. Notice that R_0, the constant portion of the reservoir discharge, was subtracted from the reservoir discharge equations prior to performing the convolution integral and then added to the result. This is done because the implicit initial condition for the convolution integral is zero input at time zero. The initial condition here, however, is steady-state input and output of R_0.

Computation of the channel discharge is simplified by considering some general forms. All the reservoir discharge equations may be written in the form given by Equation B1.26. The general form of the convolution integral is then:

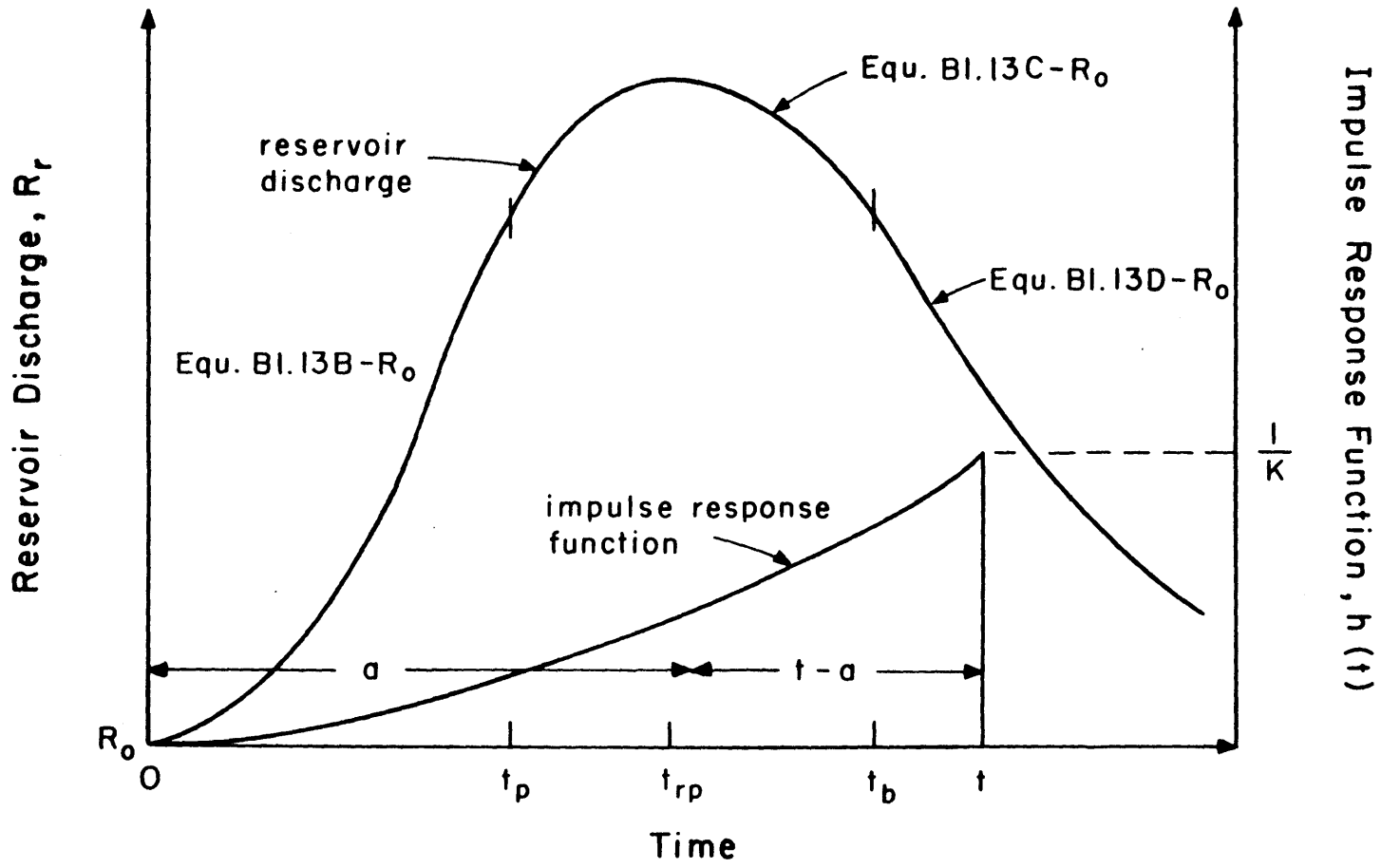

Figure B2.1: Illustration of Convolution Integral Given by Equation B2.8

$$\int_{t_1}^{t_2} \left[\frac{1}{K} \exp\left(\frac{-(a - t)}{K}\right)\right]\left[I_{pn}\ (A_1 + A_2 t + A_3 \exp\left(\frac{-a}{k_{[1,3]}}\right)\right] da$$

$$= I_{pn} \left\{\left[A_1 + A_2(t_2 - K) + \frac{A_3}{1 - K/k_{[1,3]}} \exp\left(\frac{-t_2}{k_{[1,3]}}\right)\right] \exp\left(\frac{t_2}{K}\right)\right.$$

$$\left. - \left[A_1 + A_2(t_1 - K) + \frac{A_3}{1 - K/k_{[1,3]}} \exp\left(\frac{-t_1}{k_{[1,3]}}\right)\right] \exp\left(\frac{t_1}{K}\right)\right\} \exp\left(\frac{-t}{K}\right)$$

(B2.9)

When $t_2 = t$, Equation B2.9 becomes:

$$I_{pn} \left\{(A_1 - A_2 K) + A_2 t + \frac{A_3}{1 - K/k_{[1,3]}} \exp\left(\frac{-t}{k_{[1,3]}}\right)\right.$$

$$\left. - \left[A_1 + A_2(t_1 - K) + \frac{A_3}{1 - K/k_{[1,3]}} \exp\left(\frac{-t}{k_{[1,3]}}\right)\right] \exp\left(\frac{t_1}{K}\right) \exp\left(\frac{-t}{K}\right)\right\}$$

(B2.10)

Thus, all the channel discharge equations may be written in the form:

$$Q(t) = I_{pn} \left\{D_1 + D_2 t + D_3 \exp\left(\frac{-t}{k_1}\right) + D_4 \exp\left(\frac{-t}{k_3}\right) + D_5 \exp\left(\frac{-t}{K}\right)\right\} + R_0$$

(B2.11)

where D_1 through D_5 are defined through Equations B2.9 and B2.10.

As for the reservoir discharge, the peak flow occurs when the derivative of the channel discharge equation with respect to time equals zero. The derivative of Equation B2.11 cannot be solved explicitly for time. Either of the two methods discussed in Section B1.3, Taylor's series expansion or regula falsi method, may be used to find the time of peak discharge. The regula falsi method is used in this work, with upper and lower bounds given by the time interval over which the equation applies. The time interval during which the peak occurs may be found by examining the derivatives at the end-points of the intervals. The derivative will be positive at the beginning and negative at the end of the interval in which the peak occurs.

B3 Dam Breaches

B3.1 Reservoir Breach Discharge Hydrograph Development

Dam breaches are modeled as instantaneous partial openings in the dam. The reservoir breach discharge hydrograph is represented by a triangle, as shown in Figure 2.5. Equation B3.1 describes the breach discharge hydrograph.

$$R_{db} = (R_{pb} - R_0)\left(\frac{t_{bb} + t_f - t}{t_{bb}}\right) + R_0 \qquad t_f \leq t \leq t_f + t_{bb} \tag{B3.1}$$

where:

R_{db} = total discharge rate from dam during breach

t_f = time at which dam fails

The dimensionless peak breach discharge is given by Equation 2.2, repeated here for convenience.

$$R_{pb} = B_{pg}\, B_1\, H_w^{2.22} \tag{2.2}$$

where:

$$B_{pg} = \frac{g^{0.5}\, \underline{H}_c^{2.5}}{\underline{R}_c} \tag{2.3}$$

$$B_1 = 0.29\, p_1^{1.22}\, p_2^{0.72}\, B_d^{0.28} \tag{2.4}$$

$$p_1 = \frac{H_b}{H_w} \tag{2.5}$$

$$p_2 = \frac{B_b}{H_w} \tag{2.6}$$

and H_w, B_b, and H_b are defined in Figure 2.6.

The base time of the breach discharge hydrograph, t_{bb}, is computed by equating the volume of the hydrograph shown in Figure 2.5 with the sum of the volume of water stored in the reservoir above the breach invert plus the volume of reservoir inflow after the breach has formed.

The discharge volume in terms of the hydrograph parameters is:

$$V_w = t_{bb} \left(\frac{R_{pb} - R_0}{2} + R_0\right) = \frac{t_{bb}}{2} (R_{pb} + R_0) \tag{B3.2}$$

Note that R_b has been neglected. The magnitude of R_b is likely to be much smaller than either R_{pb} or R_0 in most situations. R_0 is retained to facilitate modeling breaches with high antecendent flows.

The volume of water stored in the reservoir between the breach invert and the reservoir stage at failure can be computed from Equations 2.5 and B1.8 as:

$$V_d = (1 - (1 - p_1)^{p_4}) H_w^{p_4} \tag{B3.3}$$

The inflow volume after the breach is the sum of the steady-state and flood inflows. The steady-state inflow equals $R_0 t_{bb}$. The time of failure must be computed before the flood inflow can be computed.

The time of failure can be computed using either of the methods discussed in Appendix B1.3. The regula falsi method is used in this work. The lower and upper bounds for the solution are t = 0 and $t = t_{rp}$. (If the reservoir has not reached the failure stage at the peak stage, it will not reach the failure stage later.) The discharge at the time of failure is computed from the stage at failure, Equation B1.8, and Equation B1.5. Once the failure time is computed, the flood inflow between the failure time and t_b can be computed from the geometry of the reservoir inflow hydrograph (Figure 2.1) as:

$$V_f = \frac{I_{pn}}{2}\left(\frac{t_p^2 - t_f^2}{t_p}\right) + \frac{I_{pn}\, t_r}{2} \qquad t_f \leq t_p \qquad \text{(B3.4A)}$$

$$= \frac{I_{pn}}{2}\frac{(t_b - t_f)^2}{t_r} \qquad t_f \geq t_p \qquad \text{(B3.4B)}$$

where:

V_f = volume of reservoir flood inflow after breach

and t_f = time of failure

As discussed in Section 2.3.2.2, the breach discharge hydrograph timing error caused by using all of the reservoir flood inflow after the breach is neglected.

t_{bb} is then computed from:

$$V_w = \frac{t_{bb}}{2}(R_{pb} + R_0) = V_d + V_f + R_0\, t_{bb} \qquad \text{(B3.5)}$$

Solving for t_{bb},

$$t_{bb} = \frac{2(V_d + V_f)}{(R_{pb} - R_0)} \qquad \text{(B3.6)}$$

B3.2 Channel Routing

The channel routing method described in Section B2 is used here. As for the natural flood routing, only the peak channel discharge is needed to compute damages. Since the peak discharge will always occur before t_{bb} (the channel inflow and outflow are equal at the time of peak outflow), the recession channel hydrograph (after t_{bb}) does not need to be computed.

For non-overtopping failures, only the breach discharge need be routed downstream. For overtopping failures, there is flood flow in the stream prior to the breach. Consider first the breach discharge. Using Equations B3.1 and B2.6 in Equation B2.7, and setting $t_f = 0$,

$$Q(t) = \int_0^t \frac{1}{K} \exp\left(\frac{-t + a}{K}\right) \left(R_{pb} - R_0\right) \left(\frac{t_{bb} - a}{t_{bb}}\right) da + R_0 \qquad \text{(B3.7)}$$

where $Q(t)$ = channel discharge at time t.

Integrating,

$$Q(t) = (R_{pb} - R_0) \left((1 + \frac{K}{t_{bb}}) \left(1 - \exp\left(\frac{-t}{K}\right) - \frac{1}{t_{bb}}\right)\right) + R_0 \qquad \text{(B3.8)}$$

The time of peak discharge may be found by differentiating:

$$\frac{dQ}{dt} = (R_{pb} - R_0)\left(\left(\frac{1}{K} + \frac{1}{t_{bb}}\right) \exp\left(\frac{-t}{K}\right) - \frac{1}{t_{bb}}\right) \qquad \text{(B3.9)}$$

Setting $\frac{dQ}{dt} = 0$ and solving for t gives:

$$t_{cp} = -K \ln\left(\frac{1}{1 + \frac{t_{bb}}{K}}\right) \qquad \text{(B3.10)}$$

where t_{cp} = time of peak channel discharge.

Substituting t_{cp} in Equation B3.8 gives:

$$Q_p = (R_{pb} - R_0)\left(1 - \frac{t_{cp}}{t_{bb}}\right) + R_0 \qquad \text{(B3.11)}$$

where Q_p = peak channel discharge from breach hydrograph

The flood flow already in the stream before an overtopping failure is approximated by routing the reservoir discharge from t = 0 through $t = t_f$ downstream, using the methods of Section B2, and adding the value of that discharge at $t = t_f + t_{cp}$ to the value of Q_p computed from Equation B3.11. The effect of this antecedent flood flow on the time of peak discharge is neglected.

B4 Damage Function

The damage function is given by:

$$\underline{D} = P_{6N} (\underline{Q}_p - \underline{Q}_{nd})^{P_{7N}} \quad \text{for non-breach floods} \tag{B4.1A}$$

$$= P_{6B} (\underline{Q}_p - \underline{Q}_{nd})^{P_{7B}} + \underline{L}_d \quad \text{for dam breach floods} \tag{B4.1B}$$

where:

$P_{6[N,B]}$, $P_{7[N,B]}$ = constants

$\underline{Q}_p$ = peak channel discharge

$\underline{Q}_{nd}$ = discharge at which first damage occurs

$\underline{L}_d$ = value of dam

Non-dimensionalizing with the characteristic values from Table 2.1,

$$D = (Q_p - Q_{nd})^{P_{7N}} \quad \text{for natural floods} \tag{B4.2A}$$

$$(Q_p - Q_{nd})^{P_{7B}} + L_d \quad \text{for dam breach floods} \tag{B4.2B}$$

where $L_d = \underline{L}_d / (P_{6B} \underline{R}_c^{P_{7B}})$

Dimensional damages are then given by:

$$\underline{D} = (P_{6[N,B]} \underline{R}_c^{P_{7[N,B]}}) D \tag{B4.3}$$

B5 Computation of Mean and Variance

Means and variances of damages are computed for:

1) Successfully Passed floods
2) Overtopping Failures
3) Non-Overtopping Failures
4) 1), 2), and 3) combined
5) No-Failure floods (with dam)
6) marginal damages due to Overtopping Failure

If only item 4), the overall mean and variance, were desired, the computations could proceed much more simply than described here. The following methods are used because the intermediate results are desired. Standard procedures, which may be found in most statistics textbooks (see Benjamin and Cornell, 1970), are used. All probabilities must be given in consistent units. Annual probabilities are used in this work.

Section B5.1 describes computation of failure probability. Sections B5.2 and B5.3 describe computation of the mean and variance of flood damages, items 1) through 4) first, and then items 5) and 6).

The following notation is used for discretization of the stochastic variables:

I_j , $j = 1, N_I$ = representative values of reservoir inflow peak

H_k , $k = 1, N_H$ = representative values of reservoir stage

F_ℓ , $\ell = 1, N_F$ = representative values of failure stage

where N_I, N_H, and N_F = number of elements in I_j, H_k, and F_ℓ.

D_{jk}^{SP} = Successful Passage flood damage from reservoir inflow I_j with initial reservoir stage H_k

$D_{jk\ell}^{OF}$ = Overtopping Flood damage from reservoir inflow I_j, with initial reservoir stage H_k and failure stage F_ℓ

D_k = Non-Overtopping Failure damage, with reservoir stage H_k

P_j^I = probability mass of interval represented by I_j

P_k^H = probability mass of interval represented by H_k

P_ℓ^F = probability mass of interval represented by F_ℓ

P_k^{NOF} = probability of non-overtopping failure given stage H_k

B5.1 Failure Probabilities

For overtopping failures:

$$P_{k\ell}^{OF} = (1 - F_I (I_{k\ell}^{OF})) (1 - P_k^{NOF}) \qquad \text{(B5.1)}$$

where:

$P_{k\ell}^{OF}$ = probability of overtopping failure given initial stage H_k and failure stage F_ℓ

$F_I(x)$ = probability that the reservoir inflow flood peak is less than or equal to x.

and $I_{k\ell}^{OF}$ = smallest reservoir inflow peak which causes an Overtopping Failure, given initial stage H_k and failure stage F_ℓ. $I_{k\ell}^{OF}$ does not need to be an element of I_j.

$I_{k\ell}^{OF}$ is computed from the flood routing model using the regula falsi numerical procedure (see Carnahan, et al., 1969). The upper and lower bounds for $I_{k\ell}^{OF}$ are the largest element of I_j at which failure does not occur and the smallest element at which failure does occur.

Integrating first over the initial reservoir stage and then over the failure stage gives:

$$P_\ell^{OF} = \sum_{k=1}^{N_H} P_{k\ell}^{OF} P_k^H \qquad \text{(B5.2)}$$

where:

P_ℓ^{OF} = probability of Overtopping Failure given failure stage F_ℓ

and:

$$P^{OF} = \sum_{\ell=1}^{N_F} P_\ell^{OF} P_\ell^F \qquad \text{(B5.3)}$$

where:

P^{OF} = probability of Overtopping Failure.

For Non-Overtopping Failures:

$$P^{NOF} = \sum_{k=1}^{N_H} P_k^{NOF} P_k^H \qquad \text{(B5.4)}$$

where:

P^{NOF} = probability of Non-Overtopping Failure.

The probabilities of Successful Passage are then:

$$P_{k\ell}^{SP} = 1 - P_{k\ell}^{OF} - P_k^{NOF} = F_I(I_{k\ell}^{OF}) \ (1 - P_k^{NOF}) \tag{B5.5}$$

$$P_{\ell}^{SP} = 1 - P_{\ell}^{OF} - P^{NOF} \tag{B5.6}$$

and $$P^{SP} = 1 - P^{OF} - P^{NOF} \tag{B5.7}$$

where:

$P_{k\ell}^{SP}$ = probability of Successful Passage, given initial reservoir stage H_k and failure stage F_ℓ

P_{ℓ}^{SP} = probability of Successful Passage, given failure stage F_ℓ

P^{SP} = probability of Successful Passage

The probabilities of zero damage are:

$$P_k^{ZD} = F_I \ (I_k^{ZD}) \ (1 - P_k^{NOF}) \tag{B5.8}$$

where:

P_k^{ZD} = probability of zero damage, given initial reservoir stage H_k

and I_k^{ZD} = largest reservoir inflow flood which does not cause damage, given initial reservoir stage H_k.

Like $I^{OF}_{k\ell}$, I^{ZD}_{k} does not need to be an element of I_j. Again, like $I^{OF}_{k\ell}$, I^{ZD}_{k} is computed using the regula falsi numerical procedure. The bounds on the solution, I^{ZD}_{k} are the largest element of I_j which does not cause damage (or zero if I_1 causes damage), and the smallest element of I_j which does cause damage.

Integrating over the initial reservoir stage:

$$P^{ZD} = \sum_{k=1}^{N_H} P^{ZD}_{k} P^{H}_{k} \qquad \text{(B5.9)}$$

where:

P^{ZD} = probability of zero damage.

B5.2 Mean Damage

B5.2.1 Items 1 through 4

For Successfully Passed floods:

$$M^{SP}_{k\ell} = \left(\sum_{j=1}^{(N^{OF}_{k}-1)} D^{NF}_{jk} P^{I}_{j} \right) / F_i(I^{OF}_{k\ell}) \qquad \text{(B5.10)}$$

where:

$M^{SP}_{k\ell}$ = mean Successful Passage flood damage, given initial reservoir stage H_k, failure stage F_ℓ, and no failure occurrence, either overtopping or non-overtopping

and $N_{k\ell}^{OF}$ = index of smallest element of I_j which causes an overtopping failure, given initial reservoir stage H_k and failure stage F_ℓ

When $j = N_{k\ell}^{OF} - 1$, P_j^I is replaced by $P_j^I + PA_{k\ell}^{OF}$, where

$$PA_{k\ell}^{OF} = 1 - F_I\,(I_{k\ell}^{OF}) - F_i((I_{N_{k\ell}^{OF}} + I_{N_{k\ell}^{OF} - 1})/2) \qquad \text{(B5.11)}$$

When $j = N_k^{ZD}$, P_j^I is replaced by $P_j^I - PA_k^{ZD}$,

where:

N_k^{ZD} = index of smallest element of I_j which causes damage, given initial reservoir stage H_k.

and:

$$PA_k^{ZD} = F_I(I_k^{ZD}) - F_I((I_{N_k^{ZD} - 1} + I_{N_k^{ZD}})/2) \quad \text{when } N_k^{ZD} > 1$$

$$= F_I(I_k^{ZD}) \quad \text{when } N_k^{ZD} = 1 \qquad \text{(B5.12)}$$

When j is less than N_k^{ZD} , no adjustments are needed because D_{jk}^{SP} equals zero.

These adjustments, PA_k^{ZD} and $PA_{k\ell}^{OF}$, help compensate for the inaccuracies caused by discretization of the reservoir inflow flood peaks.

For overtopping failures,

$$M_{k\ell}^{OF} = \left(\sum_{j = N_{k\ell}^{OF}}^{N_I} D_{jk\ell}^{OF} P_j^I \right) / (1 - F_I(I_{k\ell}^{OF})) \qquad \text{(B5.13)}$$

where:

$M_{k\ell}^{OF}$ = mean flood damage, given initial reservoir stage H_k, failure stage F_ℓ, and the occurrence of an overtopping failure

When $j = N_{k\ell}^{OF}$, P_j^I is replaced by $P_j^I - PA_j^{I_{k\ell}^{OF}}$.

Integrating over the initial reservoir stage:

$$M_{\ell}^{SP} = \sum_{k=1}^{N_H} M_{k\ell}^{SP} P_k^H \qquad \text{(B5.14)}$$

$$M_{\ell}^{OF} = \sum_{k=1}^{N_H} M_{k\ell}^{OF} P_k^H \qquad \text{(B5.15)}$$

where:

M_{ℓ}^{SP} = mean Successful Passage flood damage, given failure stage F_{ℓ} and no occurrence of failure

and M_{ℓ}^{OF} = mean flood damage, given failure stage F_{ℓ} and occurrence of an overtopping failure

Finally, integrating over failure stage:

$$M^{SP} = \sum_{\ell=1}^{N_f} M_{\ell}^{SP} P_{\ell}^F \qquad \text{(B5.16)}$$

$$M^{OF} = \sum_{=1}^{N_F} M_{\ell}^{OF} P_{\ell}^F \qquad \text{(B5.17)}$$

where:

M^{SP} = mean Successful Passage damage

and M^{OF} = mean Overtopping Failure flood damage.

For Non-Overtopping Failures:

$$M^{NOF} = \left(\sum_{k=1}^{N_H} D_k P_k^H P_k^{NOF} \right) / P^{NOF} \qquad \text{(B5.18)}$$

where:

M^{NOF} = mean flood damage, given the occurrence of a non-overtopping failure

The overall mean damage is then:

$$M^{D} = M^{SP}\ P^{SP} + M^{OF}\ P^{OF} + M^{NOF}\ P^{NOF} \qquad \text{(B5.19)}$$

B5.2.2 Items 5 and 6

The mean damage when failure is not allowed is:

$$M^{NF} = \left(\sum_{j=1}^{N_I} \sum_{k=1}^{N_H} D_{jk}^{NF}\ P_k^H\ P_j^I \right)(1 - P^{NOF}) \qquad \text{(B5.20)}$$

The mean marginal damage caused by overtopping failure is:

$$M^{MD} = \left(\sum_{j=1}^{N_I} \sum_{k=1}^{N_H} \sum_{\ell=1}^{N_F} \max(0,\ D_{jk\ell}^{OF} - D_{jk}^{NF})\ P_\ell^F\ P_k^H\ P_j^I \right)(1 - P^{NOF}) \qquad \text{(B5.21)}$$

where:

max(a, b) = maximum of a and b

P_j^I is replaced by $P_j^I + PA_{k\ell}^{OF}$ when $j - N_{k\ell}^{OF} - 1$, by $P_j^I - PA_{k\ell}^{OF}$ when $j = N_{k\ell}^{OF}$, and by $P_j^I - PA_k^{ZD}$ when $j = N_k^{ZD}$ in Equations B5.20 and B5.21.

The maximum function in Equation B5.20 is necessary because $D_{jk\ell}^{OF}$ will be zero, indicating that the dam did not fail, for many values of j, k, and ℓ.

B5.3 Variance of Damages

B5.3.1 Items 1 through 4

For Successfully Passed floods:

$$V_{k\ell}^{SP} = \left(\sum_{j=1}^{N_{k\ell}^{OF} - 1} (D_{jk}^{NF} - M_{k\ell}^{NF})^2 P_j^I \right) / F_I(I_{k\ell}^{OF}) \qquad \text{(B5.22)}$$

where:

$V_{k\ell}^{SP}$ = variance of Successful Passage flood damage, given initial stage H_k and failure stage F_ℓ.

As in the computation of $M_{k\ell}^{SP}$, P_j^I is replaced by $P_j^I + PA_{k\ell}^{OF}$ when $j = N_{k\ell}^{OF} - 1$ and by $P_j^I - PA_k^{ZD}$ when $j = N_k^{ZD}$.

For Overtopping Failures,

$$V_{k\ell}^{OF} = \left(\sum_{j=N_{k\ell}^{OF}}^{N_I} (D_{jk\ell} - M_{k\ell}^{OF})^2 P_j^I \right) / (1 - F_I(I_{k\ell}^{OF})) \qquad \text{(B5.23)}$$

where:

$V_{k\ell}^{OF}$ = variance of Overtopping Failure flood damage, given initial reservoir stage H_k and failure stage F_ℓ.

As in the computation of $M_{k\ell}^{OF}$, P_j^I is replaced by $P_j^I - PA_{k\ell}^{OF}$ when $j = N_{k\ell}^{OF}$.

Integrating over the reservoir stage:

$$V_\ell^{SP} = \sum_{k=1}^{N_H} (V_{k\ell}^{SP} + (M_{k\ell}^{SP} - M_\ell^{SP})^2) P_k^H \qquad \text{(B5.24)}$$

$$V_\ell^{OF} = \sum_{k=1}^{N_h} (V_{k\ell}^{OF} + (M_{k\ell}^{OF} - M_\ell^{OF})^2) P_k^H \qquad \text{(B5.25)}$$

where:

V_ℓ^{SP} = variance of Successful Passage damage, given failure stage F_ℓ

and: V_ℓ^{OF} = variance of Overtopping Failure damage, given failure stage F_ℓ.

Integrating over the failure stage:

$$V^{SP} = \sum_{\ell=1}^{N_F} (V_\ell^{SP} + (M_\ell^{SP} - M^{SP})^2) P_\ell^F \qquad \text{(B5.26)}$$

$$V^{OF} = \sum_{\ell=1}^{N_F} (V_\ell^{OF} + (M_\ell^{OF} - M^{OF})^2) P_\ell^F \qquad \text{(B5.27)}$$

where:

V^{SP} = variance of Successful Passage damage

and: V^{OF} = variance of Overtopping Failure damage.

For Non-Overtopping Failures:

$$V^{NOF} = (\sum_{k=1}^{N_H} (D_k - M^{NOF})^2 P_k^H P_k^{NOF})/P^{NOF} \qquad \text{(B5.28)}$$

where:

V^{NOF} = variance of Non-Overtopping Failure damage.

The overall variance is given by:

$$V^D = (V^{SP} + (M^{SP} - M^D)^2) P^{SP} + (V^{OF} + (M^{OF} - M^D)^2) P^{OF}$$

$$+ (V^{NOF} + (M^{NOF} - M^D)^2) P^{NOF} \qquad (5.29)$$

where:

V^D = variance of flood damage

B5.2.3 Items 5 and 6

The variance of damage when failure is not allowed is:

$$V^{NF} = \left(\sum_{j=1}^{N_I} \sum_{k=1}^{N_H} (D_{jk}^{NF} - M^{NF})^2 P_k^H P_j^I \right)(1 - P^{NOF}) \qquad \text{(B5.30)}$$

The variance of marginal damage caused by Overtopping Failure is:

$$V^{MD} = \left(\sum_{j=1}^{N_I} \sum_{k=1}^{N_H} \sum_{\ell=1}^{N_F} (\max(0, D_{jk\ell}^{OF} - D_{jk}^{NF}) - M^{MD})^2 P_\ell^F P_k^H P_j^I \right)(1 - P^{NOF}) \qquad \text{(B5.31)}$$

P_j^I is replaced by $P_j^I + PA_{k\ell}^{OF}$ when $j = N_{k\ell}^{OF} - 1$, by $P_j^I - PA_{k\ell}^{OF}$ when $j = N_{k\ell}^{OF}$, and by $P_j^I - PA_k^{ZD}$ when $j = N_k^{ZD}$ in Equations B5.29 and B5.30.

APPENDIX C

VARIATION OF PEAK CHANNEL DISCHARGE WITH VARIATION OF CHANNEL INFLOW PEAK AND VOLUME

It is well known that flood peak attenuation in a channel is a function of both the shape of the flood wave and the shape of the channel. For example, flood waves with high peaks and low volumes will attenuate rapidly in a broad channel and slowly in a narrow channel, whereas flood waves with low peaks and high volumes will attentuate slowly in any channel.

Such observations can be quantified somewhat by routing a triangular hydrograph through a channel using the storage routing method described in Appendix B. Since the channel and reservoir routing procedures are mathematically identical, routing a triangular hydrograph through a channel is described by the reservoir routing equations for case 1, with t_d equal to zero.

Peak discharge is given by (Equation B1.22 in Table B1.3):

$$Q_p = I_{pn}\left[\frac{t_b - t_{rp}}{t_r}\right] + R_0 \qquad (C1)$$

where:

Q_p = peak discharge

I_{pn} = peak flood inflow

t_b = base time of inflow hydrograph

t_{rp} = time of peak discharge

$t_r = t_b - t_p$

t_p = time of peak inflow

and R_0 = base flow

t_{rp} is given by Equation B1.21A (see Table B1.3):

$$t_{rp} = -k \ln \left(\frac{t_p}{t_b \exp(\frac{t_p}{k}) - t_r} \right) \quad \text{for } t_p \neq 0 \tag{C2}$$

where the expression for g_{1b} from Table B1.2 has been used and the constant k has been substituted for the reservoir constant k_1.

Equation C2 cannot be computed directly when t_p equals zero, because the logarithm of zero equals negative infinity. Taking the limit of the argument for the logarithm in Equation C2, replacing t_r by $t_b - t_p$, and using L'Hospital's rule (Taylor and Mann, 1972) gives:

$$\lim_{t_p \to 0} \frac{t_p}{t_b \exp(\frac{t_p}{k}) - t_b + t_p} = \lim_{t_p \to 0} \frac{1}{\frac{t_b}{k} \exp(\frac{t_p}{k}) + 1} = \frac{1}{1 + \frac{t_b}{k}} \tag{C3}$$

Then, using Equation C3 in Equation C1, with $t_r = t_b$:

$$Q_p = I_{pn} \left[1 + \frac{k}{t_b} \ln \left(\frac{1}{1 + \frac{t_b}{k}} \right) \right] + R_0 \quad t_p = 0 \tag{C4}$$

Equation C4 has the same form as Equation B3.11, developed directly from an inflow hydrograph with t_p equal to zero, when Equation B3.10 is substituted for t_{cp} in Equation B3.11.

As $\frac{t_p}{k}$ becomes large, $\exp(\frac{t_p}{k})$ quickly becomes large enough to cause numerical problems on a computer. (The largest number which can be stored in VAX 11 FORTRAN-IV PLUS is approximately exp(80).) The following approximation for Equation C2 is helpful in this situation. As $\exp(\frac{t_p}{k})$ gets large, $t_b \exp(\frac{t_p}{k}) >> t_r$, and t_r may be neglected. Thus:

$$t_{rp} \simeq -k \ln \left(\frac{t_p}{t_b \exp(\frac{t_p}{k})}\right) = -k \left[\ln(t_p) - \ln(t_b) - \ln(\exp(\frac{t_p}{k}))\right]$$

$$= t_p + k \ln(\frac{t_b}{t_p}) \qquad \text{(C5)}$$

Using Equation C5 in Equation C1 gives:

$$Q_p \cong I_{pn} \left[1 - \frac{k}{t_r} \ln(\frac{t_b}{t_p})\right] + R_0 \qquad \text{large } \frac{t_p}{k} \qquad \text{(C6)}$$

Since we are interested here in the variation of Q_p with volume and peak for the inflow, Equation C7,

$$t_b = \frac{2V}{I_{pn}} \qquad \text{(C7)}$$

where: V = volume of flood inflow

which applies for a triangular inflow hydrograph is used to write Equations C1, C4, and C6 in terms of inflow volume and peak.

Equation C1, using Equation C7, then becomes:

$$Q_p = I_{pn} \left[\frac{2V + I_{pn}\, k\, \ell n \left(\frac{I_{pn}\, t_p}{2V\left(\exp\left(\frac{t_p}{k}\right) - 1\right) + I_{pn}\, t_p} \right)}{2V - I_{pn}\, t_p} \right] + R_0 \qquad t_p \neq 0 \tag{C8}$$

Equation C4 becomes:

$$Q_p = I_{pn} \left[1 + \frac{k\, I_{pn}}{2V}\, \ell n \left(\frac{1}{1 + \frac{2V}{k\, I_{pn}}} \right) \right] + R_0 \qquad t_p = 0 \tag{C9}$$

and Equation C6 becomes:

$$Q_p = I_{pn} \left[1 - \frac{I_{pn}\, k}{2V - I_{pn}\, t_p}\, \ell n \left(\frac{2V}{I_{pn}\, t_p} \right) \right] + R_0 \qquad \text{large } \frac{t_p}{k} \tag{C10}$$

Either Equation C9, for t_p equal to zero, or Equations C8 and C10, for t_p not equal to zero, can be used to illustrate the variation of Q_p with V and I_{pn}. Equation C9 will be used here.

Figure C1 shows Q_p and the partial derivatives of Q_p with respect to V and I_{pn} as functions of V and I_{pn} for k = 0.001, 0.01, 0.1, and 1.0. Note that the direction of the axes are reversed between the graphs of Q_p and the derivatives of Q_p.

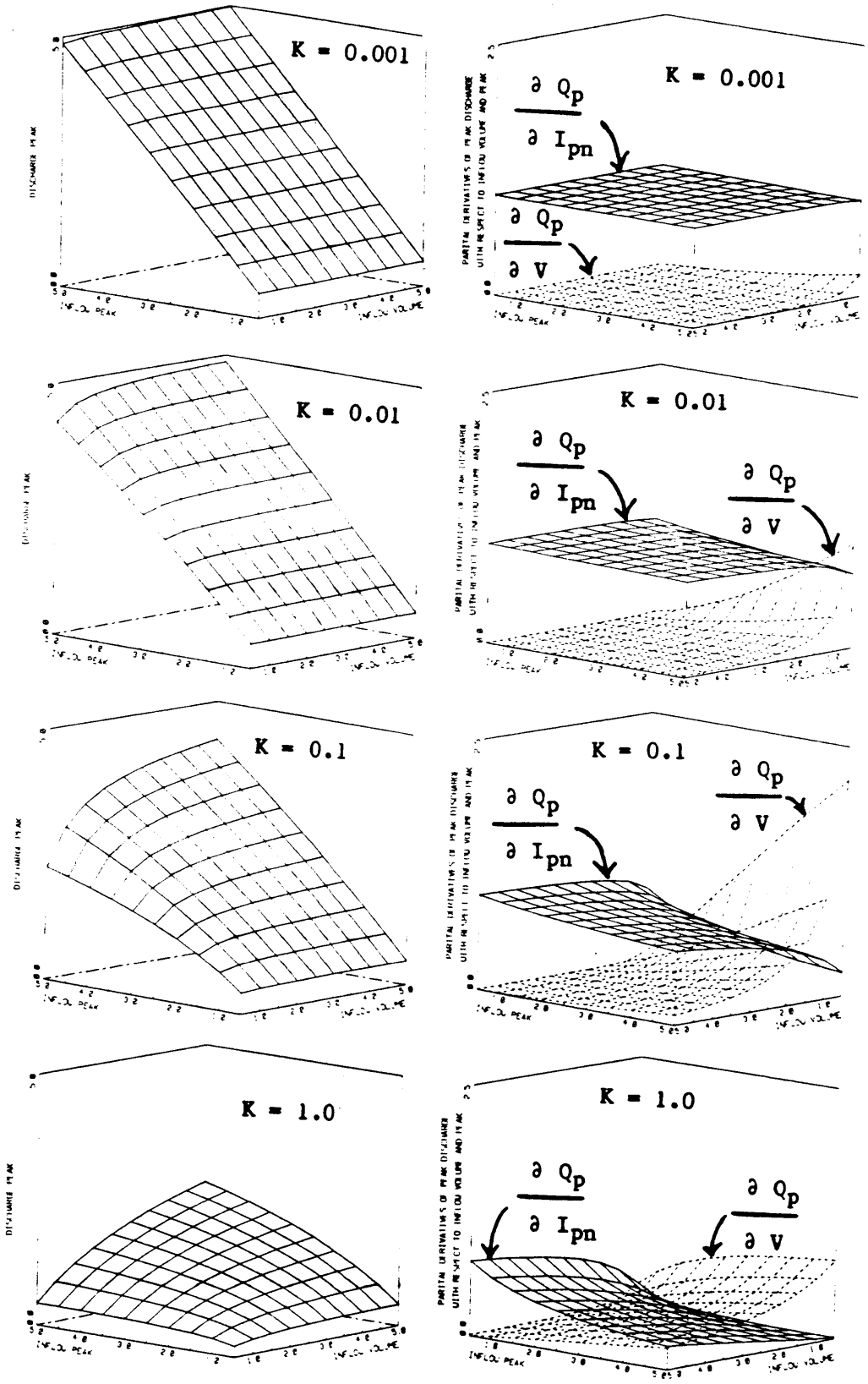

Figure C1: Variation of Discharge Peak with Variation of Inflow Peak and Volume

The partial derivatives of Equation C9 are given by:

$$\frac{\partial Q_p}{\partial V} = \frac{I_{pn}}{V}\left(\frac{-1}{1+\frac{2V}{k\,I_{pn}}}\right) - \frac{k\,I_{pn}}{2V}\,\ell n\left(\frac{1}{1+\frac{2V}{k\,I_{pn}}}\right)\right) \qquad (C11)$$

and

$$\frac{\partial Q_p}{\partial I_{pn}} = 1 + \frac{1}{1+\frac{2V}{k\,I_{pn}}} + \frac{k\,I_{pn}}{V}\,\ell n\left(\frac{1}{1+\frac{2V}{k\,I_{pn}}}\right) \qquad (C12)$$

I_{pn} and V both range from a half through five in Figures C1 through C4. These are non-dimensional numbers which imply that the inflow peak and volume range from half to five times the reference discharge and volume. The reference discharge and volume used in the body of this work are the spillway discharge and reservoir volume when the reservoir is full to the crest of the dam. Five is approximately equal to the largest non-dimensional value of the PMF and the largest non-dimensional PMF volume for the four dams considered in Chapters 3 through 5. (The largest non-dimensional peak was at Miles Pond Dam, and the largest non-dimensional volume was at Springfield Reservoir Dam.)

When k = 0.001, the peak discharge is primarily dependent on the peak inflow, regardless of volume. As k increases, the variation of Q_p with inflow volume increases for small inflow volumes. When k = 1.0, the peak discharge varies roughly equally with inflow peak

and volume when the inflow peak and volume have roughly equal values. Otherwise, still at k = 1.0, Q_p is most sensitive to changes in the smaller of the inflow peak or volume.

Appendix D

Adjustments to Non-Dimensional Parameters for Varying Spillway Size, Initial Reservoir Stage, and Spillway Crest Elevation

When the spillway size is changed, the discharge which characterizes the reservoir and which is used to remove the dimensions from the dimensional parameter values, $\underline{R_c}$, changes. Thus, several of the non-dimensional parameters needed to be adjusted so that they continue to represent the same real (dimensional) dam. Appendix D1 describes the necessary adjustments.

When the initial reservoir stage is changed at Knightville Dam (KVD), the outlet works parameters must be changed to preserve the original initial reservoir discharge and the correct outlet works discharge when the reservoir stage is at the spillway crest. Appendix D2 describes these changes.

Appendix D3 describes the parameter changes needed when the spillway crest elevation is changed.

D1 Variation of Spillway Size

Appendix D1 describes the changes in the non-dimensional parameters which are needed when the spillway size, $\underline{R_c}$, changes and all other dimensional properties do not change. Appendix D1.1 describes the changes when the spillway is modeled as the upper limb of the reservoir discharge curve (see Figure 2.2), and Appendix D1.2 describes

the changes when the spillway is modeled as the lower limb of the reservoir discharge curve.

The quantity being varied is the total discharge when the reservoir stage is at the crest of the dam. This value includes discharge through the outlet works. Thus the proportional change in $\underline{R}_c$ is not exactly equal to the proportionate change in the spillway. All of the change in total discharge, however, is reflected in the limb of the reservoir discharge curve that represents primarily the spillway.

D.1.1 Spillway as Upper Limb of Reservoir Discharge Curve

Figure D1 shows the change in the dimensional reservoir discharge curve when the spillway is changed. Dimensional $\underline{k}_3$ changes, but all other dimensional parameters do not change. The prime notation indicates the new values. Thus, $\underline{R}_c'$ is the new discharge at the crest of the dam, and $\underline{R}_c$ is the original value.

Removing the dimensions from $\underline{k}_3$ using the characteristic time from Table 2.1

$$k_3 = \frac{\underline{k}_3}{\underline{t}_c} = \frac{\underline{k}_3}{(\underline{V}_c/\underline{R}_c)} = \frac{\underline{k}_3\underline{R}_c}{\underline{V}_c} \qquad \text{(D1.1)}$$

Similarly:

$$k_3' = \frac{\underline{k}_3' \, \underline{R}_c'}{\underline{V}_c} \qquad \text{(D1.2)}$$

Dividing Equation D1.2 by Equation D1.1 gives:

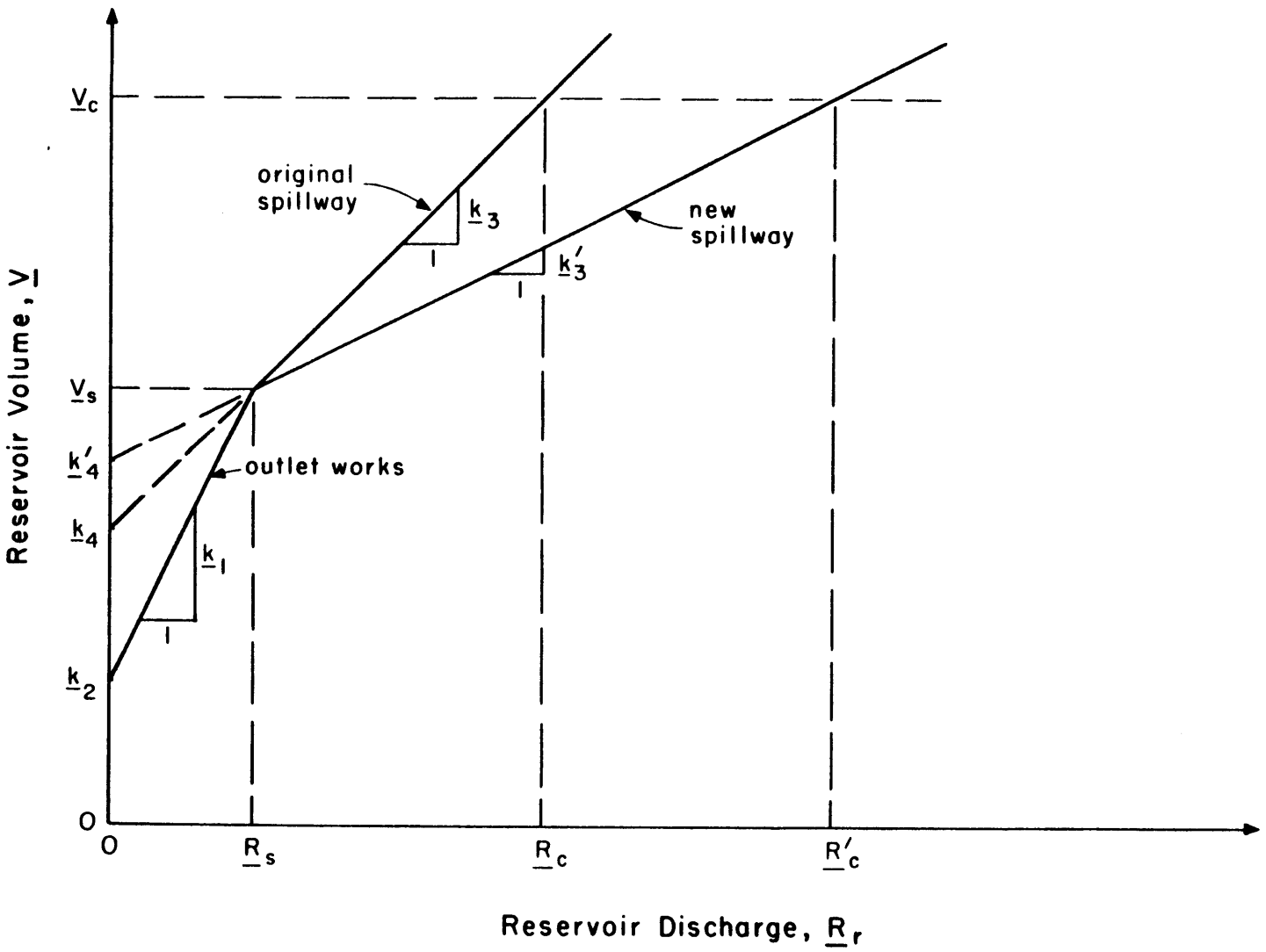

Figure D1: Change $\underline{R}_c$, Upper Limb as Spillway

$$\frac{k_3'}{k_3} = \frac{\frac{k_3'}{k_3}\frac{R_c'}{R_c}}{} \qquad \text{(D1.3)}$$

Then, from the geometry shown in Figure D1:

$$k_3 = \frac{V_c - V_s}{R_c - R_s} \qquad \text{(D1.4)}$$

and

$$k_3' = \frac{V_c - V_s}{R_c' - R_s} \qquad \text{(D1.5)}$$

Dividing Equation D1.5 by Equation D1.4 gives:

$$\frac{k_3'}{k_3} = \frac{R_c - R_s}{R_c' - R_s} \qquad \text{(D1.6)}$$

Then, using Equation D1.6 in Equation D1.3,

$$\frac{k_3'}{k_3} = \left(\frac{R_c - R_s}{R_c' - R_s}\right)\frac{R_c'}{R_c} = \frac{1 - \frac{R_s}{R_c}}{1 - \frac{R_s}{R_c'}} = \frac{1 - R_s}{1 - R_s\left(\frac{R_c}{R_c'}\right)} \qquad \text{(D1.7)}$$

Since k_3, R_s, and $\frac{R_c}{R_c'}$ are known, ($\frac{R_c}{R_c'}$ is the inverse of the values on the axis marked spillway size in Chapter 5), Equation D1.7 defines k_3'. k_4' is then given by:

$$k_4' = 1 - k_3' \tag{D1.8}$$

Equation D1.7 could have been developed from the non-dimensional reservoir discharge function by first noting that because R_c always equals a non-dimensional discharge of 1:

$$\frac{k_3'}{k_3} = \frac{1-R_s}{1-R_s'} \tag{D1.9}$$

Then, since $\underline{R}_s$ is constant, R_s' is given by

$$R_s' = \frac{\frac{R_s}{}}{\frac{R_c'}{}} = \frac{\frac{R_s}{}}{\frac{R_c}{}} \frac{\frac{R_c}{}}{\frac{R_c'}{}} = R_s \frac{\frac{R_c}{}}{\frac{R_c'}{}} \tag{D1.10}$$

Substituting Equation D1.10 into Equation D1.9 gives Equation D1.7.

Then all the other non-dimensional parameters which are functions of $\underline{R}_c$ need to be changed. These changes, given by Equations D1.11 through D1.18, are based on the reasoning shown in Equation D1.10.

$$k_1' = k_1 \frac{\frac{R_c'}{}}{\frac{R_c}{}} \tag{D1.11}$$

$$B_{pg}' = B_{pg} \frac{\frac{R_c}{}}{\frac{R_c'}{}} \tag{D1.12}$$

$$K' = K \frac{\frac{R_c'}{}}{\frac{R_c}{}} \tag{D1.13}$$

$$t_p' = t_p \frac{R_c'}{R_c} \tag{D1.14}$$

$$t_b' = t_b \frac{R_c'}{R_c} \tag{D1.15}$$

$$Q_{nd}' = Q_{nd} \frac{R_c}{R_c'} \tag{D1.16}$$

$$I_p' = I_p \frac{R_c}{R_c'} \tag{D1.17}$$

and $$R_b' = R_b \frac{R_c}{R_c'} \tag{D1.18}$$

In the computer code for this model, the new parameter values given by Equations D1.10 through D1.18 are computed first. Then k_3' is computed as

$$k_3' = \frac{1-V_s}{1-R_s'} \tag{D1.19}$$

and k_4' is computed from Equation D1.8. Equation D1.19 is equivalent to Equation D1.7.

The non-dimensional damage must also be adjusted because of the change in R_c. The required change is described in the end of Appendix D1.2.

D1.2 Spillway as Lower Limb of Reservoir Discharge Curve

Figure D2 shows the change in the reservoir discharge function, in dimensional variables, when the spillway size is changed. Dimensional $\underline{k}_1$ and $\underline{R}_s$ changed when $\underline{R}_c$ is changed. All other dimensional parameters do not change. As in Appendix D1.1, the prime notation indicates the new values. Assuming that $\underline{k}_3$ does not change is an approximation. $\underline{k}_3$ will change a little because the length of the spillway, and thus the length of the embankment crest, changes when $\underline{R}_c$ is changed. $\underline{k}_3$ increases because of the increased head over the portion of the spillway which used to be embankment.

First compute the change in k_1.

$$k_1 = \frac{\underline{k}_1}{\underline{t}_c} = \frac{\underline{k}_1}{(\underline{V}_c/\underline{R}_c)} = \frac{\underline{k}_1 \underline{R}_c}{\underline{V}_c} \qquad \text{(D1.20)}$$

and

$$k_1' = \frac{\underline{k}_1' \underline{R}_c'}{\underline{V}_c} \qquad \text{(D1.21)}$$

Dividing Equation D1.21 by Equation D1.20 gives:

$$\frac{k_1'}{k_1} = \frac{\underline{k}_1' \underline{R}_c'}{\underline{k}_1 \underline{R}_c} \qquad \text{(D1.22)}$$

From the geometry of Figure D2,

$$\underline{k}_1 = \frac{\underline{V}_c - \underline{k}_2}{\underline{R}_c} \qquad \text{(D1.23)}$$

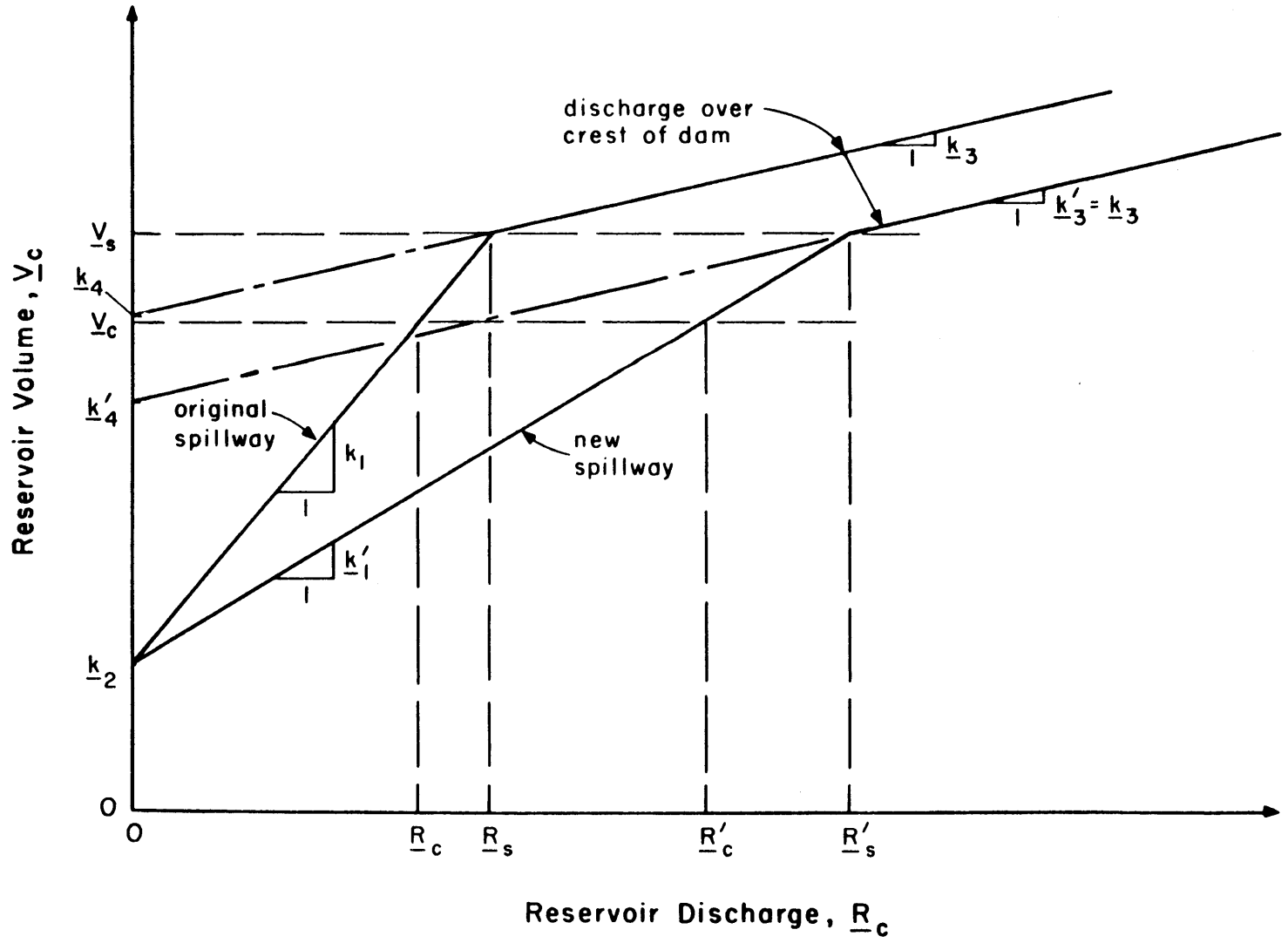

Figure D2: Change $\underline{R}_c$, Lower Limb as Spillway

and

$$\underline{k}_1' = \frac{\underline{V}_c - \underline{k}_2}{\underline{R}_c} \tag{D1.24}$$

Dividing Equation D1.24 by Equation D1.23 gives

$$\frac{\underline{k}_1'}{\underline{k}_1} = \frac{\underline{R}_c}{\underline{R}_c'} \tag{D1.25}$$

Substituting Equation D1.25 into Equation D1.22 shows that

$$\frac{k_1'}{k_1} = 1 \tag{D1.26}$$

Thus the non-dimensional value of k_1 does not change.

Now compute the change in R_s.

$$R_s = \frac{\underline{R}_s}{\underline{R}_c} \tag{D1.27}$$

and

$$R_s' = \frac{\underline{R}_s'}{\underline{R}_c'} \tag{D1.28}$$

Dividing Equation D1.28 by D1.27 gives

$$\frac{R_s'}{R_s} = \frac{\underline{R}_s' \, \underline{R}_c}{\underline{R}_c' \, \underline{R}_s} \tag{D1.29}$$

From the geometry of Figure D2,

$$\underline{R}_s = \frac{\underline{V}_s - \underline{k}_2}{\underline{k}_1} \tag{D1.30}$$

and

$$\underline{R}_s' = \frac{\underline{V}_s - \underline{k}_2}{\underline{k}_1'} \qquad \text{(D1.31)}$$

Dividing Equation D1.31 by Equation D1.30 gives

$$\frac{\underline{R}_s'}{\underline{R}_s} = \frac{\underline{k}_1}{\underline{k}_1'} \qquad \text{(D1.32)}$$

Then, substituting first Equation D1.32 and then Equation D1.25 into Equation D1.29 gives:

$$\frac{R_s'}{R_s} = \frac{\underline{k}_1 \underline{R}_c}{\underline{k}_1' \underline{R}_c'} = \frac{\underline{R}_c' \underline{R}_c}{\underline{R}_c \underline{R}_c'} = 1 \qquad \text{(D1.33)}$$

Thus the non-dimensional value of R_s does not change.

Then all the other non-dimensional parameters which are functions of $\underline{R}_c$ need to be changed. These changes are given by Equations D1.12 through D1.18, Equation D1.33, and Equation D1.8.

$$k_3' = k_3 \frac{\underline{R}_c'}{\underline{R}_c} \qquad \text{(D1.34)}$$

Adjustment to Non-Dimensional Damage

Equation B4.3 shows that the dimensional damage represented by a given value of non-dimensional damage changes when $\underline{R}_c$ changes. Thus, as originally computed, the non-dimensional damage computed for one spillway size (value of $\underline{R}_c$) can not be compared directly with the non-dimensional damage computed for a different spillway size. The non-

dimensional damages shown in the figures in Chapter 5 have been adjusted so they are directly comparable, within each figure.

We want the dimensional damage represented by a given value of non-dimensional damage to be equal, regardless of the spillway size for which it was computed. From Equation B4.3, when

$$\underline{D} = (P_6 \, \underline{R}_c^{P_7}) \, D \tag{D1.34}$$

and

$$\underline{D}' = (P_6 \, \underline{R}_c'^{P_7}) \, D' \tag{D1.35}$$

where $\underline{D} = \underline{D}'$

we have

$$(P_6 \, \underline{R}_c^{P_7}) D = (P_6 \, \underline{R}_c'^{P_7}) D' \tag{D1.36}$$

Solving for D,

$$D = P_6 \left(\frac{\underline{R}_c'}{\underline{R}_c}\right)^{P_7} D' \tag{D1.37}$$

Thus, when D', computed with $\underline{R}_c'$, is multiplied by $P_6\left(\frac{\underline{R}_c'}{\underline{R}_c}\right)^{P_7}$, it is equivalent to D computed with $\underline{R}_c$.

All non-dimensional damages in Chapater 5 are multiplied by $P_6\left(\frac{\underline{R}_c'}{\underline{R}_c}\right)^{P_7}$. Dimensional damage may then be computed by multiplying the

non-dimensional damage by $R_6 \underline{R_c}^{P_7}$.

D2 Variation of Initial Reservoir Stage at Knightville Dam

Figure D3 shows the changes in the non-dimensional reservoir discharge function when the initial stage is changed, but the original initial discharge and discharge at the spillway crest are maintained. As before, the prime notation indicates the new values.

Preservation of the initial discharge, using Equations B1.5A and B1.8, requires:

$$V_o' = H_o'^{P_4} = k_1' R_o + k_2' \qquad \text{(D2.1)}$$

Preservation of the discharge at the spillway crest requires:

$$V_s = k_1 R_s + k_2' \qquad \text{(D2.2)}$$

Solving Equations D3.1 and D3.2 for k_1' and k_2' gives:

$$k_1' = \frac{V_s - V_o'}{R_s - R_o} \qquad \text{(D2.3)}$$

and

$$k_2' = V_s - k_1' R_s \qquad \text{(D2.4)}$$

D3 Variation of Spillway Crest Elevation

Appendix D3 describes the parameter changes needed to change the spillway crest elevation when the total discharge at the crest of the

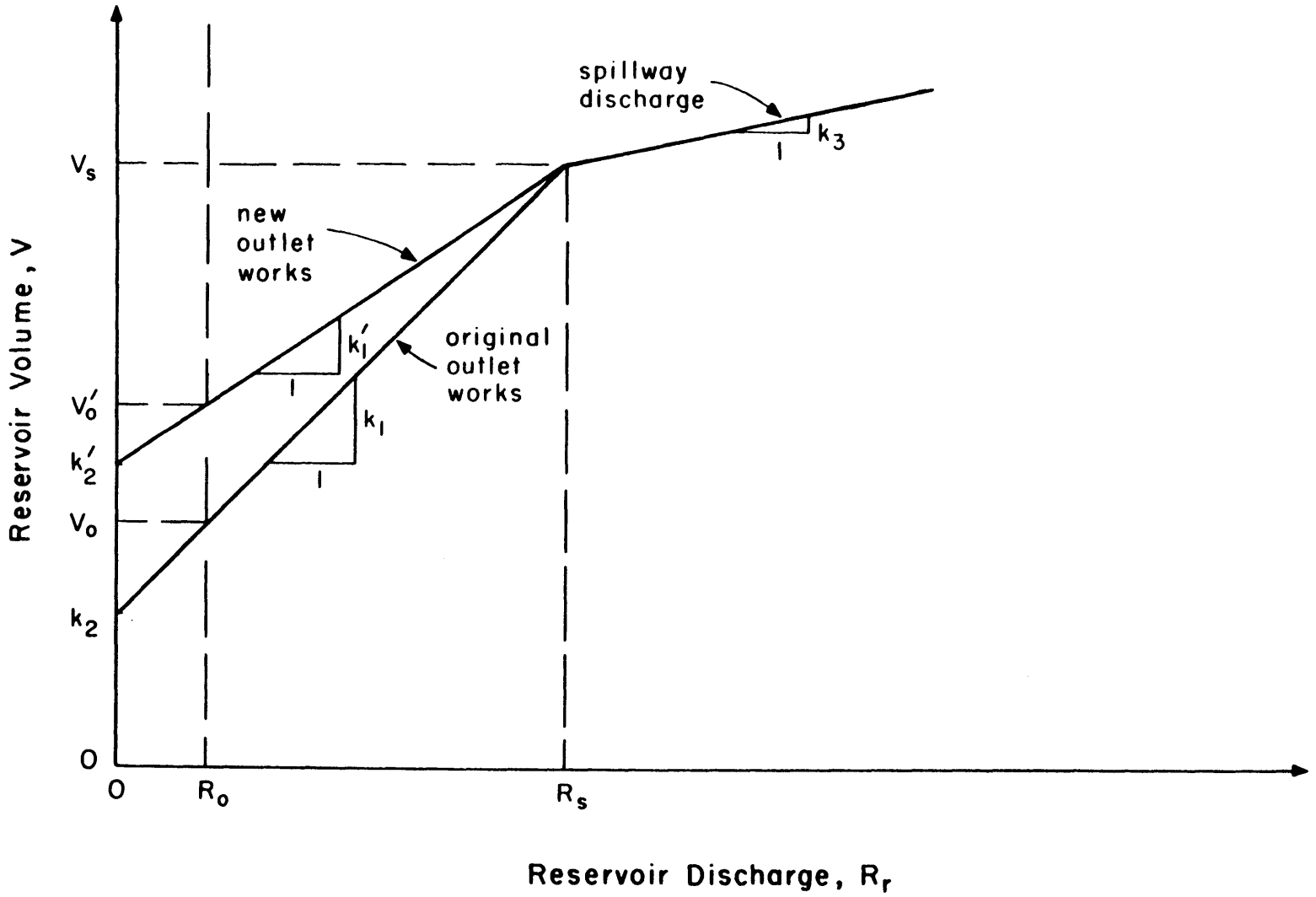

Figure D3: Reservoir Discharge Function Changes with Initial Stage Changes at Knightville Dam

dam, $\underline{R}_c$, is not changed. Appendix D3.1 describes the changes when the spillway is modeled as the upper limb of the reservoir discharge curve (see Figure 2.2), and Appendix D3.2 describes the changes when the spillway is modeled as the lower limb of the reservoir discharge curve. As before, the prime notation indicates the new values.

D3.1 Spillway as Upper Limb of Reservoir Discharge Curve

Figure D4 shows the change in the non-dimensional reservoir discharge function when the spillway crest elevation is changed. Spillway crest elevation changes are computed here in terms of the volume at the spillway crest, V_s.

From the geometry of Figure D4,

$$R_s' = \frac{V_s'-k_2}{k_1} \tag{D3.1}$$

Then, using R_s' from Equation D3.1,

$$k_3' = \frac{1-V_s'}{1-R_s'} \tag{D3.2}$$

Finally, using k_3' from Equation D3.2,

$$k_4' = 1-k_3' \tag{D3.3}$$

No other changes are needed.

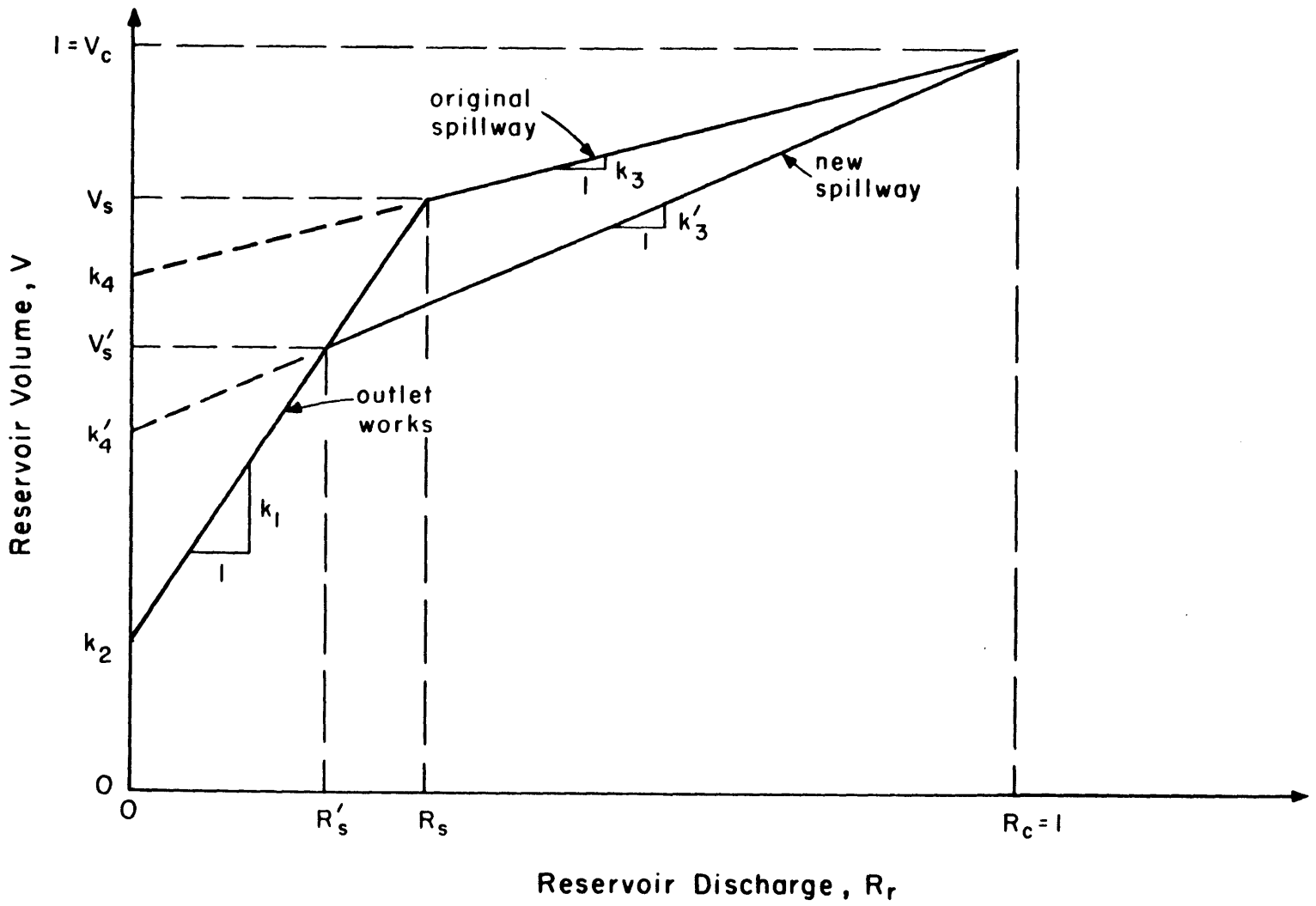

Figure D4: Change Spillway Crest Elevation, Upper Limb as Spillway

The conversion between the ratio of elevations used as the horizontal axis for the figures in Section 5.2 and the change in V_s is, using Equation B1.8 (see also Figure 2.3),

$$V' = V\left(\frac{H'}{H}\right)^{P_4} \qquad \text{(D3.4)}$$

where $\frac{H'}{H}$ is the ratio between the new and old spillway crest elevations.

D3.2 Spillway as Lower Limb of Reservoir Discharge Curve

Figure D5 shows the change in the non-dimensional reservoir discharge function when the spillway crest elevation changes. Spillway crest elevation changes are computed here as changes in the volume at the spillway crest, k_2. This method is accurate only when the outlet works are so small that the value of k_2 represents the spillway crest accurately, as for SRD. From the geometry of Figure D5,

$$k_1' = \frac{V_s - k_2'}{R_s} \qquad \text{(D3.5)}$$

No other changes are needed.

The conversion between the ratio of elevations used as the horizontal axis for the Figures in Section 5.2 and the change in k_2 is, using Equation B1.8 (see also Figure 2.3),

$$k_2' = k_2\left(\frac{H'}{H}\right)^{P_4} \qquad \text{(D3.6)}$$

where $\frac{H'}{H}$ = the ratio between the new and old spillway crest elevation.

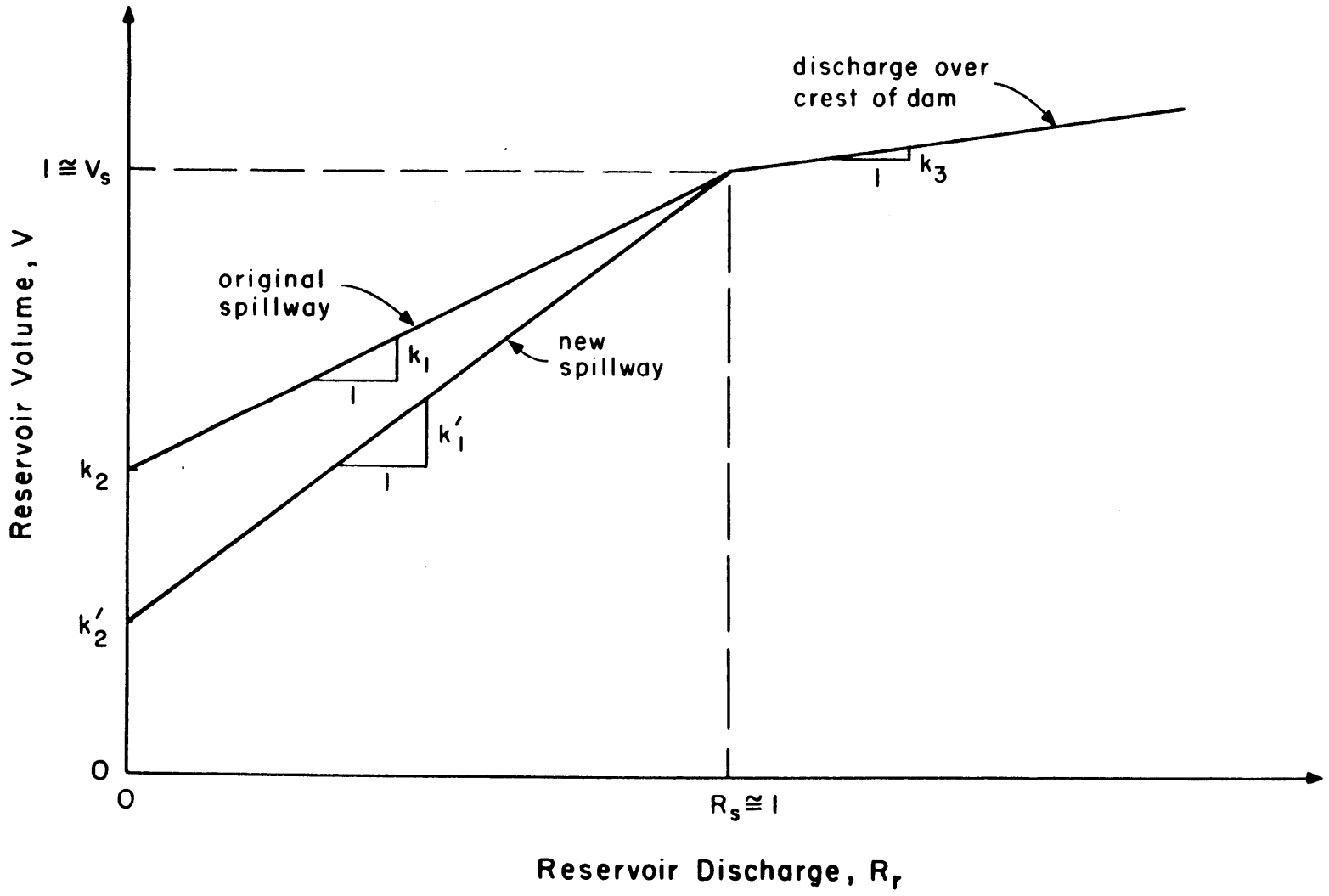

Figure D5: Change Spillway Crest Elevation, Lower Limb as Spillway

Appendix E

NATIONAL DAM INSPECTION ACT

Public Law 92-367
92nd Congress, H. R. 15951
August 8, 1972

An Act

To authorize the Secretary of the Army to undertake a national program of inspection of dams.

Be it enacted by the Senate and House of Representatives of the United States of America in Congress assembled, That the term "dam" as used in this Act means any artificial barrier, including appurtenant works, which impounds or diverts water, and which (1) is twenty-five feet or more in height from the natural bed of the stream or watercourse measured at the downstream toe of the barrier, or from the lowest elevation of the outside limit of the barrier, if it is not across a stream channel or watercourse, to the maximum water storage elevation or (2) has an impounding capacity at maximum water storage elevation of fifty acre-feet or more. This Act does not apply to any such barrier which is not in excess of six feet in height, regardless of storage capacity or which has a storage capacity at maximum water storage elevation not in excess of fifteen acre-feet, regardless of height.

National dam inspection program.
"Dam."

SEC. 2. As soon as practicable, the Secretary of the Army, acting through the Chief of Engineers, shall carry out a national program of inspection of dams for the purpose of protecting human life and property. All dams in the United States shall be inspected by the Secretary except (1) dams under the jurisdiction of the Bureau of Reclamation, the Tennessee Valley Authority, or the International Boundary and Water Commission, (2) dams which have been constructed pursuant to licenses issued under the authority of the Federal Power Act, (3) dams which have been inspected within the twelve-month period immediately prior to the enactment of this Act by a State agency and which the Governor of such State requests be excluded from inspection, and (4) dams which the Secretary of the Army determines do not pose any threat to human life or property. The Secretary may inspect dams which have been licensed under the Federal Power Act upon request of the Federal Power Commission and dams under the jurisdiction of the International Boundary and Water Commission upon request of such Commission.

Army, authorization.

Exceptions.

41 Stat. 1063; 49 Stat. 863. 16 USC 791a.

86 STAT. 506
86 STAT. 507

SEC. 3. As soon as practicable after inspection of a dam, the Secretary shall notify the Governor of the State in which such dam is located the results of such investigation. The Secretary shall immediately notify the Governor of any hazardous conditions found during an inspection. The Secretary shall provide advice to the Governor, upon request, relating to timely remedial measures necessary to mitigate or obviate any hazardous conditions found during an inspection.

Notice to Governors.

SEC. 4. For the purpose of determining whether a dam (including the waters impounded by such dam) constitutes a danger to human life or property, the Secretary shall take into consideration the possibility that the dam might be endangered by overtopping, seepage, settlement, erosion, sediment, cracking, earth movement, earthquakes, failure of bulkheads, flashboard, gates on conduits, or other conditions which exist or which might occur in any area in the vicinity of the dam.

SEC. 5. The Secretary shall report to the Congress on or before July 1, 1974, on his activities under the Act, which report shall include, but not be limited to—

Report to Congress.

(1) an inventory of all dams located in the United States;

(2) a review of each inspection made, the recommendations furnished to the Governor of the State in which such dam is located and information as to the implementation of such recommendation;

(3) recommendations for a comprehensive national program for the inspection, and regulation for safety purpose of dams of the Nation, and the respective responsibilities which should be assumed by Federal, State, and local governments and by public and private interests.

Liability.

SEC. 6. Nothing contained in this Act and no action or failure to act under this Act shall be construed (1) to create any liability in the United States or its officers or employees for the recovery of damages caused by such action or failure to act; or (2) to relieve an owner or operator of a dam of the legal duties, obligations, or liabilities incident to the ownership or operation of the dam.

Approved August 8, 1972.

LEGISLATIVE HISTORY:

HOUSE REPORT No. 92-1232 (Comm. on Public Works).
CONGRESSIONAL RECORD, Vol. 118 (1972):
July 24, considered and passed House.
July 25, considered and passed Senate.
WEEKLY COMPILATION OF PRESIDENTIAL DOCUMENTS, Vol. 8, No. 33:
Aug. 9, Presidential statement.

Appendix F

RESERVOIR STAGE DATA

Reservoir stage data from seven dams in New England were collected and analyzed by Ms. Laura Gooch for an Undergraduate Research Opportunities Project under Professor Frank E. Perkins at the Massachusetts Institute of Technology in 1981. Appendix F presents the results of the data analysis portion of that project. Except for correction of some small errors, and a few minor changes, the results presented are those developed by Ms. Gooch.

Gooch gathered seven years of daily stage data from each of three New England Division U.S. Army Corps of Engineer flood control dams and ten years of data from each of four New England Power Service Co. hydroelectric power dams. Table F1 lists the dams. Five day averages were estimated from the daily data and used for the analysis.

Figures F1 through F7 show frequency histograms computed from the five day average stages. The crest of the dam, or some elevation near the crest, was used as the datum in this work. Thus, the values decrease as the reservoir stage gets higher. The figures also show probability density functions fit to the data. Six of the dams were fit with exponential distributions. The seventh, Somerset Dam, was fit with a log-normal distribution. Parameters of the distributions were estimated from the mean and variance of the data.

The reservoir stages generally vary as expected. The hydropower dams are more frequently high and the flood control dams are more frequently low.

Bellows Falls and Wilder are run-of-the-river facilities and consequently show only small stage variations. Harriman Dam, with substantial storage and approximately 90 feet of usable drawdown capacity, shows much wider variations, but the same pattern. The stage distribution at Somerset is different than at the other three hydroelectric facilities. Somerset, like Harriman, has substantial storage and drawdown capacity (60 feet), but, unlike Harriman, has no upstream regulation. The lack of upstream regulation may be the reason for the difference in the shapes of the frequency distributions.

Reservoir stage varies more at Knightville Dam than at the other two flood control dams. Knightville provides recreation in addition to flood control, and thus must be raised during the recreational season and lowered during the flood season. The mean stage at Littleville Dam is much higher than at the other two flood control dams. Littleville provides water supply in addition to flood control and recreation and thus must be maintained at a higher stage than otherwise desirable. Franklin Falls is a purely flood control dam and can be maintained at a low stage all year.

Table F1

Descriptions of Dams for which

Reservoir Stage Data was Collected

Name	River	Purpose	Drainage Area (sq.mi.)	time period	number of data points
Wilder	Connecticut	hydropower	3375	1965-1975	792
Harriman	Deerfield	hydropower	184	1951-1965	756
Bellows Falls	Connecticut	hydropower	5414	1967-1976	702
Somerset	Deerfield	hydropower	30	1965-1974	720
Franklin Falls	Merrimack	flood control	?	1972-1979	522
Littleville	Westfield, middle branch	flood control, water supply, recreation	52	1972-1979	522
Knightville	Westfield	flood control, recreation	162	1972-1979	522

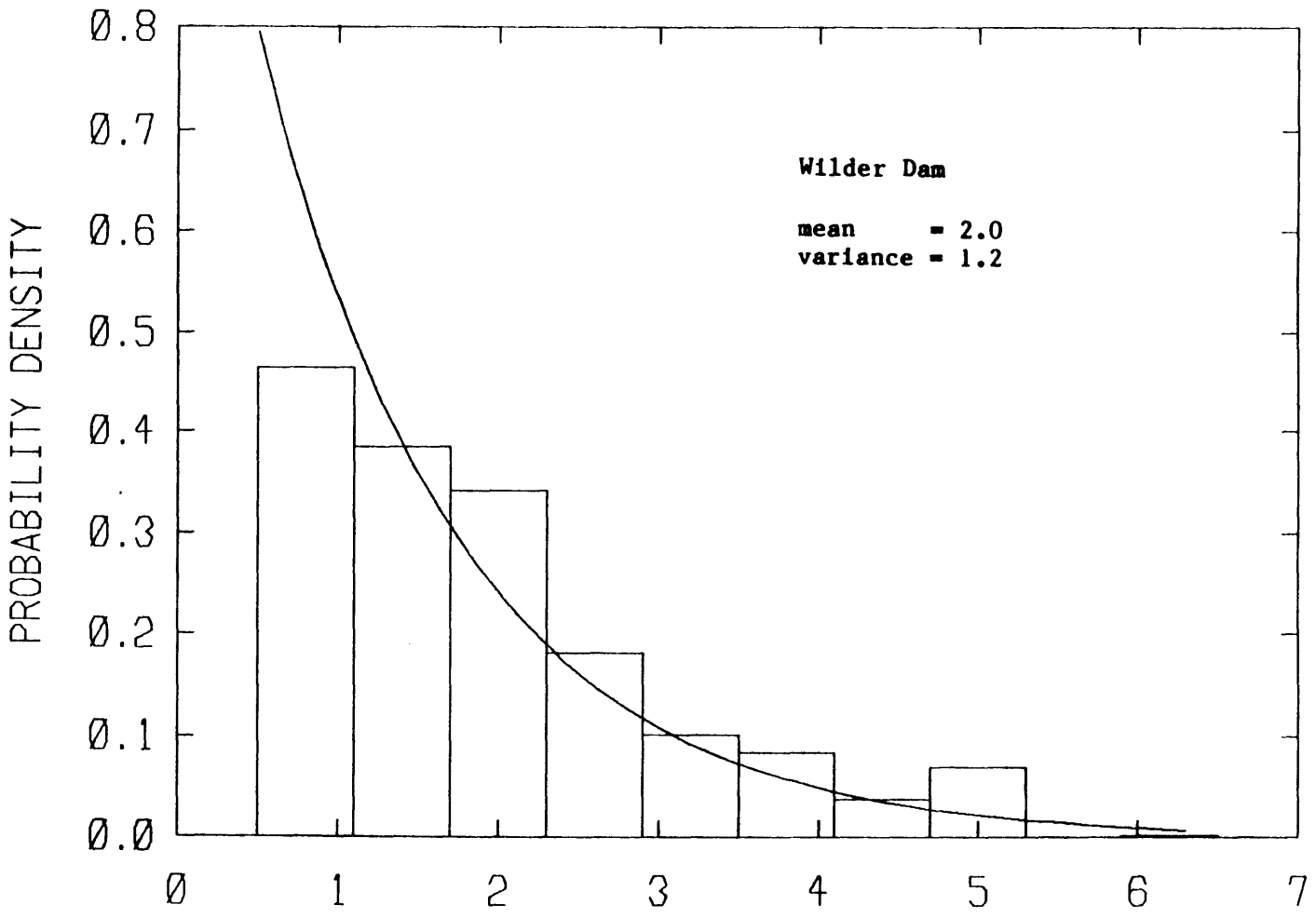

Figure F1: Reservoir Stage Distribution, Wilder Dam

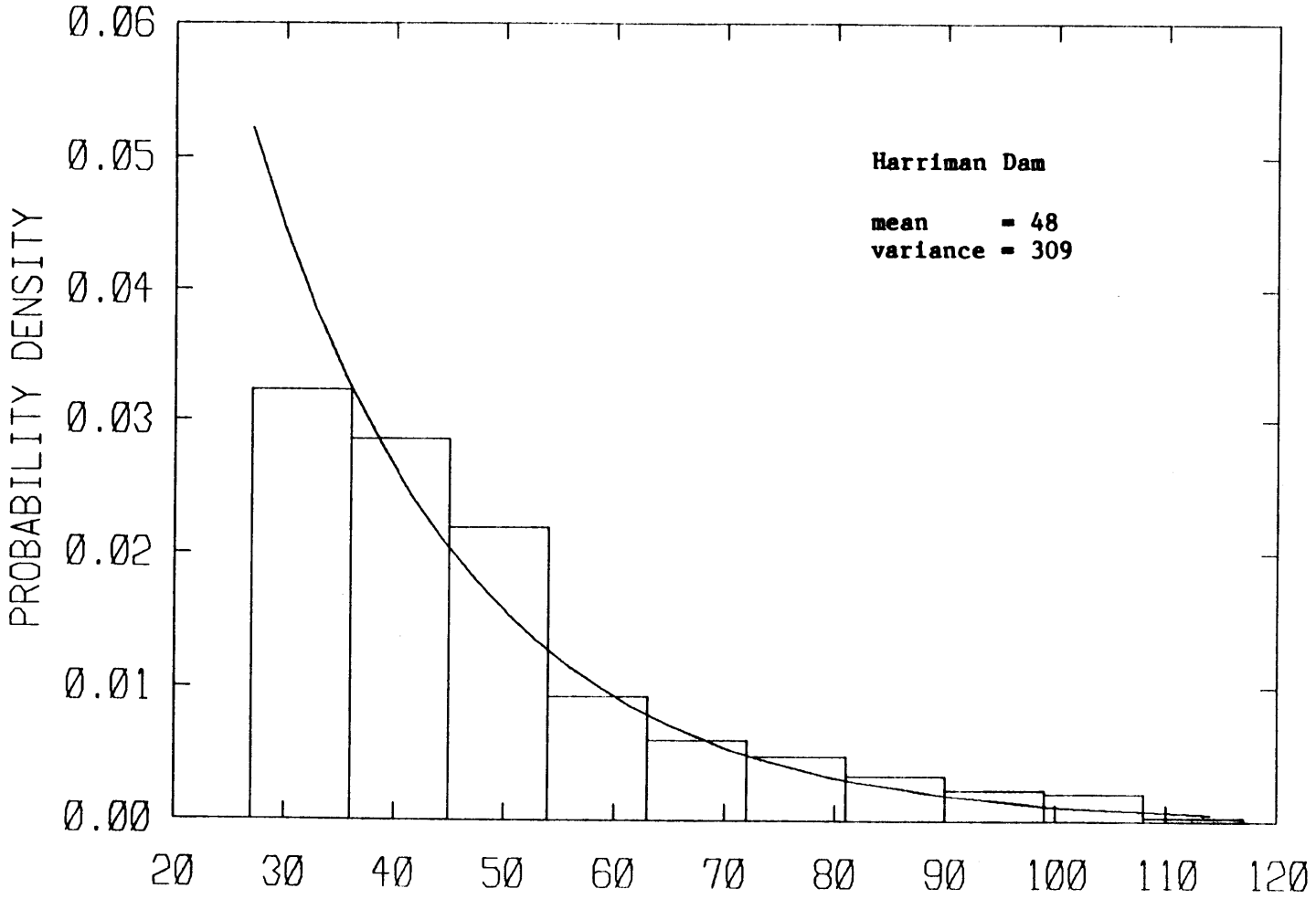

Figure F2: Reservoir Stage Distribution, Harriman Dam

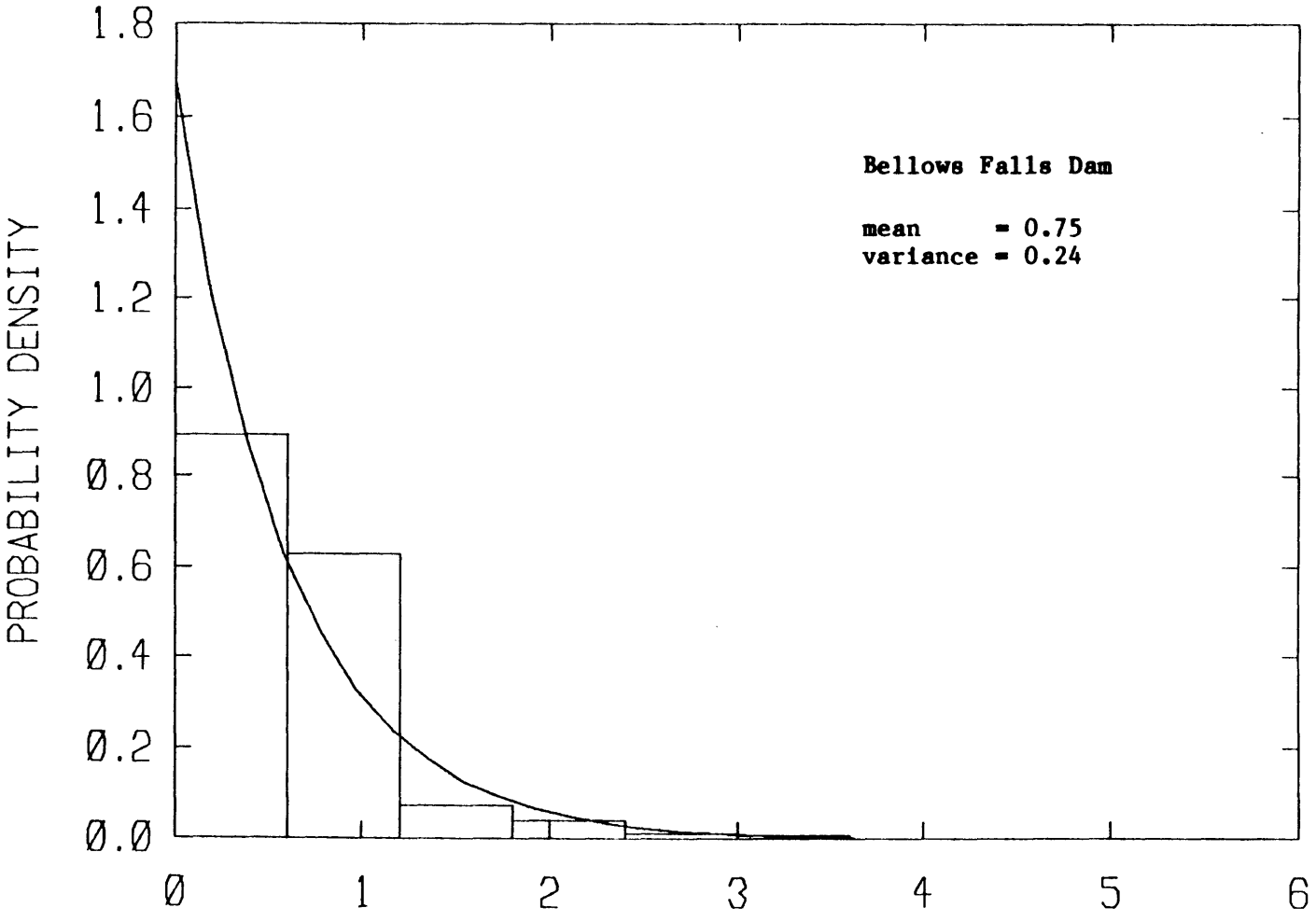

Figure F3: Reservoir Stage Distribution, Bellows Falls Dam

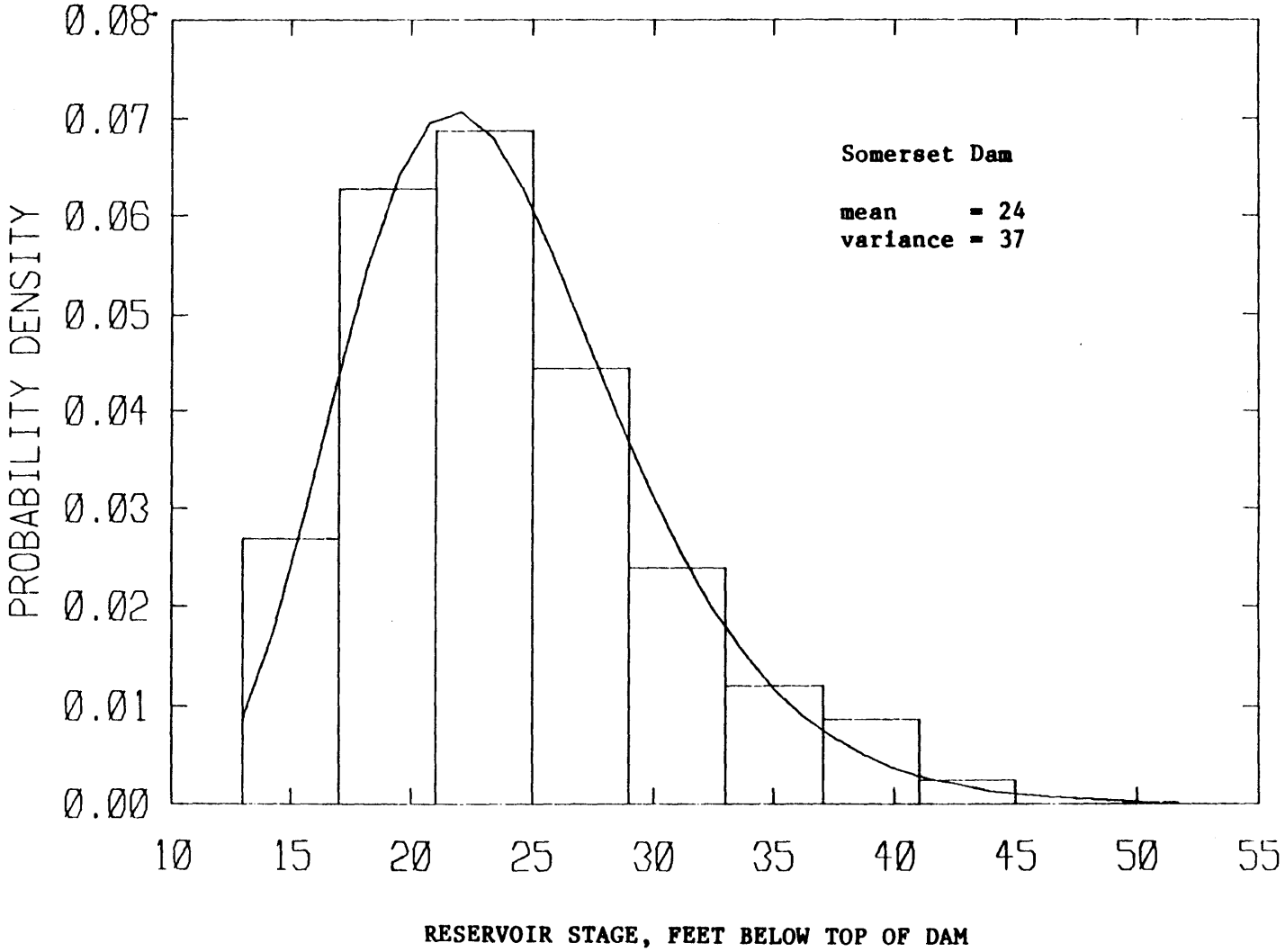

Figure F4: Reservoir Stage Distribution, Somerset Dam

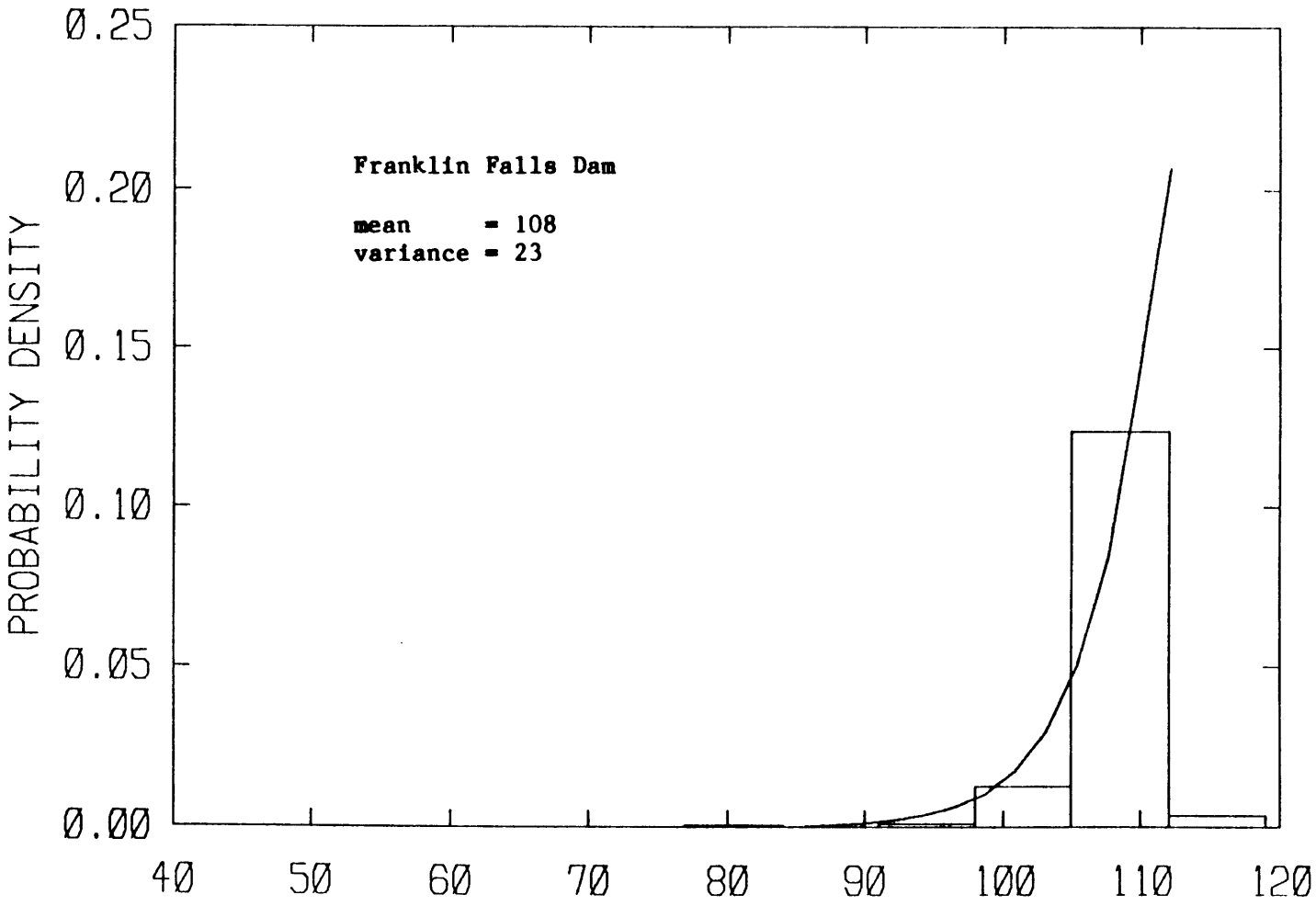

Figure F5: Reservoir Stage Distribution, Franklin Falls Dam

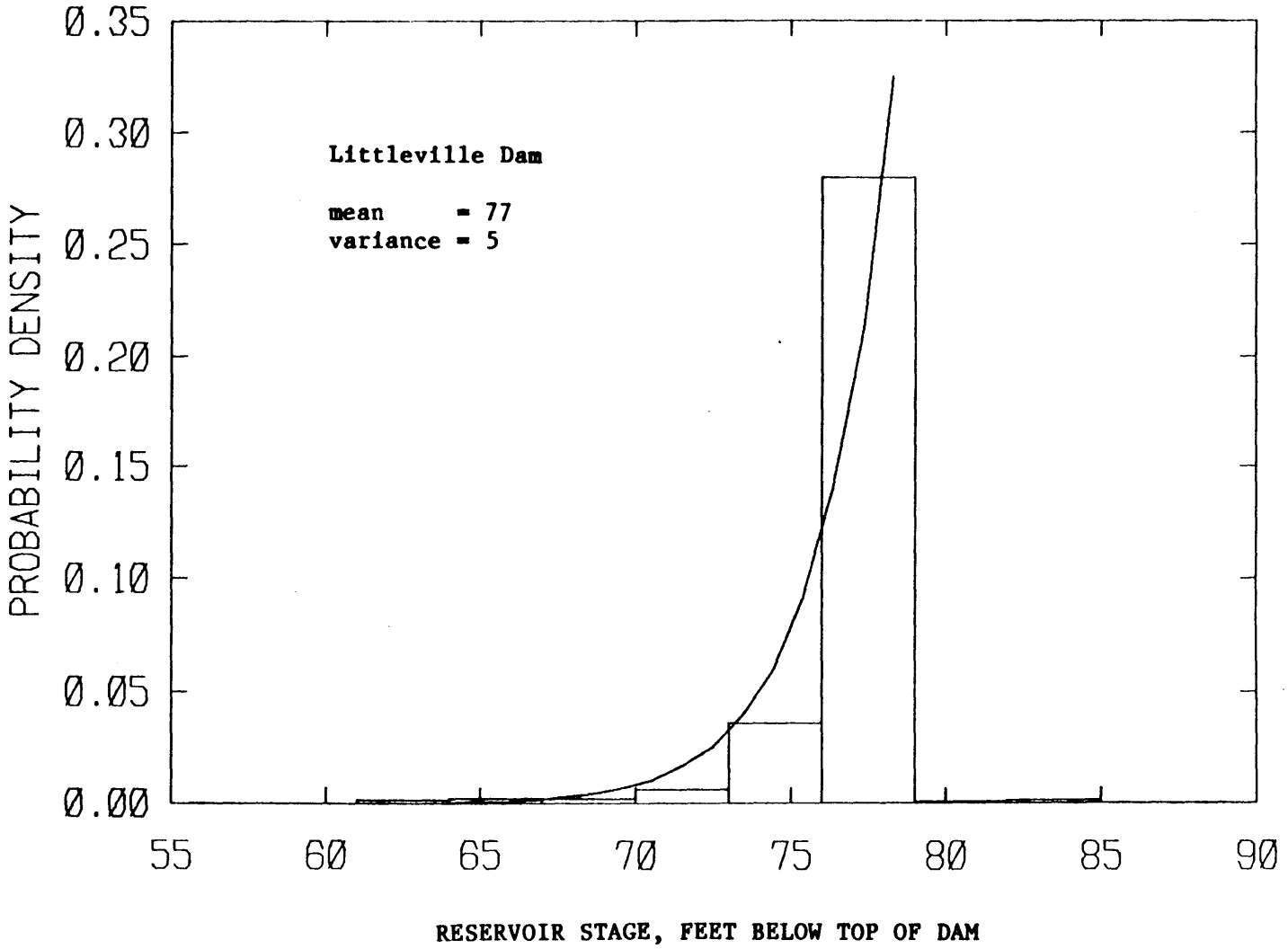

Figure F6: Reservoir Stage Distribution, Littleville Dam

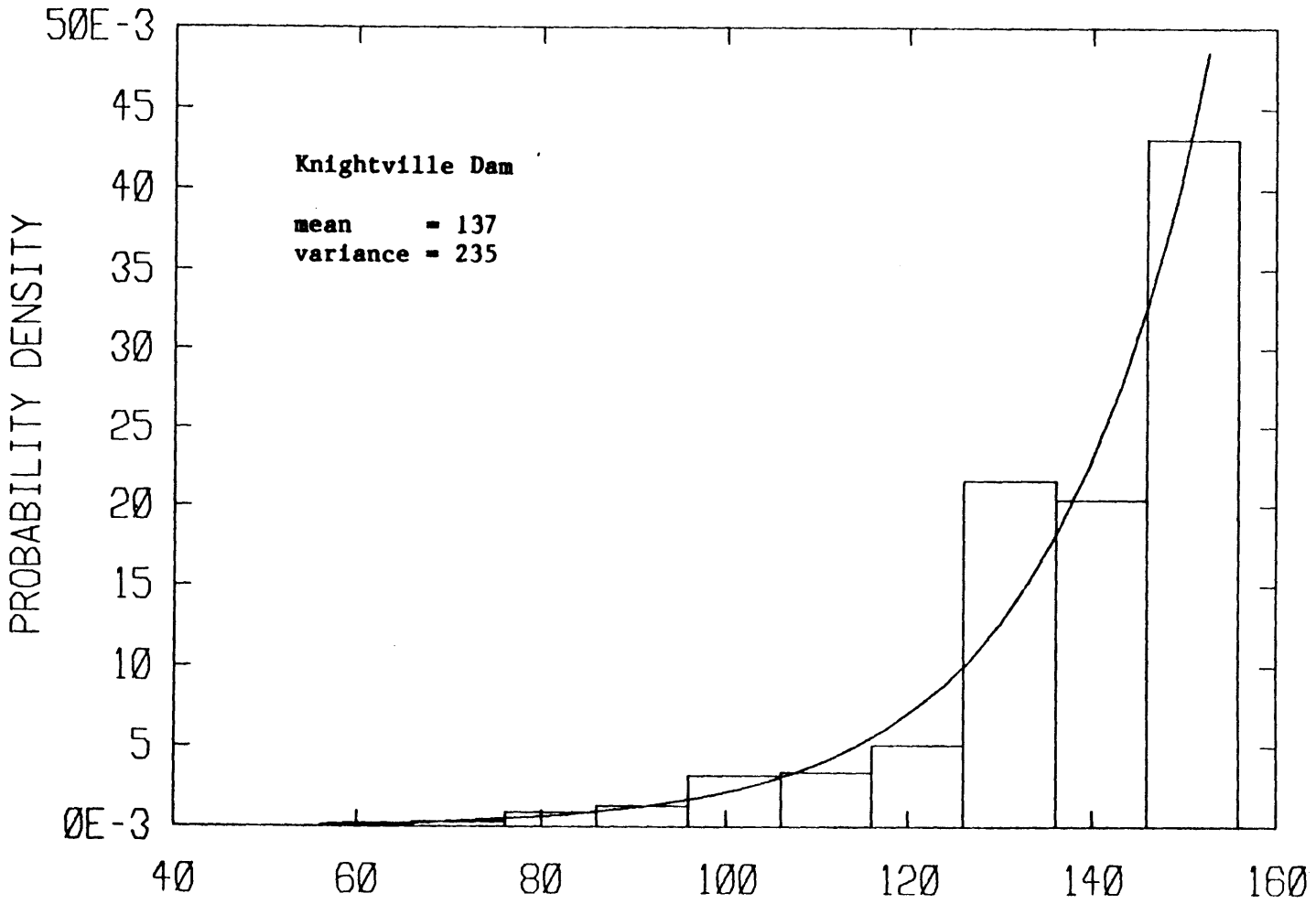

Figure F7: Reservoir Stage Distribution, Knightville Dam